Masteroppgave

BØK950 Økonomi og administrasjon

Impulse response analysis of nonlinear time series using the SNP method

Haakon Egeland og Silje Haug

Totalt antall sider inkludert forsiden: 148

Molde, 25.05.2016

Høgskolen i Molde
Vitenskapelig høgskole i logistikk

Obligatorisk egenerklæring/gruppeerklæring

Den enkelte student er selv ansvarlig for å sette seg inn i hva som er lovlige hjelpemidler, retningslinjer for bruk av disse og regler om kildebruk. Erklæringen skal bevisstgjøre studentene på deres ansvar og hvilke konsekvenser fusk kan medføre. Manglende erklæring fritar ikke studentene fra sitt ansvar.

Du/dere fyller ut erklæringen ved å klikke i ruten til høyre for den enkelte del 1-6:		
1.	**Jeg/vi erklærer herved at min/vår besvarelse er mitt/vårt eget arbeid, og at jeg/vi ikke har brukt andre kilder eller har mottatt annen hjelp enn det som er nevnt i besvarelsen.**	☒
2.	**Jeg/vi erklærer videre at denne besvarelsen:** • ikke har vært brukt til annen eksamen ved annen avdeling/universitet/høgskole innenlands eller utenlands. • ikke refererer til andres arbeid uten at det er oppgitt. • ikke refererer til eget tidligere arbeid uten at det er oppgitt. • har alle referansene oppgitt i litteraturlisten. • ikke er en kopi, duplikat eller avskrift av andres arbeid eller besvarelse.	☒
3.	Jeg/vi er kjent med at brudd på ovennevnte er å betrakte som fusk og kan medføre annullering av eksamen og utestengelse fra universiteter og høgskoler i Norge, jf. Universitets- og høgskoleloven §§4-7 og 4-8 og Forskrift om eksamen §§14 og 15.	☒
4.	Jeg/vi er kjent med at alle innleverte oppgaver kan bli plagiatkontrollert i Ephorus, se Retningslinjer for elektronisk innlevering og publisering av studiepoenggivende studentoppgaver	☒
5.	Jeg/vi er kjent med at høgskolen vil behandle alle saker hvor det forligger mistanke om fusk etter høgskolens retningslinjer for behandling av saker om fusk	☒
6.	Jeg/vi har satt oss inn i regler og retningslinjer i bruk av kilder og referanser på biblioteket sine nettsider	☒

Publiseringsavtale

Studiepoeng: 30

Veileder: Per Bjarte Solibakke

Fullmakt til elektronisk publisering av oppgaven

Forfatter(ne) har opphavsrett til oppgaven. Det betyr blant annet enerett til å gjøre verket tilgjengelig for allmennheten (Åndsverkloven. §2).
Alle oppgaver som fyller kriteriene vil bli registrert og publisert i Brage HiM med forfatter(ne)s godkjennelse.
Oppgaver som er unntatt offentlighet eller båndlagt vil ikke bli publisert.

Jeg/vi gir herved Høgskolen i Molde en vederlagsfri rett til å gjøre oppgaven tilgjengelig for elektronisk publisering: ☒ja ☐nei

Er oppgaven båndlagt (konfidensiell)? ☐ja ☒nei
(Båndleggingsavtale må fylles ut)
- Hvis ja:
Kan oppgaven publiseres når båndleggingsperioden er over? ☐ja ☐nei

Er oppgaven unntatt offentlighet? ☐ja ☒nei
(inneholder taushetsbelagt informasjon. Jfr. Offl. §13/Fvl. §13)

Dato: 12.05.2016

Antall ord: 22 127

Preface

This thesis is written as the conclusion of the Master of Science degree in Business and Administration with specialization in Economic Analysis at Molde University College. The thesis investigates how shocks influence the return and volatility in financial markets. The topic is chosen based on professional and personal interest. Working with this thesis has been both challenging and interesting, and we have gained knowledge about the structure of volatility in financial markets and market risk.

The thesis is written in Microsoft Word. The empirical analysis, estimations, and modeling have been performed in EViews 9, a statistical software package for Microsoft, and SNP, a C++ program for nonparametric time series analysis. Part of the analysis has also been performed in Microsoft Excel.

We would like to thank our supervisor Professor Per Bjarte Solibakke at NTNU, for his counseling and guidance.

Molde, May 2016

Haakon Egeland

Silje Haug

Abstract

The uncertainty associated with the price of the underlying asset is the key determinant when pricing an option. Therefore, knowledge about the dynamics of volatility is of great interest and relevant to several financial applications, such as pricing of hedging instruments and fund management. It has also become a central topic in the field of empirical studies. In this thesis, we have investigated the multi-step ahead dynamics of volatility, and the responses to shocks hitting the systems.

The study features an analysis of impulse-response dynamics of non-linear time series. Using a semi-nonparametric GARCH model, we have been able to extract conditional one-step-ahead densities and forecast one-step-ahead conditional volatility. In addition, we study shocks from conditional variance functions, analyze multi-step ahead dynamics for mean return and volatility, and calculate measures of volatility persistence. The approach includes an examination of profile bundles for evidence of damping or persistence, which is important for our thesis. We have examined univariate time series consisting of the daily return for seven stock indices, four individual company shares, and three commodity indices. The SNP-method has been applied to generate empirical evidence on the multi-step ahead price dynamics. An interesting feature is to investigate if the mean impulse responses are symmetric about the baseline and if they are heavily damped. Our results show that this symmetry is present, and we observe almost no serial dependence beyond lag one. The results suggest that an increase in volatility after a shock does not lead to a permanent change in volatility. Furthermore, we have studied the extent to which the impulse responses indicate a leverage effect, where price decrease has a greater effect on subsequent volatility than the price increase. Our findings suggest that the leverage effect is present. We find the highest degree of asymmetry for stock indices and the asymmetry seems to be persistent. Lastly, we have studied the persistence of volatility. The assets with the highest degree of asymmetry in variance also have the lowest persistence. The persistence ranges from 17 to 130 days, and it was found to be shortest for the stock indices and longest for the individual shares and commodity indices. Due to the time constraint that the master thesis composes, we have not performed significance tests of our findings. We find that the persistence of asymmetry deviate from existing literature. Although the significance of our findings is not tested, it can be an important contribution to this field of research, serving as a preliminary study for further work.

Table of Content

1.0 Introduction **1**
2.0 Descriptive Statistics **3**
2.1 The physical marketplace for commodities 3
2.1.1 Oil 4
2.1.2 Carbon 4
2.1.3 Salmon 4
2.2 Stationarity 5
2.3 Autocorrelation 6
2.4 BDS Test for Independence 7
2.5 Value at Risk (VaR) 8
2.5.1 Conditional Value at Risk (CVaR) 8
2.6 Description of Data 9
2.6.1 Dow Jones Industrial Average (DJIA) 9
2.6.2 FTSE 100 Index (FTSE) 11
2.6.3 S&P 100 Index (OEX) 13
2.6.4 S&P 500 Index (GSPC) 15
2.6.5 Oslo Stock Exchange Benchmark Index (OSEBX) 17
2.6.6 Oslo Stock Exchange Index (OBX) 19
2.6.7 Oslo Stock Exchange All Share Index (OSEAX) 21
2.6.8 Microsoft Corporation (MSFT) 23
2.6.9 Micron Technology Inc. (MU) 25
2.6.10 Norsk Hydro ASA (NHY) 27
2.6.11 Tomra Systems ASA (TOM) 29
2.6.12 The ICE Carbon one month Forward Contracts 31
2.6.13 Brent oil front month Future Contracts 33
2.6.14 Salmon Forward Contracts 34
3.0 Theoretical aspects **36**
3.1 Persistence 36
3.2 Asymmetry 36
3.3 Portfolio Theory 37
4.0 Impulse response analysis of nonlinear models **38**
4.1 Definition 38
5.0 Method **40**
5.1 The ARCH and GARCH Methodology 40
5.2 Model Selection 41
5.3 SNP Method for Nonparametric Time Series Analysis 41
5.3.1 Limitations 42
5.4 Estimation of the Conditional Density 42
5.4.1 Semi-nonparametric (SNP) Estimators 42
5.4.2 SNP- (univariate) Estimation 45
6.0 Empirical Results **107**
6.1 Impulse-Response Dynamics for Mean and Variance 107
6.2 Persistence 124
7.0 Conclusion **133**
7.1 Summary of main results 133
7.2 Further studies 135

List of Figures

Figure 1 DJIA Index Price and Returns 10
Figure 2 DJIA Index Returns 10
Figure 3 FTSE Index Price and Returns 12
Figure 4 FTSE Index Returns 12
Figure 5 S&P 100 Price and Returns 14
Figure 6 S&P 100 Returns 14
Figure 7 S&P 500 Price and Returns 16
Figure 8 S&P 500 Returns 16
Figure 9 OSEBX Index Price and Returns 18
Figure 10 OSEBX Returns 18
Figure 11 OBX Index Price and Returns 20
Figure 12 OBX Returns 20
Figure 13 OSEAX Index Price and Returns 22
Figure 14 OSEAX Index Returns 22
Figure 15 MSFT Price and Returns 24
Figure 16 MSFT Returns 24
Figure 17 MU Price and Returns 26
Figure 18 MU Returns 26
Figure 19 NHY Price and Returns 28
Figure 20 NHY Returns 28
Figure 21 TOM Price and Returns 30
Figure 22 TOM Returns 30
Figure 23 Carbon Price and Returns 32
Figure 24 Carbon Returns 32
Figure 25 Brent oil Returns 34
Figure 26 Returns Salmon 35
Figure 27 Projected conditional volatility and residuals AR (1) moving average DJIA Index 48
Figure 28 DJIA Index one-step-ahead densities (x_{t-1} = unconditional mean) 49
Figure 29 DJIA Index one-step-ahead densities (conditional mean for x_{t-1} = -40%...40%) 49
Figure 30 DJIA Index: conditional variance functions 50
Figure 31 Projected conditional volatility and residuals AR (1) moving average FTSE Index 53
Figure 32 FTSE Index one-step-ahead densities (x_{t-1} = unconditional mean) 53
Figure 33 FTSE Index one-step-ahead densities (conditional mean for x_{t-1} = -40%...40%) 54
Figure 34 FTSE Index: conditional variance function 54
Figure 35 Projected conditional volatility and residuals AR (1) moving average S&P 100 Index 57
Figure 36 S&P 100 Index one-step-ahead densities (x_{t-1} = unconditional mean) 58
Figure 37 S&P Index one-step-ahead densities (conditional mean for x_{t-1} = -40%...40%) 58
Figure 38 S&P 100 Index: conditional variance functions 59
Figure 39 Projected conditional volatility and residuals AR (1) moving average S&P 500 Index 62
Figure 40 S&P 500 Index one-step-ahead densities (x_{t-1} = unconditional mean) 62
Figure 41 S&P 500 Index one-step-ahead densities (conditional mean for x_{t-1} = -40%...40%) 63

Figure 42 S&P 500 Index: conditional variance function ... 63
Figure 43 Projected conditional volatility and residuals AR (1) moving average OSEBX Index ... 66
Figure 44 OSEBX one-step-ahead densities (x_{t-1} = unconditional mean) ... 67
Figure 45 OSEBX Index one-step-ahead densities (conditional mean for x_{t-1} = -40%...40%) ... 67
Figure 46 OSEBX Index: conditional variance functions ... 68
Figure 47 Projected conditional volatility and residuals AR (1) moving average OBX Index ... 70
Figure 48 OBX Index one-step-ahead densities (x_{t-1} = unconditional mean) ... 71
Figure 49 OBX Index one-step-ahead densities (conditional mean for x_{t-1} = -40%...40%) 71
Figure 50 OBX Index: conditional variance functions ... 72
Figure 51 Projected conditional volatility and residuals AR (1) moving average OSEAX Index ... 74
Figure 52 OSEAX Index one-step-ahead densities (x_{t-1} = unconditional mean) ... 75
Figure 53 OSEAX Index one-step-ahead densities (conditional mean for x_{t-1} = -40%...40%) ... 75
Figure 54 OSEAX Index: conditional variance functions ... 76
Figure 55 Projected conditional volatility and residuals AR (1) moving average MSFT .. 79
Figure 56 MSFT one-step-ahead densities (x_{t-1} = unconditional mean) ... 79
Figure 57 MSFT one-step-ahead densities (conditional mean for x_{t-1} = -40%...40%) ... 80
Figure 58 MSFT: conditional variance functions ... 80
Figure 59 Projected conditional volatility and residuals AR (1) moving average MU ... 83
Figure 60 MU one-step-ahead densities (x_{t-1} = unconditional mean) ... 84
Figure 61 MU one-step-ahead densities (conditional mean for x_{t-1} = -40%...40%) ... 84
Figure 62 MU: conditional variance functions ... 85
Figure 63 Projected conditional volatility and residuals AR (1) moving average NHY ... 87
Figure 64 NHY one-step-ahead densities (x_{t-1} = unconditional mean) ... 88
Figure 65 NHY one-step-ahead densities (conditional mean for xt-1 = -40%...40%) ... 88
Figure 66 NHY: conditional variance functions ... 89
Figure 67 Projected conditional volatility and residuals AR (1) moving average TOM ... 92
Figure 68 TOM one-step-ahead densities (x_{t-1} = unconditional mean) ... 92
Figure 69 TOM one-step-ahead densities (conditional mean for x_{t-1} = -40%...40%) ... 93
Figure 70 TOM: conditional variance functions ... 93
Figure 71 Projected conditional volatility and residuals AR (1) moving average Carbon 96
Figure 72 Carbon one-step-ahead densities (x_{t-1} = unconditional mean) ... 97
Figure 73 Carbon one-step-ahead densities (conditional mean for x_{t-1} = -40%...40%) ... 97
Figure 74 Carbon: conditional variance functions ... 98
Figure 75 Projected conditional volatility and residuals AR (1) moving average for Brent oil ... 100
Figure 76 Brent oil one-step-ahead densities (x_{t-1} = unconditional mean) ... 101
*Figure 77 Brent oil one-step-ahead densities (conditional mean for xt-1 = -40%...40%)*101
Figure 78 Brent oil: conditional variance functions ... 102
Figure 79 Projected conditional volatility and residuals AR (1) moving average Salmon ... 104
Figure 80 Salmon one-step-ahead densities (x_{t-1} = unconditional mean) ... 105
Figure 81 Salmon one-step-ahead densities (conditional mean for x_{t-1} = -40%...40%) .. 105
Figure 82 Salmon: conditional variance functions ... 106
Figure 83 Mean Impulse-Response Dynamics ... 114
Figure 84 Variance Impulse-Response Dynamics ... 122

Figure 85 Profile Bundles for Persistence 132

List of Tables

Table 1 Returns Characteristics from the DJIA Index 9
Table 2 Returns Characteristics from the FTSE Index 11
Table 3 Returns Characteristics from the S&P 100 Index 13
Table 4 Returns Characteristics from the S&P 500 Index 15
Table 5 Returns Characteristics from the OSEBX Index 17
Table 6 Returns Characteristics from the OBX Index 19
Table 7 Returns Characteristics from the OSEAX Index 21
Table 8 Returns Characteristics from MSFT 23
Table 9 Returns Characteristics from MU 25
Table 10 Returns Characteristics from NHY 27
Table 11 Returns Characteristics from TOM 29
Table 12 Returns Characteristics from Carbon 31
Table 13 Returns Characteristics from Brent oil 33
Table 14 Returns Characteristics from Salmon 35
Table 15 Restrictions Implied by Settings of the Tuning Parameters (Gallant and Tauchen 1990) 44
Table 16 Univariate SNP estimation: Optimized Likelihood and Model Selection Criteria (Gallant and Tauchen 1990) 45
Table 17 Characteristics of the statistical SNP Model Residuals for the DJIA Index 46
Table 18 Statistical SNP Model Parameters for the DJIA Index 47
Table 19 Characteristics of the statistical SNP Model Residuals for the FTSE Index 50
Table 20 Statistical SNP Model Parameters for the FTSE Index 51
Table 21 Characteristics of the statistical SNP Model Residuals for the S&P 100 Index . 55
Table 22 Statistical SNP Model Parameters for the S&P 100 Index 56
Table 23 Characteristics of the statistical SNP Model Residuals for the S&P 500 Index . 60
Table 24 Statistical SNP Model Parameters for the S&P 500 Index 60
Table 25 Characteristics of the statistical SNP Model Residuals for the OSEBX Index 64
Table 26 Statistical SNP Model Parameters for the OSEBX Index 65
Table 27 Characteristics of the statistical SNP Model residuals for the OBX Index 68
Table 28 Statistical SNP Model Parameters for the OBX Index 69
Table 29 Characteristics of the statistics SNP Model Residuals for the OSEAX Index 72
Table 30 Statistical SNP Model Parameters for the OSEAX Index 73
Table 31 Characteristics of the statistical SNP Model Residuals for MSFT 76
Table 32 Statistical SNP Model Parameters for the MSFT Share 77
Table 33 Characteristics of the statistical SNP Model Residuals for MU 81
Table 34 Statistical SNP Model Parameters for the MU Share 82
Table 35 Characteristics of the statistical SNP Model Residuals for NHY 85
Table 36 Statistical SNP Model Parameters for the NHY Share 86
Table 37 Characteristics of the statistical SNP Model Residuals for TOM 90
Table 38 Statistical SNP Model Parameters for TOM 90
Table 39 Characteristics of the statistical SNP Model Residuals for Carbon 94
Table 40 Statistical SNP Model Parameters for Carbon 95
Table 41 Characteristics of the statistical SNP Model Residuals for Brent oil 98
Table 42 Statistical SNP Model Parameters for Brent oil 99
Table 43 Characteristics of the statistical SNP Model Residuals for Salmon 102
Table 44 Statistical SNP Model Parameters for Salmon 103
Table 45 Variance Impulse-Response Dynamics showing the leverage effect 123
Table 46 Measures of Persistence 125

1.0 Introduction

The uncertainty associated with the price of the underlying asset is the key determinant when pricing an option. Volatility is a measure of risk associated with changes in the value of a financial instrument. Therefore, knowledge about the dynamics of volatility is of great interest and relevant to several financial applications, such as pricing of hedging instruments and fund management. This knowledge is a key input to the general understanding of market risk. We investigate the volatility dynamics by studying financial time series, which are widely acknowledged to be nonlinear processes. The series are likely to have non-normal error distributions, and the use of higher order moments is, therefore, decisive in terms of adequately describing the series. To investigate these higher order moments, features like ARCH/GARCH (Engle 1982, Bollerslev 1986), leptokurtosis (Clark 1973) and asymmetries (Nelson 1991) are of interest. Black (1976) highlighted the dependency of higher moments by finding evidence of a negative correlation between return and volatility. This has proved to be central to later research.

Impulse-response functions have been broadly used to study the dynamics of a linear process. A natural definition of the nonlinear impulse response is the net effect of the impulse, which we obtain by comparing the profile for the impulse to the baseline profile (Gallant, Rossi et al. 1993). Gallant, Rossi et al. (1993) developed an approach for analyzing the multi-step-ahead dynamics of nonlinear time series, using a nonparametric estimate of its one-step-ahead conditional density. They studied the persistence of asymmetry for the S&P composite price index and found evidence showing a heavily damped effect within six to ten days after a shock. Tauchen, Zhang et al. (1996) came to the same conclusion while examining four different individual stocks on the NYSE. They claimed that the asymmetry in volatility had a low persistence of maximum four days. The two analyses were based on sample periods from 1982-1987 and 1982-1989 respectively. Another study conducted by Figlewski and Wang (2000) examined the individual stocks in the S&P 100 Index and the index itself. They found that the degree of asymmetry in volatility was higher for indices than for individual shares. We expect to find similar features of volatility dynamics; still we are aware that our samples, which include additional periods of substantial price fluctuations, might give different results.

The framework for impulse-response analysis developed by Gallant, Rossi et al. (1993) will be of great importance to our thesis. We are going to study the impulse-response dynamics in a *uni*variate case for the time series. In this setting, forecasts depend only on present and past values of the single time series. The objective is to study the persistence properties of stochastic volatility, as well as to examine the asymmetric property of the conditional variance function. We measure the persistence by calculating the half-life of volatility. Engle/Patton (2000) did this in a similar study and measured the volatility half-life of the DJIA. Based on the broad selection of financial assets, we want to extract the different characteristics of stock indices, individual stocks, and commodity indices. By doing so, we hope to contribute by giving more empirical insight to this field of research.

The remainder of the thesis is structured as follows. Section 2.0 presents the descriptive statistics for each of the studied time series. Theoretical aspects are described in section 3.0. Section 4.0 outlines the definition of nonlinear impulse-response functions. Section 5.0 explains the method of semi-nonparametric estimation of univariate conditional densities for each of the time series. The empirical results and discussions are presented in section 6.0. Section 7.0 concludes the thesis.

The thesis is structured in a way so that the reader can interpret each of the time series separately.

2.0 Descriptive Statistics

We have considered long data sets, which provide sufficient information about the conditional and unconditional distribution of returns, as well as giving a broad range in the composition of volatility. The raw data consist of daily returns on seven different stock indices; Dow Jones industrial average (DJIA), FTSE 100 Index (FTSE), S&P 100 Index (OEX), S&P 500 Index (GSPC), Oslo Stock Exchange Benchmark Index (OSEBX), Oslo Stock Exchange Index (OBX) and the Oslo Stock Exchange All Share Index (OSEAX), four shares; Microsoft Corporation (MSFT), Micron Technology, Inc. (MU), Norsk Hydro ASA (NHY) and Tomra Systems ASA (TOM) and three commodity indices; the ICE Carbon Forward Contract, Brent Oil Future Contracts and Salmon Forward Contracts.
All data regarding the stock indices, as well Micron Technology, Inc. and Microsoft Corporation, are obtained from the stock database obtained by Yahoo! Finance (2016). Prices for Oslo Stock Exchange Index (OBX), Oslo Stock Exchange All Share Index (OSEAX), Norsk Hydro ASA and Tomra Systems ASA are extracted from the stock database provided by Netfonds Bank (2016). The Intercontinental Exchange (2016) and Fish Pool ASA (2016) provide the prices for Brent oil, carbon and salmon future/forward contracts.

2.1 The physical marketplace for commodities

The Intercontinental Exchange, Inc. (ICE) was founded in 2000, and it was introduced as an electronic trading platform that brought transparency and accessibility to the OTC energy markets. Other markets were later added and today it consists of regulated exchanges and clearing houses for financial and commodity markets. The exchange markets are diverse and provide trading and clearing of international derivatives such as futures and options on interest risk, commodities, indexes, and FX, as well as equities and equity options. The company operates exchanges such as The ICE Commodity Exchange, which is the market for trading energy and metals commodities, and The ICE Derivatives Markets, an electronic order book that mainly trades forwards/futures and options. The usage of these markets often consist of risk management activities (Intercontinental Exchange 2016).

2.1.1 Oil

The crude oil market is the largest commodity market in the world. The world benchmark price for purchases of oil is the Brent Crude, which is extracted from the North Sea. We have applied the Brent oil prices to our analysis.
The Brent oil futures contracts are standardized, exchange-traded contracts, where the buyer of the contract agrees to take delivery from the seller, a given quantity of crude oil (one contract equals 1,000 barrels quotes in U.S. dollars) at a predetermined price, on a future delivery date. The Brent oil futures contracts are traded at the ICE Futures Europe and work as cash-settled contracts. The term “front month contract” refers to the contract month with an expiration date closest to the current date, typically in the same month. This means that the front month contracts have the shortest duration of the contracts that are available in the futures market. They are also the ICE markets underlying assets for active option trading, which makes it interesting in terms of pricing mechanisms and risk management activities (Intercontinental Exchange 2016).

2.1.2 Carbon

The carbon market originates from the trading of carbon emission allowances to help nations and companies limit their carbon dioxide (CO_2) emissions. It is a way of cutting down the greenhouse gasses caused by the polluters. Exceeding the allowance of carbon emission means that the company has to purchase further permits to cover this. If the limit is never reached, the unused permits may be sold in the carbon market.
The carbon products are mainly traded as forward/futures and options, and the market is typically used for risk management activities. The front December forward contracts act as the underlying asset for all-active derivative trading and will be utilized in this analysis. This thesis is based upon contracts traded at the ICE Futures Europe (Intercontinental Exchange 2016).

2.1.3 Salmon

The price of salmon is volatile, and it is, therefore, a great source of risk to both the producing company and to the consumer. Forward- and future contracts aims to protect against the risk of price fluctuations. The forward contracts are agreements to buy/sell a given quantity of a commodity (salmon) at some particular time in the future for a

predetermined price, determined from the daily closing prices of an index (the forward price). These contracts are common derivative assets in today's commodity markets and provide a more realistic indication of future salmon prices. They are widely traded for risk management purposes, such as pricing of hedging instruments and fund management.
This thesis is based upon Salmon forward contracts that are traded at Fish Pool. Fish Pool ASA is an international, regulated market for the trading of financial salmon contracts, and its main shareholder is Oslo Stock Exchange ASA. Physical trading of salmon is not offered in this marketplace. The contracts are cleared through Nasdaq OMX (Fish Pool ASA 2016).

The return (logarithmic) of a forward/future contract is computed using one-month contracts. As an example, we calculate the return between the prices of a January contract within the month. When January ends, we find the return of the first trading day in February, by taking the difference between the price of the February contract and the price at the first trading day in February.

2.2 Stationarity

All traded assets have a price. In order to use the extended GARCH model in the SNP model properly, we need stationary time series. The price of an asset is non-stationary in the way that it shows a positive or negative trend over time.
In order to make the time series stationary, we compute the return (logarithmic) as

$$y_t = 100 * [ln(P_t) - ln(P_{t-1})]$$

As non-stationary series moves in a large variety, stationary series moves around its mean. A stationary series has the property of being mean reverting because it moves to its mean return in the long run. Stationary processes also have the property that the variance and autocorrelation structure do not change over time. If the price moves based on an event, it keeps going from this new level in the following time (autocorrelation). This is not the case with stationary series. It will have a jump in the return and then move back to its mean; the autocorrelation seems to decline within few days. This suggests that a stationary series only has a transient effect of stochastic shocks, which is an important property for statistical analysis (Verbeek 2012).

To find out if the time series are stationary, we use the Augmented Dickey-Fuller test (ADF) (Dickey and Fuller 1979) and the Kwiatkowski, Phillips, Schmidt, and Shin test (KPSS) (Kwiatowski, Phillips et al. 1992). Both tests are conducted in EViews.
Under the null hypothesis of a unit root, the ADF statistic does not follow the typical Student's *t-distribution*, and it derives asymptotic results and simulates critical values for various test and sample sizes (Dickey and Fuller 1979). Rejection of the null hypothesis at some level of confidence means that the time series have no unit root present and that the series are stationary.
The KPSS test differs from the ADF test in that the series is assumed stationary under the null hypothesis. "The series is expressed as the sum of a deterministic trend, a random walk, and a stationary error and the test is the LM test of the hypothesis that the random walk has zero variance" (Kwiatowski, Phillips et al. 1992).

2.3 Autocorrelation

Before applying the GARCH/SNP model to a time series, we need to check for autocorrelation in the raw series. To estimate autocorrelation we use the Ljung Box test statistic (Q) (Ljung and Box 1978). If autocorrelation is present, it is a sign of dependency in the data. This relationship between lags makes it possible to build a model that incorporates this phenomenon and describes the innovations in a good manner. A good measure of a model describing the time series is whether the residuals reject the null hypothesis of no autocorrelation or not. If the residuals of the model show no autocorrelation, this tells us that the model has managed to incorporate the autocorrelation of the raw data, and the residuals are approximately white noise.
We use EViews to check for autocorrelation of raw data and residuals. The test is computed for both normal (Q) and squared (Q^2) data. The Ljung-Box test statistic is

$$Q_K = T(T+2)\sum_{k=1}^{K}\frac{1}{T-k}r_k^2$$

where r_k is the estimated autocorrelation coefficients of the residuals. K is the number of lags we want to investigate; in this case, we use 12 lags for all the time series. The statistic Q_K is approximately Chi Squared distributed with K-p-q degrees of freedom for an ARMA

(p,q) process under the null hypothesis that the ARMA is correctly specified (Verbeek 2012).

We use the 12th lag of the Q-test for all the time series.

2.4 BDS Test for Independence

The BDS test is a non-parametric method for testing for serial dependence and nonlinear structure in a time series. The test examines a time series by its correlation integral, considering repeated patterns in the data. The correlation integral, given n observations of a series X, can be estimated by

$$C_{m,n}(\epsilon) = \frac{2}{n - m + 1\,(n - m)} \sum_{s=1}^{n-m+1} \sum_{t=s+1}^{n-m+1} \prod_{j=0}^{m-1} I_\epsilon\,(X_{s+j}, X_{t+j})$$

where I_ε is the indicator function

$$I_\epsilon(x, y) = \begin{cases} 1 & if\ |x - y| \leq \in \\ 0 & otherwise. \end{cases}$$

The test can be applied to the estimated residuals of fitted models. It detects nonlinear structures and serial dependence in a time series, by testing the null hypothesis that the sample comes from a generating process which is independent and identically distributed (IID). There is no alternative hypothesis specified.
The estimates of $C_{m,n}(\epsilon)$ is used to generate a test statistic for independence:

$$b_{m,n}(\in) = C_{m,n}(\in) - C_{1,n-m+1}(\in)^m$$

This statistic should be close to zero if we assume no dependence in the sample.
The standard deviation can be estimated consistently. The “goodness of fit” of an estimated model can be measured by checking if the residuals are IID. If the null hypothesis is rejected, it suggests that there is a remaining structure in the data which can include nonlinearity and nonstationarity. If the null hypothesis is rejected when testing the residuals, the model is misspecified (Brock, Dechert et al. 1996).

We use EViews to compute the BDS test, with epsilon (ϵ) value of 1 and maximum correlation dimension of *5*. The ϵ is calculated based on the standard deviation of the series.

2.5 Value at Risk (VaR)

Value at risk (VaR) is a risk measure applied to time series consisting of financial data. JPMorgan developed VaR to capture the total risk of a portfolio, and it is in the form of stating that we will not lose more than V in time T at X percent certainty. V is the VaR of the investigated security, T is the time horizon and the X describes the confidence level. VaR is frequently used by companies and regulators in the financial industry to measure the amount of assets needed to cover possible future losses (Hull 2015).

2.5.1 Conditional Value at Risk (CVaR)

Conditional value at risk measures the average loss in the tail of the loss distribution. Financial time series often has fatter tails compared to a normal distribution. The CVaR is often higher than the VaR, supporting this phenomenon. The tail, in this case, is the excess beyond the confidence band of the VaR. It is a good technique to ensure that we do not overlook potentially massive losses (Hull 2015).

2.6 *Description of Data*

2.6.1 Dow Jones Industrial Average (DJIA)

The daily return (logarithmic) of the DJIA data set from the beginning of 1987 to the end of 2015 is y_t, t= 1, . . . , 7299. Features of the DJIA Index are reported in ***Table 1***. The mean is positive and the standard deviation is 1.15. The index reports a maximum (minimum) value of 10.50 (-25.63), which is relatively high (low). The kurtosis is high, indicating that the data are heavy-tailed relative to a normal distribution. The table reports *excess* kurtosis, meaning that positive kurtosis indicates leptokurtosis features. The Cramer-von-Mises and Quantile normal test statistic support non-normal return distributions. Serial correlation in the mean equation is strong and the Ljung-Box Q-statistic is significant. The Ljung-Box test statistic for squared returns (Q^2) and the ARCH statistic show that volatility clustering is significantly present.

Both the KPSS statistic and the ADF test support stationary series. The BDS test statistic reports highly significant dependence in the data. The price and return series are plotted in ***Figure 1*** and the return series, together with a Kernel distribution to the left, is shown in ***Figure 2***. From the price plot, we clearly see that the series is non-stationary, unlike the price change (log-returns) which is stationary. From the return plot, the series show some volatility clustering, as illustrated by higher volatility when prices are falling. The return level seems to change randomly. The fact that the skewness is different from zero supports the feature of non-normal distribution.

Table 1 *Returns Characteristics from the DJIA Index*

Statistics for DJI Index

Mean / Mode	Median Std.dev.	Maximum / Minimum	Moment Kurt/Skew	Quantile Kurt/Skew	Quantile Normal	Cramer-von-Mises	Serial dependence Q(12)	$Q^2(12)$
0.03039	0.05293	10.5083	41.64478	0.27054	22.2676	22.33867	57.2580	692.670
0.00000	1.14625	-25.6320	-1.67450	0.00260	{0.0000}	{0.0000}	{0.0000}	{0.0000}
BDS-Z-statistic (Ɛ = 1)				**KPSS (Stationary)**		**Augmented**	**ARCH**	**VaR 2.5% /**
m=2	**m=3**	**m=4**	**m=5**	**Intercept**	**Trend**	**DF-test**	**(12)**	**CVaR 2.5%**
14.1290	20.1089	24.4952	28.8058	0.04868	-0.00001	-65.3260	438.294	-2.2322
{0.0000}	{0.0000}	{0.0000}	{0.0000}	{0.0697}	{0.4312}	{0.0000}	{0.0000}	-3.4676

The figures in braces are P-values for statistical significance

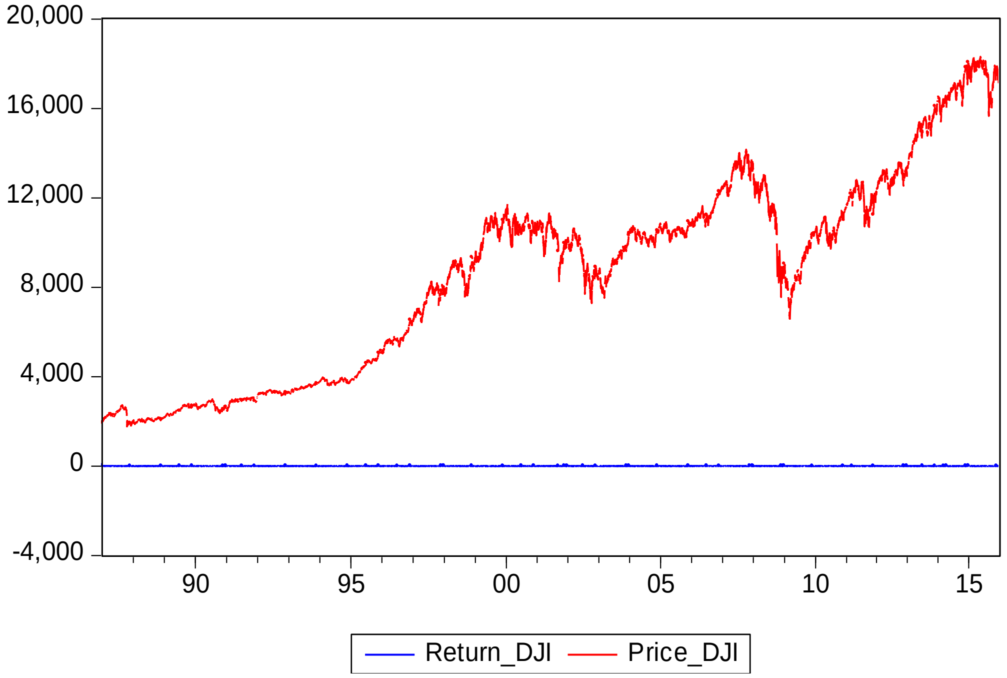

Figure 1 *DJIA Index Price and Returns*

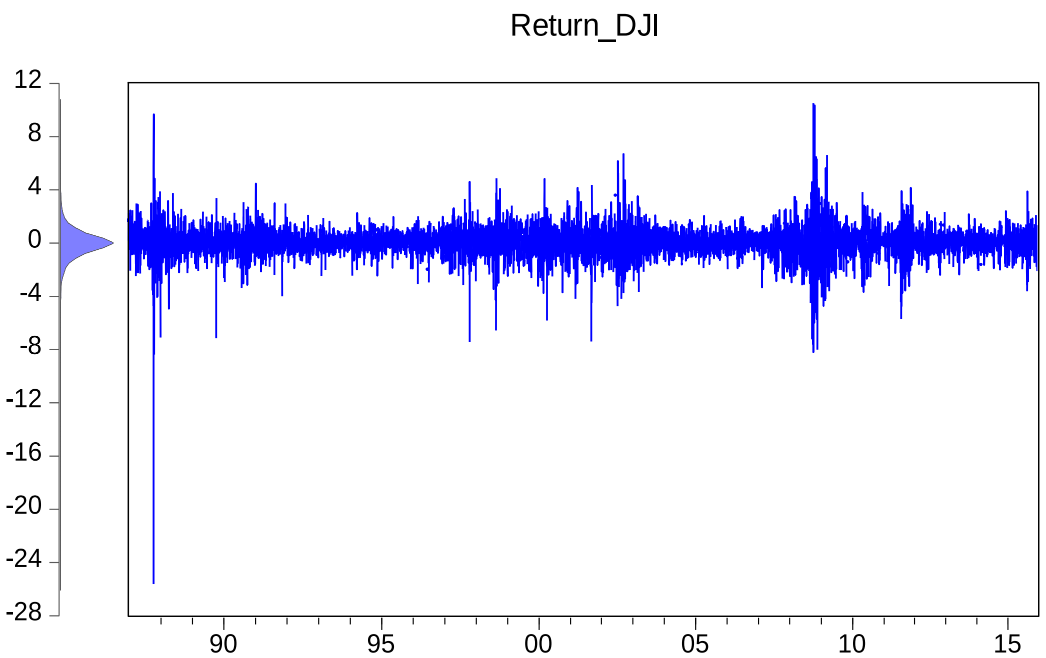

Figure 2 *DJIA Index Returns*

2.6.2 FTSE 100 Index (FTSE)

The daily return (logarithmic) of the FTSE data set from the beginning of 1987 to the end of 2015 is y_t, t= 1, . . . , 7551. Features of the FTSE 100 Index are reported in ***Table 2.*** The mean is positive and the standard deviation is 1.11. The index reports a maximum (minimum) value of 9.38 (-13.03), which is relatively high (low). The kurtosis is high, indicating that the data are heavy-tailed relative to a normal distribution. The table reports *excess* kurtosis, meaning that positive kurtosis indicates leptokurtosis features. The Cramer-von-Mises and Quantile normal test statistic support non-normal return distributions. Serial correlation in the mean equation is strong and the Ljung-Box Q-statistic is significant. The Ljung-Box test statistic for squared returns (Q^2) and the ARCH statistic show that volatility clustering is significantly present. Both the KPSS statistic and the ADF test support stationary series. The BDS test statistic reports highly significant dependence in the data. The price and return series are plotted in ***Figure 3*** and the return series, together with a Kernel distribution to the left, is shown in ***Figure 4.*** From the price plot, we clearly see that the series is non-stationary, unlike the price change (log-returns) which is stationary. From the return plots, the series show some volatility clustering, as shown by higher volatility when prices are falling. The return level seems to change randomly. The fact that the skewness is different from zero supports the feature of non-normal distribution.

Table 2 *Returns Characteristics from the FTSE Index*

Statistics for FTSE 100 Index

Mean /	Median	Maximum /	Moment	Quantile	Quantile	Cramer-	Serial dependence	
Mode	Std.dev.	Minimum	Kurt/Skew	Kurt/Skew	Normal	von-Mises	Q(12)	Q^2(12)
0.01739	0.00998	9.3842	10.64884	0.17434	13.0371	15.23015	73.1870	4365.600
0.00000	1.11340	-13.0286	-0.48944	0.05254	{0.0015}	{0.0000}	{0.0040}	{0.0000}
BDS-Z-statistic (Ɛ = 1)				KPSS (Stationary)		Augmented	ARCH	VaR 2.5% /
m=2	m=3	m=4	m=5	Intercept	Trend	DF-test	(12)	CVaR 2.5%
16.9418	22.7004	27.3308	31.4319	0.03868	-0.00001	-40.4579	1578.519	-2.2994
{0.0000}	{0.0000}	{0.0000}	{0.0000}	{0.1312}	{0.3374}	{0.0000}	{0.0000}	-3.3893

The figures in braces are P-values for statistical significance

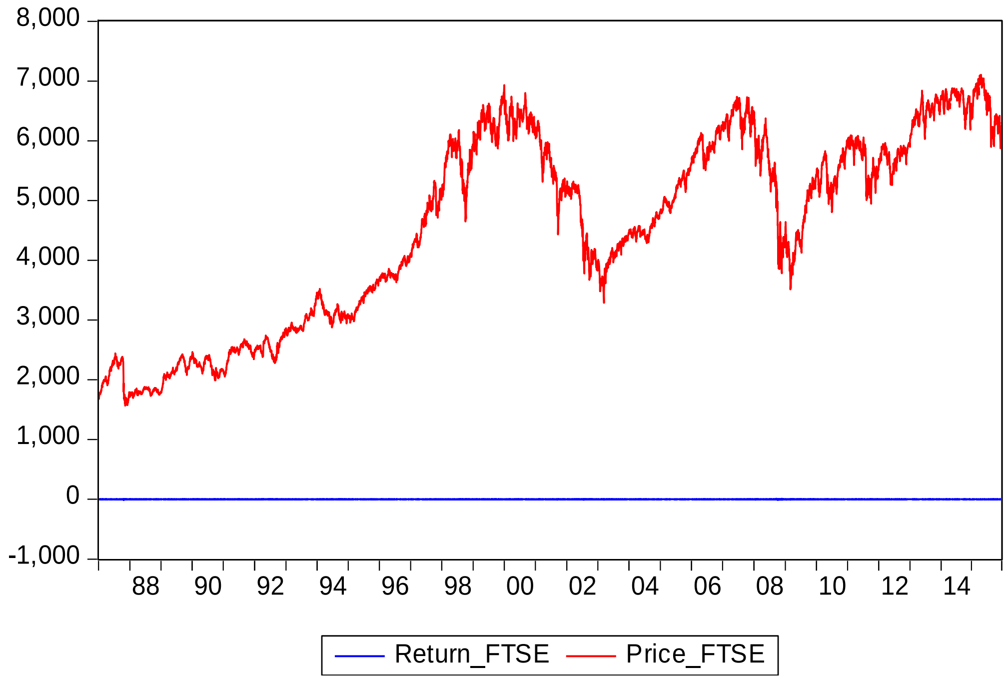

Figure 3 *FTSE Index Price and Returns*

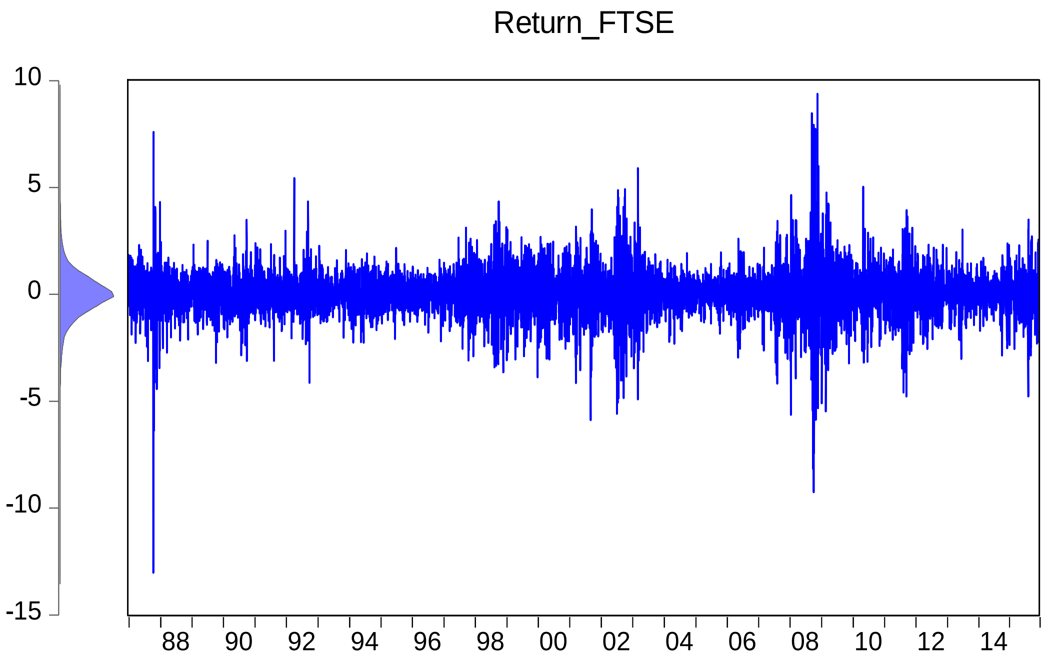

Figure 4 *FTSE Index Returns*

2.6.3 S&P 100 Index (OEX)

The daily return (logarithmic) of the S&P 100 data set from the beginning of 1987 to the end of 2015 is y_t, t= 1, . . . , 7311. Features of the S&P 100 Index are reported in ***Table 3.*** The mean is positive and the standard deviation is 1.19. The index reports a maximum (minimum) value of 10.65 (-23.78), which is relatively high (low). The kurtosis is high, indicating that the data are heavy-tailed relative to a normal distribution. The table reports *excess* kurtosis, meaning that positive kurtosis indicates leptokurtosis features. The Cramer-von-Mises and Quantile normal test statistic support non-normal return distributions. Serial correlation in the mean equation is strong and the Ljung-Box Q-statistic is significant. The Ljung-Box test statistic for squared returns (Q^2) and the ARCH statistic show that volatility clustering is significantly present. Both the KPSS statistic and the ADF test support stationary series. The BDS test statistic reports highly significant dependence in the data. The price and return series are plotted in ***Figure 5*** and the return series, together with a Kernel distribution to the left, is shown in ***Figure 6***. From the price plot, we clearly see that the series is non-stationary, unlike the price change (log-returns) which is stationary. From the return plots, the series show some volatility clustering, as shown by higher volatility when prices are falling. The return level seems to change randomly. The fact that the skewness is different from zero supports the feature of non-normal distribution.

Table 3 *Returns Characteristics from the S&P 100 Index*

Statistics for S&P 100 Index

Mean / Mode	Median Std.dev.	Maximum / Minimum	Moment Kurt/Skew	Quantile Kurt/Skew	Quantile Normal	Cramer-von-Mises	Serial dependence Q(12)	Q^2(12)
0.02825	0.05627	10.6551	28.71837	0.30141	27.8945	22.83270	69.4010	1117.200
0.00000	1.19334	-23.7769	-1.27747	-0.01343	{0.0000}	{0.0000}	{0.0000}	{0.0000}
BDS-Z-statistic (Ɛ = 1)				KPSS (Stationary)		Augmented	ARCH	VaR 2.5% /
m=2	m=3	m=4	m=5	Intercept	Trend	DF-test	(12)	CVaR 2.5%
15.4415	22.4543	27.3440	32.5046	0.04542	0.00000	-65.8377	601.120	-2.3391
{0.0000}	{0.0000}	{0.0000}	{0.0000}	{0.1037}	{0.4774}	{0.0000}	{0.0000}	-3.6202

The figures in braces are P-values for statistical significance

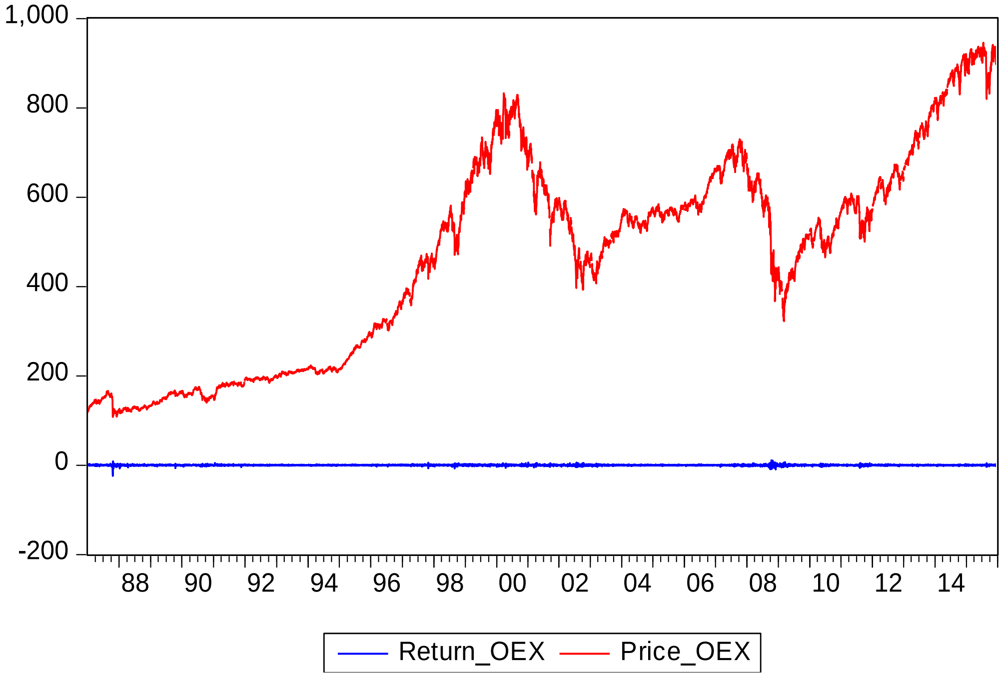

Figure 5 *S&P 100 Price and Returns*

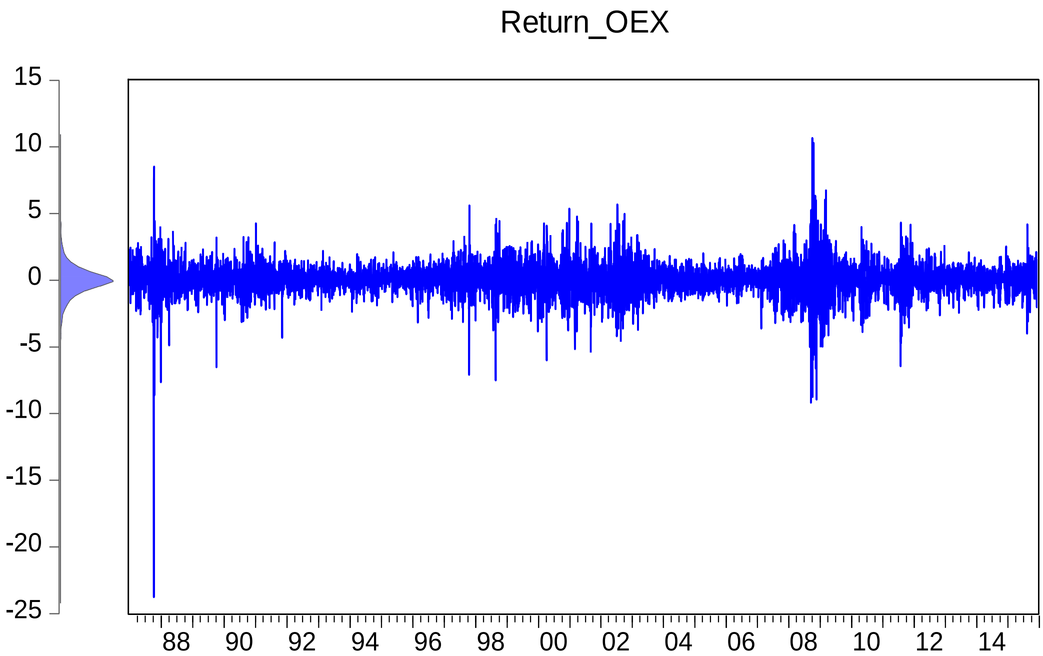

Figure 6 *S&P 100 Returns*

2.6.4 S&P 500 Index (GSPC)

The daily return (logarithmic) of the GSPC data set from the beginning of 1987 to the end of 2015 is y_t, t= 1, . . . , 7311. Features of the GSPC Index are reported in ***Table 4***. The mean is positive and the standard deviation is 1.17. The index reports a maximum (minimum) value of 10.96 (-22.90), which is relatively high (low). The kurtosis is high, indicating that the data are heavy-tailed relative to a normal distribution. The table reports *excess* kurtosis, meaning that positive kurtosis indicates leptokurtosis features. The Cramer-von-Mises and Quantile normal test statistic support non-normal return distributions. Serial correlation in the mean equation is strong and the Ljung-Box Q-statistic is significant. The Ljung-Box test statistic for squared returns (Q^2) and the ARCH statistic show that volatility clustering is significantly present. Both the KPSS statistic and the ADF test support stationary series. The BDS test statistic reports highly significant dependence in the data. The price and return series are plotted in ***Figure 7*** and the return series, together with a Kernel distribution to the left, is shown in ***Figure 8***. From the price plots, we clearly see that this series is non-stationary, unlike the price change (log-returns) which is stationary. From the return plots, the series show some volatility clustering, as shown by higher volatility when prices are falling. The return level seems to change randomly. The fact that the skewness is different from zero supports the feature of non-normal distribution.

Table 4 *Returns Characteristics from the S&P 500 Index*

Statistics for S&P 500 Index

Mean / Mode	Median Std.dev.	Maximum / Minimum	Moment Kurt/Skew	Quantile Kurt/Skew	Quantile Normal	Cramer-von-Mises	Serial dependence Q(12)	$Q^2(12)$
0.02918	0.05852	10.9572	27.68730	0.31743	30.8648	23.51701	58.4880	1281.900
0.00000	1.17322	-22.8997	-1.27273	-0.01180	{0.0000}	{0.0000}	{0.0000}	{0.0000}
BDS-Z-statistic (Ɛ = 1)				**KPSS (Stationary)**		**Augmented**	**ARCH**	**VaR 2.5% /**
m=2	m=3	m=4	m=5	Intercept	Trend	DF-test	(12)	CVaR 2.5%
14.6550	21.9052	26.7649	31.7154	0.04406	0.00000	-65.1543	657.633	-2.3390
{0.0000}	{0.0000}	{0.0000}	{0.0000}	{0.1084}	{0.5312}	{0.0000}	{0.0000}	-3.5885

The figures in braces are P-values for statistical significance

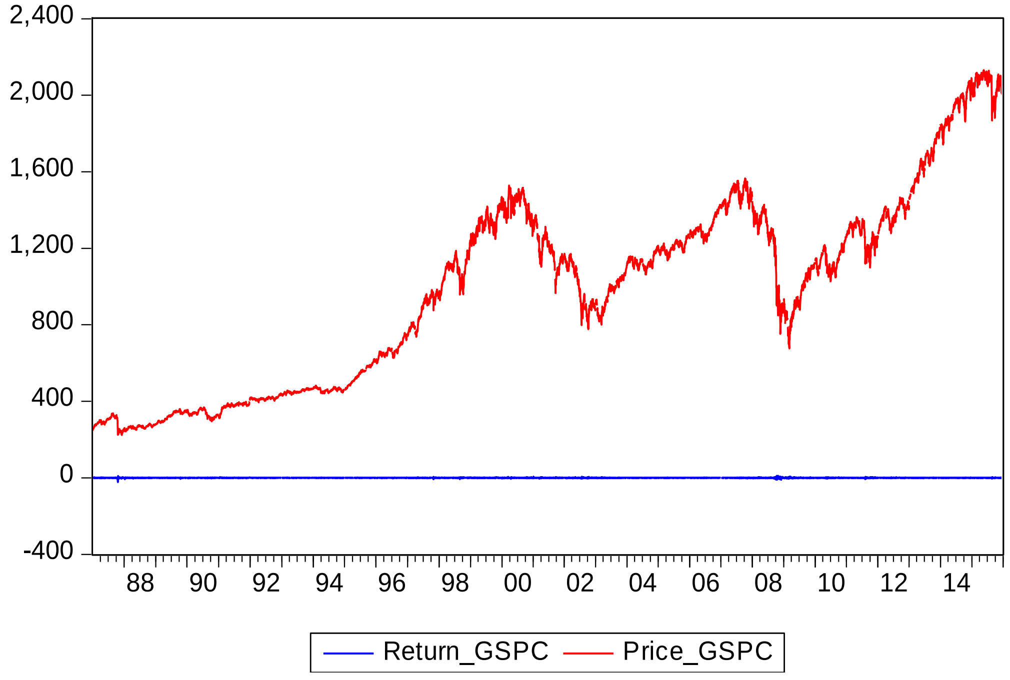

Figure 7 *S&P 500 Price and Returns*

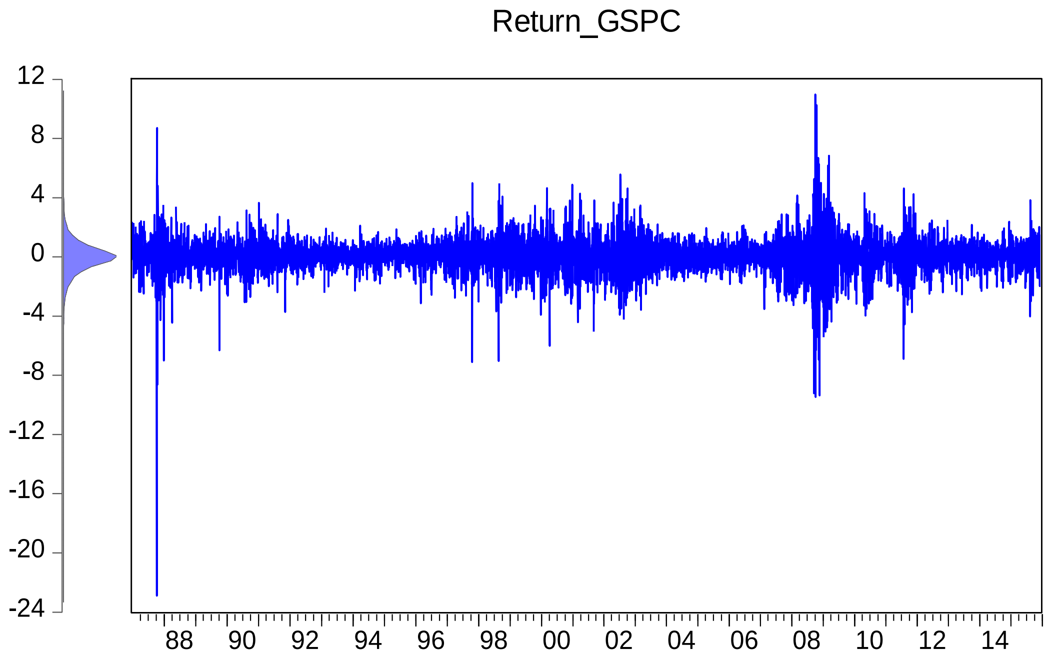

Figure 8 *S&P 500 Returns*

2.6.5 Oslo Stock Exchange Benchmark Index (OSEBX)

The daily return (logarithmic) of the OSEBX Index data set from the beginning of 1987 to the end of 2015 is y_t, t= 1, . . . , 7277. Features of the OSEBX Index are reported in ***Table 5.*** The mean is positive and the standard deviation is 1.37. The index reports a maximum (minimum) value of 10.14 (-10.74), which is relatively high (low). The kurtosis is relatively high, indicating that the data are heavy-tailed relative to a normal distribution. The table reports *excess* kurtosis, meaning that positive kurtosis indicates leptokurtosis features. The Cramer-von-Mises and Quantile normal test statistic support non-normal return distributions. Serial correlation in the mean equation is strong and the Ljung-Box Q-statistic is significant. The Ljung-Box test statistic for squared returns (Q^2) and the ARCH statistic show that volatility clustering is significantly present. Both the KPSS statistic and the ADF test support stationary series. The BDS test statistic reports highly significant dependence in the data. The price and return series are plotted in ***Figure 9*** and the return series, together with a Kernel distribution to the left, is shown in ***Figure 10***. From the price plots, we clearly see that this series is non-stationary, unlike the price change (log-returns) which is stationary. From the return plots, the series show some volatility clustering, as shown by higher volatility when prices are falling. The return level seems to change randomly. The fact that the skewness is different from zero supports the feature of non-normal distribution.

Table 5 *Returns Characteristics from the OSEBX Index*

Statistics for OSEBX Index

Mean / Mode	Median Std.dev.	Maximum / Minimum	Moment Kurt/Skew	Quantile Kurt/Skew	Quantile Normal	Cramer-von-Mises	Serial dependence Q(12)	$Q^2(12)$
0.03672	0.08932	10.1387	7.50623	0.19271	12.1261	17.94628	59.8550	6515.900
0.00000	1.37085	-10.7379	-0.61930	-0.02671	{0.0023}	{0.0000}	{0.0000}	{0.0000}
BDS-Z-statistic (Ɛ = 1)				KPSS (Stationary)		Augmented	ARCH	VaR 2.5% /
m=2	m=3	m=4	m=5	Intercept	Trend	DF-test	(12)	CVaR 2.5%
21.8789	29.1330	33.9507	38.3601	0.04573	0.00000	-79.6684	1673.268	-2.8626
{0.0000}	{0.0000}	{0.0000}	{0.0000}	{0.1549}	{0.7464}	{0.0001}	{0.0000}	-4.4471

The figures in braces are P-values for statistical significance

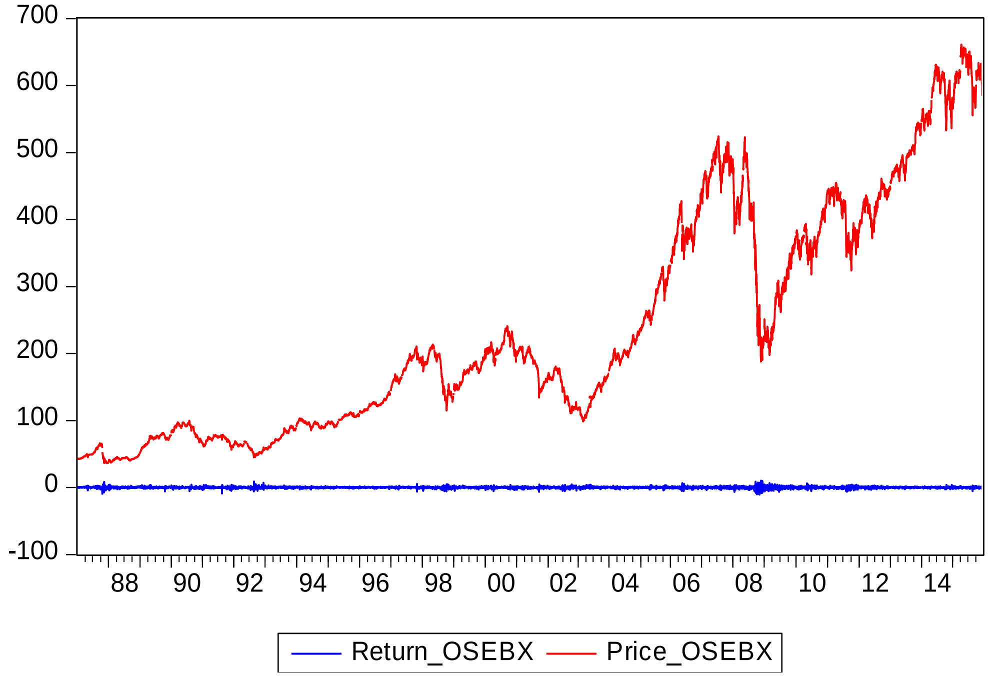

Figure 9 *OSEBX Index Price and Returns*

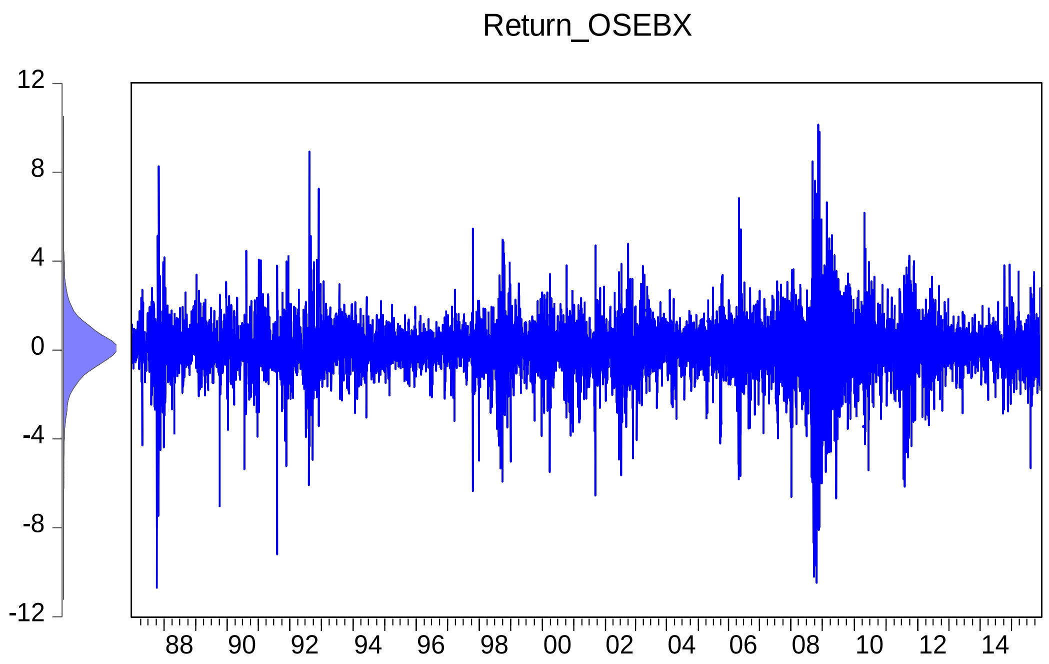

Figure 10 *OSEBX Returns*

2.6.6 Oslo Stock Exchange Index (OBX)

The daily return (logarithmic) of the OBX Index data set from the beginning of 1998 to the end of 2015 is y_t, t= 1, . . . , 4512. Features of the OBX Index are reported in ***Table 6***.The mean is positive and the standard deviation is 1.58. The index reports a maximum (minimum) value of 11.02 (-11.27), which is relatively high (low). The kurtosis is relatively high, indicating that the data are heavy-tailed relative to a normal distribution. The table reports *excess* kurtosis, meaning that positive kurtosis indicates leptokurtosis features. The Cramer-von-Mises and Quantile normal test statistic support non-normal return distributions. Serial correlation in the mean equation is strong and the Ljung-Box Q-statistic is significant. The Ljung-Box test statistic for squared returns (Q^2) and the ARCH statistic show that volatility clustering is significantly present. Both the KPSS statistic and the ADF test support stationary series. The BDS test statistic reports highly significant dependence in the data. The price and return series are plotted in ***Figure 11*** and the return series, together with a Kernel distribution to the left, is shown in ***Figure 12***. From the price plot, we clearly see that the series is non-stationary, unlike the price change (log-returns) which is stationary. From the return plots, the series show some volatility clustering, as shown by higher volatility when prices are falling. The return level seems to change randomly. The fact that the skewness is different from zero supports the feature of non-normal distribution.

Table 6 *Returns Characteristics from the OBX Index*

Statistics for OBX-index

Mean /	Median	Maximum /	Moment	Quantile	Quantile	Cramer-	Serial dependence	
Mode	Std.dev.	Minimum	Kurt/Skew	Kurt/Skew	Normal	von-Mises	Q(12)	Q^2(12)
0.03072	0.09264	11.0198	6.06763	0.17319	6.3228	9.56415	28.6540	5626.400
0.72728	1.58331	-11.2730	-0.51277	-0.03015	{0.0424}	{0.0000}	{0.0040}	{0.0000}
BDS-Z-statistic (Ɛ = 1)				KPSS (Stationary)		Augmented	ARCH	VaR 2.5% /
m=2	m=3	m=4	m=5	Intercept	Trend	DF-test	(12)	CVaR 2.5%
17.3060	23.1739	27.3544	31.0860	0.02051	0.00000	-66.8920	1343.320	-3.3708
{0.0000}	{0.0000}	{0.0000}	{0.0000}	{0.6635}	{0.8026}	{0.0000}	{0.0000}	-5.0370

The figures in braces are P-values for statistical significance

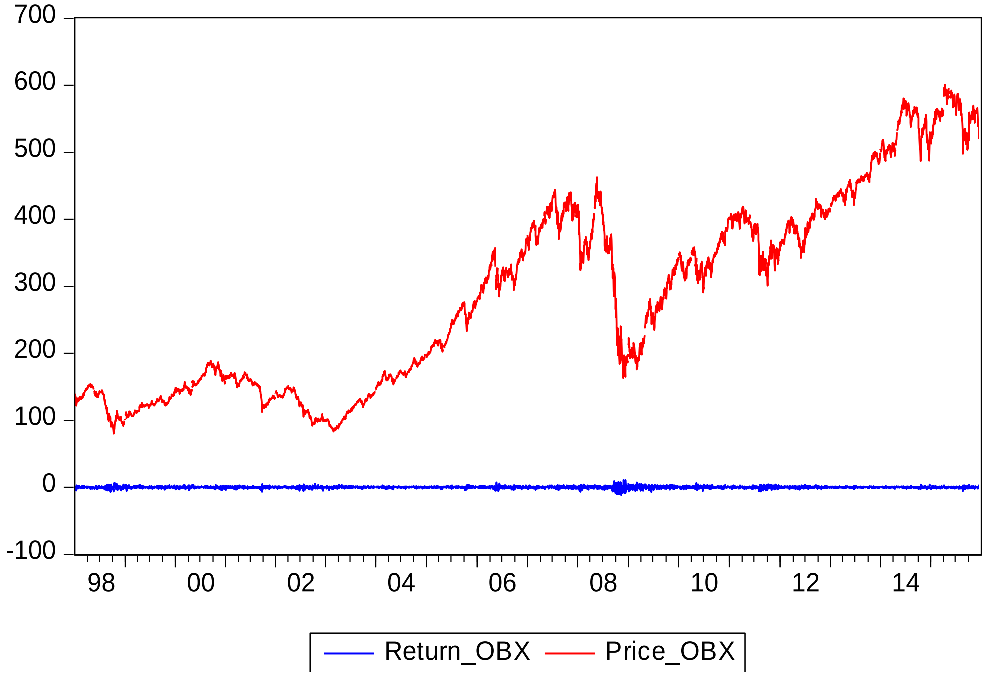

Figure 11 *OBX Index Price and Returns*

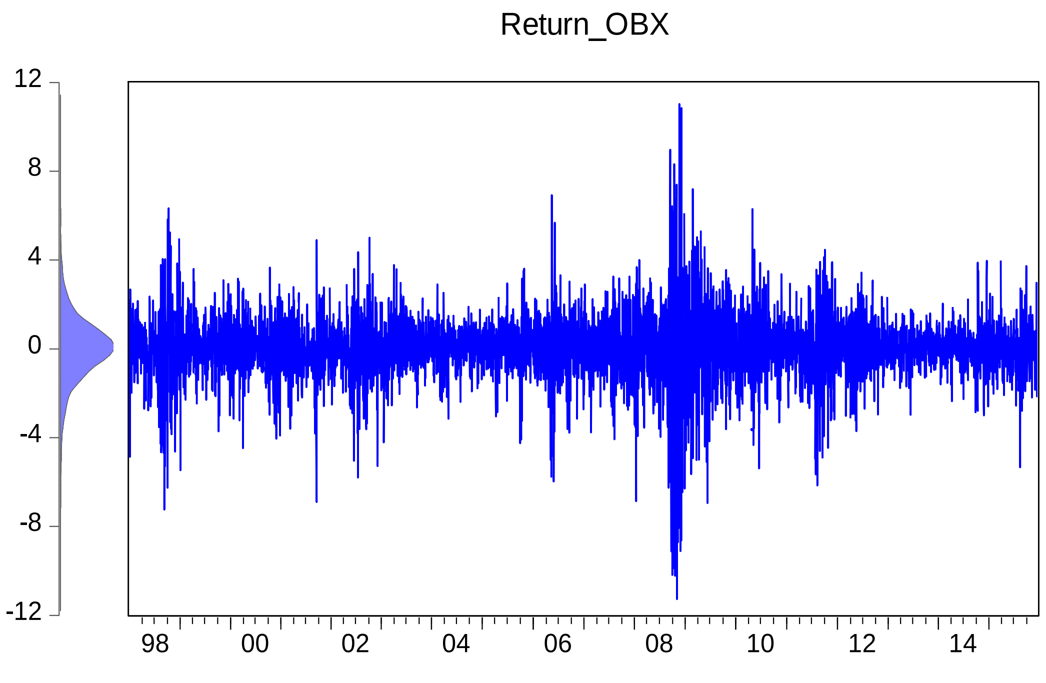

Figure 12 *OBX Returns*

2.6.7 Oslo Stock Exchange All Share Index (OSEAX)

The daily return (logarithmic) of the OSEAX Index data set from the beginning of 1998 to the end of 2015 is y_t, t= 1, . . . ,4514. Features of the OSEAX Index are reported in ***Table 7***. The mean is positive and the standard deviation is 1.41. The index reports a maximum (minimum) value of 9.19 (-9.71), which is relatively high (low). The kurtosis is relatively high, indicating that the data are heavy-tailed relative to a normal distribution. The table reports *excess* kurtosis, meaning that positive kurtosis indicates leptokurtosis features. The Cramer-von-Mises and Quantile normal test statistic support non-normal return distributions. Serial correlation in the mean equation is strong and the Ljung-Box Q-statistic is significant. The Ljung-Box test statistic for squared returns (Q^2) and the ARCH statistic show that volatility clustering is significantly present. Both the KPSS statistic and the ADF test support stationary series. The BDS test statistic reports highly significant dependence in the data. The price and return series are plotted in ***Figure 13*** and the return series, together with a Kernel distribution to the left, is shown in ***Figure 14***. From the price plot, we clearly see that the series is non-stationary, unlike the price change (log-returns) which is stationary. From the return plots, the series show some volatility clustering, as shown by higher volatility when prices are falling. The return level seems to change randomly. The fact that the skewness is different from zero supports the feature of non-normal distribution.

Table 7 *Returns Characteristics from the OSEAX Index*

Statistics for OSEAX Index

Mean / Mode	Median Std.dev.	Maximum / Minimum	Moment Kurt/Skew	Quantile Kurt/Skew	Quantile Normal	Cramer-von-Mises	Serial dependence Q(12)	Q^2(12)
0.02982	0.09580	9.1864	5.73096	0.17450	6.0794	9.17645	28.2530	5188.300
0.00000	1.41334	-9.7088	-0.58741	-0.02164	{0.0478}	{0.0000}	{0.0050}	{0.0000}
BDS-Z-statistic (Ɛ = 1)				KPSS (Stationary)		Augmented	ARCH	VaR 2.5% /
m=2	m=3	m=4	m=5	Intercept	Trend	DF-test	(12)	CVaR 2.5%
16.8152	22.1216	26.0232	29.5705	0.02109	0.00002	-66.0007	1267.595	-2.9933
{0.0000}	{0.0000}	{0.0000}	{0.0000}	{0.6163}	{0.8105}	{0.0000}	{0.0000}	-4.5130

The figures in braces are P-values for statistical significance

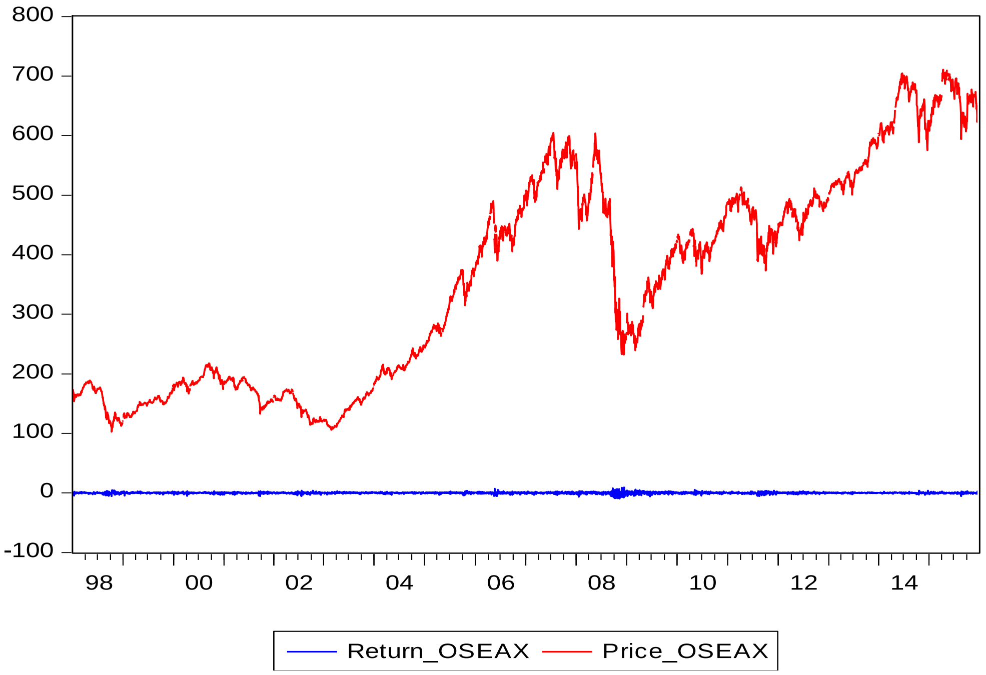

Figure 13 *OSEAX Index Price and Returns*

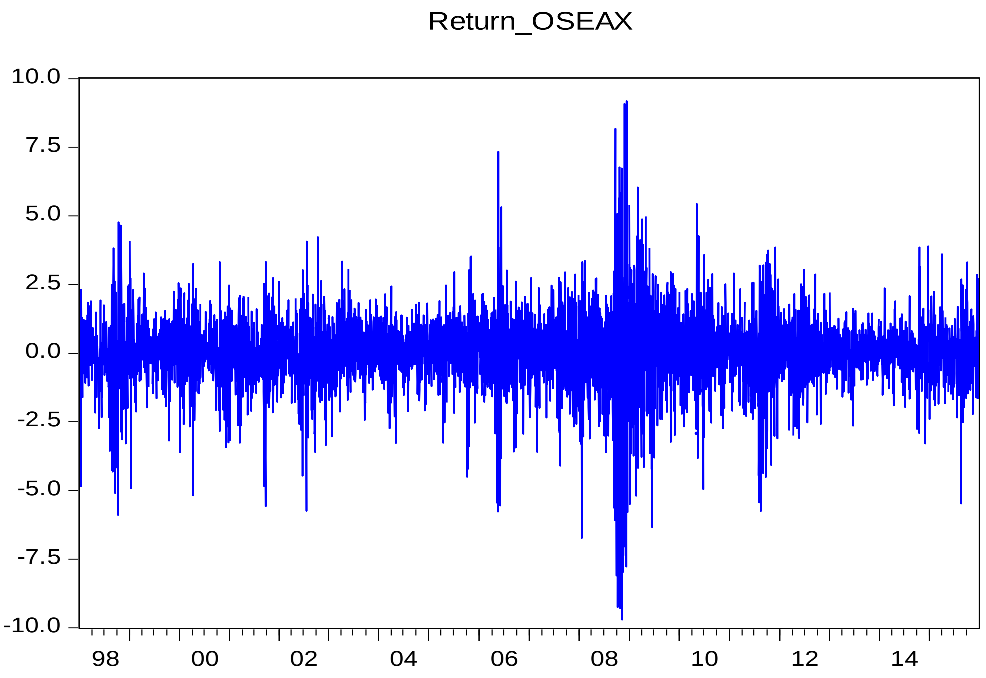

Figure 14 *OSEAX Index Returns*

2.6.8 Microsoft Corporation (MSFT)

The daily return (logarithmic) of the MSFT data set from the beginning of 1987 to the end of 2015 is y_t, t= 1, . . . , 7311. Features of the MSFT are reported in ***Table 8***. The mean is positive and the standard deviation is 2.21. The index reports a maximum (minimum) value of 17.87 (-35.83), which is high (low). The kurtosis is high, indicating that the data are heavy-tailed relative to a normal distribution. The table reports *excess* kurtosis, meaning that positive kurtosis indicates leptokurtosis features. The Cramer-von-Mises and Quantile normal test statistic support non-normal return distributions. Serial correlation in the mean equation is strong and the Ljung-Box Q-statistic is significant. The Ljung-Box test statistic for squared returns (Q^2) and the ARCH statistic show that volatility clustering is significantly present. Both the KPSS statistic and the ADF test support stationary series. The BDS test statistic reports highly significant dependence in the data. The price and return series are plotted in ***Figure 15*** and the return series, together with a Kernel distribution to the left, is shown in ***Figure 16***. From the price plot, we clearly see that the series is non-stationary, unlike the price change (log-returns) which are stationary. From the return plots, the series show some volatility clustering, as shown by higher volatility when prices are falling. The return level seems to change randomly. The fact that the skewness is different from zero supports the feature of non-normal distribution.

Table 8 *Returns Characteristics from MSFT*

Statistics for MSFT Share

Mean /	Median	Maximum /	Moment	Quantile	Quantile	Cramer-	Serial dependence	
Mode	Std.dev.	Minimum	Kurt/Skew	Kurt/Skew	Normal	von-Mises	Q(12)	Q^2(12)
0.08429	0.00000	17.8692	15.49519	0.21526	23.4622	14.56884	33.2970	1081.700
0.00000	2.21104	-35.8310	-0.65275	0.08759	{0.0000}	{0.0000}	{0.0010}	{0.0000}
BDS-Z-statistic (Ɛ = 1)				KPSS (Stationary)		Augmented	ARCH	VaR 2.5% /
m=2	m=3	m=4	m=5	Intercept	Trend	DF-test	(12)	CVaR 2.5%
19.0659	24.6665	29.3205	34.4300	0.17707	0.00003	-52.7417	648.637	-4.1751
{0.0000}	{0.0000}	{0.0000}	{0.0000}	{0.0006}	{0.0383}	{0.0000}	{0.0000}	-6.3621

The figures in braces are P-values for statistical significance

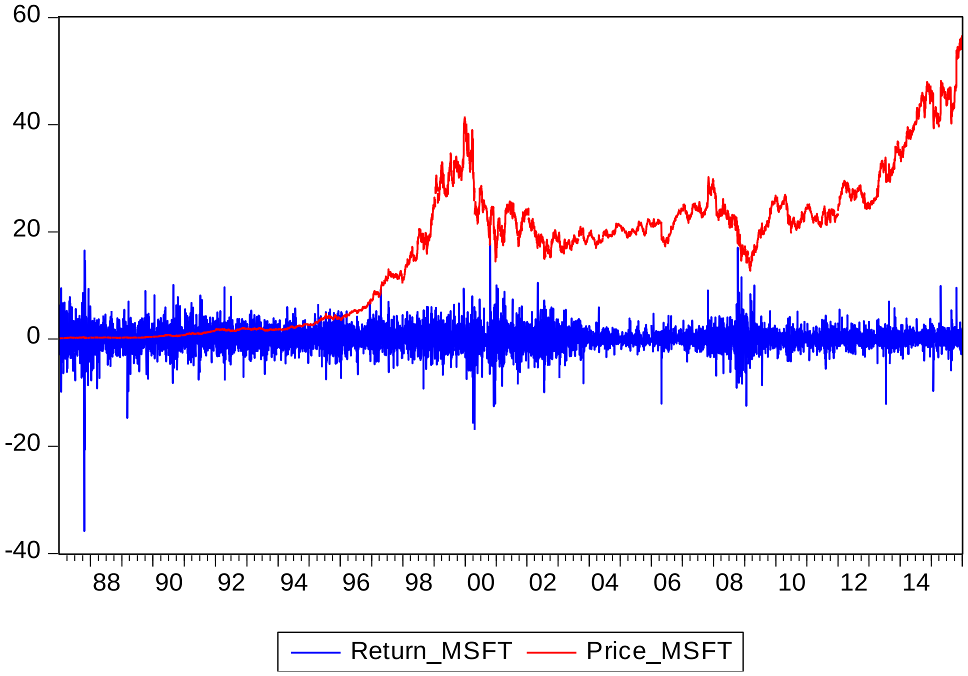

Figure 15 *MSFT Price and Returns*

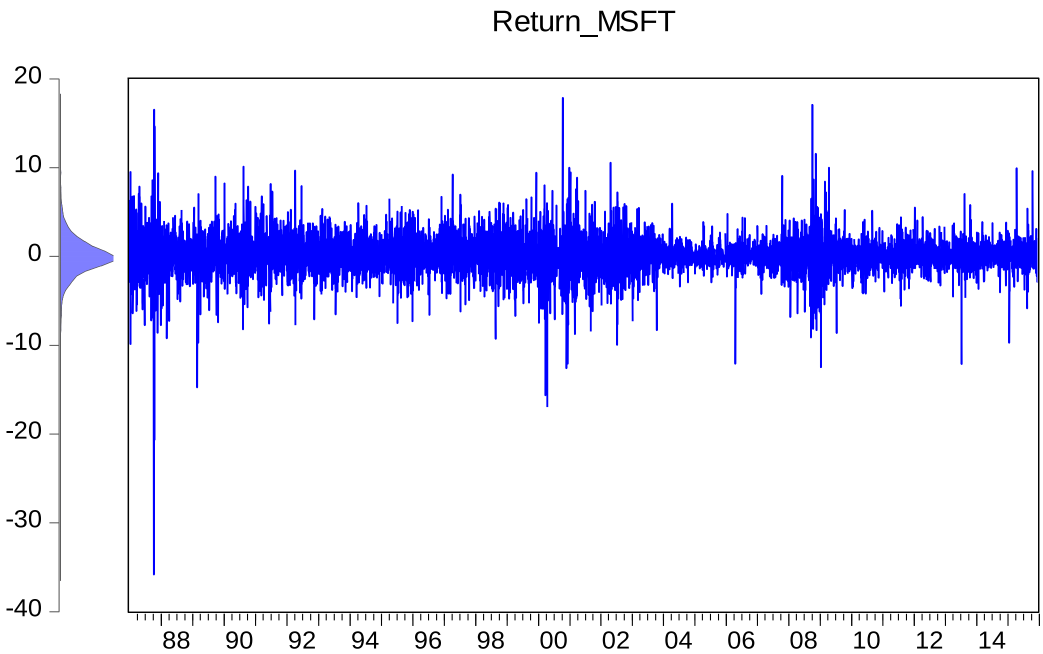

Figure 16 *MSFT Returns*

2.6.9 Micron Technology Inc. (MU)

The daily return (logarithmic) of the MU data set from the beginning of 1998 to the end of 2015 is y_t, t= 1, . . . , 4529. Features of the MU Share are reported in ***Table 9***. The mean is positive and the standard deviation is 3.88. The index reports a maximum (minimum) value of 21.06 (-26.19), which is relatively high (low). The kurtosis is relatively high, indicating that the data are heavy-tailed relative to a normal distribution. The table reports *excess* kurtosis, meaning that positive kurtosis indicates leptokurtosis features. The Cramer-von-Mises and Quantile normal test statistic support non-normal return distributions. Serial correlation in the mean equation is not strong and the Ljung-Box Q-statistic is not significant. The Ljung-Box test statistic for squared returns (Q^2) and the ARCH statistic show that volatility clustering is significantly present. Both the KPSS statistic and the ADF test support stationary series. The BDS test statistic reports highly significant dependence in the data. The price and return series are plotted in ***Figure 17*** and the return series, together with a Kernel distribution to the left, is shown in ***Figure 18***. From the price plots, we clearly see that this series is non-stationary, unlike the price change (log-returns) which is stationary. From the return plots, the series show some volatility clustering, as shown by higher volatility when prices are falling. The return level seems to change randomly. The fact that the skewness is different from zero supports the feature of non-normal distribution.

Table 9 *Returns Characteristics from MU*

Statistics for MU Share

Mean / Mode	Median Std.dev.	Maximum / Minimum	Moment Kurt/Skew	Quantile Kurt/Skew	Quantile Normal	Cramer-von-Mises	Serial dependence Q(12)	$Q^2(12)$
0.00194	0.00000	21.0611	3.36057	0.16134	4.9652	5.77836	19.5780	1451.200
0.00000	3.87548	-26.1913	-0.11271	-0.00836	{0.0835}	{0.0000}	{0.0750}	{0.0000}
BDS-Z-statistic (Ɛ = 1)				KPSS (Stationary)		Augmented	ARCH	VaR 2.5% /
m=2	m=3	m=4	m=5	Intercept	Trend	DF-test	(12)	CVaR 2.5%
14.7219	20.1111	24.2027	28.0643	0.00809	0.00000	-65.8956	544.870	-7.9625
{0.0000}	{0.0000}	{0.0000}	{0.0000}	{0.9440}	{0.9509}	{0.0000}	{0.0000}	-11.1315

The figures in braces are P-values for statistical significance

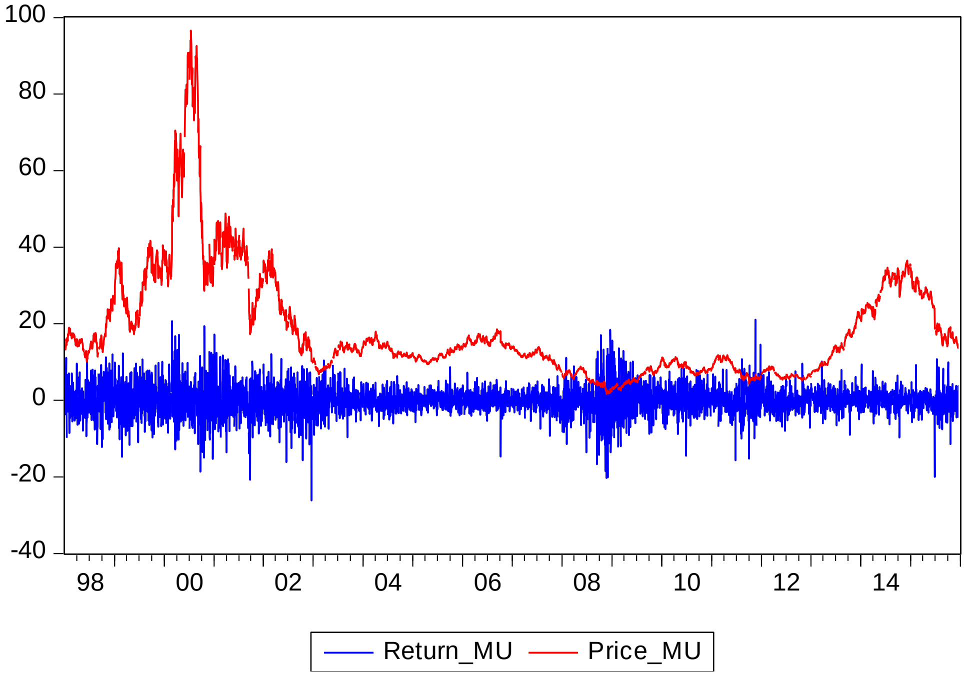

Figure 17 *MU Price and Returns*

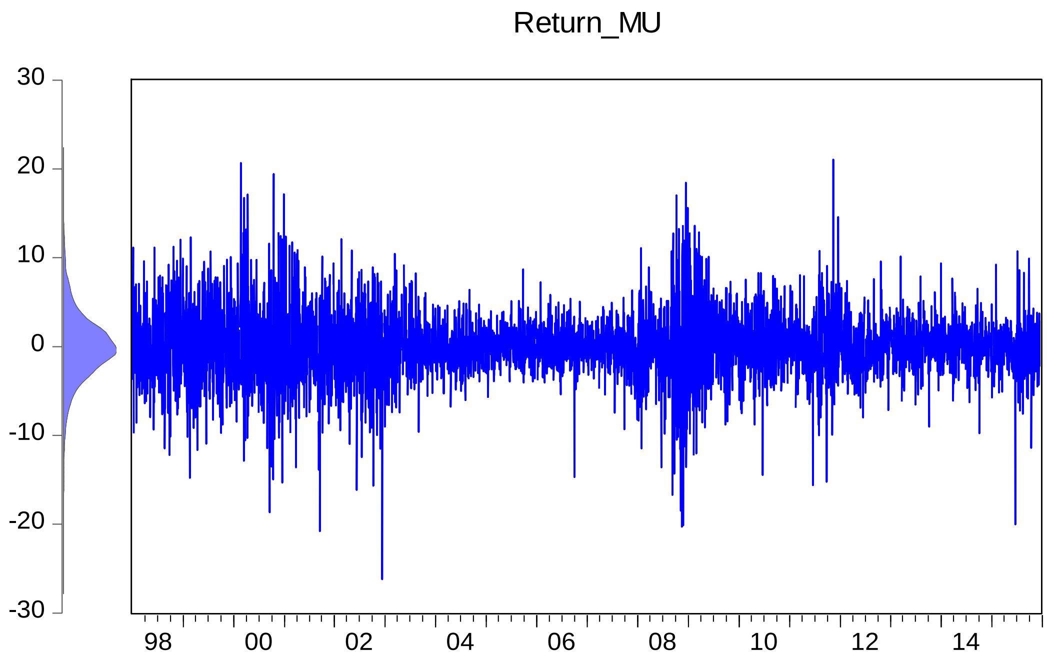

Figure 18 *MU Returns*

2.6.10 Norsk Hydro ASA (NHY)

The daily return (logarithmic) of the NHY data set from the beginning of 1998 to the end of 2015 is y_t, t= 1, . . . , 4499. Features of the NHY Share are reported in ***Table 10***. The mean is positive and the standard deviation is 2.22. The index reports a maximum (minimum) value of 18.76 (-16.47), which is relatively high (low). The kurtosis is relatively high, indicating that the data are heavy-tailed relative to a normal distribution. The table reports *excess* kurtosis, meaning that positive kurtosis indicates leptokurtosis features. The Cramer-von-Mises and Quantile normal test statistic support non-normal return distributions. Serial correlation in the mean equation is strong and the Ljung-Box Q-statistic is significant. The Ljung-Box test statistic for squared returns (Q^2) and the ARCH statistic show that volatility clustering is significantly present. Both the KPSS statistic and the ADF test support stationary series. The BDS test statistic reports highly significant dependence in the data. The price and return series are plotted in ***Figure 19*** and the return series, together with a Kernel distribution to the left, is shown in ***Figure 20***. From the price plots, we clearly see that this series is non-stationary, unlike the price change (log-returns) which is stationary. From the return plots, the series show some volatility clustering, as shown by higher volatility when prices are falling. The return level seems to change randomly. The fact that the skewness is different from zero supports the feature of non-normal distribution.

Table 10 *Returns Characteristics from NHY*

Statistics for NHY Share

Mean / Mode	Median Std.dev.	Maximum / Minimum	Moment Kurt/Skew	Quantile Kurt/Skew	Quantile Normal	Cramer-von-Mises	Serial dependence Q(12)	$Q^2(12)$
0.00904	0.00000	18.7601	6.96596	0.18066	6.9478	7.23170	40.5220	2540.700
0.00000	2.22250	-16.4733	-0.13780	0.03327	{0.0310}	{0.0000}	{0.0000}	{0.0000}
BDS-Z-statistic (Ɛ = 1)				**KPSS (Stationary)**		**Augmented**	**ARCH**	**VaR 2.5% /**
m=2	**m=3**	**m=4**	**m=5**	**Intercept**	**Trend**	**DF-test**	**(12)**	**CVaR 2.5%**
14.5442	19.2582	22.0472	24.1960	0.03077	0.00001	-69.1574	783.659	-4.4090
{0.0000}	{0.0000}	{0.0000}	{0.0000}	{0.6499}	{0.7139}	{0.0000}	{0.0000}	-6.5517

The figures in braces are P-values for statistical significance

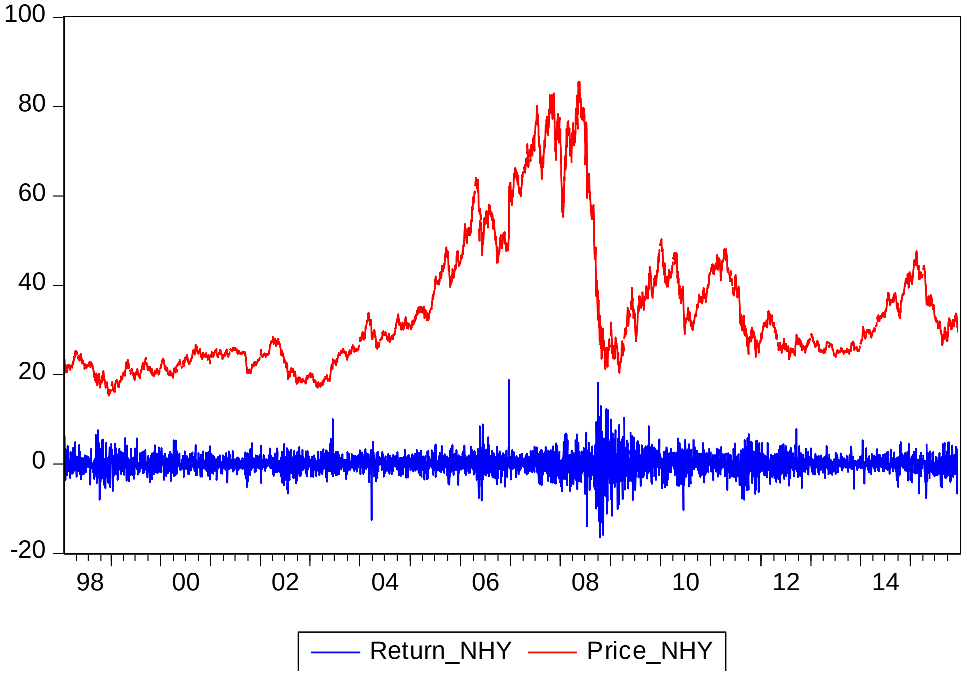

Figure 19 *NHY Price and Returns*

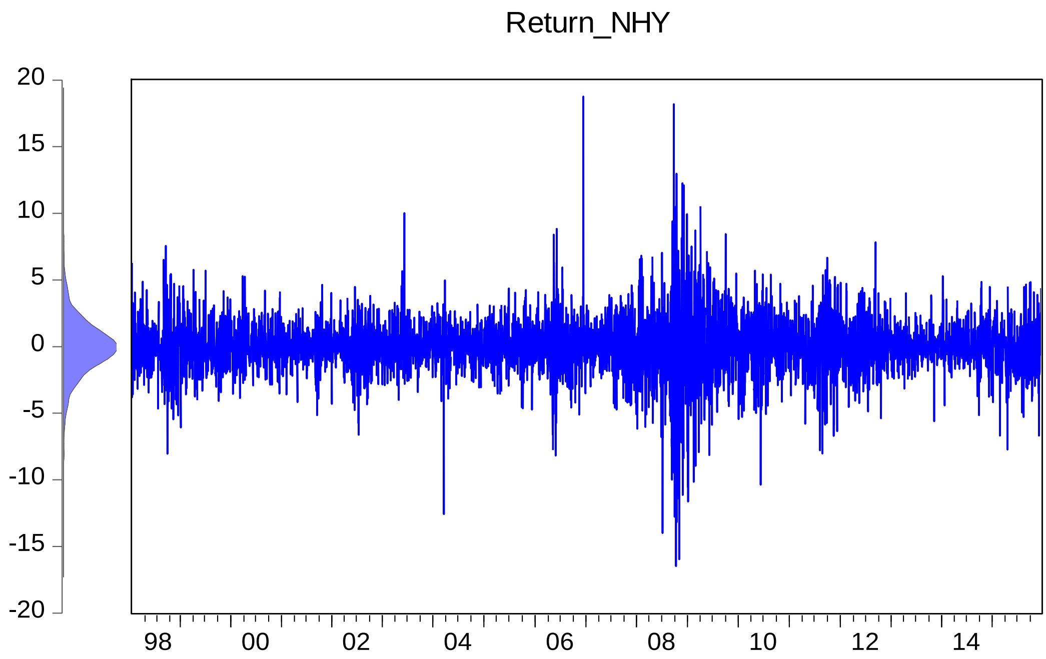

Figure 20 *NHY Returns*

2.6.11 Tomra Systems ASA (TOM)

The daily return (logarithmic) of the TOM data set from the beginning of 1998 to the end of 2015 is y_t, t= 1, . . . , 4499. Features of the TOM Share are reported in ***Table 11***. The mean is positive and the standard deviation is 2.92. The index reports a maximum (minimum) value of 21.65 (-47.57), which is high (low). The kurtosis is high, indicating that the data are heavy-tailed relative to a normal distribution. The table reports *excess* kurtosis, meaning that positive kurtosis indicates leptokurtosis features. The Cramer-von-Mises and Quantile normal test statistic support non-normal return distributions. Serial correlation in the mean equation is present and the Ljung-Box Q-statistic is significant. The Ljung-Box test statistic for squared returns (Q^2) and the ARCH statistic show that volatility clustering is not significantly present. Both the KPSS statistic and the ADF test support stationary series. The BDS test statistic reports highly significant dependence in the data. The price and return series are plotted in ***Figure 21*** and the return series together with a Kernel distribution to the left is shown in ***Figure 22***. From the price plot, we clearly see that the series is non-stationary, unlike the price change (log-returns) which is stationary. From the return plots, the series show little volatility clustering, as suggested by the test statistics for Q^2 and ARCH. The return level seems to change randomly. The fact that the skewness is different from zero supports the feature of non-normal distribution.

Table 11 *Returns Characteristics from TOM*

Statistics for TOM Share

Mean /	Median	Maximum /	Moment	Quantile	Quantile	Cramer-	Serial dependence	
Mode	Std.dev.	Minimum	Kurt/Skew	Kurt/Skew	Normal	von-Mises	Q(12)	$Q^2(12)$
0.01920	0.00000	21.6455	22.87798	0.20072	7.6355	10.90318	23.5600	18.649
0.00000	2.92436	-47.5734	-1.12335	-0.01053	{0.0220}	{0.0000}	{0.0230}	{0.0970}
BDS-Z-statistic (ε = 1)				KPSS (Stationary)		Augmented	ARCH	VaR 2.5% /
m=2	m=3	m=4	m=5	Intercept	Trend	DF-test	(12)	CVaR 2.5%
12.2077	16.1311	18.6860	20.5971	-0.01293	0.00001	-69.5023	16.369	-5.5308
{0.0000}	{0.0000}	{0.0000}	{0.0000}	{0.8821}	{0.6704}	{0.0000}	{0.1749}	-8.3849

The figures in braces are P-values for statistical significance

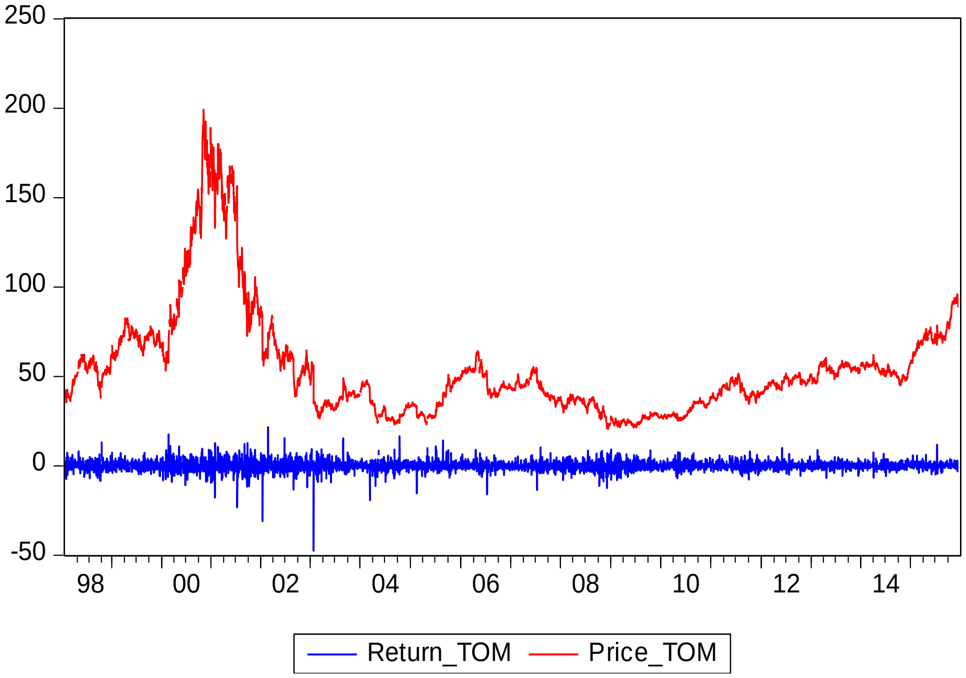

Figure 21 *TOM Price and Returns*

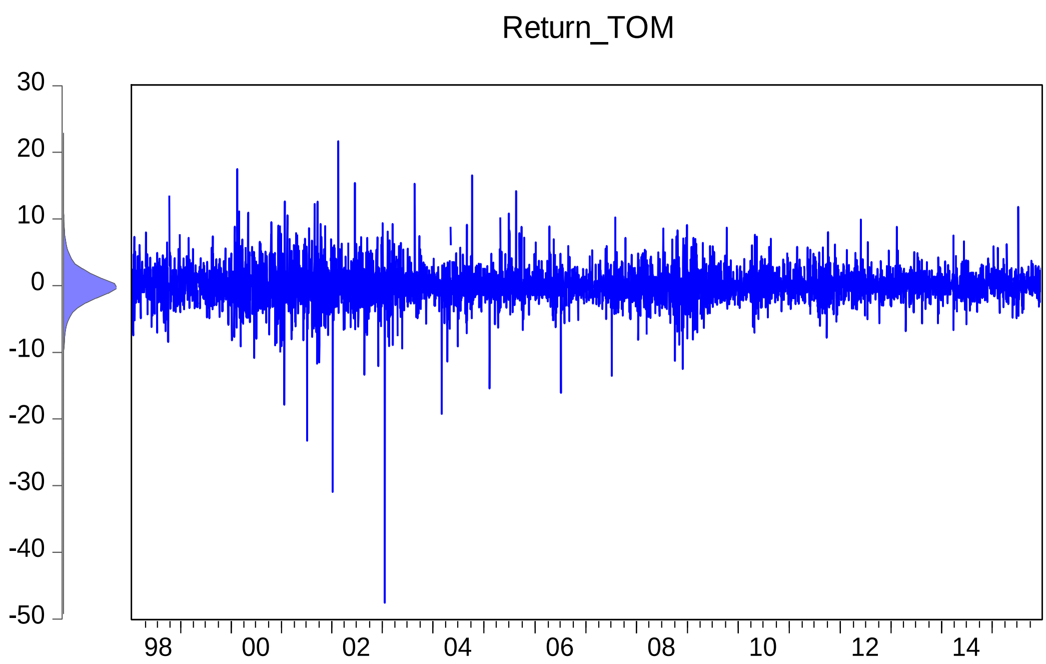

Figure 22 *TOM Returns*

2.6.12 The ICE Carbon one month Forward Contracts

The daily return (logarithmic) of the Carbon Forward Contracts data set from the beginning of 2008 to the end of 2015 is y_t, t= 1, . . . , 2007. Features of the Carbon Forward Contracts are reported in ***Table 12.*** The mean is negative and the standard deviation is 3.22. The index reports a maximum (minimum) value of 24.02 (-45.23), which is relatively high (low). The kurtosis is high, indicating that the data are heavy-tailed relative to a normal distribution. The table reports *excess* kurtosis, meaning that positive kurtosis indicates leptokurtosis features. The Cramer-von-Mises and Quantile normal test statistic support non-normal return distributions. Serial correlation in the mean equation is strong and the Ljung-Box Q-statistic is significant. The Ljung-Box test statistic for squared returns (Q^2) and the ARCH statistic show that volatility clustering is significantly present. Both the KPSS statistic and the ADF test support stationary series. The BDS test statistic reports highly significant dependence in the data. The price and return series are plotted in ***Figure 23*** and the return series, together with a Kernel distribution to the left, is shown in ***Figure 24***. From the price plot, we clearly see that the series is non-stationary, unlike the price change (log-returns) which is stationary. From the return plots, the series show some volatility clusters, as shown by higher volatility when prices are falling. The return level seems to change randomly. The fact that the skewness is different from zero supports the feature of non-normal distribution.

Table 12 *Returns Characteristics from Carbon*

Statistics for Front December Forward Contracts Carbon

Mean /	Median	Maximum /	Moment	Quantile	Quantile	Cramer-	Serial dependence	
Mode	Std.dev.	Minimum	Kurt/Skew	Kurt/Skew	Normal	von-Mises	Q(12)	Q^2(12)
-0.05279	0.00000	24.0141	25.18876	0.30561	8.0832	7.90779	62.5190	157.080
0.00000	3.21655	-45.2282	-1.16896	0.02857	{0.0176}	{0.0000}	{0.0000}	{0.0000}
BDS-Z-statistic (Ɛ = 1)				KPSS (Stationary)		Augmented	ARCH	VaR 2.5% /
m=2	m=3	m=4	m=5	Intercept	Trend	DF-test	(12)	CVaR 2.5%
11.7125	15.2580	18.3065	21.3580	-0.14668	0.00009	-22.8697	115.864	-6.8051
{0.0000}	{0.0000}	{0.0000}	{0.0000}	{0.3070}	{0.4502}	{0.0000}	{0.0000}	-10.0746

The figures in braces are P-values for statistical significance

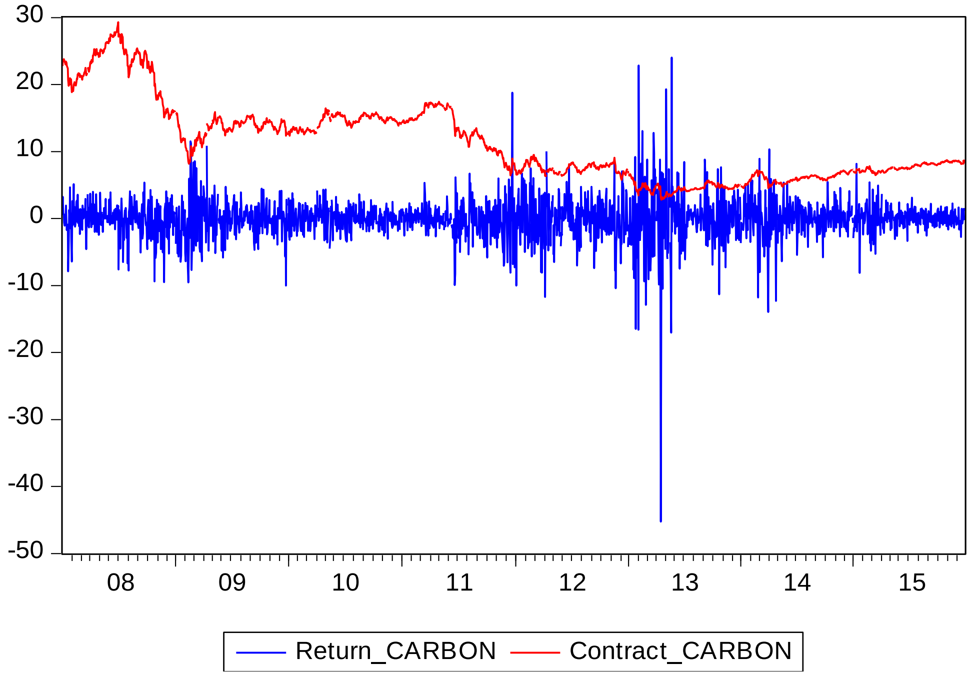

Figure 23 *Carbon Price and Returns*

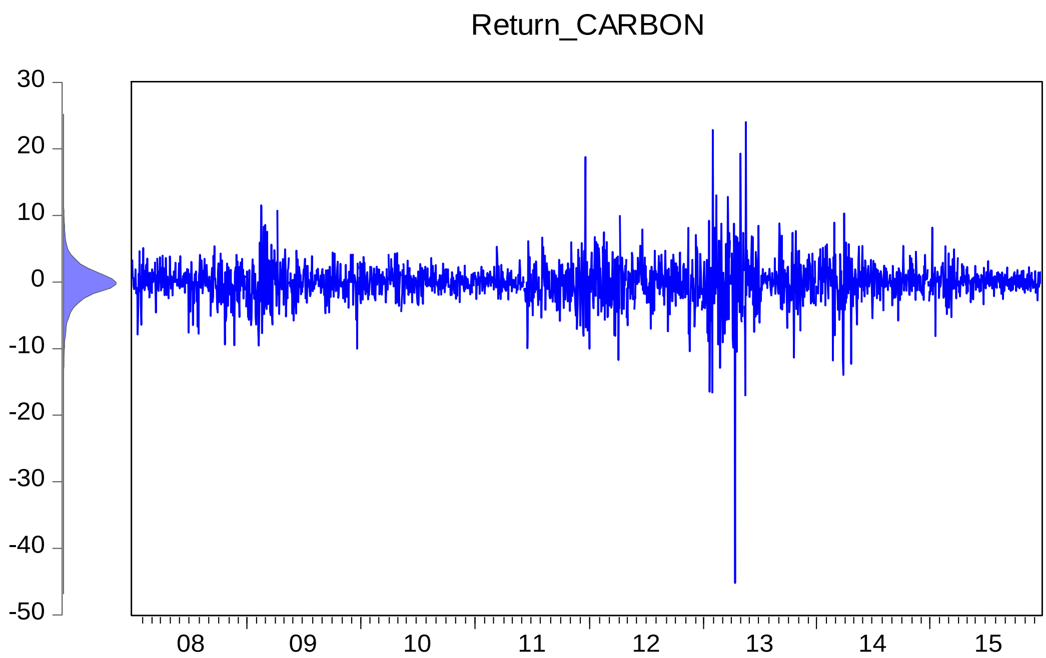

Figure 24 *Carbon Returns*

2.6.13 Brent oil front month Future Contracts

The daily return (logarithmic) of the Brent Oil Future Contracts data set from the beginning of 2008 to the end of 2015 is y_t, t= 1, . . . , 2063. Features of the Brent Oil Derivative are reported in ***Table 13.*** The mean is negative and the standard deviation is 2.18. The index reports a maximum (minimum) value of 12.71 (-10.95), which is relatively high (low). The kurtosis is relatively high, indicating that the data are heavy-tailed relative to a normal distribution. The table reports *excess* kurtosis, meaning that positive kurtosis indicates leptokurtosis features. The Cramer-von-Mises and Quantile normal test statistic support non-normal return distributions. Serial correlation in the mean equation is strong and the Ljung-Box Q-statistic is significant. The Ljung-Box test statistic for squared returns (Q^2) and the ARCH statistic show that volatility clustering is significantly present. Both the KPSS statistic and the ADF test support stationary series. The BDS test statistic reports highly significant dependence in the data. The return series is plotted in ***Figure 25*** together with a Kernel distribution to the left. From this plot, we clearly see that the return series is stationary. It also shows some volatility clustering, as shown by higher volatility when prices are falling. The return level seems to change randomly. The fact that the skewness is different from zero supports the feature of non-normal distribution.

Table 13 *Returns Characteristics from Brent oil*

Statistics for Brent Oil Derivative

Mean / Mode	Median Std.dev.	Maximum / Minimum	Moment Kurt/Skew	Quantile Kurt/Skew	Quantile Normal	Cramer-von-Mises	Serial dependence Q(12)	$Q^2(12)$
-0.06281	-0.01505	12.7066	3.81490	0.36369	11.6166	4.90892	23.4200	1398.800
0.00000	2.17998	-10.9455	-0.14027	-0.02681	{0.0030}	{0.0000}	{0.0240}	{0.0000}
BDS-Z-statistic (Ɛ = 1)				**KPSS (Stationary)**		**Augmented**	**ARCH**	**VaR 2.5% /**
m=2	**m=3**	**m=4**	**m=5**	**Intercept**	**Trend**	**DF-test**	**(12)**	**CVaR 2.5%**
12.5894	15.5706	18.1255	21.0406	0.02616	-0.00009	-48.2876	425.805	-4.9395
{0.0000}	{0.0000}	{0.0000}	{0.0000}	{0.7852}	{0.2844}	{0.0000}	{0.0000}	-6.7188

The figures in braces are P-values for statistical significance

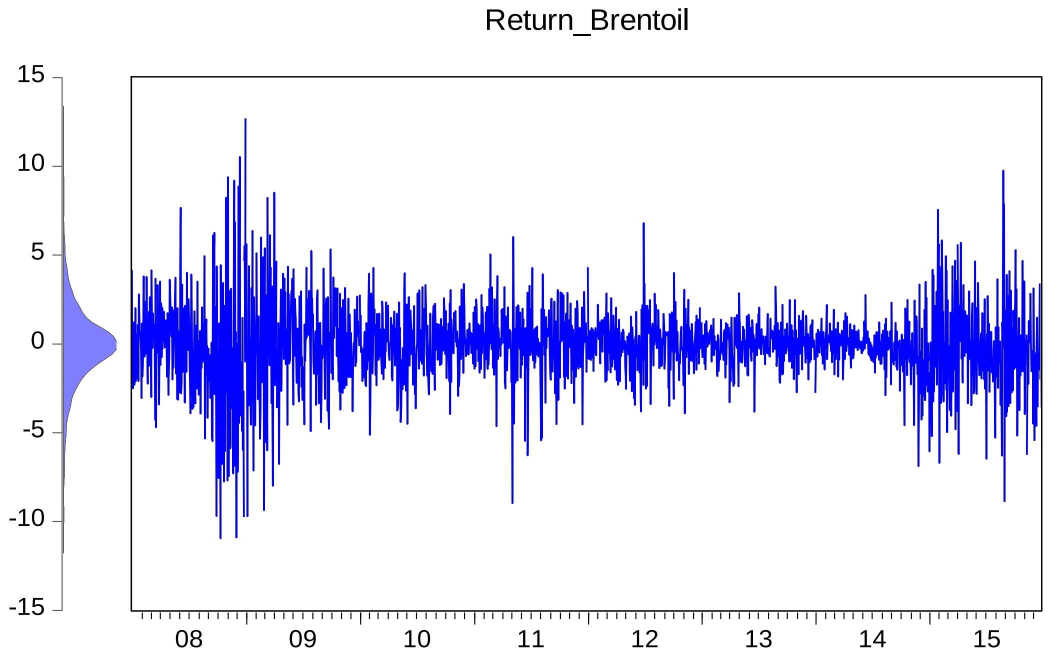

Figure 25 *Brent oil Returns*

2.6.14 Salmon Forward Contracts

The daily return (logarithmic) of the one month Salmon Forward Contracts data set from June 2006 to the end of 2015 is y_t, $t= 1, \ldots, 2400$. Features of the Salmon Forward Contracts are reported in ***Table 14.*** The mean is positive and the standard deviation is 1.12. The index reports a maximum (minimum) value of 8.41 (-9.31), which is relatively high (low). The kurtosis is relatively high, indicating that the data are heavy-tailed relative to a normal distribution. The table reports excess kurtosis, meaning that positive kurtosis indicates leptokurtosis features. The Cramer-von-Mises and Quantile normal test statistic support non-normal return distributions. Serial correlation in the mean equation is strong and the Ljung-Box Q-statistic is significant. The Ljung-Box test statistic for squared returns (Q^2) and the ARCH statistic show that volatility clustering is significantly present. Both the KPSS statistic and the ADF test support stationary series. The BDS test statistic reports highly significant dependence in the data. The return series is plotted in ***Figure 26*** together with a Kernel distribution to the left. From this plot, we clearly see that the return series is stationary. It also shows some volatility clustering, as shown by higher volatility when prices are falling. The return level seems to change randomly. The fact that the skewness is different from zero supports the feature of non-normal distribution.

Table 14 Returns Characteristics from Salmon

Statistics for Salmon one month Forward Contract

Mean /	Median	Maximum /	Moment	Quantile	Quantile	Cramer-	Serial dependence	
Mode	Std.dev.	Minimum	Kurt/Skew	Kurt/Skew	Normal	von-Mises	Q(12)	$Q^2(12)$
0.02360	0.00000	8.4083	7.72358	0.72941	54.3777	13.97996	116.5200	93.949
0.00000	1.11540	-9.3149	0.03555	0.05417	{0.0000}	{0.0000}	{0.0000}	{0.0000}
BDS-Z-statistic (Ɛ = 1)				KPSS (Stationary)		Augmented	ARCH	VaR 2.5% /
m=2	m=3	m=4	m=5	Intercept	Trend	DF-test	(12)	CVaR 2.5%
5.9157	7.3299	7.7997	8.3252	-0.02326	-0.00004	-40.8526	72.043	-2.3119
{0.0000}	{0.0000}	{0.0000}	{0.0000}	{0.6098}	{0.2349}	{0.0000}	{0.0000}	-3.3308

The figures in braces are P-values for statistical significance

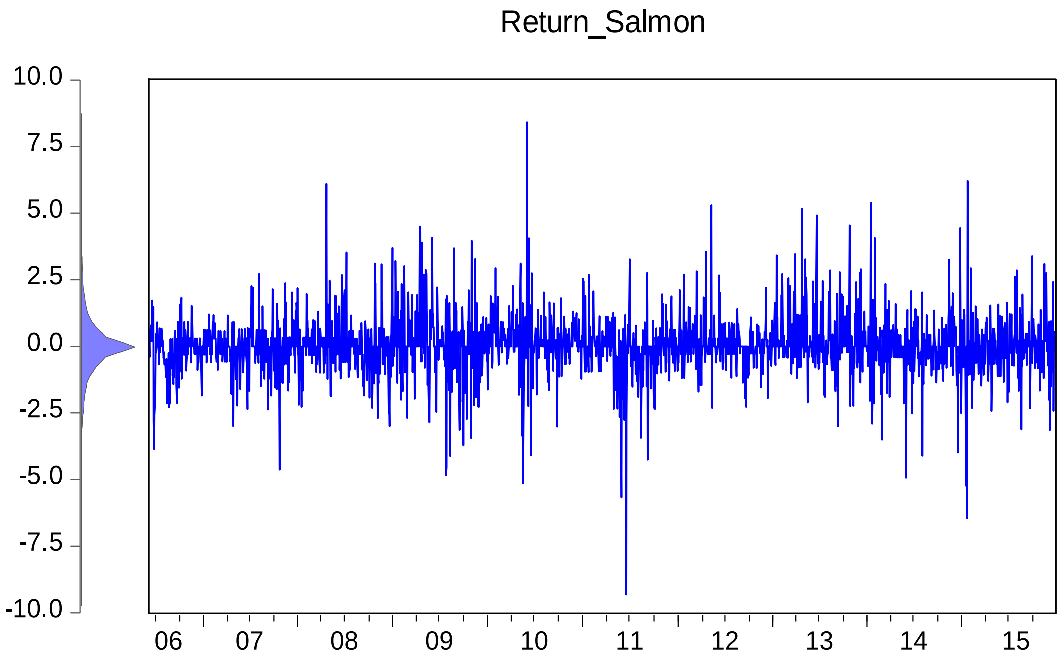

Figure 26 *Returns Salmon*

3.0 Theoretical aspects

3.1 Persistence

A stationary time series is said to be *mean reverting,* meaning that it tends to return to its mean in the long run. It suggests that today's information has no influence on long-run estimates. If today's return has a large impact on the forecast variance several periods in the future, the volatility is said to be persistent. Due to this fact, persistence is of great interest examining the effect of a shock to a time series. A time series with a unit root has persistence indefinitely in the way that it never returns to its mean. The half-life of a shock is a good measure of persistence. It measures the time span needed for the volatility to move halfway back to its unconditional mean.
It is given by:

$$\tau = \mathrm{k} : \left| h_{t+k|t} - \sigma^2 \right| = \frac{1}{2} \left| h_{t+1|t} - \sigma^2 \right|$$

where $h_{t+1|t}$ is the expected value of the variance in return *k* periods in the future, and σ^2 is the long-term volatility (Engle and Patton 2001).
The persistence is interesting in the way that if the volatility after a shock is highly persistent, it can change the risk premium in the stock market. This can influence the stock prices in later periods. However, if the half-life is low, it only affects required returns for a short period. In response to this, volatility shocks have little impact on the stock market prices (Poterba and Summers 1986). Higher risk premium raises the required return on capital. With ceteris paribus, the discounted value of a company's income decline, and so does the value.

3.2 Asymmetry

Asymmetry is a common feature of financial time series. In the period after a shock in the market, like the great shocks in 1987 and 2007-2008, we have a significant correction in the price of assets. Between 2007 and 2009 the DJIA index went from 14.000 to 6.600. The volatility was high while the stock prices declined dramatically. This suggests that there is a correlation between volatility and return. Nelson (1991) argues that this is the case, referring to the events of October 1987, saying that stock market volatility does not necessarily change randomly over time. There is evidence of a negative correlation between changes in return and volatility (Christie 1982). “Bad news” leads to higher volatility and “good news” leads to lower volatility. This asymmetry is explained by the *leverage effect* and the *risk premium effect.* The volatility tends to rise when the stock prices fall. This is because when bad news occurs, and the price of stocks falls, the debt-to-equity ratio grows. The value of the equity falls relative to the debt and the volatility rise. Meanwhile, investors get news of higher volatility, leading to lower demand for shares because of risk aversion. This asymmetric response of volatility to large price movements is referred to as the *leverage effect* (Engle and Patton 2001). In this setting, the term “leverage” is used to explain asymmetry in the conditional variance function (Gallant, Rossi et al. 1993).

3.3 Portfolio Theory

In 1952, Markowitz presented a paper describing the portfolio theory. Every investor wants to (or should) maximize their return. Because of uncertainty about the future, the expected return counts. A risk adverse investor will minimize the risk for the given return. The portfolio theory states that we can get rid of unsystematic risk by combining different shares. It is not the variance of each share that is interesting; it is the covariance between them. In this way, we can construct a portfolio where different shares outweigh each other. As an example, we have a situation in Norway today with low oil price. If we in front of the price fall had one share, we would have experienced a great loss if this share were within the oil industry. If it were in the Salmon industry, the return would be very good. When the price of oil decline, the oil company can get its value decreased. On the other side, we see that lower oil price increase the disposable income for people buying fish for dinner, leading to a rise in demand. The lower oil price has reduced the value of the Norwegian Krone, which makes it more profitable to export salmon. In this way, if we had two shares in front of the oil-drop, the salmon shares would outweigh the drop in oil shares. The covariance of salmon and oil shares has indeed been negative the last year, and this makes it a great example for showing the value of diversifying.

It is widely discussed how many shares a well-diversified portfolio should consist of, ranging from over 100 to about 20. Diversification cannot remove all variance. An efficient portfolio is one where the investor can’t get more return without raising the variance and vice versa (Markowitz 1952).

4.0 Impulse response analysis of nonlinear models

Impulse response functions (IRF) have been widely used to study the dynamics of a linear process. The IRF measure the effect of shocks on future values of a time series relative to some reference value. It may be used for studying the persistence of shocks as well as asymmetric effects (Koop 1996), and it works as an important tool in empirical causal analysis. As discussed by Gallant, Rossi and Tauchen (Gallant, Rossi et al. 1993) the analysis of dynamics can also be extended to be applied to non-linear time series.
This approach includes an examination of profile bundles for evidence of damping or persistence, which embraces some of the key aspects to this thesis.
In the general non-linear case, a structural model is needed to link shocks to endogenous variables back to shocks in underlying exogenous or policy variables (Gallant, Rossi et al. 1993). A natural definition of the nonlinear impulse response is the net effect of the impulse, which is obtained by comparing the profile for the impulse to the baseline profile. Both the effect of shocks to the mean (return) and the effects on volatility will be considered. The SNP- method will be applied to generate empirical evidence on the multi-step ahead price dynamics. The focus lies in the persistence of the response of volatility to price shocks, as well as studying the asymmetrical effects. The analysis uses the nonparametric estimate of the conditional density of price changes (Gallant and Tauchen 1990).

4.1 Definition

The simplest and most prevalent form of impulse response function is referred to as the *traditional impulse response function.*

> The traditional impulse response function is defined as the difference between two different realizations of y_{t+n} that are identical up to *t-1*. One realization assumes that between *t* and *t+n* the system is hit only by a shock of size δ at period t, while the second realization, being the benchmark profile, assumes that the system is not hit by any shocks between *t* and *t+n*. The function is defined as
>
> $$I_Y(n,\delta,w_{t-1}) = E[Y_{t+n}|V_t = \delta, V_{t+1} = 0, \dots, V_{t+n} = 0, w_{t-1}] - E[Y_{t+n}|V_t = 0, V_t = 0, V_{t+1} = 0, \dots, V_{t+n} = 0, w_{t-1}],$$
>
> For *n = 1,2,3,….*

> The traditional impulse response aims to disclose the effect of a shock of size δ hitting the system at time *t* on the state of the system at time *t+1,* given that no other shocks hit the system. In the case of nonlinear models, the traditional IRF generally depends on w_{t-1} , the history chosen as the baseline profile for comparison of the two realizations. The impulse responses rely on the initial condition, reflecting the nonlinearity of the system. Assuming stationarity, the mean of the baseline forecast is the unconditional mean. The traditional IRF also depends on the size of the shock, δ (Koop, Pesaran et al. 1996).

Both the effect of shocks on the means of subsequent returns and the effects on subsequent volatility are of interest.

5.0 Method

5.1 The ARCH and GARCH Methodology

Time-varying volatility clustering is a well-known phenomenon in financial time series. Volatility one day seems to have a positive correlation with the volatility of the next day. ARCH and GARCH models may be used for modeling this feature.
The ARCH model developed by Engle (Engle 1982) uses earlier observations to estimate the one-period forecast variance. The lag structure of the model uses the last observation of squared residuals in order to derive the next days' volatility.

$$\sigma_t^2 = \alpha_0 + \sum_{j=1}^{p} \alpha_j \varepsilon_{t-j}^2$$

The GARCH (Generalized Autoregressive Conditional Heteroscedastic) model (Bollerslev 1986) is used to calculate the one-step-ahead volatility. This is done by including both the last period squared return and the last period forecast.

GARCH (p,q)

$$\sigma_t^2 = \alpha_0 + \sum_{j=1}^{p} \alpha_j \varepsilon_{t-j}^2 + \sum_{j=1}^{q} \beta_j \sigma_{t-j}^2$$

GARCH (1,1)

$$\sigma_t^2 = \alpha_0 + \alpha_1 \varepsilon_{t-1}^2 + \beta_1 \sigma_{t-1}^2$$

Where $\alpha_0 > 0$, $\varepsilon_1 > 0$, $\beta_1 > 0$, and $\alpha_1 + \beta_1 < 1$ to ensure stationarity.

By including the last period forecast of the volatility, the model manages to cooperate better with the persistence of a shock than an ARCH model, where next periods variance only depends on the squared residuals from last period. The model has proved to give a good fit to empirical data. Maximum likelihood is used to estimation and specification of the GARCH (Verbeek 2012).

5.2 Model Selection

Bayesian Information Criterion (BIC) or Schwarz criterion is an index used to help us find the appropriate dimensionality of a model that will fit our set of observations (Schwarz 1978). The criterion chooses the model with the best fit, measured by the maximum likelihood function, subject to a penalty term that increases with the number of parameters included. This should diminish the possibility of overfitting the model. The penalty term is greater for BIC than for the related Akaike Information Criterion (AIC) (Akaike 1969). In time-series analysis, the BIC should be preferred to the ordinary AIC, especially when the number of model parameters is high compared to the number of observations (Chatfield 2000). In large-sample cases, the Bayes solution ideally corresponds to the model which is *a posteriori* most probable, i.e. the model that is considered most credible by the data at hand (Schwarz 1978).

The BIC can be defined as:

$$BIC = -2 \ln f\left(y \middle| \hat{\theta}_k\right) + k \ \ln n$$

where y is the observed data, $\hat{\theta}_k$ are the parameter values that maximizes the likelihood function; n is the sample size and k is the total number of parameters estimated. The term $f\left(y \middle| \hat{\theta}_k\right)$ is the maximized value of the likelihood function of the model. The model with the lowest BIC is preferred while models with higher values are rejected (Schwarz 1978). Using this procedure, the selected model for our dataset is a semi-nonparametric GARCH-model (Gallant and Tauchen 1990).

5.3 SNP Method for Nonparametric Time Series Analysis

SNP is a semi-nonparametric method, based on an expansion in Hermite functions, for the estimation of the conditional density. The Hermite polynomial expansion used by Gallant and Tauchen (1990) is based on ARCH, and it allows a deviation without knowing the property of normality and conditional heterogeneity. By applying this to univariate time series, we get an estimation of the fitted conditional density. This expansion works well for simulation, and we eliminate the problem of non-normality (Walter 1977).

The semi-nonparametric term tells us that it lies halfway between being a nonparametric (number and nature of parameters are adjustable and not fixed in the advance) and parametric method. The one-step-ahead conditional density incorporates all the information about various characteristics of time series including conditional heteroscedasticity, non-normality, time irreversibility and other forms of nonlinearities. The SNP model is, therefore, a moment generator and well described by Gallant and Tauchen (1990). The model is flexible written in C++ and therefore available on many platforms. The model specification provides an appropriate and detailed statistical description of uni- and multivariate data series. Starting from a VAR model, the methodology if necessary, elaborates the description of the data set from VAR, to Normal (G) ARCH, to Semi-parametric GARCH, and to Nonlinear Nonparametric. It features an extension of the GARCH model with parameters for level and asymmetric (leverage) effects. The Schwarz criterion (BIC) is used for model selection (Schwarz 1978). The preferred model for the data set is selected with a minimum of four Hermite polynomials for non-normal features of data series. The statistical methodology describes the GARCH process using a BEKK (Engle and Kroner 1995) formulation for the conditional variance allowing for BIC-efficient volatility asymmetry and level effects. Moreover, for evaluation purposes, the residuals are easily available for an appropriate model test statistic (Gallant and Tauchen 1990). The program provides an opportunity of specifying a good model and simulates shocks with corresponding output, which is important in our analysis.

5.3.1 Limitations

Due to the time constraint that the master thesis composes, we are not able to perform significance tests of our findings. This is a limitation of this paper, but it can work as a preliminary study, in hope of uncovering some interesting features.

5.4 Estimation of the Conditional Density

5.4.1 Semi-nonparametric (SNP) Estimators

As mentioned above, the SNP method depends on the fact that a Hermite expansion can be used as a common method for approximating the density function.

> Letting z denote an M-vector, the Hermite density has the form $h(z)\alpha[P(z)]^2\emptyset(z)$ where $P(z)$ denotes a multivariate polynomial of degree K_z and $\emptyset(z)$ denotes the density function of the (multivariate) Gaussian distribution with mean zero and the

identity as its variance-covariance matrix. The constant of proportionality is $1/\int[P(s)]^2\,\emptyset(s)ds$ which makes $h(z)$ integrate to one. Because of this division, the coefficients can only be determined to within a scalar multiple. To achieve a unique representation, the constant term of the polynomial part is set to one.

The location/scale shift $y = R_z + \mu$, where R is an upper triangular matrix and μ is an M-vector, leads to a parameterization denoted as $f(y|\theta)\alpha\{P[R^{-1}(y - \mu)]\}^2\{\emptyset[R^{-1}(y - \mu)]/|\det(R)|\}$. Because $\{\emptyset[R^{-1}(y - \mu)]/|\det(R)|\}$ is the density function of the M-dimensional multivariate Gaussian distribution with mean μ

and variance-covariance matrix $\sum = RR'$, and because the main term of the polynomial part equals unity, the leading term of the entire expansion is the multivariate Gaussian density function. The parameters θ of $f(y|\theta)$ are made up of the coefficients of the polynomial $P(z)$ plus μ and R and are estimated by maximum likelihood.

Since the method is parametric yet has nonparametric properties, it is termed semi-nonparametric to suggest that it lies halfway between the two procedures. The conditional density, given the entire past, depends only on L lags from the past. This basic approach is characterized as having a Markovian structure.

A density is then obtained by a location/scale shift $y_t = Rz_t + \mu_x$ off a sequence of normalized errors $\{z_t\}$. This makes the leading term of the expansion a Gaussian vector autoregression (VAR).

In time series analysis, the $\{z_t\}$ are usually referred to as linear innovations. In order to let them me conditionally heterogeneous, the coefficients of the polynomial $P(z)$ are polynomials of degree K_x in x_{t-1}. This polynomial is denoted as $P(z, x)$. When $K_x = 0$, the $\{z_t\}$ are homogeneous, as the conditional density of z_t does not depend on x_{t-1}. The tuning parameter K_z controls the extent to which the model deviates from normality while the K_x controls the extent to which these deviations vary with the history of the process. One additional tuning parameter is added, I_x, to control the high order of interactions caused by large values of M. $I_x = 0$ in all univariate estimation.

The SNP method distinguishes between several different lag descriptions. The total number of lags under consideration is denoted L. We then use the following notations:

L_u: Number of lags in VAR

L_g: Number of lags in GARCH

L_p: Total number of lags in the x part of the polynomial $P(z,x)$

L_r: Number of lags of y_t in R_x (number of lags in ARCH)

L_v: Lags in leverage effect of GARCH

L_w: Lags in additive level effect

Setting certain of the tuning parameters to zero will lead to strong restrictions on the process of $\{y_t\}$. These implied restrictions are shown in ***Table 15***. In this table, the parameters L_v and L_w are set to zero. The parameter I_x has no effect when $M = 1$ (Gallant and Tauchen 1990).

Table 15 *Restrictions Implied by Settings of the Tuning Parameters (Gallant and Tauchen 1990)*

SNP Models

Parameter setting						Characterization of $\{y_t\}$
$L_u = 0$	$L_g = 0$	$L_r \geq 0$	$L_p \geq 0$	$K_z = 0$	$K_x = 0$	Iid Gaussian
$L_u > 0$	$L_g = 0$	$L_r \geq 0$	$L_p \geq 0$	$K_z = 0$	$K_x = 0$	Gaussian VAR
$L_u > 0$	$L_g = 0$	$L_r \geq 0$	$L_p \geq 0$	$K_z > 0$	$K_x = 0$	Semi-parametric VAR
$L_u \geq 0$	$L_g = 0$	$L_r \geq 0$	$L_p \geq 0$	$K_z = 0$	$K_x = 0$	Gaussian ARCH
$L_u \geq 0$	$L_g = 0$	$L_r \geq 0$	$L_p \geq 0$	$K_z > 0$	$K_x = 0$	Semiparametric ARCH
$L_u \geq 0$	$L_g > 0$	$L_r \geq 0$	$L_p \geq 0$	$K_z = 0$	$K_x = 0$	Gaussian GARCH
$L_u \geq 0$	$L_g > 0$	$L_r \geq 0$	$L_p \geq 0$	$K_z > 0$	$K_x = 0$	Semi-parametric GARCH
$L_u \geq 0$	$L_g \geq 0$	$L_r \geq 0$	$L_p > 0$	$K_z > 0$	$K_x > 0$	Nonlinear nonparametric

The method starts by setting one lag in the VAR model, which is later extended to two lags. The lags in ARCH are set to find the best-fitted ARCH model, before adding a GARCH lag. The next is to check whether the leverage effect and additive level are significant. Applying the Schwarz criterion (Schwarz 1978) for model selection, we choose the best-fitted model before adding the degree of polynomials in z. We start with a polynomial degree of 4 (Gallant and Tauchen 1990) and extend this to 6 and 8, in order to find the model that gives us the best fit, being the model with the lowest BIC. We end up with a semi-nonparametric GARCH model for each of our datasets.

5.4.2 SNP- (univariate) Estimation

This section follows an estimation of the conditional density of the univariate return process. ***Table 16*** presents the final model selected for each of the time series. Again, $I_x = 0$ throughout the univariate estimation.

Table 16 *Univariate SNP estimation: Optimized Likelihood and Model Selection Criteria (Gallant and Tauchen 1990)*

Time series	L_u	L_p	L_r	L_g	L_v	L_w	K_z	K_x	I_x	S_n	AIC	HQ	BIC
DJI	2	1	1	1	1	0	8	0	0	1.17087	1.17279	1.17506	1.17940
FTSE	2	1	1	1	1	0	8	0	0	1.21589	1.21775	1.21995	1.22417
OEX	2	1	1	1	1	0	8	0	0	1.16065	1.16257	1.16484	1.16917
GSPC	2	1	1	1	1	0	8	0	0	1.15782	1.59730	1.16200	1.66340
OSEBX	2	1	1	1	1	0	8	0	0	1.19359	1.19552	1.19780	1.20215
OBX	1	1	1	1	0	0	4	0	0	1.19541	1.19741	1.19966	1.20380
OSEAX	2	1	1	1	1	0	4	0	0	1.20806	1.21027	1.21278	1.21738
MSFT	1	1	1	1	1	1	8	0	0	1.23311	1.23502	1.23729	1.24163
MU	2	1	1	1	1	0	6	0	0	1.25669	1.25934	1.26233	1.26784
NHY	2	1	1	1	1	0	6	0	0	1.23941	1.24207	1.24509	1.25062
TOM	1	1	1	1	1	1	8	0	0	1.23915	1.24223	1.24574	1.25220
Carbon	2	1	1	1	1	0	6	0	0	1.12172	2.12770	1.13385	1.44450
Brentoil	1	1	1	1	1	1	4	0	0	1.19643	1.20128	1.20628	1.21493
Salmon	2	1	1	1	1	0	8	0	0	1.21672	1.22256	1.22859	1.23943

5.4.2.1 Dow Jones Industrial Average (DJIA)

The specification tests for the optimal SNP GARCH model are reported in ***Table 17***. The residual statistics show that the data is closer to the normal distribution, with a kurtosis of 4.8. There is no volatility clustering, having *P*-values of 0.79 and 0.76 for Q^2 (12) and ARCH (12) respectively. The mean is approximately zero, and the standard deviation is one, referring to the normal distribution denoted as N (0, 1). There is still some dependency in the data. The null hypothesis of the BDS test is rejected, suggesting that the model is misspecified (Brock, Dechert et al. 1996). There is some structure in the data, which can include nonlinearity and nonstationarity. This problem often occurs when analyzing American indices, because they usually have very high liquidity. We choose to use the semi-nonparametric GARCH model as it is for the impulse response analysis, bearing in mind that the model can have sub-optimal performance.

Table 17 *Characteristics of the statistical SNP Model Residuals for the DJIA Index*

Residual Statistics for DJI Index

Mean	Median / Std.dev.	Maximum / Minimum	Moment Kurt/Skew	Quantile Kurt/Skew	Quantile Normal	Cramer-von-Mises	Serial dependence Q(12)	$Q^2(12)$
-0.00446	0.03016	4.37162	4.80183	0.18453	10.92827	4.23554	23.5224	7.9694
	0.99999	-11.37832	-0.64693	-0.02206	{0.0042}	{0.0000}	{0.0240}	{0.7900}

BDS-statistic (ε=1) m=2	m=3	m=4	m=5	ARCH (12)	VaR 2.5%/0.5%	CVaR 2.5%/0.5%
-4.533555	-4.106013	-3.781507	-3.105822	8.268002	-2.1112	-2.8217
{0.0000}	{0.0000}	{0.0002}	{0.0019}	{0.7639}	-3.0418	-4.2092

The figures in braces are P-values for statistical significance

The model selected under the Schwarz Criterion is a semi-nonparametric GARCH with eight Hermite polynomials (K_z) for non-normal features of the series. The model is a GARCH (1,1) (L_g, L_r) model with two lags in VAR (L_u). The asymmetric volatility effect is significant for the time series, which indicates that the volatility of the stock shows greater response to a negative shock than a positive shock. The eigenvalue of variance function is 0.9366, and the eigenvalue of the mean function is 0.1626, as shown below.

Table 18 *Statistical SNP Model Parameters for the DJIA Index*

DJI Index

Statistical Model SNP-11118000 -fit model
Parameters Semiparametric-GARCH.

η		Mode	Standard error
η_1	a0[1]	-0.00278	0.00613
η_2	a0[2]	-0.22329	0.01372
η_3	a0[3]	-0.00869	0.01117
η_4	a0[4]	0.08242	0.01771
η_5	a0[5]	0.03551	0.02545
η_6	a0[6]	-0.06772	0.02798
η_7	a0[7]	-0.02134	0.02447
η_8	a0[8]	0.06135	0.01439
η_9	A(1,1)	1.00000	0.00000
η_{10}	B(1,1)	-0.02409	0.01201
η_{11}	B(1,2)	-0.02644	0.01189
η_{12}	R0[1]	0.17211	0.00774
η_{13}	P(1,1)	0.20107	0.02496
η_{14}	Q(1,1)	0.94667	0.00298
η_{15}	V(1,1)	-0.50759	0.01778

Largest eigen value of mean function companion matrix = 0.162593
Largest eigen value of variance function P & Q companion matrix = 0.936619

Figure 27 displays the characteristics of the projected time series. The plots show the projected conditional volatility, together with a moving average (*m*=number of lags) of the squared residuals of an AR (1) regression model of the returns. It seems like the volatility change randomly, and the projected volatility tends to be relatively compact between *m*=4 and *m*=15. ***Figure 29*** displays the volatility at the mean of the time series, being the one-step-ahead densities $f_k(y_t|x_{t-1}.\theta)$, conditional on the values for x_{t-1} (where x_{t-1} = unconditional mean). The plot shows fatter tails than the normal distribution and advocatess only small non-normal elements of the time series. We find that the DJIA Index has a distribution that is narrower than the normal distribution. These features are commonly seen when analyzing data from a financial market, and confirm the purpose of using Hermite polynomials to describe the density in the best possible way. ***Figure 29*** shows the one-step-ahead densities of shocks ranging from - 40 % to + 40 %, together with the baseline profile (*m*=0.032451). Comparing the different impulse profiles to the baseline profile (the mean), we find that the densities are wider after adding an impulse (shock) to the series. The largest negative shock of - 40 % shows a much wider density compared to the equivalent positive shock. This indicates a higher degree of uncertainty after a negative shock and is a confirmation of the observed asymmetry. The relationship between the one-step-ahead dynamics of the conditional variance and the percentage growth is displayed in ***Figure 30***. The graph represents the reactions to shocks hitting the system (asset price). The difference in responses suggests asymmetry due to the "leverage -" and "risk premium" effects. For the DJIA Index, we find that the responses from negative shocks are much higher than from positive, showing an apparent asymmetry.

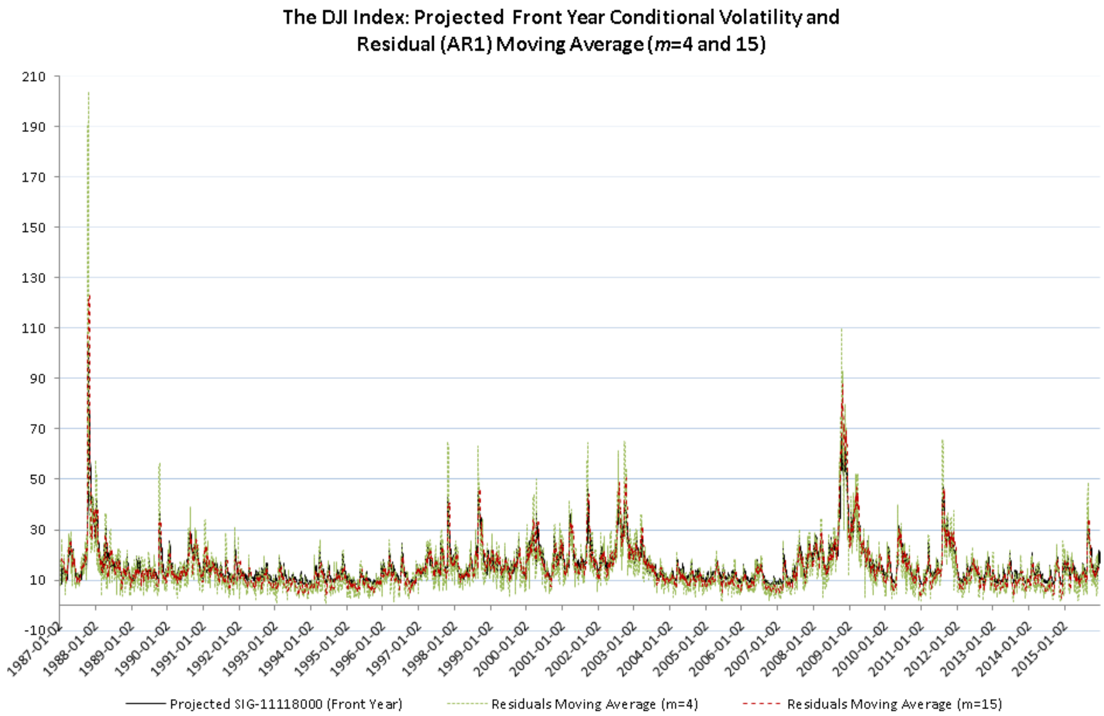

***Figure 27** Projected conditional volatility and residuals AR (1) moving average DJIA Index*

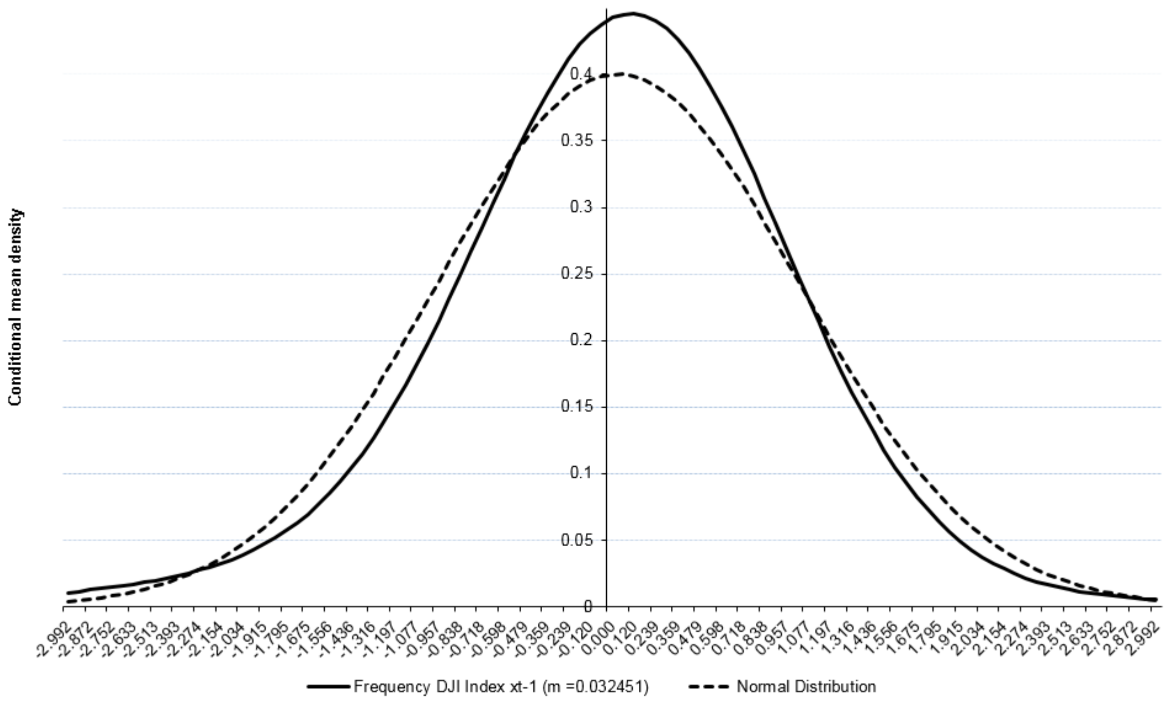

Figure 28 *DJIA Index one-step-ahead densities (x_{t-1} = unconditional mean)*

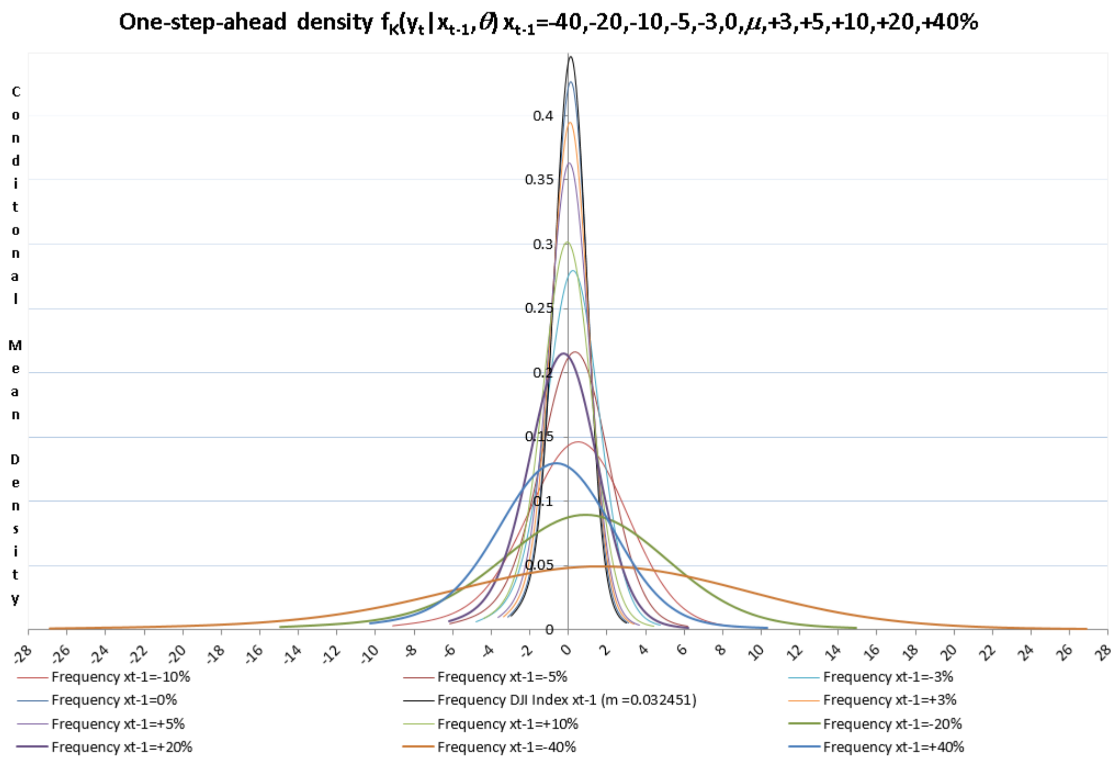

Figure 29 *DJIA Index one-step-ahead densities (conditional mean for x_{t-1} = -40%...40%)*

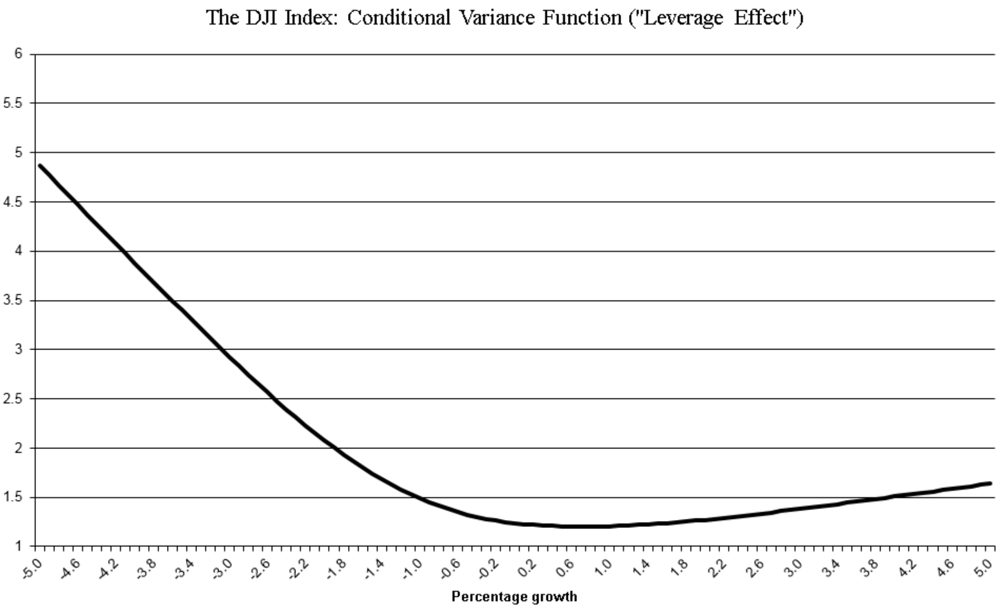

Figure 30 *DJIA Index: conditional variance functions*

5.4.2.2 FTSE 100 Index (FTSE)

The specification tests for the optimal SNP GARCH model are reported in ***Table 19.*** The residual statistics show that the data is closer to the normal distribution, with a kurtosis of 4.29. There is still some volatility clustering, having *P*-values of 0.026 and 0.024 for Q^2 (12) and ARCH (12) respectively. However, serial correlation is not present. The mean is approximately zero, and the standard deviation is one, referring to the normal distribution denoted as N (0, 1). The BDS-test show significant values at correlation dimension two and three. We choose to use the semi-nonparametric GARCH model as it is for the impulse response analysis, bearing in mind that the model can have sub-optimal performance (Brock, Dechert et al. 1996).

Table 19 *Characteristics of the statistical SNP Model Residuals for the FTSE Index*

Residual Statistics for FTSE 100 Index

Mean	Median / Std.dev.	Maximum / Minimum	Moment Kurt/Skew	Quantile Kurt/Skew	Quantile Normal	Cramer-von-Mises	Serial dependence Q(12)	Q^2(12)
0.00132	0.00319	6.06399	4.28767	0.08468	3.35076	2.05688	7.9332	23.223
	0.99998	-12.68592	-0.48338	0.02957	{0.1872}	{0.0000}	{0.7900}	{0.0260}
BDS-statistic (ε=1)				ARCH	VaR	CVaR		
m=2	m=3	m=4	m=5	(12)	2.5%/0.5%	2.5%/0.5%		
-3.514959	-2.527237	-1604985	-1.17713	23.44199	-2.0777	-2.6775		
{0.0006}	{0.0115}	{0.1085}	{0.2391}	{0.0242}	-2.9755	-3.7720		

The figures in braces are P-values for statistical significance

The model selected under the Schwarz Criterion is a semi-nonparametric GARCH with eight Hermite polynomials (K_z) for non-normal features of the series. The model is a GARCH (1,1) (L_g, L_r) model with two lags in VAR (L_u). The asymmetric volatility effect is significant for the time series, which indicates that the volatility of the stock shows greater response to a negative shock than a positive shock. The eigenvalue of variance function is 0.9593, and the eigenvalue of the mean function is 0.1105, as shown in the table below.

Table 20 *Statistical SNP Model Parameters for the FTSE Index*

FTSE 100 Index

Satistical Model SNP-11118000-fit model
Parameters Semiparametric-GARCH

η		Mode	Standard error
η_1	a0[1]	-0.01339	0.00631
η_2	a0[2]	-0.26162	0.01078
η_3	a0[3]	-0.02055	0.00831
η_4	a0[4]	0.10712	0.00971
η_5	a0[5]	0.01947	0.00760
η_6	a0[6]	-0.07512	0.01007
η_7	a0[7]	-0.01620	0.01040
η_8	a0[8]	0.04507	0.01268
η_9	A(1,1)	1.00000	0.00000
η_{10}	B(1,1)	0.00336	0.01213
η_{11}	B(1,2)	-0.01222	0.01173
η_{12}	R0[1]	0.17194	0.01115
η_{13}	P(1,1)	0.22421	0.03156
η_{14}	Q(1,1)	0.95341	0.00316
η_{15}	V(1,1)	-0.50088	0.02003

Largest eigen value of mean function companion matrix = 0.110542
Largest eigen value of variance function P & Q companion matrix = 0.959266

Figure 31 displays the characteristics of the projected time series. The plots show the projected conditional volatility, together with a moving average (*m*=number of lags) of the squared residuals of an AR (1) regression model of the returns. It seems like the volatility change randomly, and the projected volatility tends to be relatively compact between *m*=4 and *m*=15. ***Figure 32*** displays the volatility at the mean of the time series, being the one-step-ahead densities $f_k(y_t|x_{t-1}.\theta)$, conditional on the values for x_{t-1} (where x_{t-1} =

unconditional mean). The plot shows slightly fatter tails than the normal distribution and advocates only small non-normal elements of the time series. We find that the FTSE Index has a distribution that is narrower than the normal distribution. These features are commonly seen when analyzing data from a financial market, and confirm the purpose of using Hermite polynomials to describe the density in the best possible way. ***Figure 33*** shows the one-step-ahead densities of shocks ranging from - 40 % to + 40 %, together with the baseline profile (m=0.013947). Comparing the different impulse profiles to the baseline profile (the mean), we find that the densities are wider after adding an impulse (shock) to the series. The largest negative shock of - 40 % shows a much wider density compared to the equivalent positive shock. This indicates a higher degree of uncertainty after a negative shock and is a confirmation of the observed asymmetry. The relationship between the one-step-ahead dynamics of the conditional variance and the percentage growth is displayed in ***Figure 34***. The graph represents the reactions to shocks hitting the system (asset price). The difference in responses suggests asymmetry due to the "leverage -" and "risk premium" effects. For the FTSE Index, we find that the responses from negative shocks are much higher than from positive, showing an apparent asymmetry.

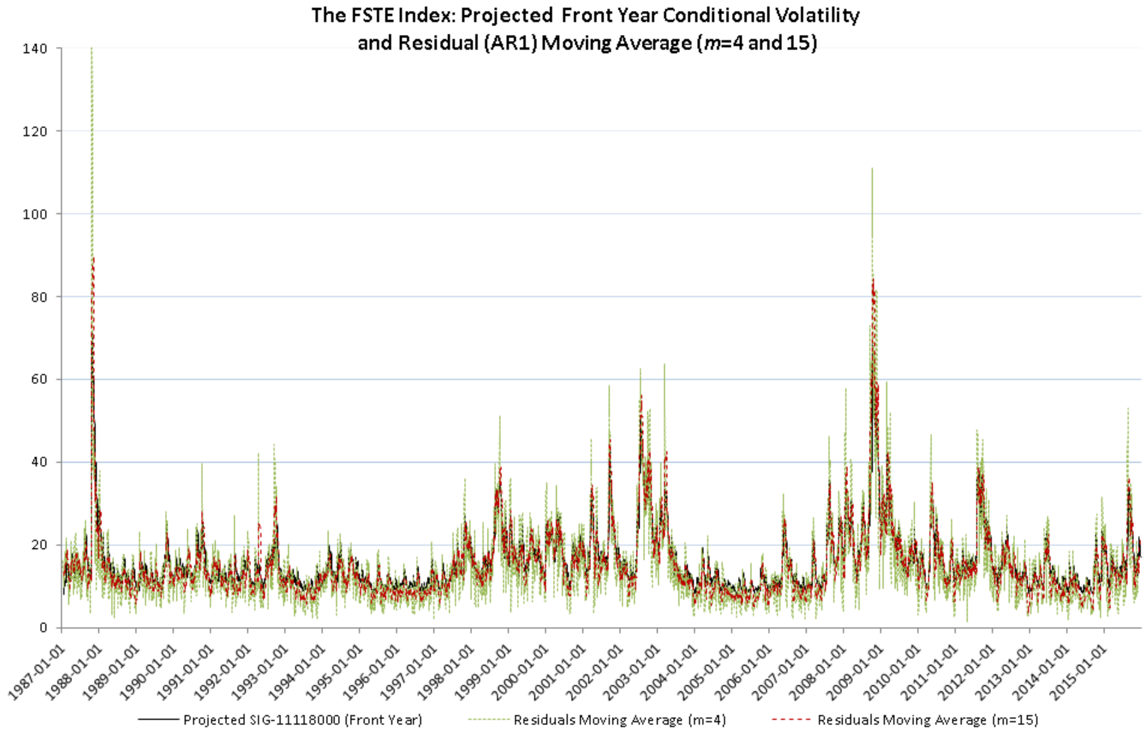

Figure 31 *Projected conditional volatility and residuals AR (1) moving average FTSE Index*

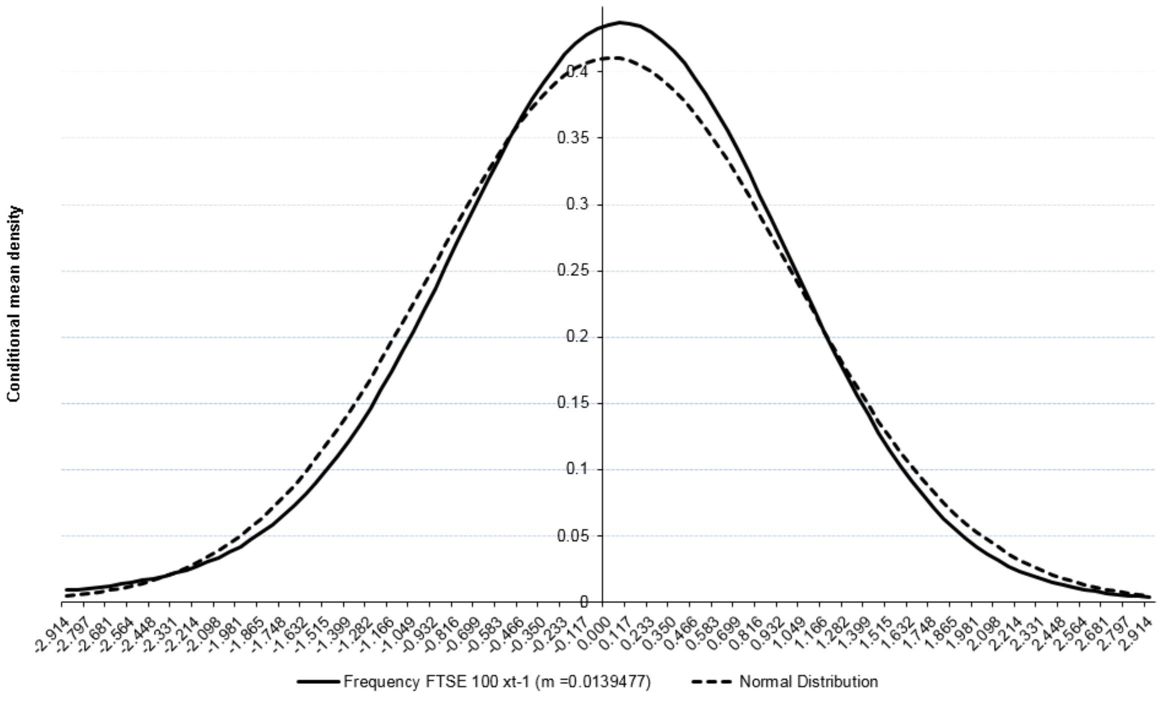

Figure 32 *FTSE Index one-step-ahead densities (x_{t-1} = unconditional mean)*

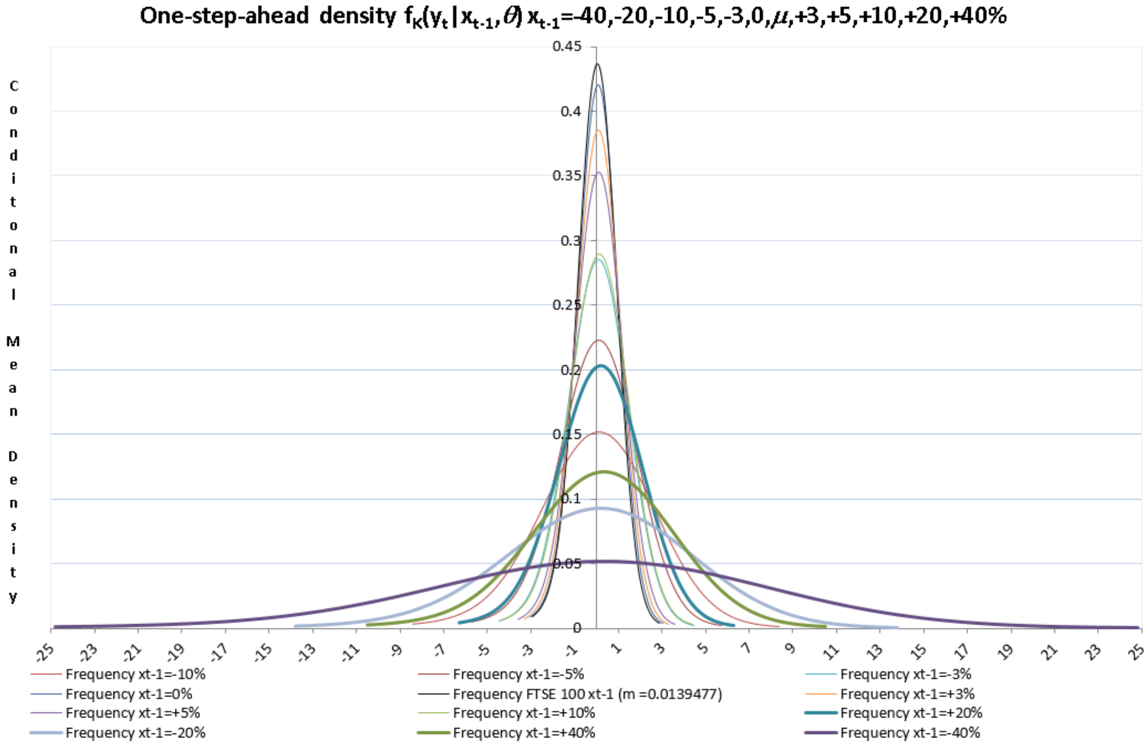

Figure 33 *FTSE Index one-step-ahead densities (conditional mean for x_{t-1} = -40%...40%)*

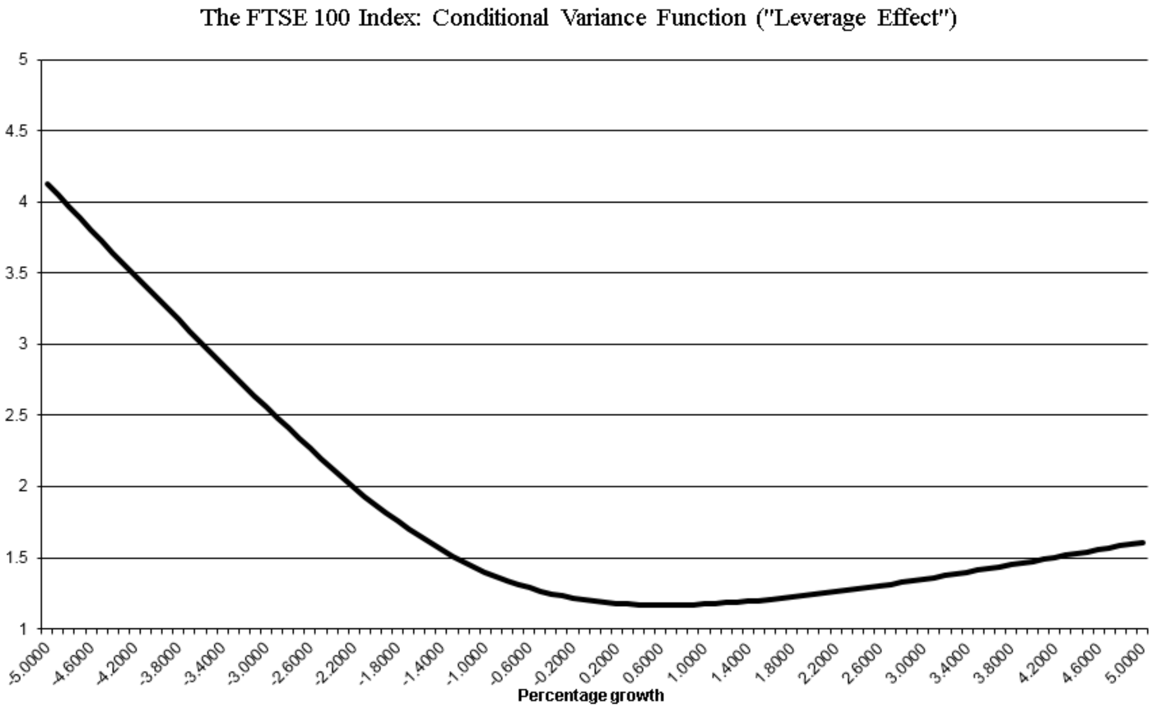

Figure 34 *FTSE Index: conditional variance function*

5.4.2.3 S&P 100 Index (OEX)

The specification tests for the optimal SNP GARCH model are reported in ***Table 21***. The residual statistics show that the data is closer to the normal distribution, with a kurtosis of 3.9. There is no volatility clustering, having *P*-values of 0.94 and 0.93 for Q^2 (12) and ARCH (12) respectively. The mean is approximately zero, and the standard deviation is one, referring to the normal distribution denoted as N (0, 1). There is still some dependency in the data. The null hypothesis of the BDS test is rejected, suggesting that the model is misspecified (Brock, Dechert et al. 1996). There is some structure in the data, which can include nonlinearity and nonstationarity. This problem often occurs when analyzing American indices, because they are characterized by having very high liquidity. We choose to use the semi-nonparametric GARCH model as it is for the impulse response analysis, bearing in mind that the model can have sub-optimal performance.

Table 21 *Characteristics of the statistical SNP Model Residuals for the S&P 100 Index*

Residual Statistics for S&P 100 Index

Mean	Median / Std.dev.	Maximum / Minimum	Moment Kurt/Skew	Quantile Kurt/Skew	Quantile Normal	Cramer-von-Mises	Serial dependence Q(12)	Q^2(12)
-0.00011	0.03987	4.79848	3.89974	0.16895	9.67359	4.33546	26.3970	5.5327
	0.99995	-10.37470	-0.60000	-0.02859	{0.0079}	{0.0000}	{0.0090}	{0.9380}
BDS-statistic (ε=1)				ARCH	VaR	CVaR		
m=2	m=3	m=4	m=5	(12)	2.5%/0.5%	2.5%/0.5%		
-5.195092	-3.972041	-3.62307	-2.793552	5.704204	-2.1304	-2.8089		
{0.0000}	{0.0001}	{0.0003}	{0.0052}	{0.9303}	-3.0490	-4.1558		

The figures in braces are P-values for statistical significance

The model selected under the Schwarz Criterion is a semi-nonparametric GARCH with eight Hermite polynomials (K_z) for non-normal features of the series. The model is a GARCH (1,1) (L_g, L_r) model with two lags in VAR (L_u). The asymmetric volatility effect is significant for the time series, which indicates that the volatility of the stock shows greater response to a negative shock than a positive shock. The eigenvalue of variance function is 0.9236, and the eigenvalue of the mean function is 0.1645, as shown below.

Table 22 *Statistical SNP Model Parameters for the S&P 100 Index*

S&P 100 Index

Statistical Model SNP-11118000 -fit model
Parameters Semiparametric-GARCH.

η		Mode	Standard error
η_1	a0[1]	-0.00643	0.00601
η_2	a0[2]	-0.13593	0.01041
η_3	a0[3]	-0.04775	0.00599
η_4	a0[4]	0.06401	0.00664
η_5	a0[5]	-0.00643	0.00751
η_6	a0[6]	-0.03814	0.00909
η_7	a0[7]	-0.01826	0.00901
η_8	a0[8]	0.05169	0.00845
η_9	A(1,1)	1.00000	0.00000
η_{10}	B(1,1)	-0.04181	0.01248
η_{11}	B(1,2)	-0.02707	0.01180
η_{12}	R0[1]	0.13555	0.00720
η_{13}	P(1,1)	-0.13319	0.02974
η_{14}	Q(1,1)	0.95176	0.00300
η_{15}	V(1,1)	-0.44466	0.01393

Largest eigen value of mean function companion matrix = 0.164542
Largest eigen value of variance function P & Q companion matrix = 0.923583

Figure 35 displays the characteristics of the projected time series. The plots show the projected conditional volatility, together with a moving average (*m*=number of lags) of the squared residuals of an AR (1) regression model of the returns. It seems like the volatility change randomly, and the projected volatility tends to be relatively compact between *m*=4 and *m*=15. ***Figure 36*** displays the volatility at the mean of the time series, being the one-step-ahead densities $f_k(y_t|x_{t-1}.\theta)$, conditional on the values for x_{t-1} (where x_{t-1} = unconditional mean). The plot shows slightly fatter tails than the normal distribution and advocates only small non-normal elements of the time series. We find that the S&P 100 Index has a distribution that is narrower than the normal distribution. These features are commonly seen when analyzing data from a financial market, and confirm the purpose of using Hermite polynomials to describe the density in the best possible way. ***Figure 37*** shows the one-step-ahead densities of shocks ranging from - 40 % to + 40 %, together with the baseline profile (*m*=0.025360). Comparing the different impulse profiles to the baseline profile (the mean), we find that the densities are wider after adding an impulse (shock) to the series. The largest negative shock of - 40 % shows a much wider density compared to the equivalent positive shock. This indicates a higher degree of uncertainty after a negative shock and is a confirmation of the observed asymmetry. The relationship between the one-step-ahead dynamics of the conditional variance and the percentage growth is displayed in ***Figure 38***. The graph represents the reactions to shocks hitting the system (asset price). The difference in responses suggests asymmetry due to the "leverage -" and "risk premium" effects. For the S&P 100 Index, we find that the responses from negative shocks are much higher than from positive, showing an apparent asymmetry.

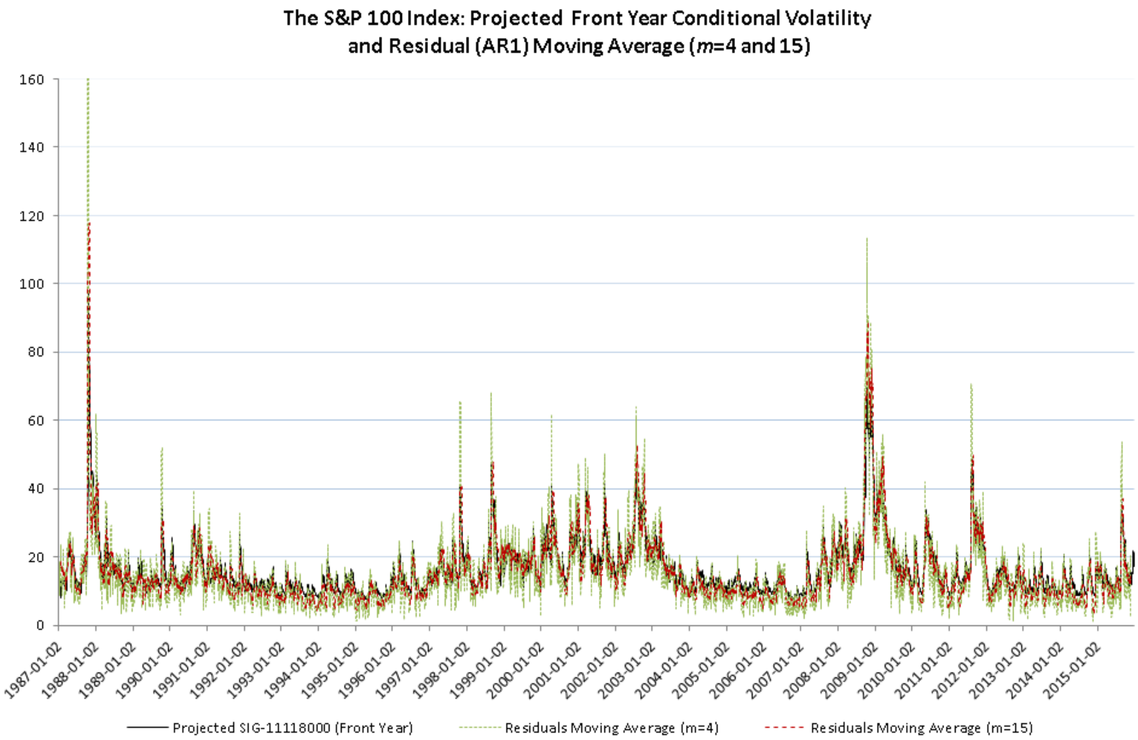

Figure 35 *Projected conditional volatility and residuals AR (1) moving average S&P 100 Index*

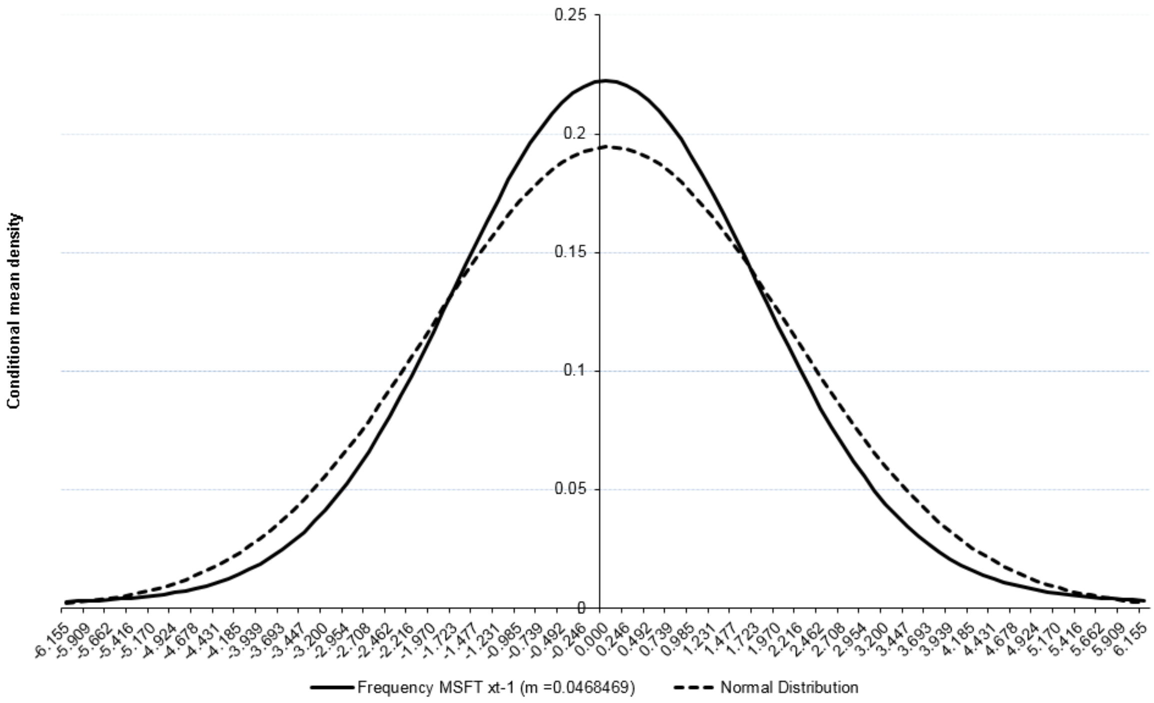

Figure 36 *S&P 100 Index one-step-ahead densities (x_{t-1} = unconditional mean)*

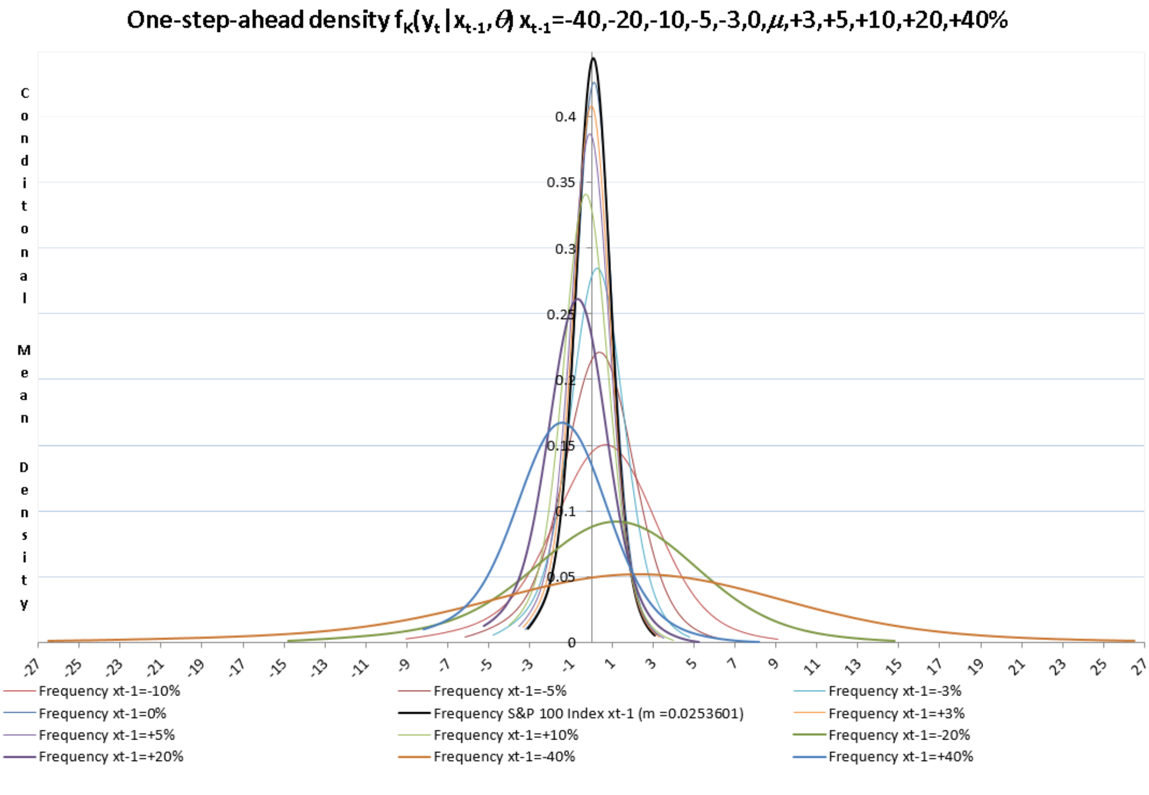

Figure 37 *S&P Index one-step-ahead densities (conditional mean for x_{t-1} = -40%...40%)*

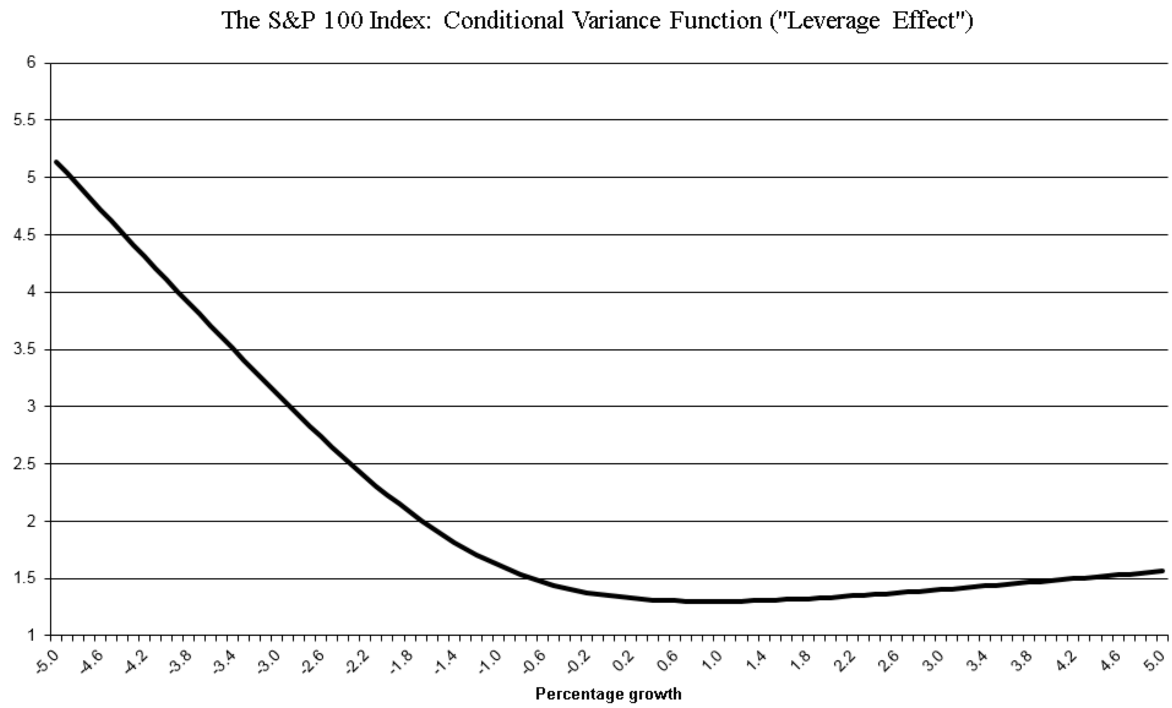

Figure 38 *S&P 100 Index: conditional variance functions*

5.4.2.4 S&P 500 Index (GSPC)

The specification tests for the optimal SNP GARCH model are reported in ***Table 23***. The residual statistics show that the data is closer to the normal distribution, with a kurtosis of 3.7. There is no volatility clustering, having *P*-values of 0.99 and 0.98 for Q^2 (12) and ARCH (12) respectively. The mean is approximately zero, and the standard deviation is one, referring to the normal distribution denoted as N (0, 1). There is still some dependency in the data. The null hypothesis of the BDS test is rejected, suggesting that the model is misspecified (Brock, Dechert et al. 1996). There is some structure in the data, which can include nonlinearity and nonstationarity. This problem often occurs when analyzing American indices, because they usually have very high liquidity. We choose to use the semi-nonparametric GARCH model as it is for the impulse response analysis, bearing in mind that the model can have sub-optimal performance.

***Table 23** Characteristics of the statistical SNP Model Residuals for the S&P 500 Index*

Residual Statistics for S&P 500 Index

Mean	Median / Std.dev.	Maximum / Minimum	Moment Kurt/Skew	Quantile Kurt/Skew	Quantile Normal	Cramer-von-Mises	Serial dependence Q(12)	$Q^2(12)$
-0.00006	0.04004	4.80374	3.68508	0.18374	11.00142	4.43498	17.7250	3.9154
	1.00000	-10.09384	-0.60934	-0.02459	{0.0041}	{0.0000}	{0.1240}	{0.9850}
BDS-statistic (ε=1)				ARCH	VaR	CVaR		
m=2	m=3	m=4	m=5	(12)	2.5%/0.5%	2.5%/0.5%		
-5.759872	-4.589539	-4.148204	-3.372182	4.310437	-2.1351	-2.8112		
{0.0000}	{0.0000}	{0.0000}	{0.0007}	{0.9772}	-3.1117	-4.1868		

The figures in braces are P-values for statistical significance

The model selected under the Schwarz Criterion is a semi-nonparametric GARCH with eight Hermite polynomials (K_z) for non-normal features of the series. The model is a GARCH (1,1) (L_g, L_r) model with two lags in VAR (L_u). The asymmetric volatility effect is significant for the time series, which indicates that the volatility of the stock shows greater response to a negative shock than a positive shock. The eigenvalue of variance function is 0.9125, and the eigenvalue of the mean function is 0.1725, as shown in the table below.

***Table 24** Statistical SNP Model Parameters for the S&P 500 Index*

S&P 500 Index

Statistical Model SNP-11118000 -fit model
Parameters Semiparametric-GARCH.

η		Mode	Standard error
η_1	a0[1]	-0.00747	0.00607
η_2	a0[2]	-0.14977	0.01122
η_3	a0[3]	-0.04480	0.00621
η_4	a0[4]	0.07470	0.00708
η_5	a0[5]	0.00083	0.00696
η_6	a0[6]	-0.03624	0.00821
η_7	a0[7]	-0.02431	0.00847
η_8	a0[8]	0.04459	0.00864
η_9	A(1,1)	1.00000	0.00000
η_{10}	B(1,1)	-0.01816	0.01270
η_{11}	B(1,2)	-0.02975	0.01193
η_{12}	R0[1]	0.14266	0.00748
η_{13}	P(1,1)	-0.09635	0.03819
η_{14}	Q(1,1)	0.95037	0.00314
η_{15}	V(1,1)	-0.48443	0.01449

Largest eigen value of mean function companion matrix = 0.172472
Largest eigen value of variance function P & Q companion matrix = 0.912488

Figure 39 displays the characteristics of the projected time series. The plots show the projected conditional volatility, together with a moving average (*m*=number of lags) of the squared residuals of an AR (1) regression model of the returns. It seems like the volatility change randomly, and the projected volatility tends to be relatively compact between *m*=4 and *m*=15. ***Figure 40*** displays the volatility at the mean of the time series, being the one-step-ahead densities $f_k(y_t|x_{t-1}.\theta)$, conditional on the values for x_{t-1} (where x_{t-1} = unconditional mean). The plot shows fatter tails than the normal distribution and advocates only small non-normal elements of the time series. We find that the S&P 500 Index has a distribution that is narrower than the normal distribution. These features are commonly seen when analyzing data from a financial market, and confirm the purpose of using Hermite polynomials to describe the density in the best possible way. ***Figure 41*** shows the one-step-ahead densities of shocks ranging from - 40 % to + 40 %, together with the baseline profile (*m*=0.025313). Comparing the different impulse profiles to the baseline profile (the mean), we find that the densities are wider after adding an impulse (shock) to the series. The largest negative shock of - 40 % shows a much wider density compared to the equivalent positive shock. This indicates a higher degree of uncertainty after a negative shock and is a confirmation of the observed asymmetry. The relationship between the one-step-ahead dynamics of the conditional variance and the percentage growth is displayed in ***Figure 42***. The graph represents the reactions to shocks hitting the system (asset price). The difference in responses suggests asymmetry due to the “leverage -” and “risk premium” effects. For the S&P 500 Index, we find that the responses from negative shocks are much higher than from positive, showing an apparent asymmetry.

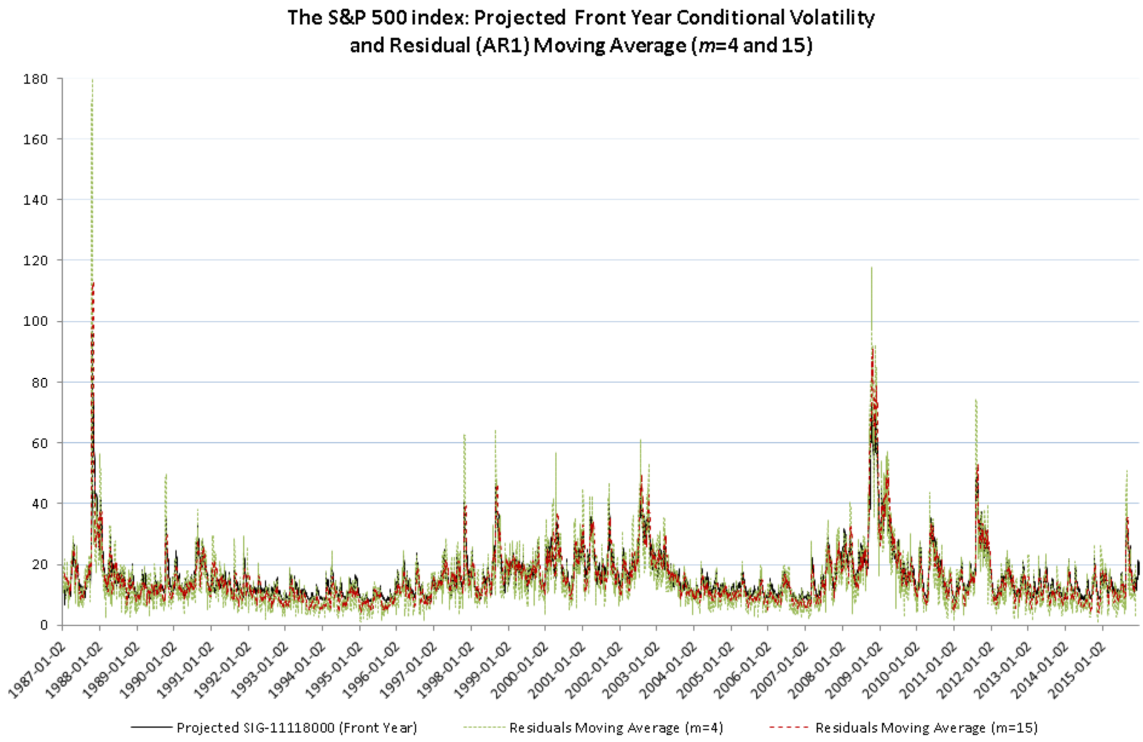

Figure 39 *Projected conditional volatility and residuals AR (1) moving average S&P 500 Index*

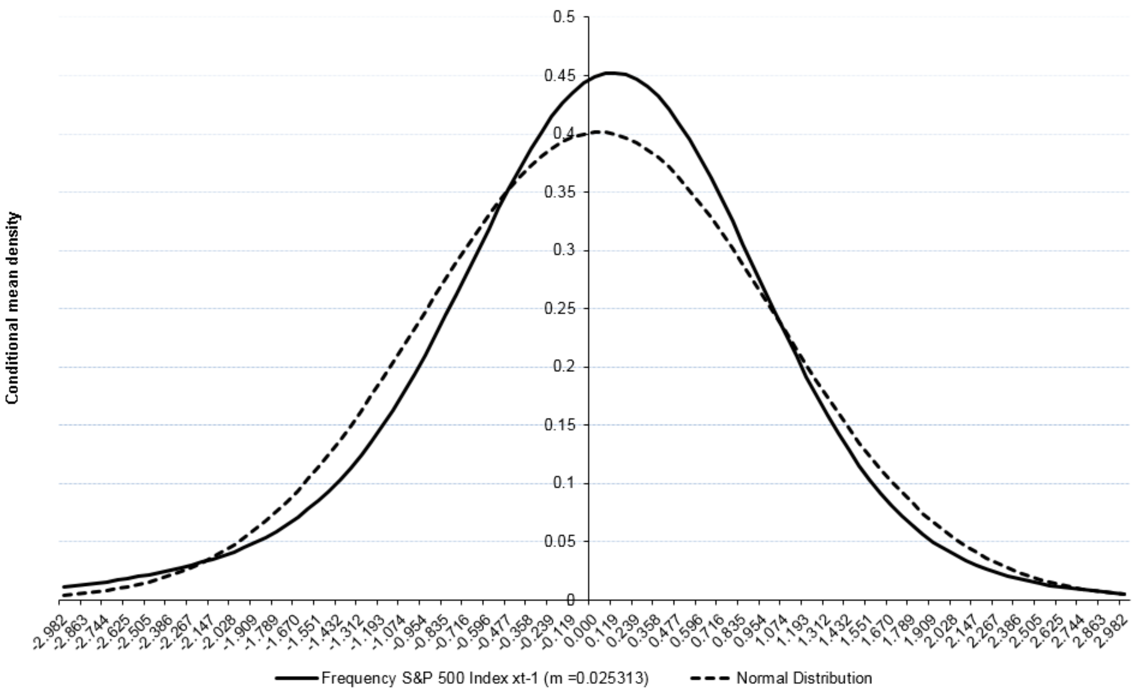

Figure 40 *S&P 500 Index one-step-ahead densities (x_{t-1} = unconditional mean)*

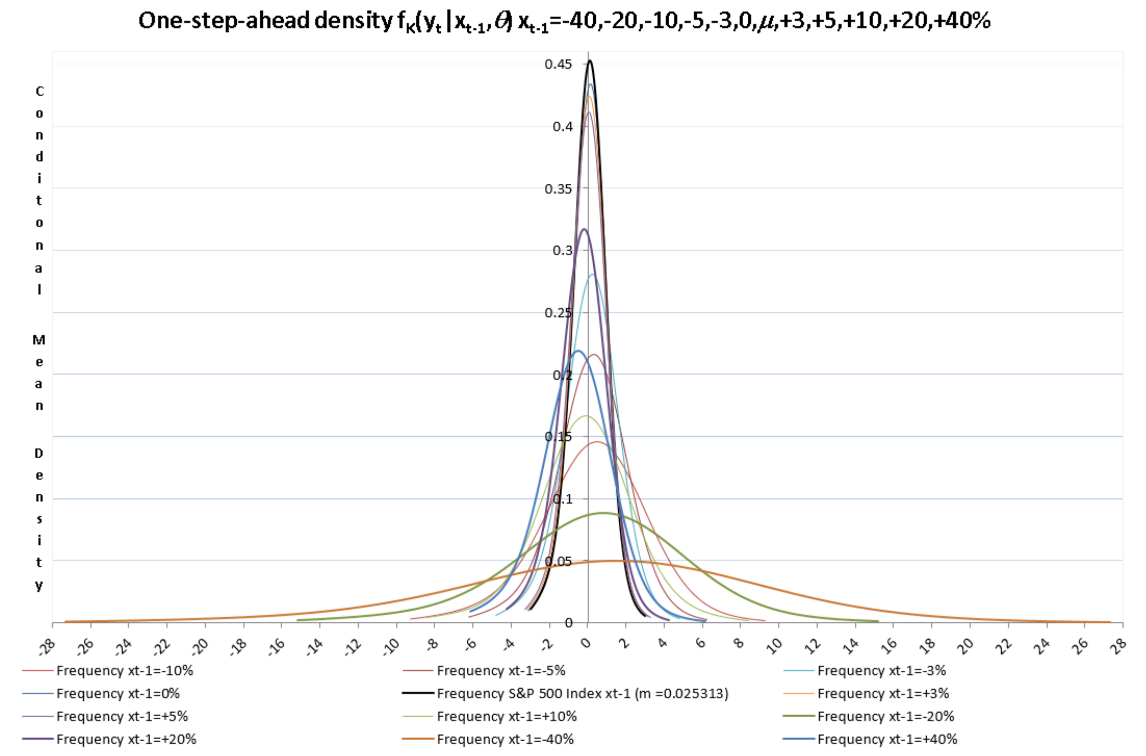

***Figure 41** S&P 500 Index one-step-ahead densities (conditional mean for x_{t-1} = -40%...40%)*

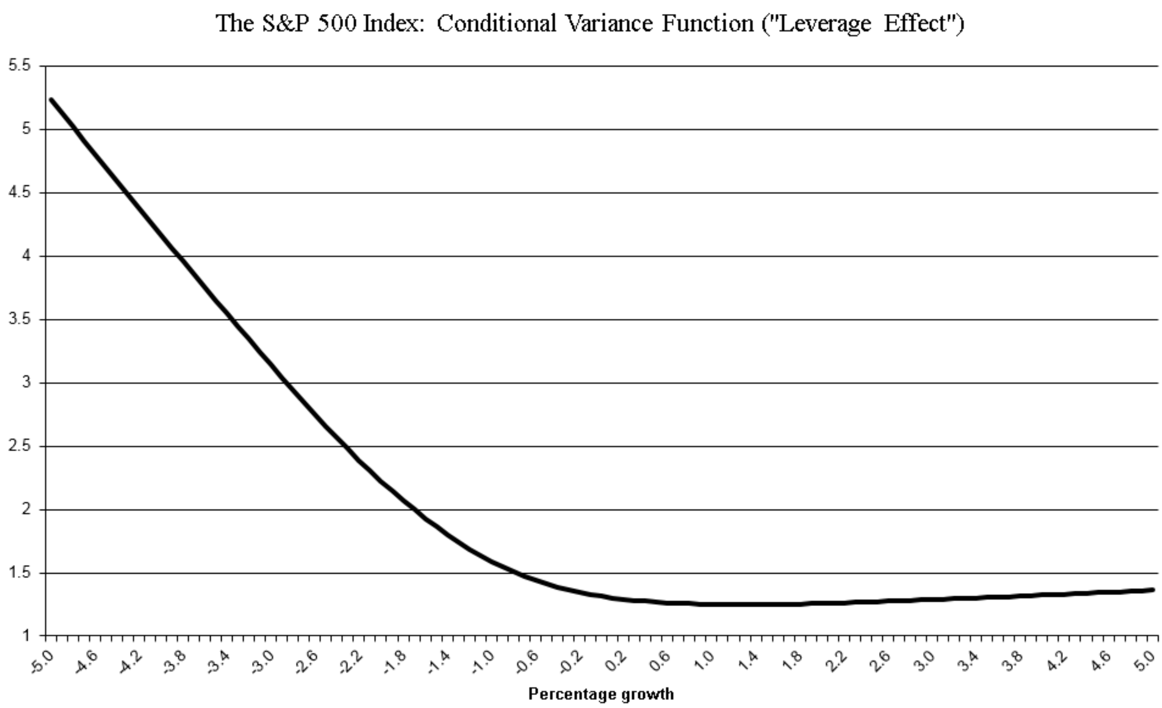

***Figure 42** S&P 500 Index: conditional variance function*

5.4.2.5 Oslo Stock Exchange Benchmark Index (OSEBX)

The specification tests for the optimal SNP GARCH model are reported in ***Table 25***. The residual statistics show that the data is closer to the normal distribution, with a kurtosis of 4.0. There is no volatility clustering, having *P*-values of 0.77 and 0.76 for Q^2 (12) and ARCH (12) respectively. The mean is approximately zero, and the standard deviation is one, referring to the normal distribution denoted as N (0, 1). The BDS-test states that the residuals are IID, meaning data dependence is no longer present. By this, the model misspecification seems minimized, and the semi-nonparametric GARCH model is selected for the impulse response analysis.

Table 25 *Characteristics of the statistical SNP Model Residuals for the OSEBX Index*

Residual Statistics for OSEBX Index

Mean	Median /	Maximum /	Moment	Quantile	Quantile	Cramer-	Serial dependence	
	Std.dev.	Minimum	Kurt/Skew	Kurt/Skew	Normal	von-Mises	Q(12)	Q^2(12)
-0.00129	0.02802	5.46626	4.01469	0.06710	1.73512	1.86231	25.9510	8.2287
	0.99999	-11.63768	-0.46320	-0.01753	{0.4200}	{0.0000}	{0.0110}	{0.7670}
BDS-statistic (ε=1)				ARCH	VaR	CVaR		
m=2	m=3	m=4	m=5	(12)	2.5%/0.5%	2.5%/0.5%		
-0.553981	0.042615	0.256883	0.240129	8.264149	-2.0319	-2.7096		
{0.5796}	{0.9660}	{0.7973}	{0.8102}	{0.7642}	-2.9826	-3.8825		

The figures in braces are P-values for statistical significance

The model selected under the Schwarz Criterion is a semi-nonparametric GARCH with eight Hermite polynomials (K_z) for non-normal features of the series. The model is a GARCH (1,1) (L_g, L_r) model with two lags in VAR (L_u). The asymmetric volatility effect is significant for the time series, which indicates that the volatility of the stock shows greater response to a negative shock than a positive shock. The eigenvalue of variance function is 0.9760, and the eigenvalue of the mean function is 0.1591, as shown in the table below.

Table 26 *Statistical SNP Model Parameters for the OSEBX Index*

OSEBX Index			
Satistical Model SNP-11118000-fit model			
Parameters Semiparametric-GARCH			
η		Mode	Standard error
η_1	a0[1]	-0.00079	0.00626
η_2	a0[2]	-0.23476	0.01177
η_3	a0[3]	-0.01878	0.00658
η_4	a0[4]	0.09616	0.00810
η_5	a0[5]	0.01419	0.00774
η_6	a0[6]	-0.06356	0.00901
η_7	a0[7]	-0.02146	0.00940
η_8	a0[8]	0.05424	0.00966
η_9	A(1,1)	1.00000	0.00000
η_{10}	B(1,1)	0.08596	0.01235
η_{11}	B(1,2)	0.01164	0.01224
η_{12}	R0[1]	0.21904	0.01127
η_{13}	P(1,1)	0.35046	0.02792
η_{14}	Q(1,1)	0.92370	0.00499
η_{15}	V(1,1)	-0.51624	0.02753

Largest eigen value of mean function companion matrix = 0.159096
Largest eigen value of variance function P & Q companion matrix = 0.976037

Figure 43 displays the characteristics of the projected time series. The plots show the projected conditional volatility, together with a moving average (m=number of lags) of the squared residuals of an AR (1) regression model of the returns. It seems like the volatility change randomly, and the projected volatility tends to be relatively compact between m=4 and m=15. ***Figure 44*** displays the volatility at the mean of the time series, being the one-step-ahead densities $f_k(y_t|x_{t-1}.\theta)$, conditional on the values for x_{t-1} (where x_{t-1} = unconditional mean). The plot shows fatter tails than the normal distribution and advocates only small non-normal elements of the time series. We find that the OSEBX Index has a distribution that is narrower than the normal distribution. These features are commonly seen when analyzing data from a financial market, and confirm the purpose of using Hermite polynomials to describe the density in the best possible way. ***Figure 45*** shows the one-step-ahead densities of shocks ranging from - 40 % to + 40 %, together with the baseline profile (m=0.049823). Comparing the different impulse profiles to the baseline profile (the mean), we find that the densities are wider after adding an impulse (shock) to the series. The largest negative shock of - 40 % shows a much wider density compared to the equivalent positive shock. This indicates a higher degree of uncertainty after a negative shock and is a confirmation of the observed asymmetry. The relationship between the one-step-ahead dynamics of the conditional variance and the percentage growth is displayed in ***Figure 46***. The graph represents the reactions to shocks hitting the system (asset price). The difference in responses suggests asymmetry due to the “leverage -” and “risk premium” effects. For the OSEBX Index, we find that the responses from negative shocks are much higher than from positive, showing an apparent asymmetry.

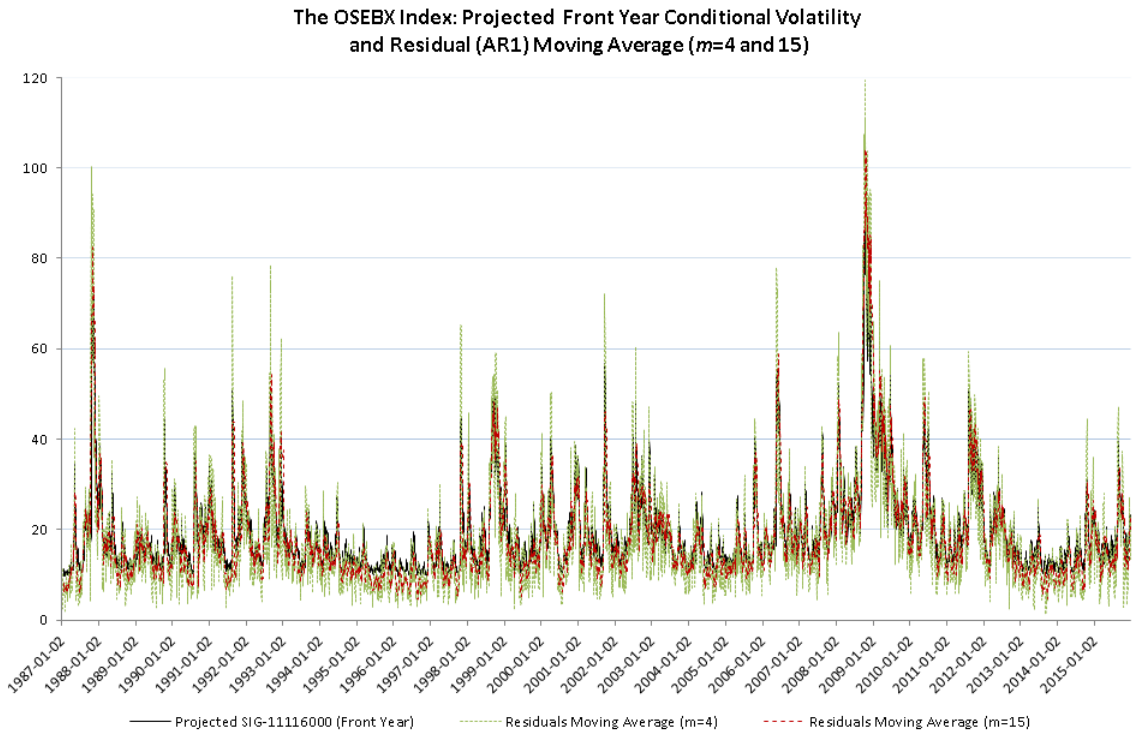

Figure 43 *Projected conditional volatility and residuals AR (1) moving average OSEBX Index*

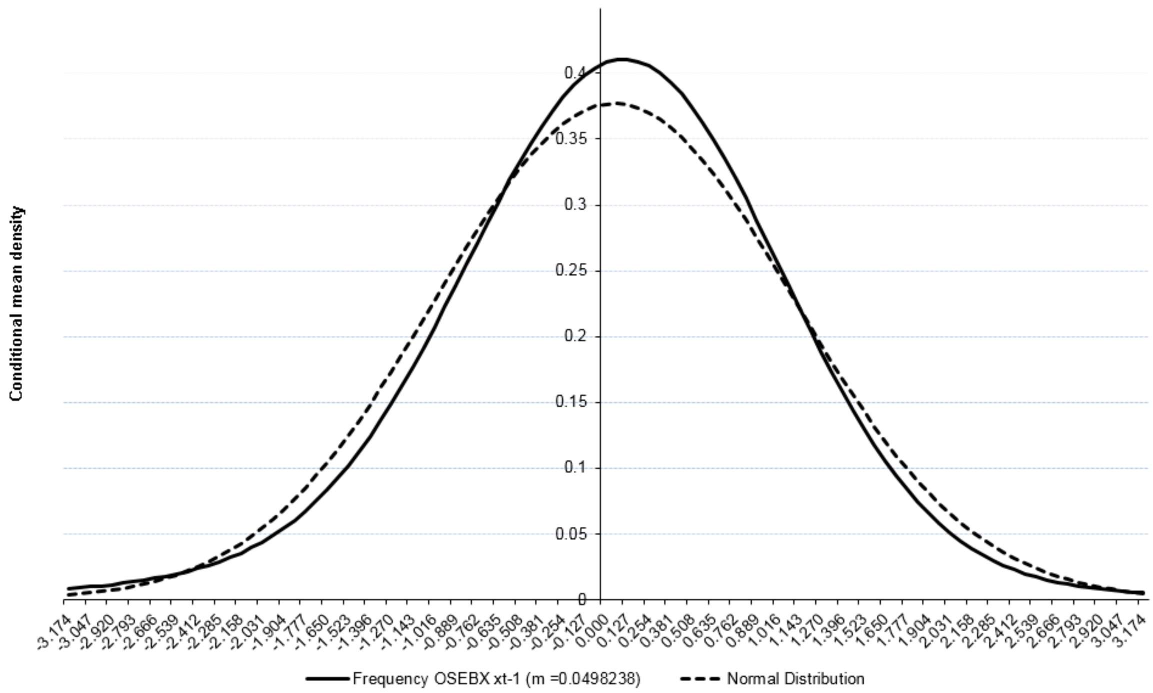

Figure 44 *OSEBX one-step-ahead densities (x_{t-1} = unconditional mean)*

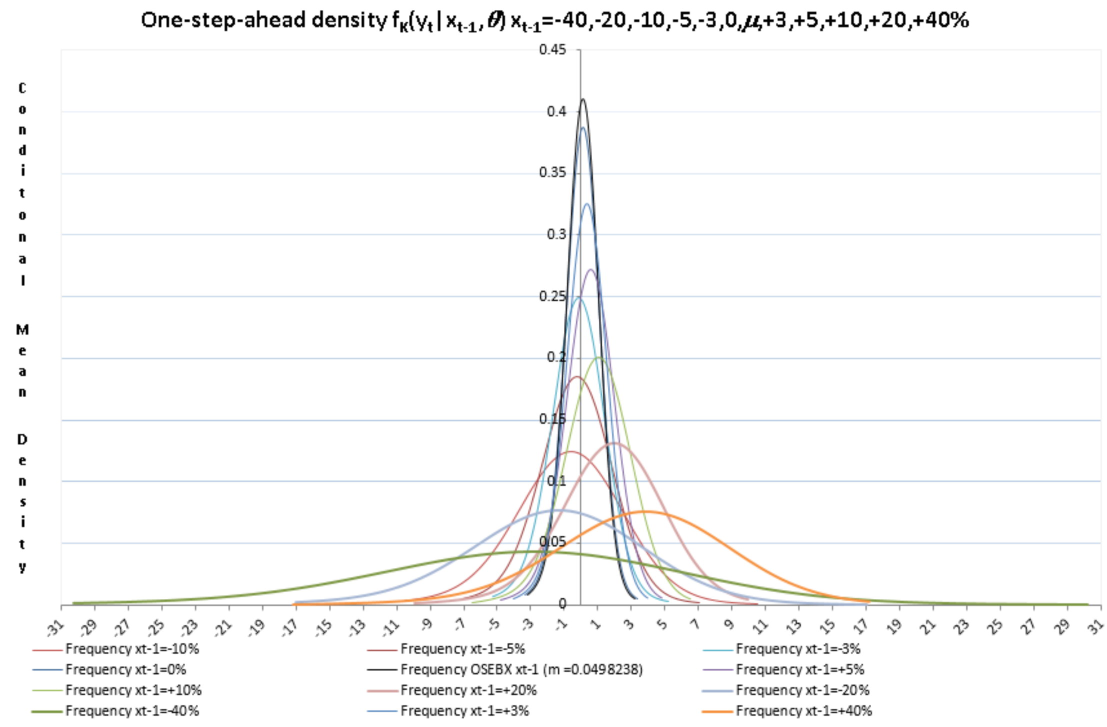

Figure 45 *OSEBX Index one-step-ahead densities (conditional mean for x_{t-1} = -40%...40%)*

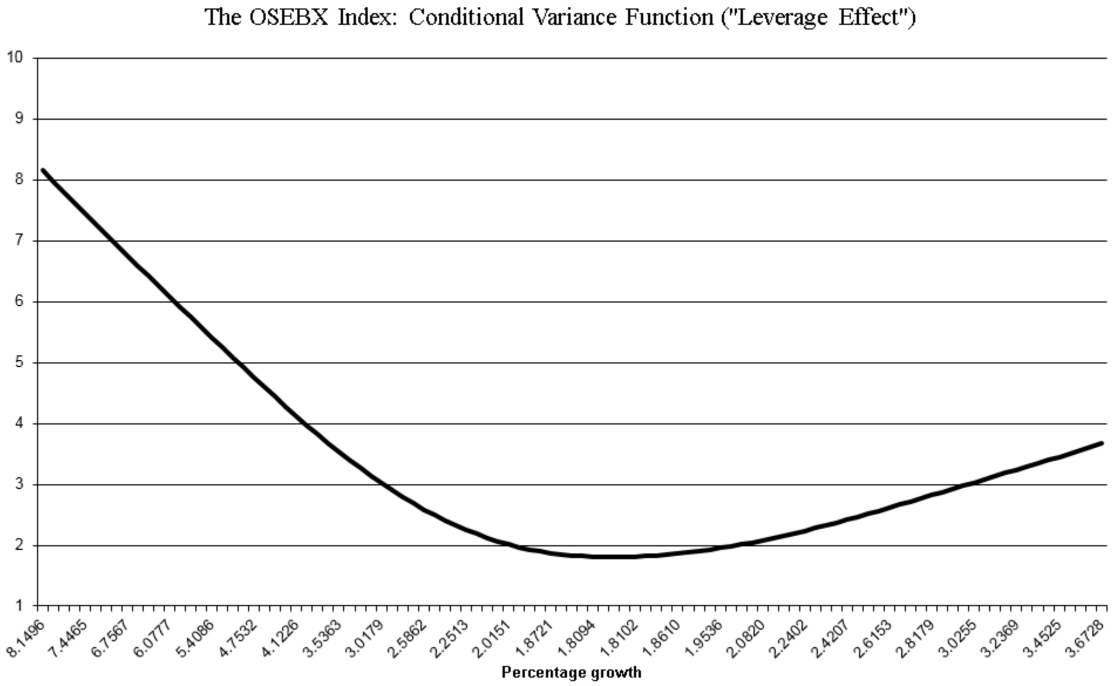

Figure 46 *OSEBX Index: conditional variance functions*

5.4.2.6 Oslo Stock Exchange Index (OBX)

The specification tests for the optimal SNP GARCH model are reported in ***Table 27***. The residual statistics show that the data is closer to the normal distribution, with a kurtosis of 0.6. There is no volatility clustering, having *P*-values of 0.40 and 0.43 for Q^2 (12) and ARCH (12) respectively. The mean is approximately zero, and the standard deviation is one, referring to the normal distribution denoted as N (0, 1). The BDS-test states that the residuals are IID, meaning data dependence is no longer present. By this, the model misspecification seems minimized, and the semi-nonparametric GARCH model is selected for the impulse response analysis.

Table 27 *Characteristics of the statistical SNP Model residuals for the OBX Index*

Residual Statistics for OBX-index

Mean	Median / Std.dev.	Maximum / Minimum	Moment Kurt/Skew	Quantile Kurt/Skew	Quantile Normal	Cramer-von-Mises	Serial dependence Q(12)	Q^2(12)
0.00208	0.04809	4.53259	0.60579	0.04259	0.95732	1.02467	8.6257	12.584
	1.00001	-4.12109	-0.23199	-0.02869	{0.6196}	{0.0000}	{0.7350}	{0.4000}

BDS-statistic (ε=1) m=2	m=3	m=4	m=5	ARCH (12)	VaR 2.5%/0.5%	CVaR 2.5%/0.5%
-0.372445	0.206405	0.740186	0.950046	12.22452	-2.1379	-2.6230
{0.7096}	{0.8365}	{0.4592}	{0.3421}	{0.4278}	-2.8972	-3.3131

The figures in braces are P-values for statistical significance

The model selected under the Schwarz Criterion is a semi-nonparametric GARCH with four Hermite polynomials (K_z) for non-normal features of the series. The model is a GARCH (1,1) (L_g, L_r) model with one lag in VAR (L_u). The asymmetric volatility effect is significant for the time series, which indicates that the volatility of the stock shows greater response to a negative shock than a positive shock. The eigenvalue of variance function is 0.9252, and the eigenvalue of the mean function is 0.0057, as shown in the table below.

Table 28 *Statistical SNP Model Parameters for the OBX Index*

OBX Index share			
Satistical Model SNP-11114000-fit model			
Parameters Semiparametric-GARCH			
η		Mode	Standard error
η_1	a0[1]	0.01216	0.00796
η_2	a0[2]	0.05511	0.02710
η_3	a0[3]	-0.04603	0.00776
η_4	a0[4]	0.05279	0.00863
η_5	A(1,1)	1.00000	0.00000
η_6	B(1,1)	-0.00574	0.01575
η_7	R0[1]	0.10766	0.00934
η_8	P(1,1)	0.16295	0.02619
η_9	Q(1,1)	0.94797	0.00489
η_{10}	V(1,1)	-0.29195	0.02202

Largest eigen value of mean function companion matrix = 0.00574204
Largest eigen value of variance function P & Q companion matrix = 0.925195

Figure 47 displays the characteristics of the projected time series. The plots show the projected conditional volatility, together with a moving average (*m*=number of lags) of the squared residuals of an AR (1) regression model of the returns. It seems like the volatility change randomly, and the projected volatility tends to be relatively compact between *m*=4 and *m*=15. ***Figure 48*** displays the volatility at the mean of the time series, being the one-step-ahead densities $f_k(y_t|x_{t-1}.\theta)$, conditional on the values for x_{t-1} (where x_{t-1} = unconditional mean). The plot shows fatter tails than the normal distribution and advocates only small non-normal elements of the time series. We find that the OBX Index has a distribution that is narrower than the normal distribution. These features are commonly seen when analyzing data from a financial market, and confirm the purpose of using

Hermite polynomials to describe the density in the best possible way. ***Figure 49*** shows the one-step-ahead densities of shocks ranging from - 40 % to + 40 %, together with the baseline profile (*m*=0.039154). Comparing the different impulse profiles to the baseline profile (the mean), we find that the densities are wider after adding an impulse (shock) to the series. The largest negative shock of - 40 % shows a much wider density compared to the equivalent positive shock. This indicates a higher degree of uncertainty after a negative shock and is a confirmation of the observed asymmetry. The relationship between the one-step-ahead dynamics of the conditional variance and the percentage growth is displayed in ***Figure 50***. The graph represents the reactions to shocks hitting the system (asset price). The difference in responses suggests asymmetry due to the "leverage -" and "risk premium" effects. For the OBX Index, we find that the responses from negative shocks are much higher than from positive, showing an apparent asymmetry.

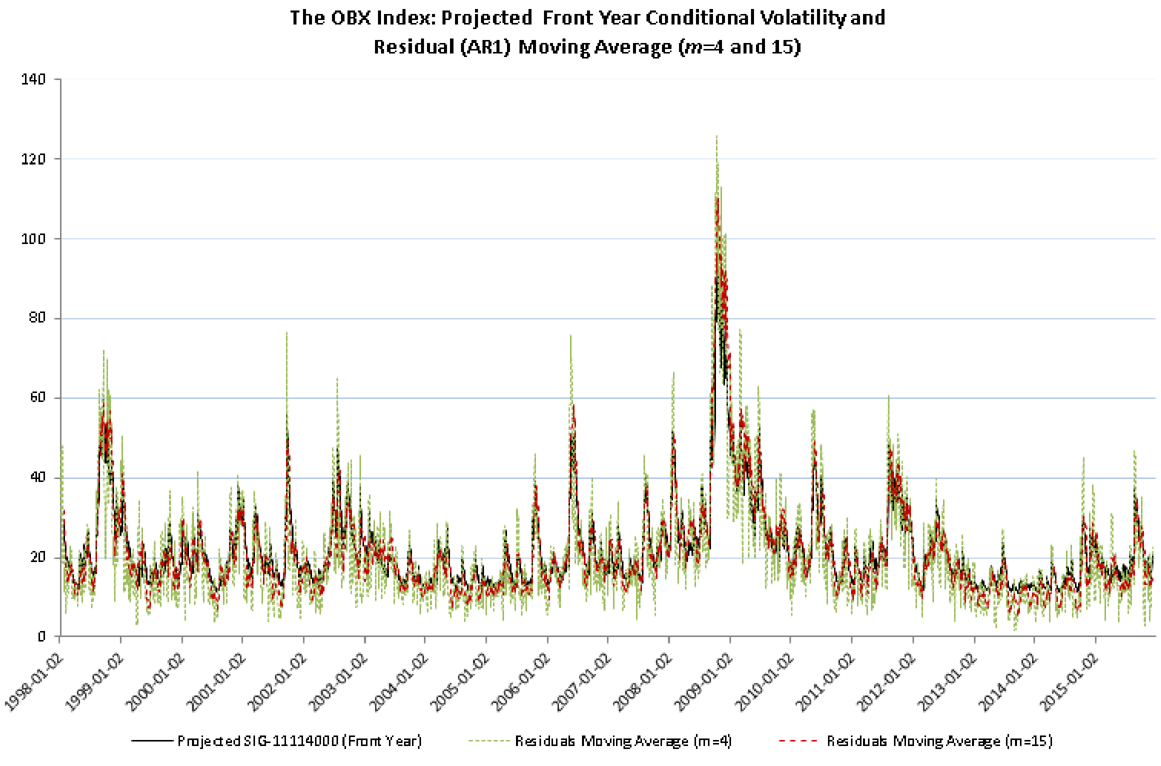

Figure 47 *Projected conditional volatility and residuals AR (1) moving average OBX Index*

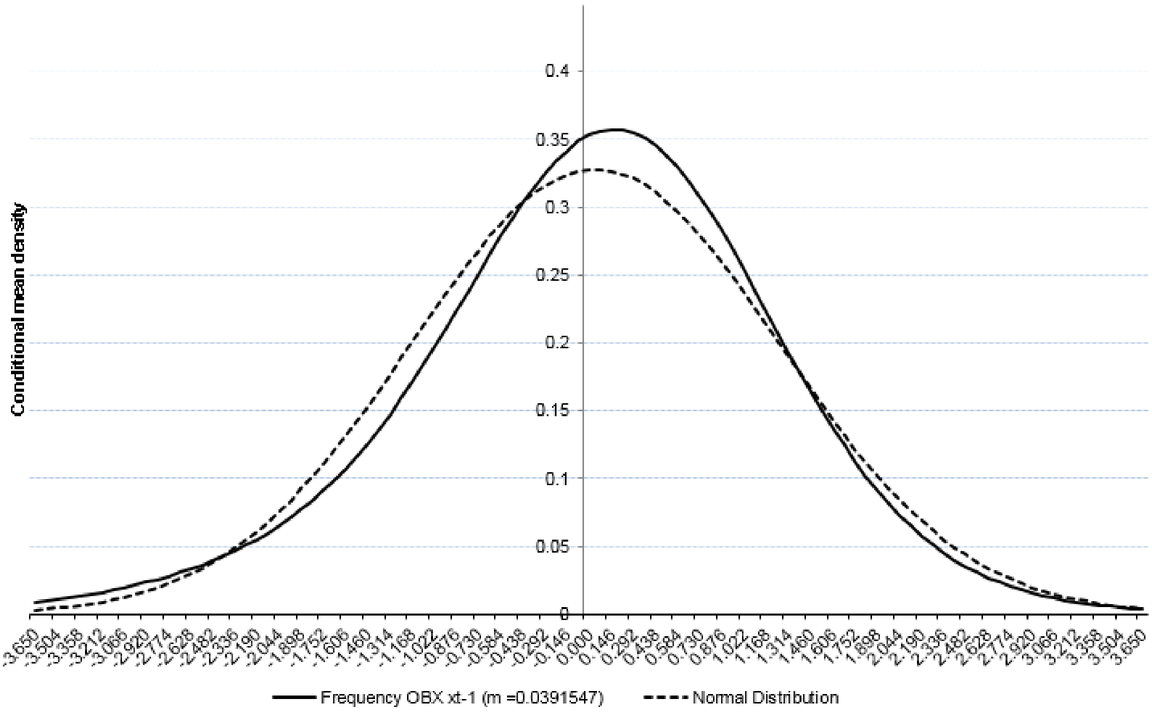

Figure 48 *OBX Index one-step-ahead densities (x_{t-1} = unconditional mean)*

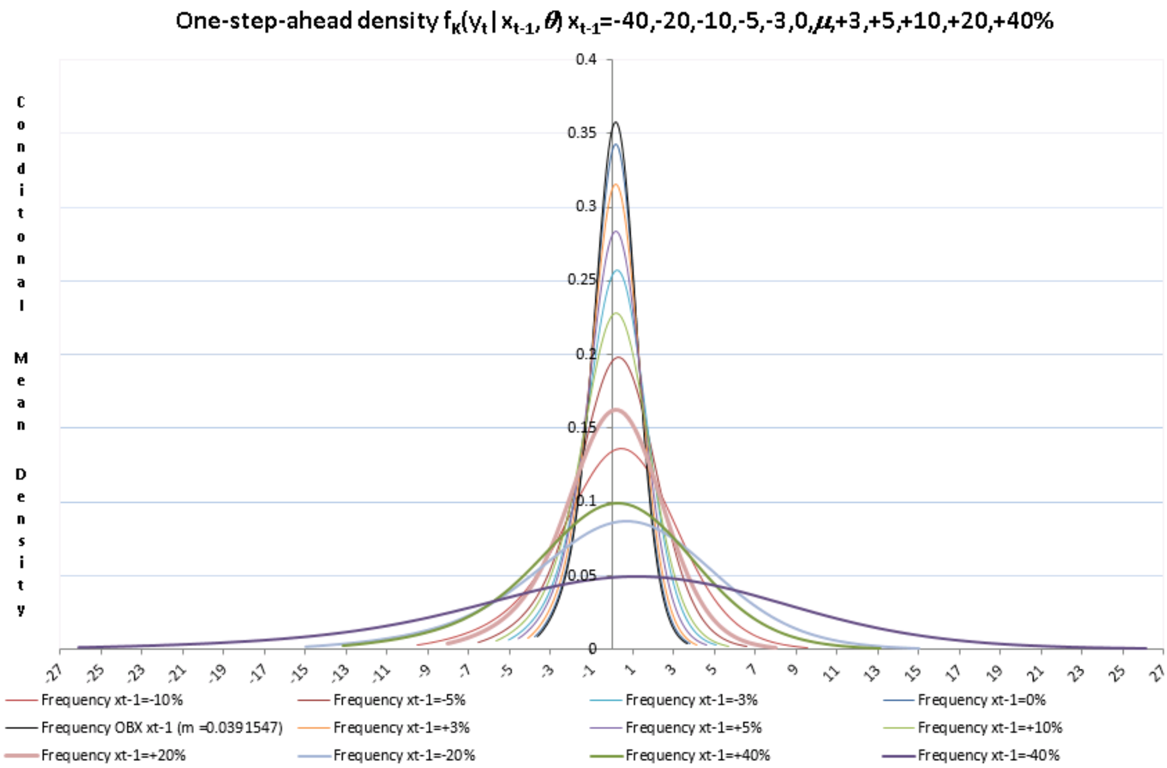

Figure 49 *OBX Index one-step-ahead densities (conditional mean for x_{t-1} = -40%...40%)*

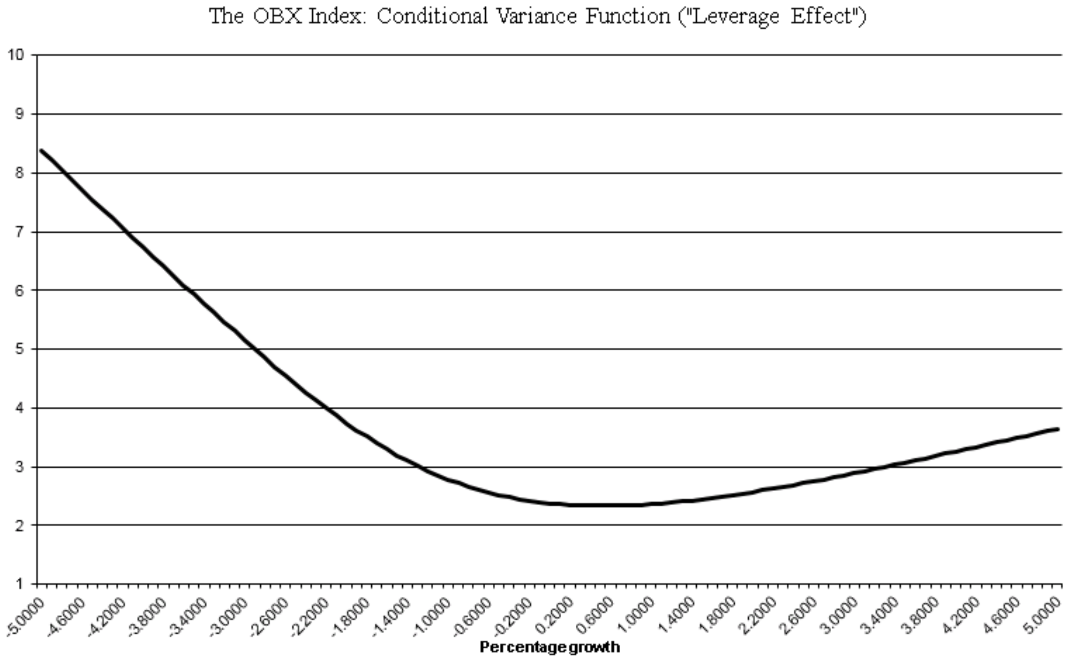

Figure 50 *OBX Index: conditional variance functions*

5.4.2.7 Oslo Stock Exchange All Share Index (OSEAX)

The specification tests for the optimal SNP GARCH model are reported in ***Table 29***. The residual statistics show that the data is closer to the normal distribution, with a kurtosis of 0.7. There is no volatility clustering, having *P*-values of 0.49 and 0.49 for Q^2 (12) and ARCH (12) respectively. The mean is approximately zero, and the standard deviation is one, referring to the normal distribution denoted as N (0, 1). The BDS-test states that the residuals are IID, meaning data dependence is no longer present. By this, the model misspecification seems minimized, and the semi-nonparametric GARCH model is selected for the impulse response analysis.

Table 29 *Characteristics of the statistics SNP Model Residuals for the OSEAX Index*

Residual Statistics for OSEAX Index

Mean	Median / Std.dev.	Maximum / Minimum	Moment Kurt/Skew	Quantile Kurt/Skew	Quantile Normal	Cramer-von-Mises	Serial dependence Q(12)	Q^2(12)
0.00117	0.05397	4.57874	0.64512	0.07587	2.28607	1.18426	20.0680	11.407
	0.99998	-4.23449	-0.27302	-0.04010	{0.3188}	{0.0000}	{0.0660}	{0.4940}

BDS-statistic (ε=1) m=2	m=3	m=4	m=5	ARCH (12)	VaR 2.5%/0.5%	CVaR 2.5%/0.5%
-0.438671	-0.2186	0.042301	0.241671	11.36966	-2.1418	-2.6431
{0.6609}	{0.8270}	{0.9663}	{0.8090}	{0.4975}	-3.0029	-3.4243

The figures in braces are P-values for statistical significance

The model selected under the Schwarz Criterion is a semiparametric GARCH with four Hermite polynomials (K_z) for non-normal features of the series. The model is a GARCH (1,1) (L_g, L_r) model with two lags in VAR (L_u). The asymmetric volatility effect is significant for the time series, which indicates that the volatility of the stock shows greater response to a negative shock than a positive shock. The eigenvalue of variance function is 0.9148, and the eigenvalue of the mean function is 0.0874, as shown in the table below.

Table 30 *Statistical SNP Model Parameters for the OSEAX Index*

OSEAX index

Satistical Model SNP-11114000-fit model
Parameters Semiparametric-GARCH

η		Mode	Standard error
η_1	a0[1]	0.01345	0.00799
η_2	a0[2]	0.04282	0.02672
η_3	a0[3]	-0.04877	0.00782
η_4	a0[4]	0.05054	0.00841
η_5	A(1,1)	1.00000	0.00000
η_6	B(1,1)	0.01211	0.01589
η_7	B(1,2)	-0.00765	0.01550
η_8	R0[1]	0.13063	0.01067
η_9	P(1,1)	0.19710	0.02459
η_{10}	Q(1,1)	0.93593	0.00593
η_{11}	V(1,1)	-0.30578	0.02289

Largest eigen value of mean function companion matrix = 0.0874471
Largest eigen value of variance function P & Q companion matrix = 0.914819

Figure 51 displays the characteristics of the projected time series. The plots show the projected conditional volatility, together with a moving average (m=number of lags) of the squared residuals of an AR (1) regression model of the returns. It seems like the volatility change randomly, and the projected volatility tends to be relatively compact between m=4 and m=15. ***Figure 52*** displays the volatility at the mean of the time series, being the one-step-ahead densities $f_k(y_t|x_{t-1}.\theta)$, conditional on the values for x_{t-1} (where x_{t-1} = unconditional mean). The plot shows fatter tails than the normal distribution and advocates only small non-normal elements of the time series. We find that the OSEAX Index has a distribution that is narrower than the normal distribution. These features are commonly seen when analyzing data from a financial market, and confirm the purpose of using

Hermite polynomials to describe the density in the best possible way. ***Figure 53*** shows the one-step-ahead densities of shocks ranging from - 40 % to + 40 %, together with the baseline profile (*m*=0.041896). Comparing the different impulse profiles to the baseline profile (the mean), we find that the densities are wider after adding an impulse (shock) to the series. The largest negative shock of - 40 % shows a much wider density compared to the equivalent positive shock. This indicates a higher degree of uncertainty after a negative shock and is a confirmation of the observed asymmetry. The relationship between the one-step-ahead dynamics of the conditional variance and the percentage growth is displayed in ***Figure 54***. The graph represents the reactions to shocks hitting the system (asset price). The difference in responses suggests asymmetry due to the "leverage -" and "risk premium" effects. For the OSEAX Index, we find that the responses from negative shocks are much higher than from positive, showing an apparent asymmetry.

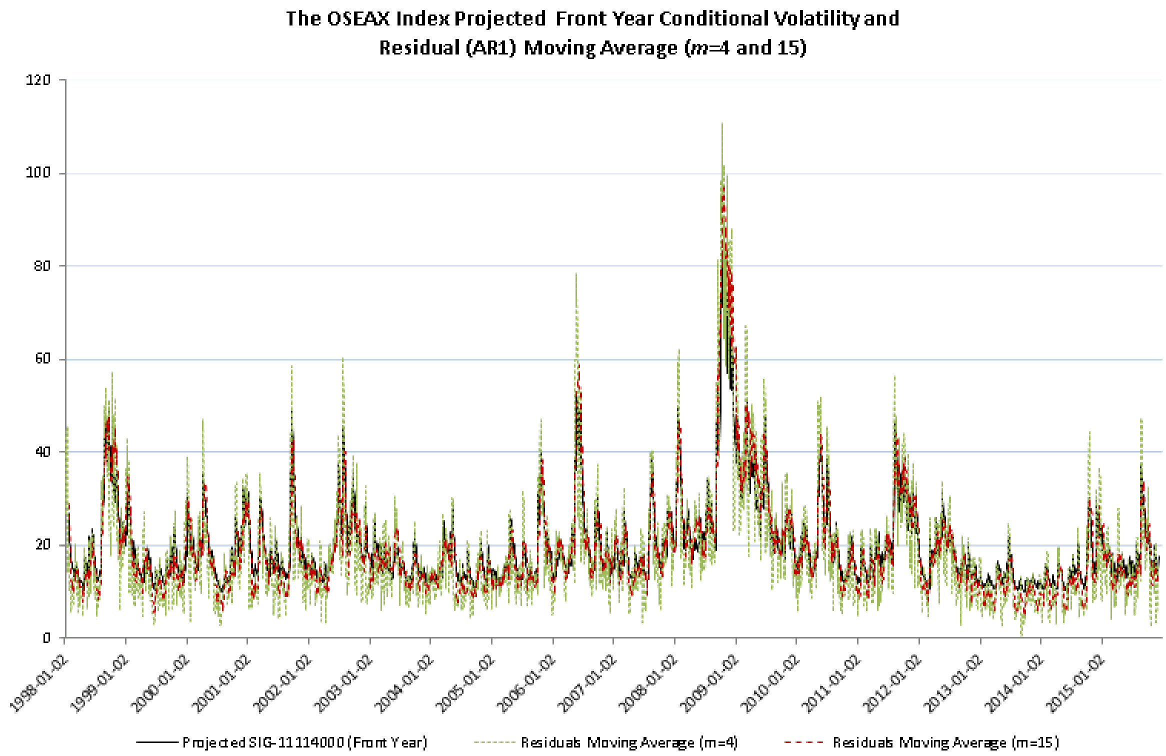

Figure 51 *Projected conditional volatility and residuals AR (1) moving average OSEAX Index*

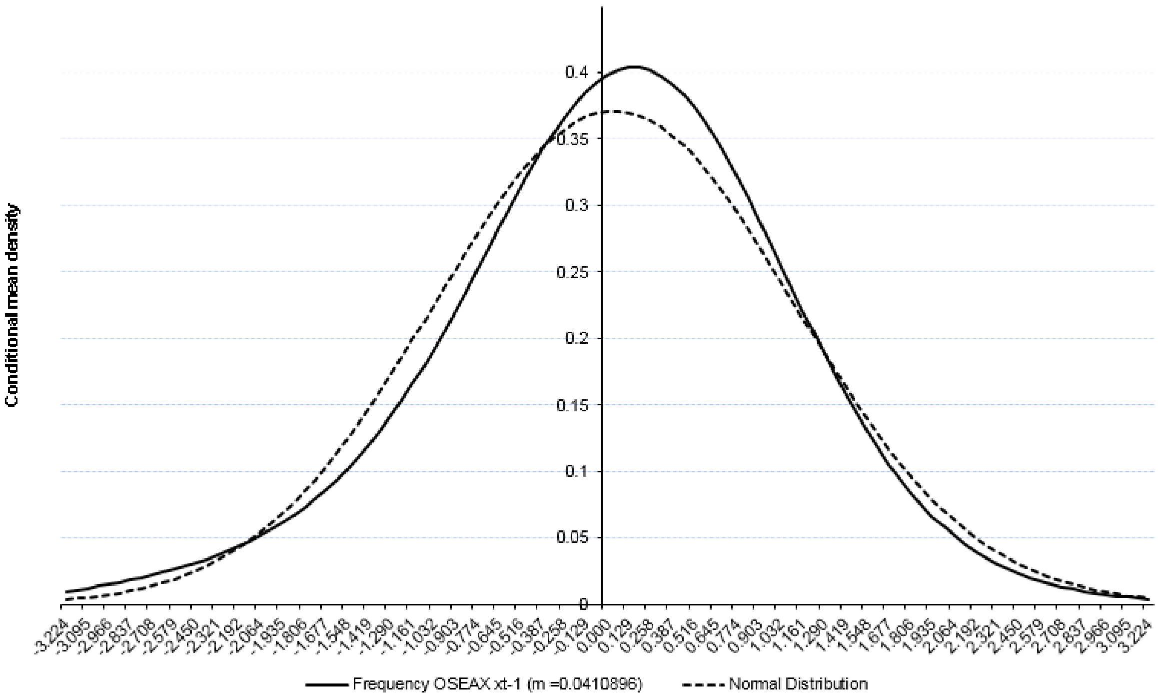

Figure 52 *OSEAX Index one-step-ahead densities (x_{t-1} = unconditional mean)*

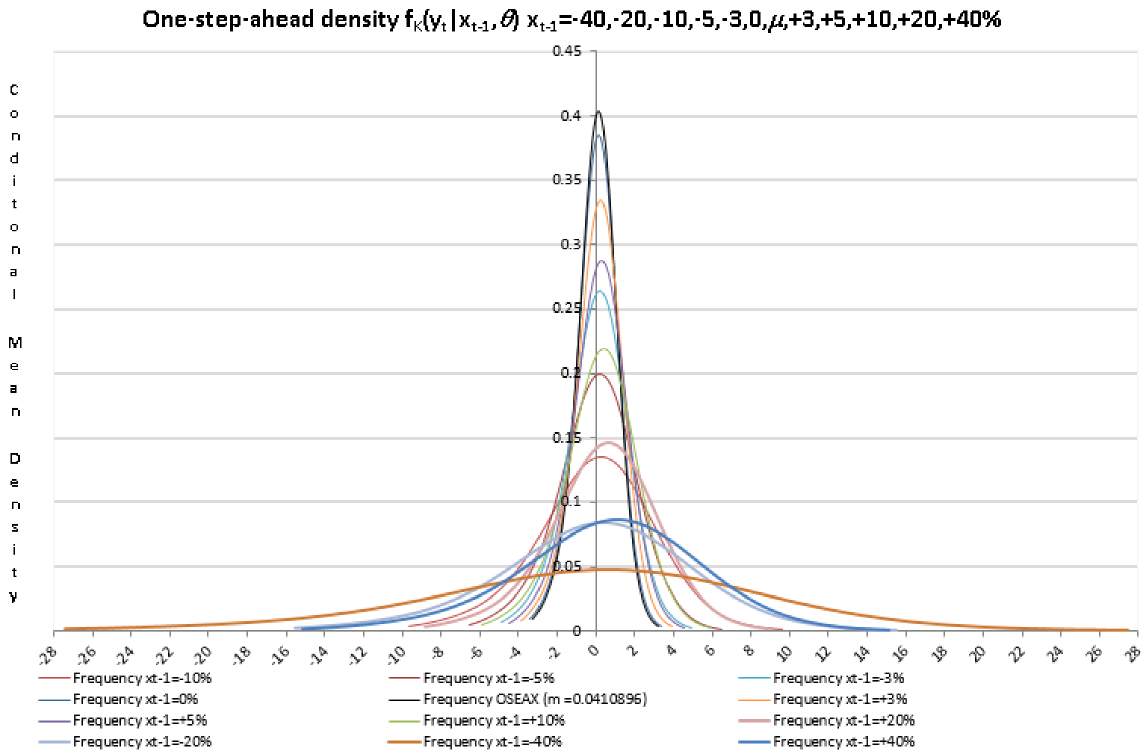

Figure 53 *OSEAX Index one-step-ahead densities (conditional mean for x_{t-1} = -40%...40%)*

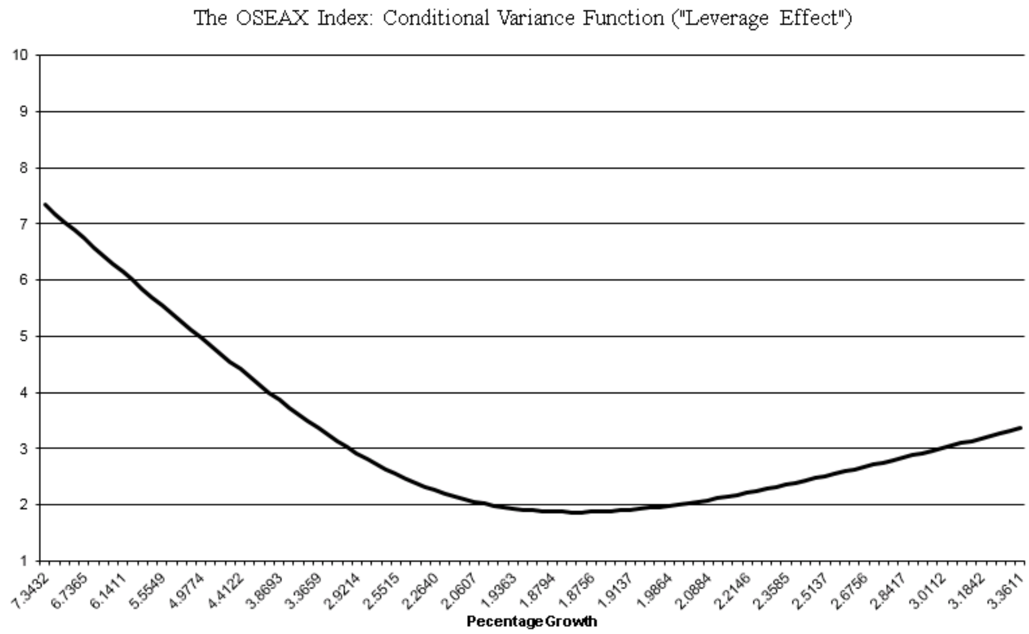

Figure 54 *OSEAX Index: conditional variance functions*

5.4.2.8 Microsoft Corporation (MSFT)

The specification tests for the optimal SNP GARCH model are reported in ***Table 31***. The residual statistics show that the data is closer to the normal distribution, with a kurtosis of 8.5. There is no volatility clustering, having *P*-values of 1.00 and 0.99 for Q^2 (12) and ARCH (12) respectively. The mean is approximately zero, and the standard deviation is one, referring to the normal distribution denoted as N (0, 1). The BDS-test show significant values at correlation dimension two and three. We choose to use the semi-nonparametric GARCH model as it is for the impulse response analysis, bearing in mind that the model can have sub-optimal performance (Brock, Dechert et al. 1996).

Table 31 *Characteristics of the statistical SNP Model Residuals for MSFT*

Residual Statistics for MSFT Share

Mean	Median / Std.dev.	Maximum / Minimum	Moment Kurt/Skew	Quantile Kurt/Skew	Quantile Normal	Cramer-von-Mises	Serial dependence Q(12)	Q^2(12)
-0.01056	-0.03771	6.95276	8.47190	0.08500	4.63579	4.84764	12.2930	1.6368
	1.00006	-13.00836	-0.35572	0.04478	{0.0985}	{0.0000}	{0.4220}	{1.0000}

BDS-statistic (ε=1) m=2	m=3	m=4	m=5	ARCH (12)	VaR 2.5%/0.5%	CVaR 2.5%/0.5%
0.695635	1.93145	2.44825	2.997429	1.70808	-1.8955	-2.7041
{0.4867}	{0.0534}	{0.0248}	{0.0027}	{0.9997}	-3.0107	-4.3773

The figures in braces are P-values for statistical significance

The model selected under the Schwarz Criterion is a semiparametric GARCH with eight Hermite polynomials (K_z) for non-normal features of the series. The model is a GARCH (1,1) (L_g, L_r) model with one lag in VAR (L_u). The asymmetric volatility effect is significant for the time series, which indicates that the volatility of the stock shows greater response to a negative shock than a positive shock. The lags in additive level effect are also significant indicating additive outliers in the series. The eigenvalue of variance function is 1.0319, and the eigenvalue of the mean function is 0.01030, as shown in the table below.

Table 32 *Statistical SNP Model Parameters for the MSFT Share*

Microsoft share

Satistical Model SNP-11118000-fit model
Parameters Semiparametric-GARCH

η		Mode	Standard error
η_1	a0[1]	0.00314	0.00607
η_2	a0[2]	-0.22891	0.01063
η_3	a0[3]	0.00689	0.00608
η_4	a0[4]	0.15807	0.00717
η_5	a0[5]	0.00355	0.00643
η_6	a0[6]	-0.06338	0.00811
η_7	a0[7]	0.00806	0.00696
η_8	a0[8]	0.06209	0.00768
η_9	A(1,1)	1.00000	0.00000
η_{10}	B(1,1)	-0.01030	0.01206
η_{11}	R0[1]	0.09393	0.00802
η_{12}	P(1,1)	0.30210	0.02167
η_{13}	Q(1,1)	0.96987	0.00247
η_{14}	V(1,1)	-0.23296	0.03448
η_{15}	W(1,1)	-0.29261	0.05941

Largest eigen value of mean function companion matrix = 0.0103047
Largest eigen value of variance function P & Q companion matrix = 1.03192

Figure 55 displays the characteristics of the projected time series. The plots show the projected conditional volatility, together with a moving average (m=number of lags) of the squared residuals of an AR (1) regression model of the returns. It seems like the volatility change randomly, and the projected volatility tends to be relatively compact between m=4 and m=15. ***Figure 56*** displays the volatility at the mean of the time series, being the one-step-ahead densities $f_k(y_t|x_{t-1}.\theta)$, conditional on the values for x_{t-1} (where x_{t-1} = unconditional mean). The plot shows fatter tails than the normal distribution and advocates only small non-normal elements of the time series. We find that the MSFT series has a distribution that is narrower than the normal distribution. These features are commonly seen when analyzing data from a financial market, and confirm the purpose of using Hermite polynomials to describe the density in the best possible way. ***Figure 57*** shows the one-step-ahead densities of shocks ranging from - 40 % to + 40 %, together with the baseline profile (*m*=0.046846). Comparing the different impulse profiles to the baseline profile (the mean), we find that the densities are wider after adding an impulse (shock) to the series. The densities given by a shock of +/- 3% are narrower than the baseline profile. The largest negative shock of - 40 % shows a slightly wider density compared to the equivalent positive shock. This indicates a higher degree of uncertainty after a negative shock and is a confirmation of the observed asymmetry. The relationship between the one-step-ahead dynamics of the conditional variance and the percentage growth is displayed in ***Figure 58***. The graph represents the reactions to shocks hitting the system (asset price). The difference in responses suggests a asymmetry due to the "leverage -" and "risk premium" effects. For the MSFT series, we find that the responses from negative shocks are little higher than from positive, showing a tendency of asymmetry.

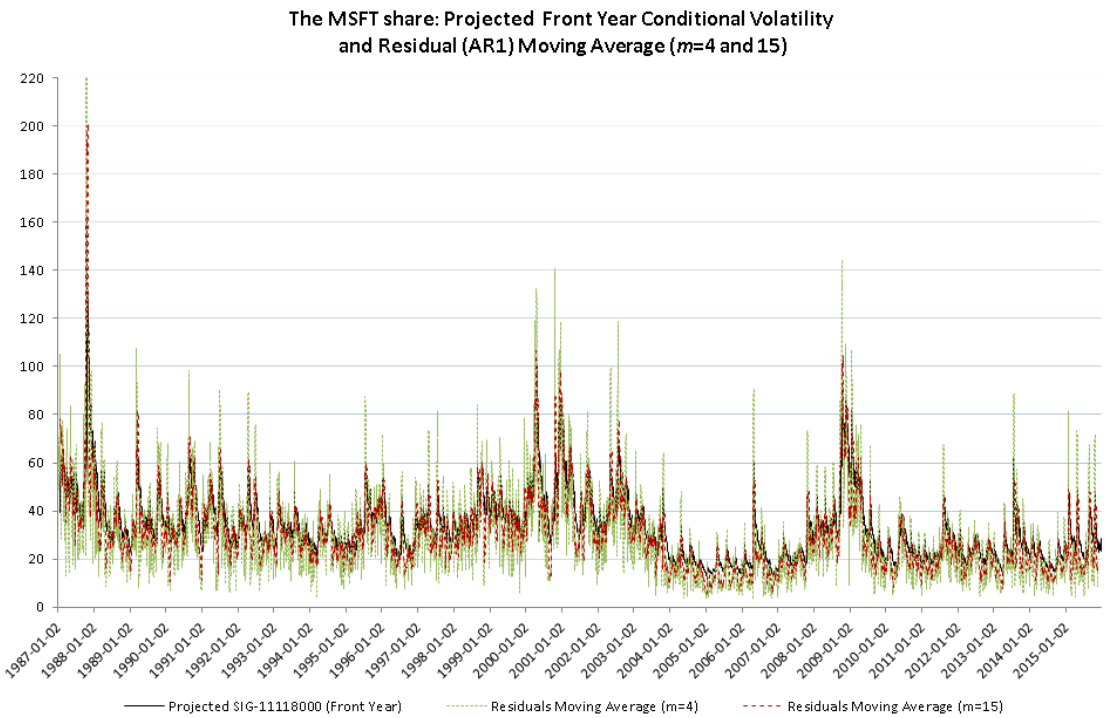

Figure 55 *Projected conditional volatility and residuals AR (1) moving average MSFT*

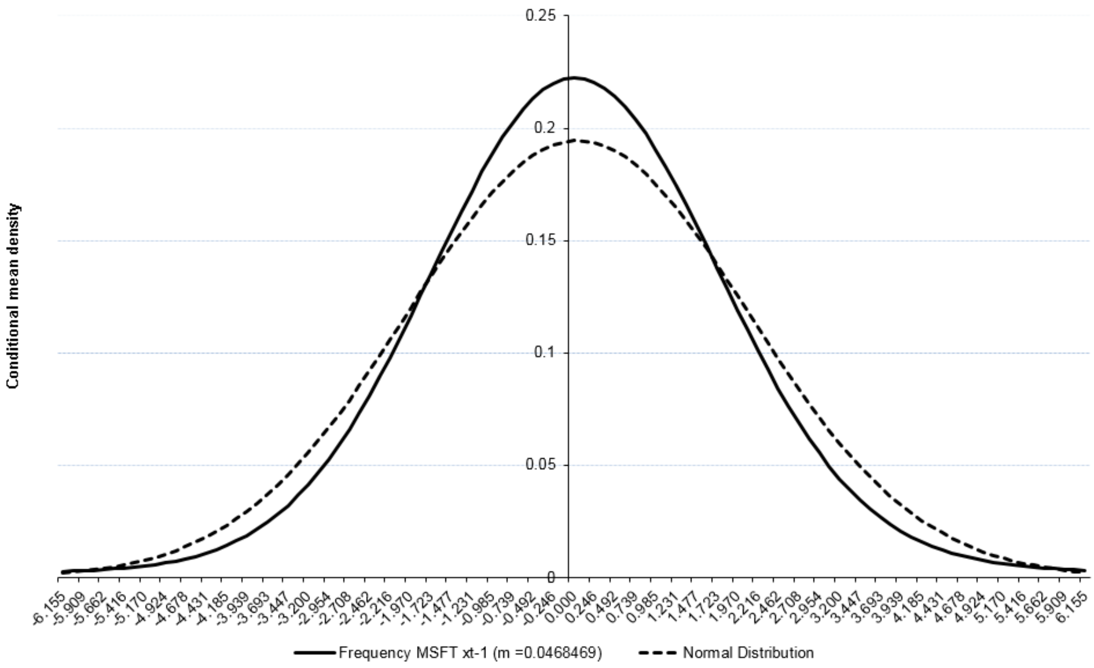

Figure 56 *MSFT one-step-ahead densities (x_{t-1} = unconditional mean)*

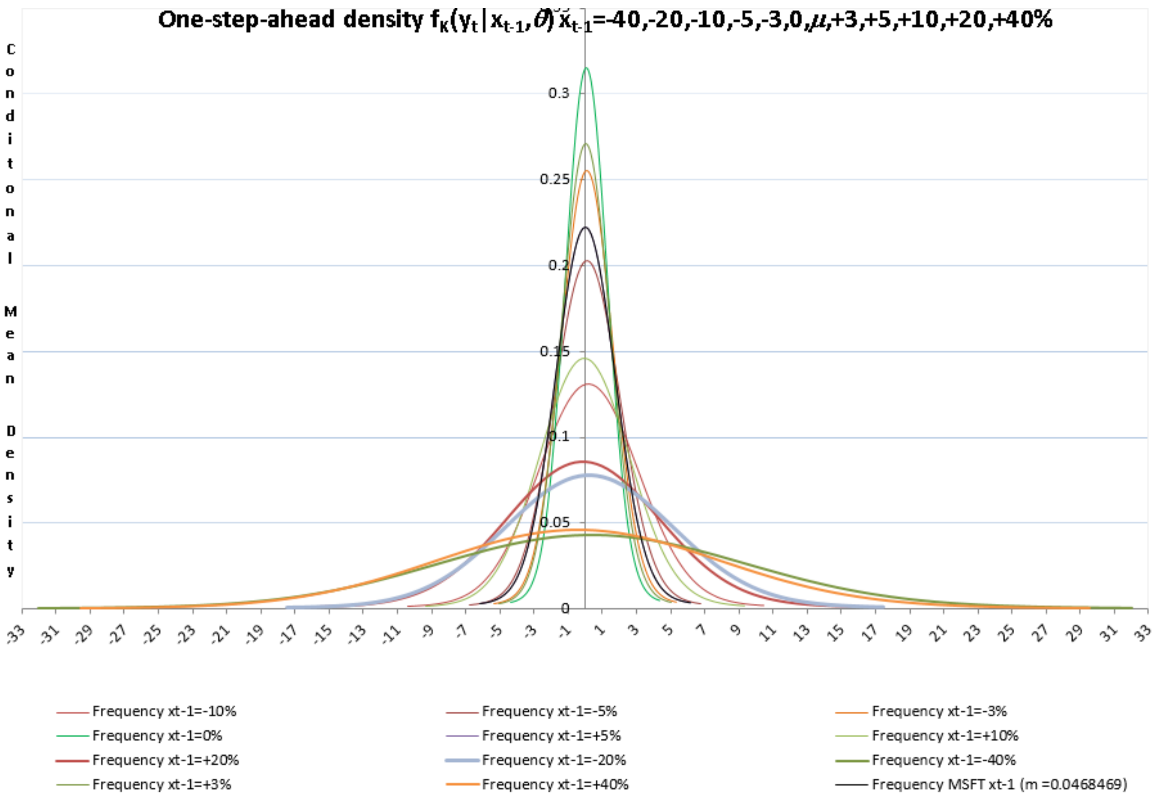

Figure 57 *MSFT one-step-ahead densities (conditional mean for x_{t-1} = -40%...40%)*

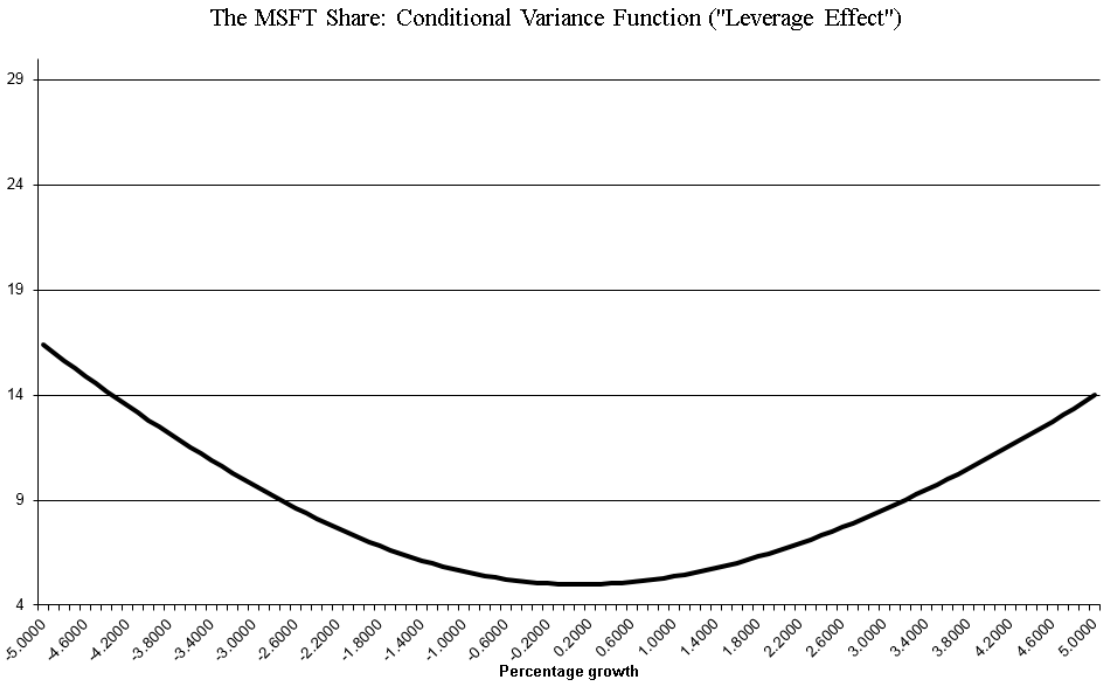

Figure 58 *MSFT: conditional variance functions*

5.4.2.9 Micron Technology Inc. (MU)

The specification tests for the optimal SNP GARCH model are reported in ***Table 33***. The residual statistics show that the data is closer to the normal distribution, with a kurtosis of 3.7. There is no volatility clustering, having *P*-values of 0.87 and 0.86 for Q^2 (12) and ARCH (12) respectively. The mean is approximately zero, and the standard deviation is one, referring to the normal distribution denoted as N (0, 1). The BDS-test states that the residuals are IID, meaning data dependence is no longer present. By this, the model misspecification seems minimized, and the semi-nonparametric GARCH model is selected for the impulse response analysis

Table 33 *Characteristics of the statistical SNP Model Residuals for MU*

Residual Statistics for MU Share

Mean	Median / Std.dev.	Maximum / Minimum	Moment Kurt/Skew	Quantile Kurt/Skew	Quantile Normal	Cramer-von-Mises	Serial dependence Q(12)	Q^2(12)
-0.00664	-0.00766	5.07055	3.72390	0.03533	0.24239	0.97640	9.6795	6.8857
	1.00006	-9.87175	-0.32024	0.00317	{0.8859}	{0.0000}	{0.6440}	{0.8650}
BDS-statistic (ε=1)				ARCH	VaR	CVaR		
m=2	m=3	m=4	m=5	(12)	2.5%/0.5%	2.5%/0.5%		
0.173401	0.612795	0.671377	0.681438	6.93662	-1.8980	-2.6833		
{0.8623}	{0.5400}	{0.5020}	{0.6956}	{0.8618}	-3.0085	-4.1253		

The figures in braces are P-values for statistical significance

The model selected under the Schwarz Criterion is a semiparametric GARCH with six Hermite polynomials (K_z) for non-normal features of the series. The model is a GARCH (1,1) (L_g, L_r) model with two lags in VAR (L_u). The asymmetric volatility effect is significant for the time series, which indicates that the volatility of the stock shows greater response to a negative shock than a positive shock. The eigenvalue of variance function is 1.0011, and the eigenvalue of the mean function is 0.1183, as shown in the table below.

Table 34 *Statistical SNP Model Parameters for the MU Share*

MU share

Statistical Model SNP-11116000 -fit model
Parameters Semiparametric-GARCH.

η		Mode	Standard error
η_1	a0[1]	0.00063	0.00768
η_2	a0[2]	-0.22074	0.01447
η_3	a0[3]	-0.00691	0.00829
η_4	a0[4]	0.12450	0.00888
η_5	a0[5]	-0.00247	0.00897
η_6	a0[6]	-0.07037	0.01246
η_7	A(1,1)	1.00000	0.00000
η_8	B(1,1)	0.02619	0.01488
η_9	B(1,2)	-0.01400	0.01489
η_{10}	R0[1]	0.06228	0.01182
η_{11}	P(1,1)	0.19499	0.02703
η_{12}	Q(1,1)	0.98137	0.00206
η_{13}	V(1,1)	-0.26777	0.02522

Largest eigen value of mean function companion matrix = 0.118338
Largest eigen value of variance function P & Q companion matrix = 1.00111

Figure 59 displays the characteristics of the projected time series. The plots show the projected conditional volatility, together with a moving average (*m*=number of lags) of the squared residuals of an AR (1) regression model of the returns. It seems like the volatility change randomly, and the projected volatility tends to be relatively compact between *m*=4 and *m*=15. ***Figure 60*** displays the volatility at the mean of the time series, being the one-step-ahead densities $f_k(y_t|x_{t-1}.\theta)$, conditional on the values for x_{t-1} (where x_{t-1} = unconditional mean). The plot shows fatter tails than the normal distribution and advocates only small non-normal elements of the time series. We find that the MU series has a distribution that is narrower than the normal distribution. These features are commonly seen when analyzing data from a financial market, and confirm the purpose of using Hermite polynomials to describe the density in the best possible way. ***Figure 61*** shows the one-step-ahead densities of shocks ranging from - 40 % to + 40 %, together with the baseline profile (*m*=0.010148). Comparing the different impulse profiles to the baseline profile (the mean), we find that the densities are wider after adding an impulse (shock) to the series. The largest negative shock of - 40 % shows a much wider density compared to the equivalent positive shock. This indicates a higher degree of uncertainty after a negative shock and is a confirmation of the observed asymmetry. The relationship between the one-step-ahead dynamics of the conditional variance and the percentage growth is displayed in ***Figure 62***. The graph represents the reactions to shocks hitting the system (asset price). The difference in responses suggests asymmetry due to the "leverage -" and "risk premium" effects. For the MU series, we find that the responses from negative shocks are much higher than from positive, showing an apparent asymmetry.

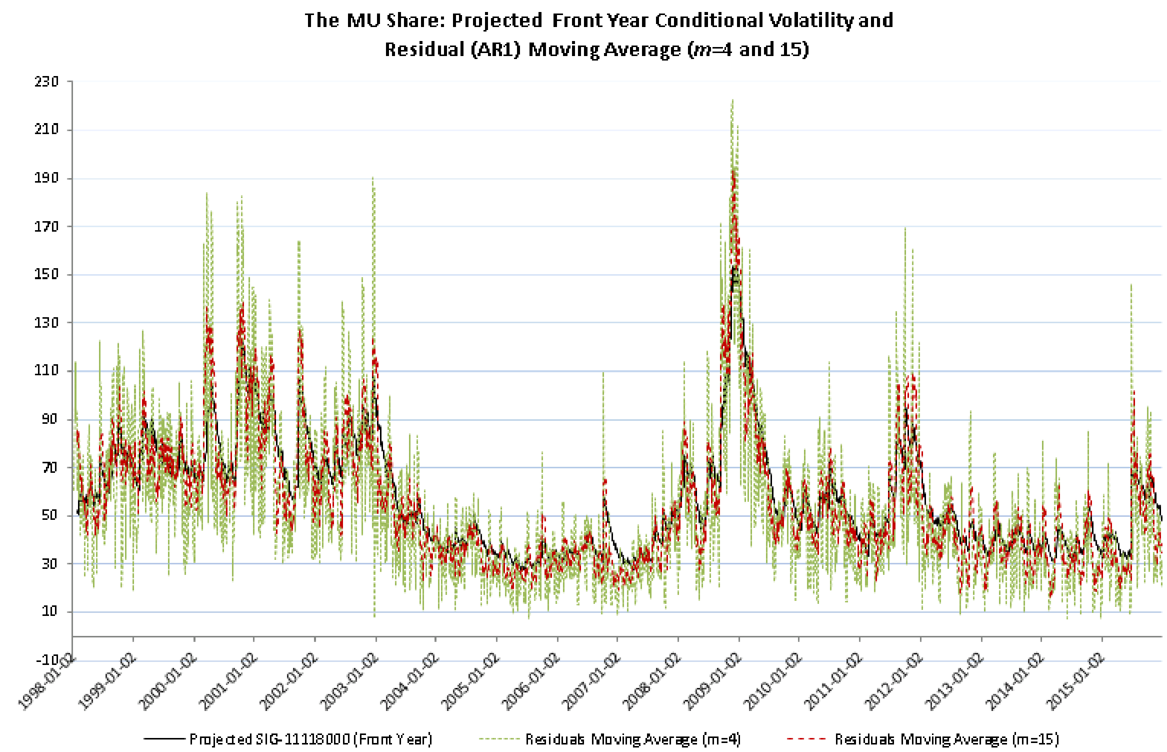

Figure 59 *Projected conditional volatility and residuals AR (1) moving average MU*

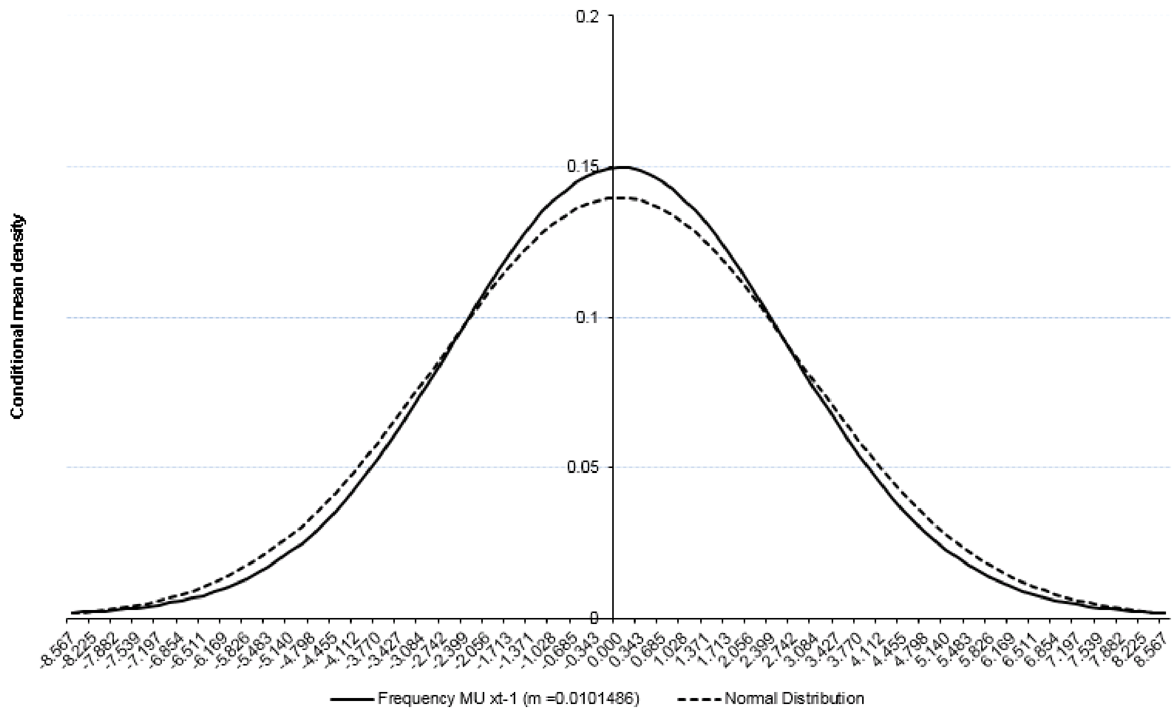

Figure 60 *MU one-step-ahead densities (x_{t-1} = unconditional mean)*

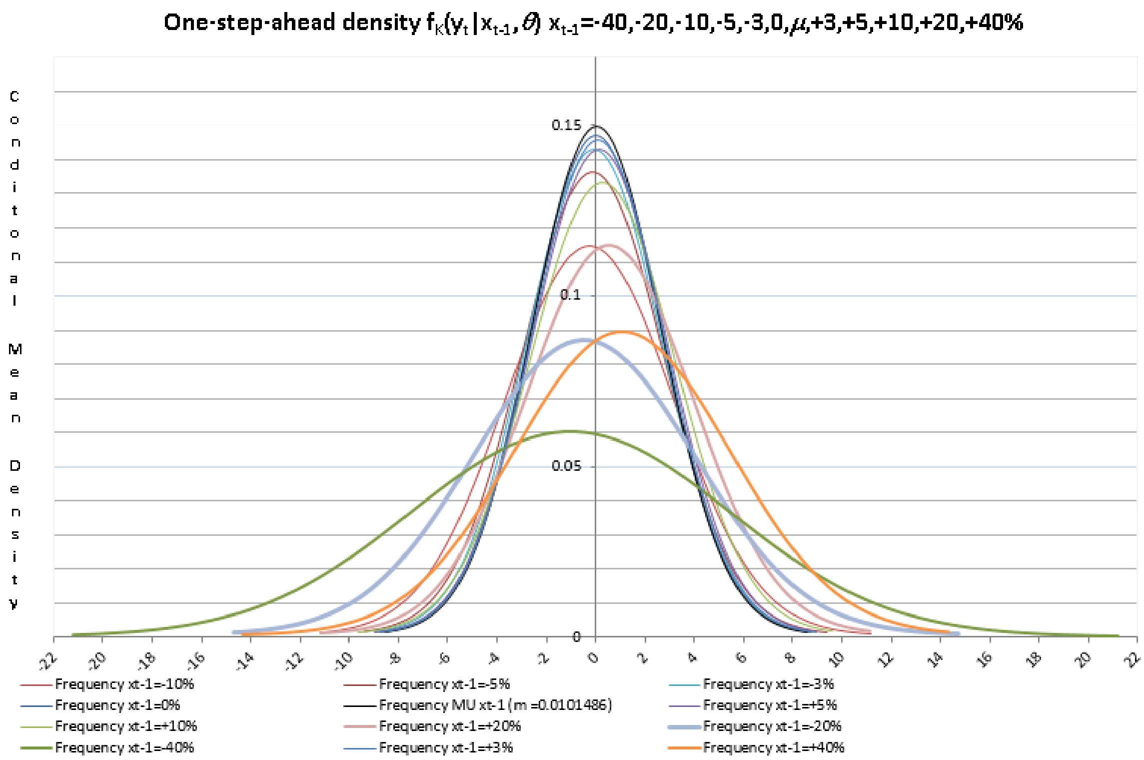

Figure 61 *MU one-step-ahead densities (conditional mean for x_{t-1} = -40%...40%)*

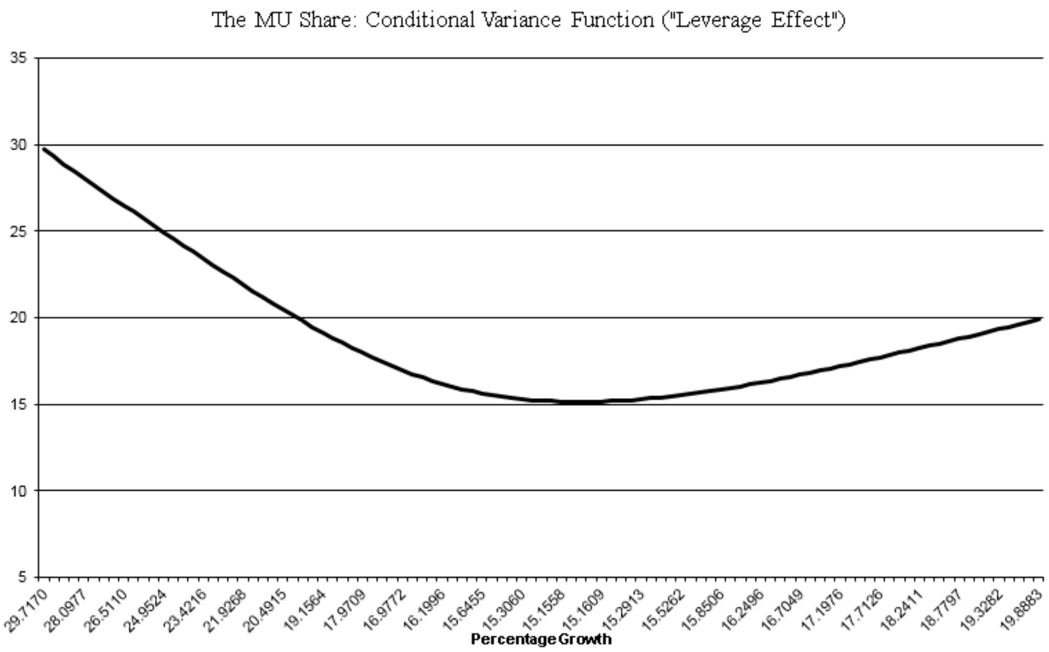

Figure 62 *MU: conditional variance functions*

5.4.2.10 Norsk Hydro ASA (NHY)

The specification tests for the optimal SNP GARCH model are reported in ***Table 35***. The residual statistics show that the data is closer to the normal distribution, with a kurtosis of 4.1. There is no volatility clustering, having *P*-values of 0.82 and 0.84 for Q^2 (12) and ARCH (12) respectively. The mean is approximately zero, and the standard deviation is one, referring to the normal distribution denoted as N (0, 1). The BDS-test states that the residuals are IID, meaning data dependence is no longer present. By this, the model misspecification seems minimized, and the semi-nonparametric GARCH model is selected for the impulse response analysis

Table 35 *Characteristics of the statistical SNP Model Residuals for NHY*

Residual Statistics for NHY Share

Mean	Median / Std.dev.	Maximum / Minimum	Moment Kurt/Skew	Quantile Kurt/Skew	Quantile Normal	Cramer-von-Mises	Serial dependence Q(12)	Q^2(12)
0.00127	0.00402	10.36203	4.05481	0.03485	0.22702	1.06591	11.0070	7.5982
	1.00004	-7.33716	0.12180	-0.00006	{0.8927}	{0.0000}	{0.5280}	{0.8160}

BDS-statistic (ε=1) m=2	m=3	m=4	m=5	ARCH (12)	VaR 2.5%/0.5%	CVaR 2.5%/0.5%
0.258477	0.981165	1.043539	0.7869	7.228142	-1.9702	-2.5566
{0.7960}	{0.3265}	{0.2967}	{0.4313}	{0.8422}	-2.8678	-3.6242

The figures in braces are P-values for statistical significance

The model selected under the Schwarz Criterion is a semiparametric GARCH with six Hermite polynomials (K_z) for non-normal features of the series. The model is a GARCH (1,1) (L_g, L_r) model with two lags in VAR (L_u). The asymmetric volatility effect is significant for the time series, which indicates that the volatility of the stock shows greater response to a negative shock than a positive shock. The eigenvalue of variance function is 0.9986, and the eigenvalue of the mean function is 0.0689, as shown in the table below.

Table 36 *Statistical SNP Model Parameters for the NHY Share*

Norsk Hydro share

Satistical Model SNP-11116000-fit model

Parameters Semiparametric-GARCH

η		Mode	Standard error
η_1	a0[1]	0.00175	0.00773
η_2	a0[2]	-0.22311	0.01269
η_3	a0[3]	-0.00427	0.00838
η_4	a0[4]	0.11526	0.00969
η_5	a0[5]	0.00806	0.00880
η_6	a0[6]	-0.06868	0.01075
η_7	A(1,1)	1.00000	0.00000
η_8	B(1,1)	0.02070	0.01550
η_9	B(1,2)	0.00332	0.01477
η_{10}	R0[1]	-0.11839	0.01422
η_{11}	P(1,1)	0.24728	0.02915
η_{12}	Q(1,1)	0.96821	0.00323
η_{13}	V(1,1)	-0.33332	0.03357

Largest eigen value of mean function companion matrix = 0.0689271

Largest eigen value of variance function P & Q companion matrix = 0.99857

Figure 63 displays the characteristics of the projected time series. The plots show the projected conditional volatility, together with a moving average (*m*=number of lags) of the squared residuals of an AR (1) regression model of the returns. It seems like the volatility change randomly, and the projected volatility tends to be relatively compact between *m*=4 and *m*=15. ***Figure 64*** displays the volatility at the mean of the time series, being the one-step-ahead densities $f_k(y_t|x_{t-1}.\theta)$, conditional on the values for x_{t-1} (where x_{t-1} = unconditional mean). The plot shows fatter tails than the normal distribution and advocates only small non-normal elements of the time series. We find that the NHY series has a distribution that is narrower than the normal distribution. These features are commonly seen when analyzing data from a financial market, and confirm the purpose of using Hermite polynomials to describe the density in the best possible way. ***Figure 65*** shows the one-step-ahead densities of shocks ranging from - 40 % to + 40 %, together with the baseline profile (m=0.023007). Comparing the different impulse profiles to the baseline profile (the mean), we find that the densities are wider after adding an impulse (shock) to the series. The largest negative shock of - 40 % shows a much wider density compared to the equivalent positive shock. This indicates a higher degree of uncertainty after a negative shock and is a confirmation of the observed asymmetry. The relationship between the one-step-ahead dynamics of the conditional variance and the percentage growth is displayed in ***Figure 66***. The graph represents the reactions to shocks hitting the system (asset price). The difference in responses suggests asymmetry due to the "leverage -" and "risk premium" effects. For the NHY series, we find that the responses from negative shocks are much higher than from positive, showing an apparent asymmetry.

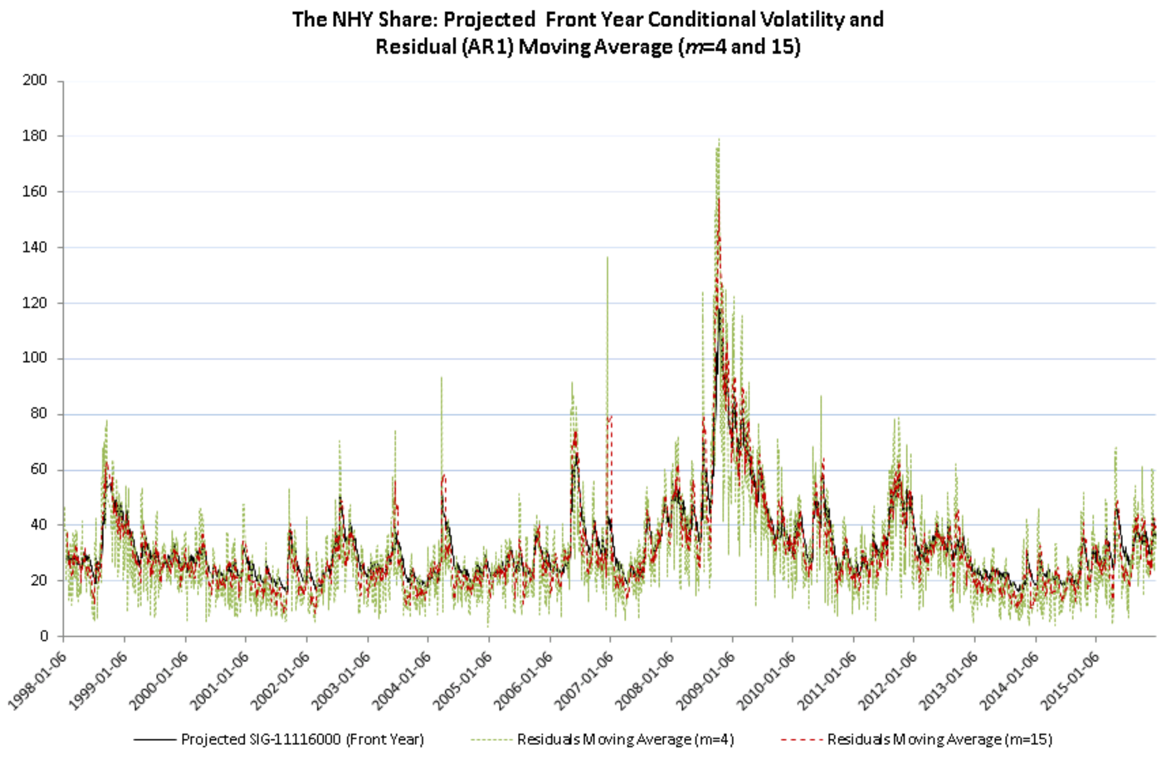

Figure 63 *Projected conditional volatility and residuals AR (1) moving average NHY*

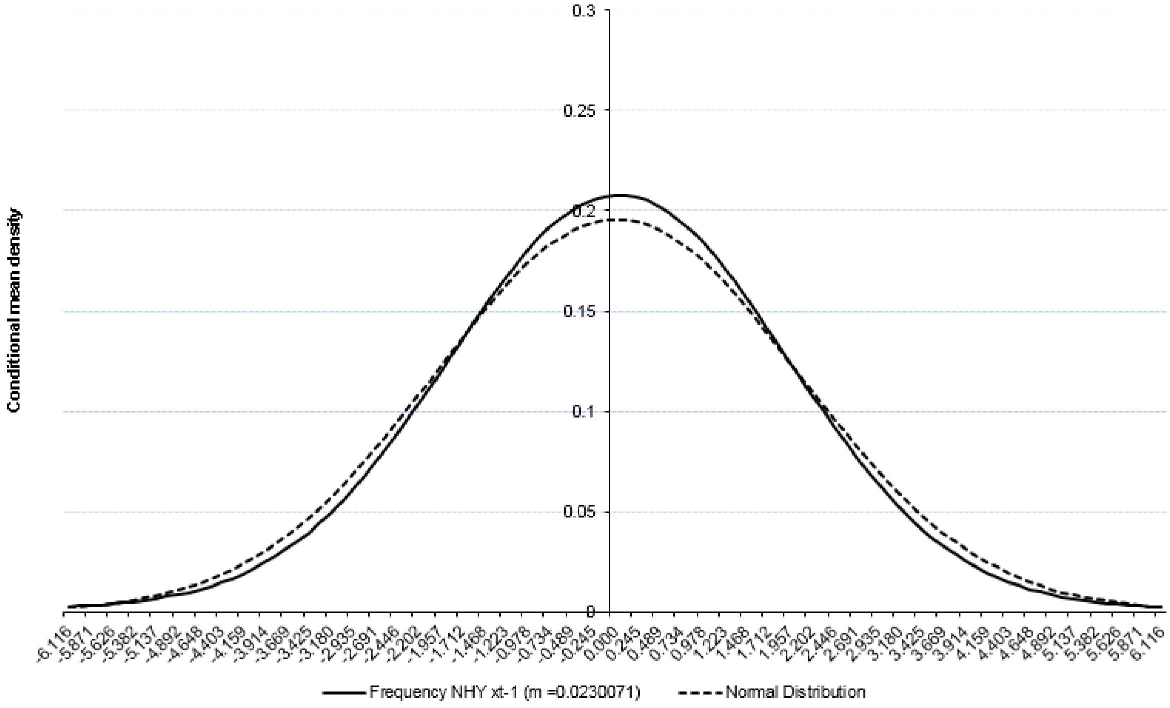

Figure 64 *NHY one-step-ahead densities (x_{t-1} = unconditional mean)*

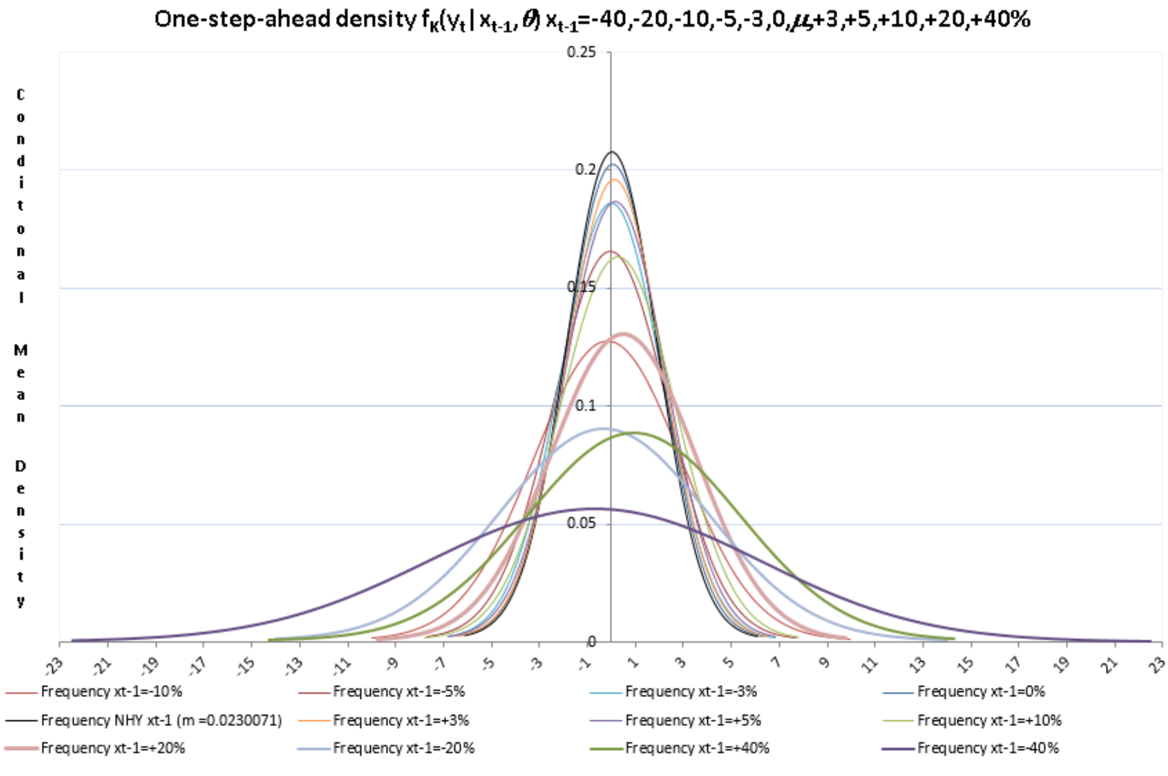

Figure 65 *NHY one-step-ahead densities (conditional mean for xt-1 = -40%...40%)*

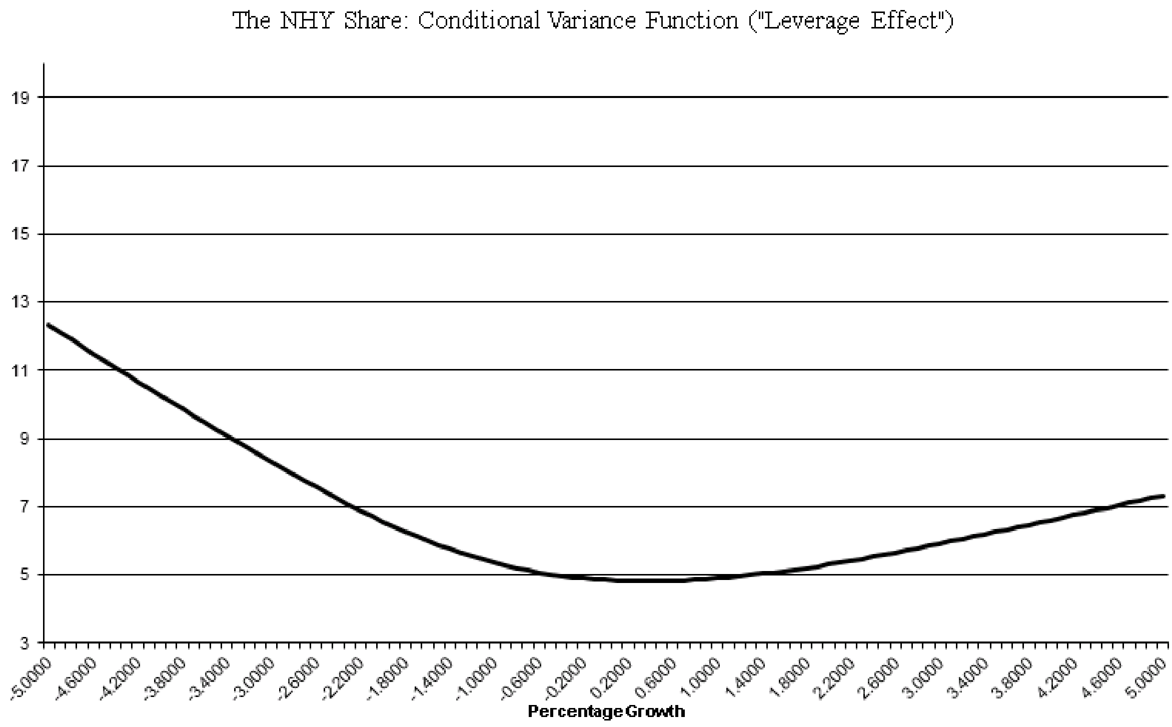

Figure 66 *NHY: conditional variance functions*

5.4.2.11 Tomra Systems ASA (TOM)

The specification tests for the optimal SNP GARCH model are reported in ***Table 37***. The residual statistics show that the data is closer to the normal distribution, with a kurtosis of 13.89, but we still observe leptokurtosis features of the series. There is no volatility clustering, having *P*-values of 0.99 and 0.99 for Q^2 (12) and ARCH (12) respectively. The mean is approximately zero, and the standard deviation is one, referring to the normal distribution denoted as N (0, 1). There is still some dependency in the data. The null hypothesis of the BDS test is rejected, suggesting that the model is misspecified (Brock, Dechert et al. 1996). There is some structure in the data, which can include nonlinearity and nonstationarity. We choose to use the semi-nonparametric GARCH model as it is for the impulse response analysis, bearing in mind that the model can have sub-optimal performance. This might be related to the low trading volume for this stock, making it difficult to describe.

Table 37 *Characteristics of the statistical SNP Model Residuals for TOM*

Residual Statistics for TOM Share

Mean	Median / Std.dev.	Maximum / Minimum	Moment Kurt/Skew	Quantile Kurt/Skew	Quantile Normal	Cramer-von-Mises	Serial dependence Q(12)	$Q^2(12)$
-0.00951	-0.02562	6.12387	13.88975	0.17665	5.94640	6.10353	14.0970	3.1915
	1.00001	-12.99357	-0.69910	-0.01231	{0.0511}	{0.0000}	{0.2950}	{0.9940}
BDS-statistic (ε=1)				ARCH	VaR	CVaR		
m=2	m=3	m=4	m=5	(12)	2.5%/0.5%	2.5%/0.5%		
2.398546	3.8049	4.221029	4.388699	3.268925	-1.7734	-2.7280		
{0.0165}	{0.0001}	{0.0000}	{0.0000}	{0.9933}	-2.9290	-4.9024		

The figures in braces are P-values for statistical significance

The model selected under the Schwarz Criterion is a semiparametric GARCH with eight Hermite polynomials (K_z) for non-normal features of the series. The model is a GARCH (1,1) (L_g, L_r) model with two lags in VAR (L_u). The asymmetric volatility effect is significant for the time series, which indicates that the volatility of the stock shows greater response to a negative shock than a positive shock. The eigenvalue of variance function is 1.007, and the eigenvalue of the mean function is 0.046, as shown in the table below.

Table 38 *Statistical SNP Model Parameters for TOM*

Tomra share

Satistical Model SNP-11118000-fit model
Parameters Semiparametric-GARCH

η		Mode	Standard error
η_1	a0[1]	0.00358	0.00786
η_2	a0[2]	-0.25043	0.01063
η_3	a0[3]	-0.01797	0.00913
η_4	a0[4]	0.10482	0.00979
η_5	a0[5]	-0.05328	0.01027
η_6	a0[6]	-0.09158	0.00933
η_7	a0[7]	-0.00145	0.00986
η_8	a0[8]	0.09670	0.01090
η_9	A(1,1)	1.00000	0.00000
η_{10}	B(1,1)	-0.04597	0.01438
η_{11}	R0[1]	0.07525	0.01040
η_{12}	P(1,1)	0.19310	0.01547
η_{13}	Q(1,1)	0.98467	0.00140
η_{14}	V(1,1)	-0.18644	0.02700
η_{15}	W(1,1)	0.28733	0.05820

Largest eigen value of mean function companion matrix = 0.0459711
Largest eigen value of variance function P & Q companion matrix = 1.00685

Figure 67 displays the characteristics of the projected time series. The plots show the projected conditional volatility, together with a moving average (*m*=number of lags) of the squared residuals of an AR (1) regression model of the returns. It seems like the volatility change randomly, and the projected volatility tends to be relatively compact between *m*=4 and *m*=15. ***Figure 68*** displays the volatility at the mean of the time series, being the one-step-ahead densities $f_k(y_t|x_{t-1}.\theta)$, conditional on the values for x_{t-1} (where x_{t-1} = unconditional mean). The plot shows fatter tails than the normal distribution and advocates only small non-normal elements of the time series. We find that the TOM series has a distribution that is narrower than the normal distribution. These features are commonly seen when analyzing data from a financial market, and confirm the purpose of using Hermite polynomials to describe the density in the best possible way. ***Figure 69*** shows the one-step-ahead densities of shocks ranging from - 40 % to + 40 %, together with the baseline profile (*m*=0.042934). Comparing the different impulse profiles to the baseline profile (the mean), we find that the densities are wider after adding an impulse (shock) to the series. The largest negative shock of - 40 % shows a slightly wider density compared to the equivalent positive shock. This indicates a higher degree of uncertainty after a negative shock and is a confirmation of the observed asymmetry. The relationship between the one-step-ahead dynamics of the conditional variance and the percentage growth is displayed in ***Figure 70***. The graph represents the reactions to shocks hitting the system (asset price). The difference in responses suggests asymmetry due to the “leverage -” and “risk premium” effects. For the TOM series, we find that the responses from negative shocks are slightly higher than from positive, showing a tendency of asymmetry.

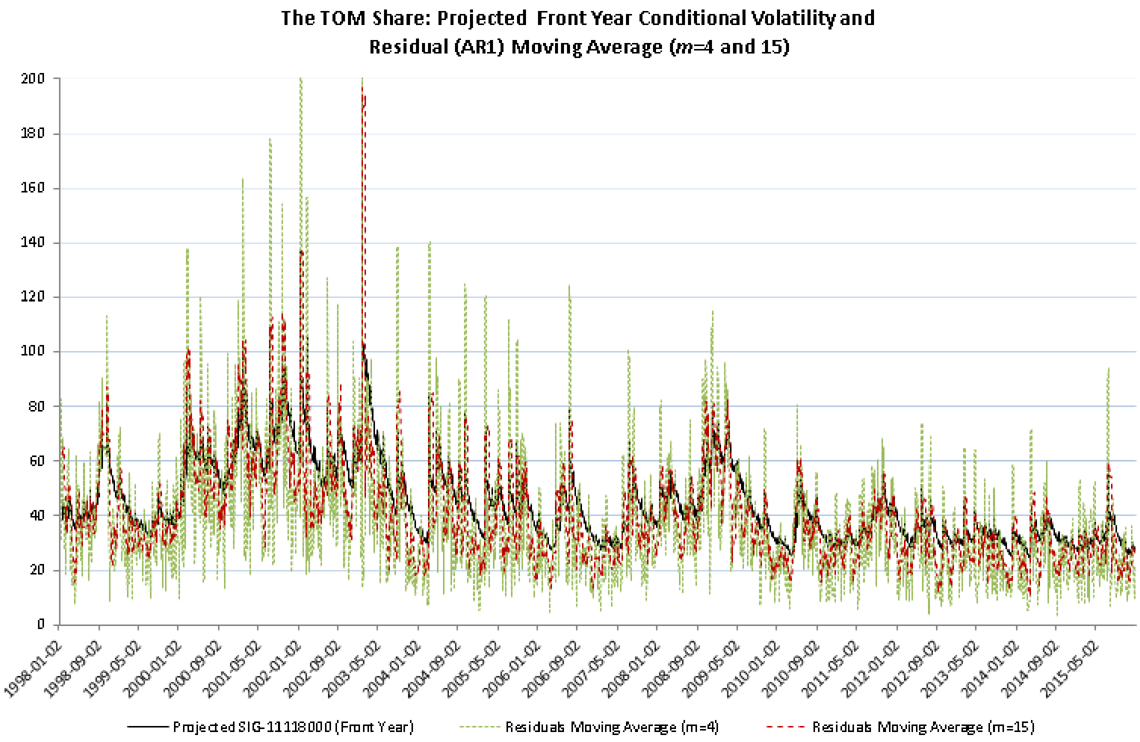

Figure 67 *Projected conditional volatility and residuals AR (1) moving average TOM*

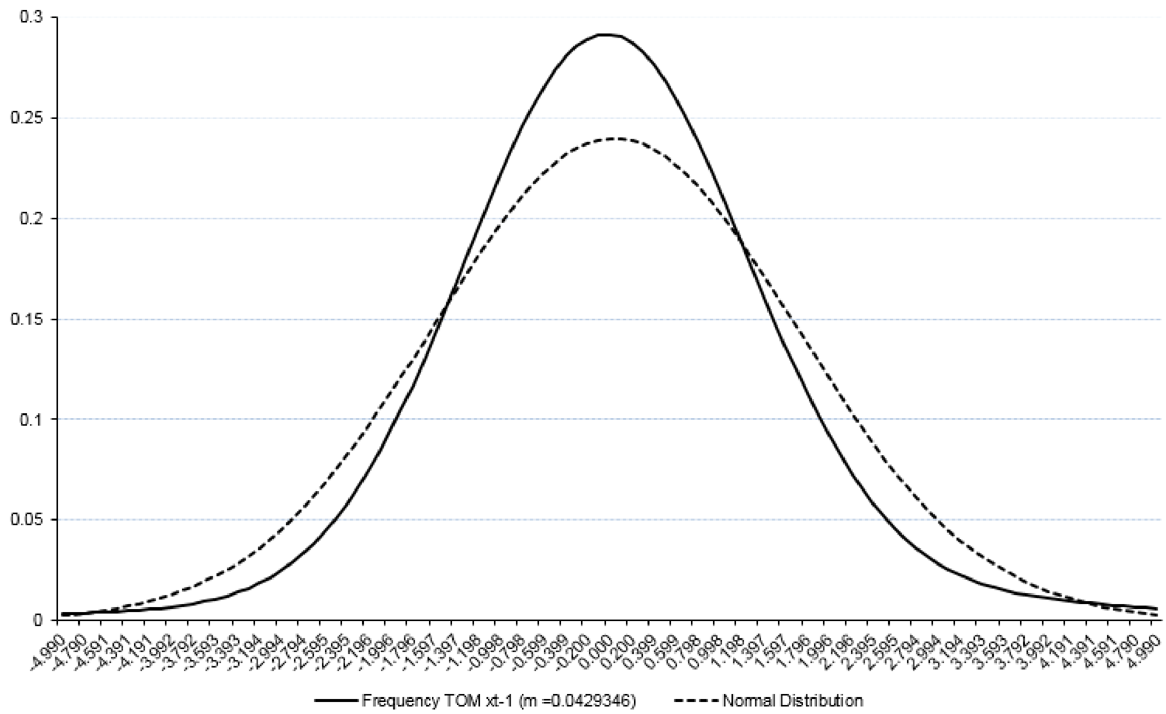

Figure 68 *TOM one-step-ahead densities (x_{t-1} = unconditional mean)*

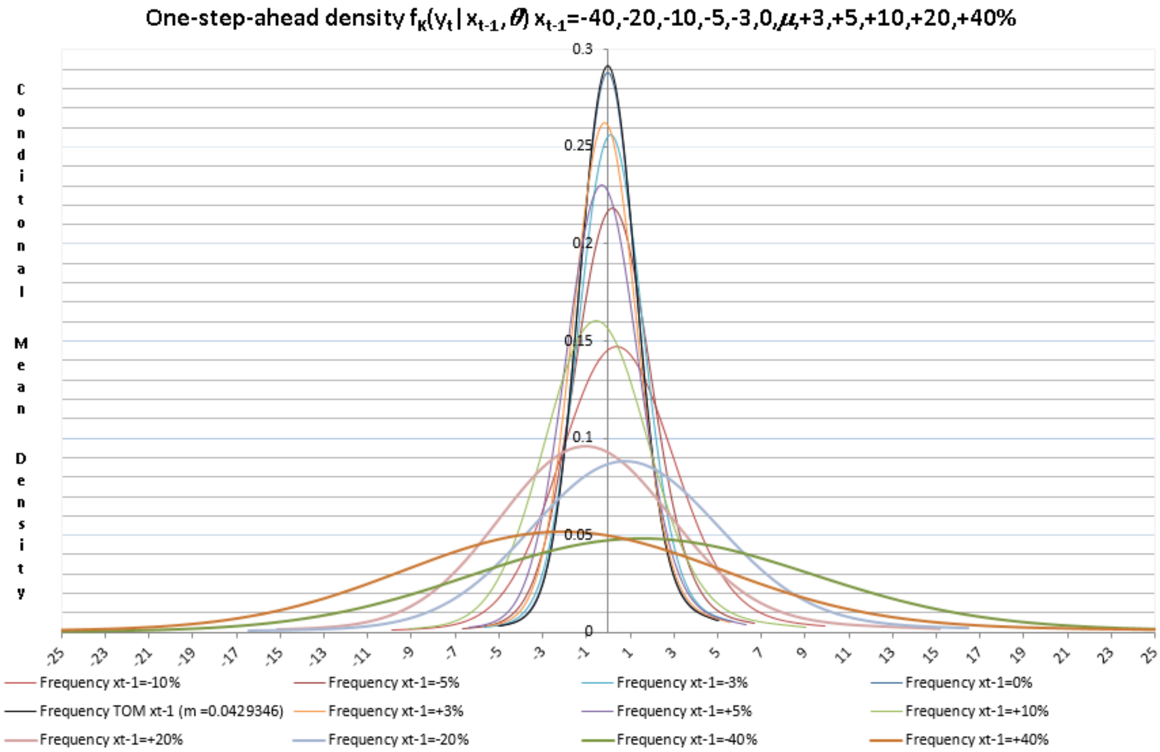

Figure 69 *TOM one-step-ahead densities (conditional mean for x_{t-1} = -40%...40%)*

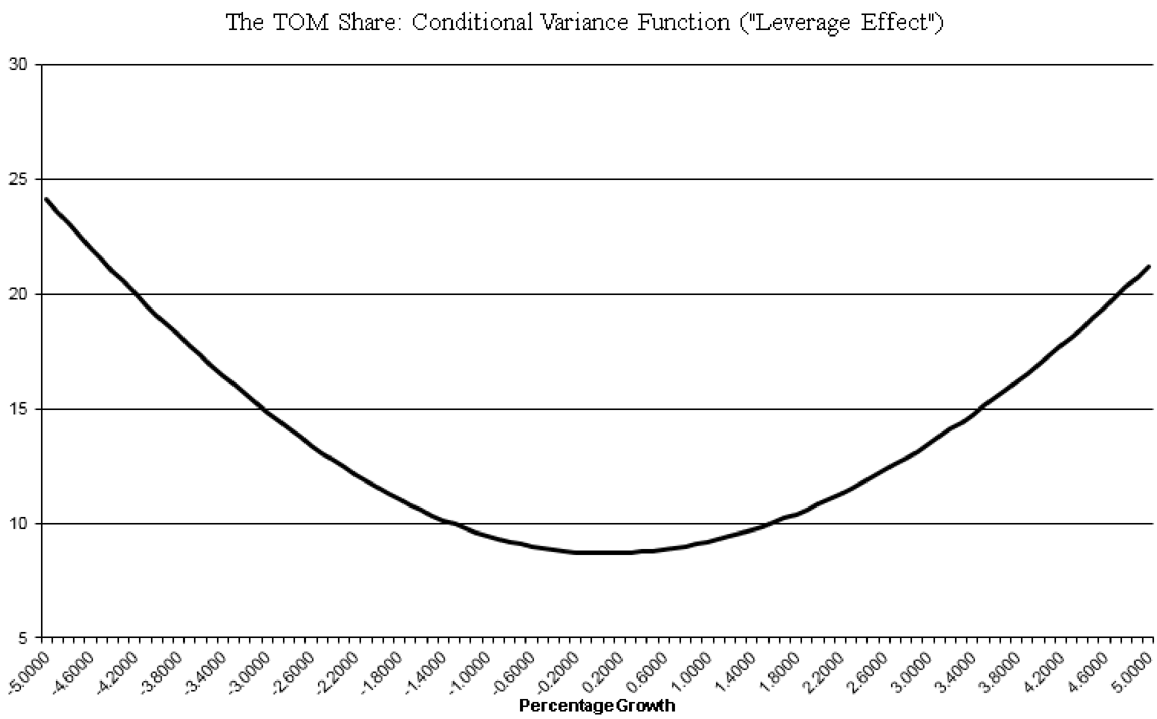

Figure 70 *TOM: conditional variance functions*

5.4.2.12 The ICE Carbon one month Forward Contracts

The specification tests for the optimal SNP GARCH model are reported in ***Table 39***. The residual statistics show that the data is closer to the normal distribution, with a kurtosis of 4.4. There is no volatility clustering, having *P*-values of 0.98 and 0.95 for Q^2 (12) and ARCH (12) respectively. The mean is approximately zero, and the standard deviation is one, referring to the normal distribution denoted as N (0, 1). The BDS-test states that the residuals are IID, meaning data dependence is no longer present. By this, the model misspecification seems minimized, and the semi-nonparametric GARCH model is selected for the impulse response analysis

Table 39 *Characteristics of the statistical SNP Model Residuals for Carbon*

Residual Statistics for Front December Forward Contracts Carbon

Mean	Median / Std.dev.	Maximum / Minimum	Moment Kurt/Skew	Quantile Kurt/Skew	Quantile Normal	Cramer-von-Mises	Serial dependence Q(12)	Q^2(12)
-0.01049	0.01416	5.08209	4.38445	0.10929	1.05649	1.73651	12.8440	4.2798
	0.99995	-7.59808	-0.46072	-0.01388	{0.5896}	{0.0000}	{0.3800}	{0.9780}

BDS-statistic (ε=1)				ARCH	VaR	CVaR
m=2	m=3	m=4	m=5	(12)	2.5%/0.5%	2.5%/0.5%
-1.300481	-0.994773	-1.034807	-1.111832	5.109644	-2.0687	-2.9601
{0.1934}	{0.3198}	{0.3008}	{0.2662}	{0.9542}	-3.2412	-4.6219

The figures in braces are P-values for statistical significance

The model selected under the Schwarz Criterion is a semiparametric GARCH with six Hermite polynomials (K_z) for non-normal features of the series. The model is a GARCH (1,1) (L_g, L_r) model with two lags in VAR (L_u). The asymmetric volatility effect is significant for the time series, which indicates that the volatility of the stock shows greater response to a negative shock than a positive shock. The eigenvalue of variance function is 0.9995, and the eigenvalue of the mean function is 0.2430, as shown in the table below.

Table 40 *Statistical SNP Model Parameters for Carbon*

Carbon Forward Contract

Satistical Model SNP-11116000-fit model
Parameters Semiparametric-GARCH

η		Mode	Standard error
η_1	a0[1]	0.00377	0.01152
η_2	a0[2]	-0.12600	0.01912
η_3	a0[3]	-0.04476	0.01178
η_4	a0[4]	0.03912	0.01168
η_5	a0[5]	-0.00364	0.01140
η_6	a0[6]	-0.11370	0.01213
η_7	A(1,1)	1.00000	0.00000
η_8	B(1,1)	-0.02322	0.02289
η_9	B(1,2)	-0.05903	0.02233
η_{10}	R0[1]	0.08129	0.01333
η_{11}	P(1,1)	0.30900	0.02988
η_{12}	Q(1,1)	0.95079	0.00537
η_{13}	V(1,1)	-0.24761	0.04026

Largest eigen value of mean function companion matrix = 0.242951
Largest eigen value of variance function P & Q companion matrix = 0.999487

Figure 71 displays the characteristics of the projected time series. The plots show the projected conditional volatility, together with a moving average (*m*=number of lags) of the squared residuals of an AR (1) regression model of the returns. It seems like the volatility change randomly, and the projected volatility tends to be relatively compact between *m*=4 and *m*=15. ***Figure 72*** displays the volatility at the mean of the time series, being the one-step-ahead densities $f_k(y_t|x_{t-1}.\theta)$, conditional on the values for x_{t-1} (where x_{t-1} = unconditional mean). The plot shows fatter tails than the normal distribution and advocates only small non-normal elements of the time series. We find that the carbon series has a distribution that is narrower than the normal distribution. These features are commonly seen when analyzing data from a financial market, and confirm the purpose of using Hermite polynomials to describe the density in the best possible way. ***Figure 73*** shows the one-step-ahead densities of shocks ranging from - 40 % to + 40 %, together with the baseline profile (*m*=0.026486). Comparing the different impulse profiles to the baseline profile (the mean), we find that the densities are wider after adding an impulse (shock) to the series. The largest negative shock of - 40 % shows a wider density compared to the equivalent positive shock. This indicates a higher degree of uncertainty after a negative shock and is a confirmation of the observed asymmetry. The relationship between the one-step-ahead dynamics of the conditional variance and the percentage growth is displayed in ***Figure 74***. The graph represent the reactions to shocks hitting the system (asset price). The difference in responses suggests asymmetry due to the “leverage -” and “risk premium” effects. For the carbon series, we find that the responses from negative shocks are much higher than from positive, showing an apparent asymmetry.

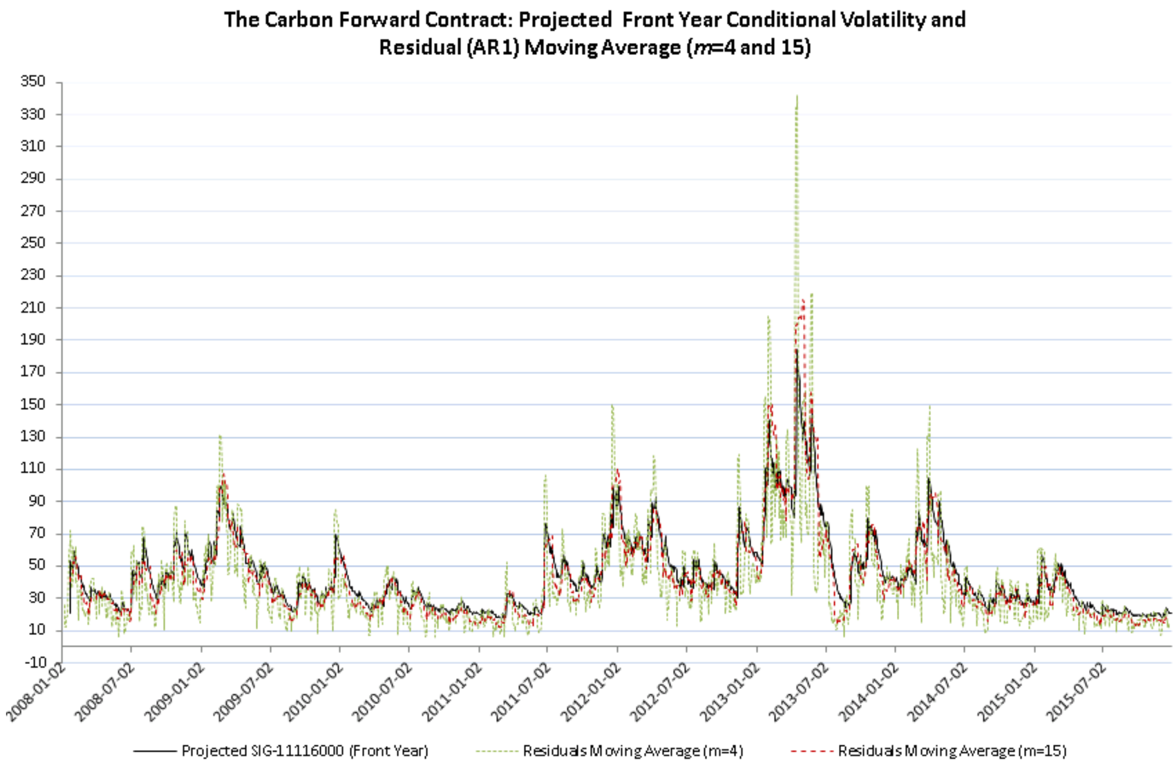

Figure 71 *Projected conditional volatility and residuals AR (1) moving average Carbon*

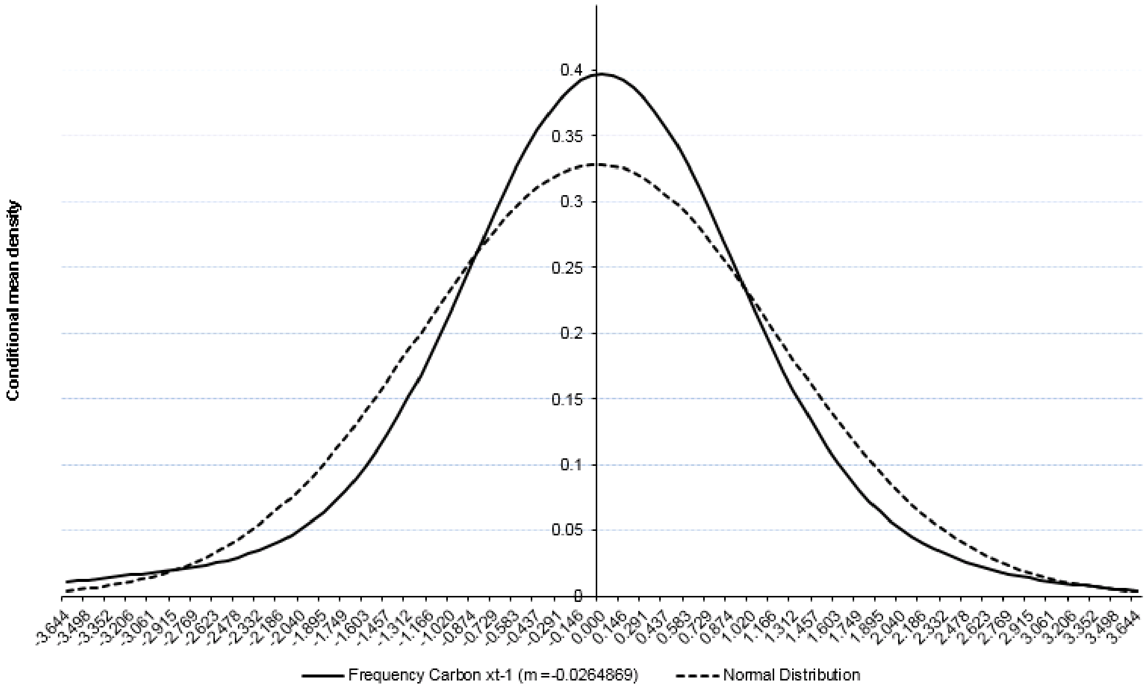

Figure 72 *Carbon one-step-ahead densities (x_{t-1} = unconditional mean)*

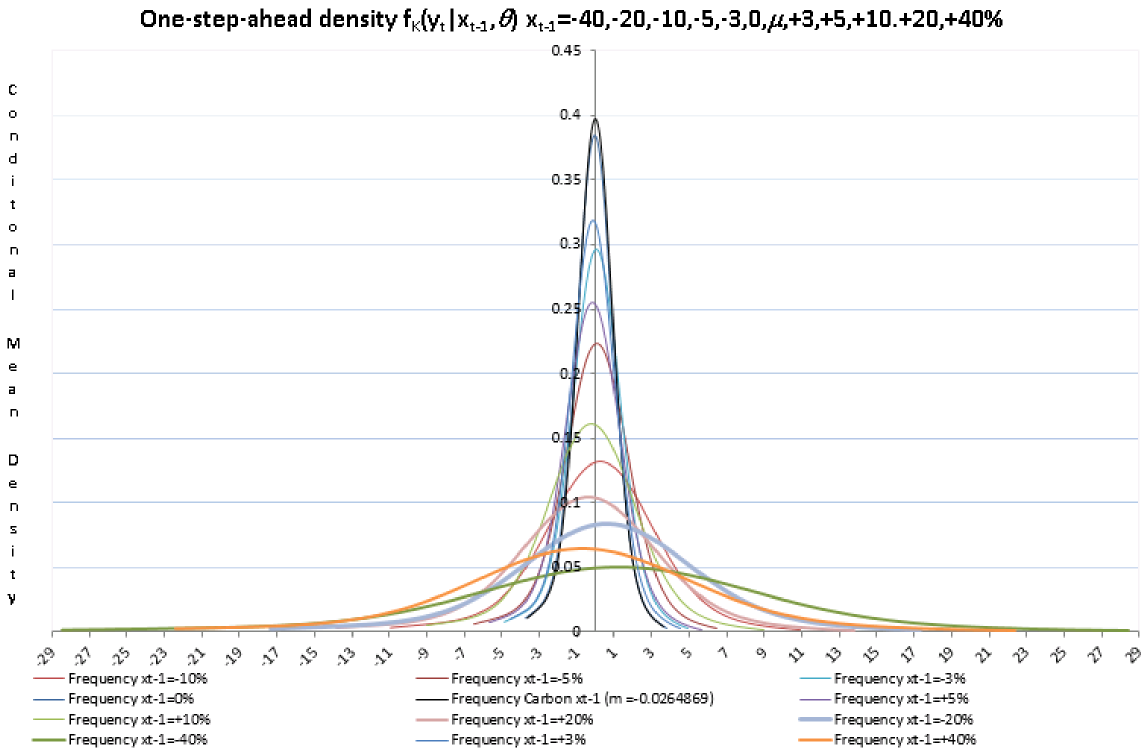

Figure 73 *Carbon one-step-ahead densities (conditional mean for x_{t-1} = -40%...40%)*

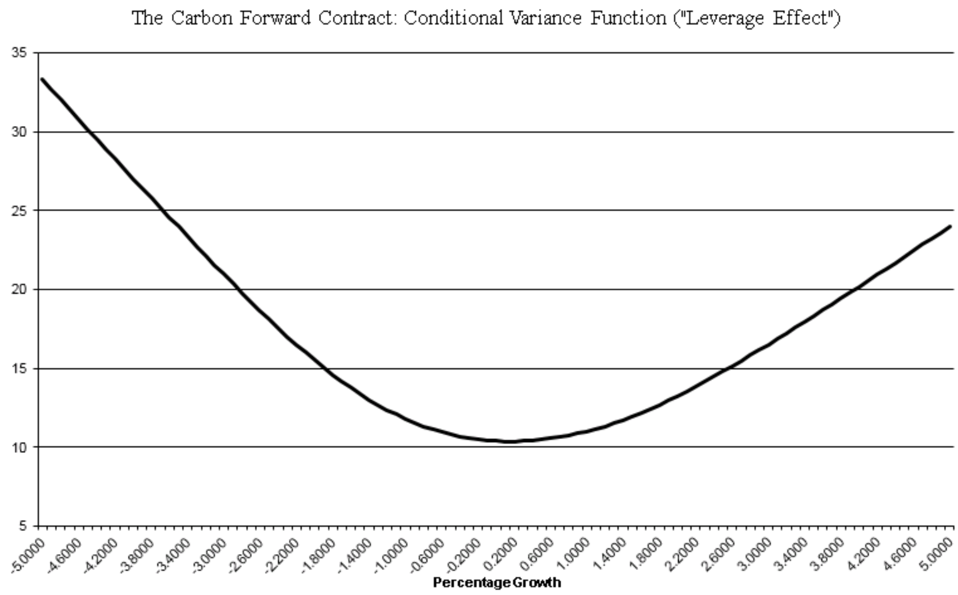

Figure 74 *Carbon: conditional variance functions*

5.4.2.13 Brent oil front month Future Contracts

The specification tests for the optimal SNP GARCH model are reported in **Table 41**. The residual statistics show that the data is closer to the normal distribution, with a kurtosis of 1.5. There is no volatility clustering, having *P*-values of 0.19 and 0.18 for Q^2 (12) and ARCH (12) respectively. The mean is approximately zero, and the standard deviation is one, referring to the normal distribution denoted as N (0, 1). The BDS-test states that the residuals are IID, meaning data dependence is no longer present. By this, the model misspecification seems minimized, and the semi-nonparametric GARCH model is selected for the impulse response analysis

Table 41 *Characteristics of the statistical SNP Model Residuals for Brent oil*

Residual Statistics for Brent Oil Derivatives

Mean	Median / Std.dev.	Maximum / Minimum	Moment Kurt/Skew	Quantile Kurt/Skew	Quantile Normal	Cramer-von-Mises	Serial dependence Q(12)	$Q^2(12)$
0.00432	0.01628	4.14855	1.53487	0.12467	1.32753	0.70963	8.1122	16.087
	0.99995	-6.26755	-0.24563	-0.00006	{0.5149}	{0.0000}	{0.7760}	{0.1870}
BDS-statistic (ε=1)				ARCH	VaR	CVaR		
m=2	m=3	m=4	m=5	(12)	2.5%/0.5%	2.5%/0.5%		
0.136521	0.44962	0.145858	0.16214	16.31221	-2.1032	-2.6731		
{0.8914}	{0.6530}	{0.8840}	{0.8712}	{0.1774}	-3.0171	-3.6311		

The figures in braces are P-values for statistical significance

The model selected under the Schwarz Criterion is a semiparametric GARCH with four Hermite polynomials (K_z) for non-normal features of the series. The model is a GARCH (1,1) (L_g, L_r) model with one lag in VAR (L_u). The asymmetric volatility effect is significant for the time series, which indicates that the volatility of the stock shows greater response to a negative shock than a positive shock. Lags in additive level (L_w) is also significant indicating additive outliers in the series. The eigenvalue of variance function is 0.9752, and the eigenvalue of the mean function is 0.0537, as shown in the table below.

Table 42 *Statistical SNP Model Parameters for Brent oil*

Brent Oil Derivative

Statistical Model SNP-11114000 -fit model
Parameters Semiparametric-GARCH.

η		Mode	Standard error
η_1	a0[1]	0.00759	0.01126
η_2	a0[2]	-0.05462	0.02399
η_3	a0[3]	-0.03231	0.01164
η_4	a0[4]	0.07174	0.01137
η_5	A(1,1)	1.00000	0.00000
η_6	B(1,1)	-0.05371	0.02352
η_7	R0[1]	0.05024	0.01327
η_8	P(1,1)	0.16656	0.03201
η_9	Q(1,1)	0.97336	0.00446
η_{10}	V(1,1)	-0.24875	0.03408
η_{11}	W(1,1)	-0.24868	0.07772

Largest eigen value of mean function companion matrix = 0.053706
Largest eigen value of variance function P & Q companion matrix = 0.975178

Figure 75 displays the characteristics of the projected time series. The plots show the projected conditional volatility, together with a moving average (*m*=number of lags) of the squared residuals of an AR (1) regression model of the returns. It seems like the volatility change randomly, and the projected volatility tends to be relatively compact between *m*=4 and *m*=15. ***Figure 76*** displays the volatility at the mean of the time series, being the one-step-ahead densities $f_k(y_t|x_{t-1}.\theta)$, conditional on the values for x_{t-1} (where x_{t-1} = unconditional mean). The plot shows fatter tails than the normal distribution and advocates only small non-normal elements of the time series. We find that the Brent oil series has a distribution that is narrower than the normal distribution. These features are commonly seen when analyzing data from a financial market, and confirm the purpose of using

Hermite polynomials to describe the density in the best possible way. ***Figure 77*** shows the one-step-ahead densities of shocks ranging from - 40 % to + 40 %, together with the baseline profile (*m*=0.033740). Comparing the different impulse profiles to the baseline profile (the mean), we find that the densities are wider after adding an impulse (shock) to the series. The largest negative shock of - 40 % shows a much wider density compared to the equivalent positive shock. This indicates a higher degree of uncertainty after a negative shock and is a confirmation of the observed asymmetry. The relationship between the one-step-ahead dynamics of the conditional variance and the percentage growth is displayed in ***Figure 78***. The graph represents the reactions to shocks hitting the system (asset price). The difference in responses suggests asymmetry due to the "leverage -" and "risk premium" effects. For the Brent oil series, we find that the responses from negative shocks are much higher than from positive, showing an apparent asymmetry.

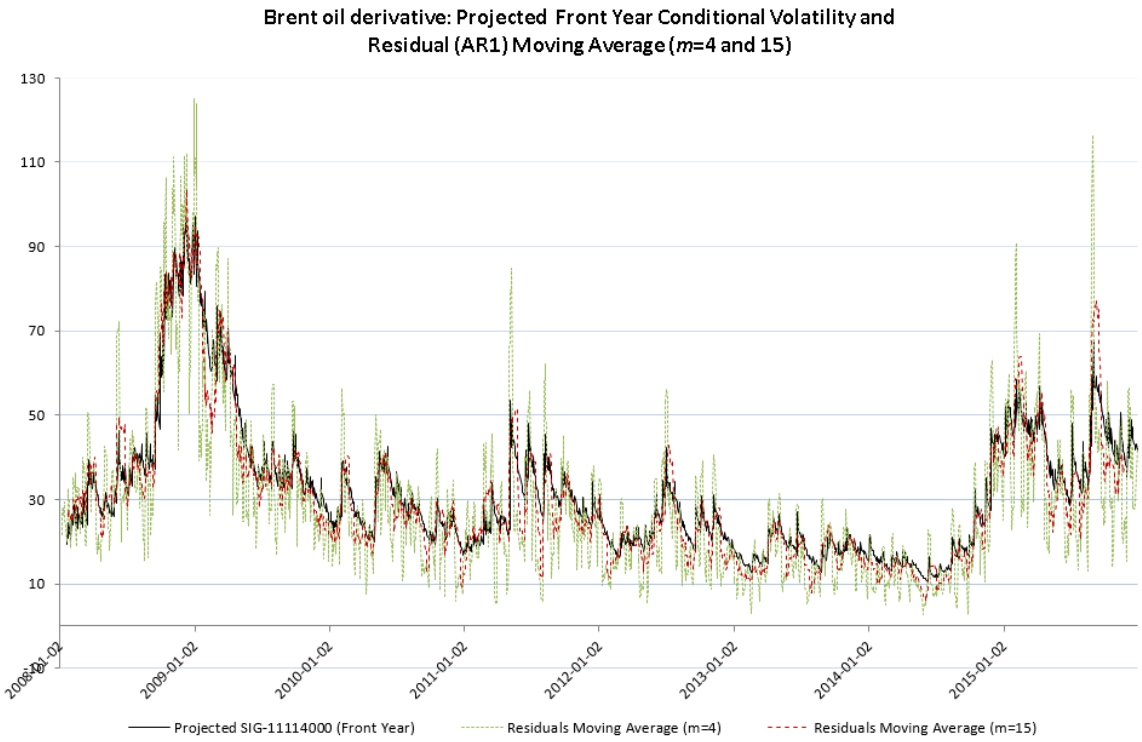

Figure 75 *Projected conditional volatility and residuals AR (1) moving average for Brent oil*

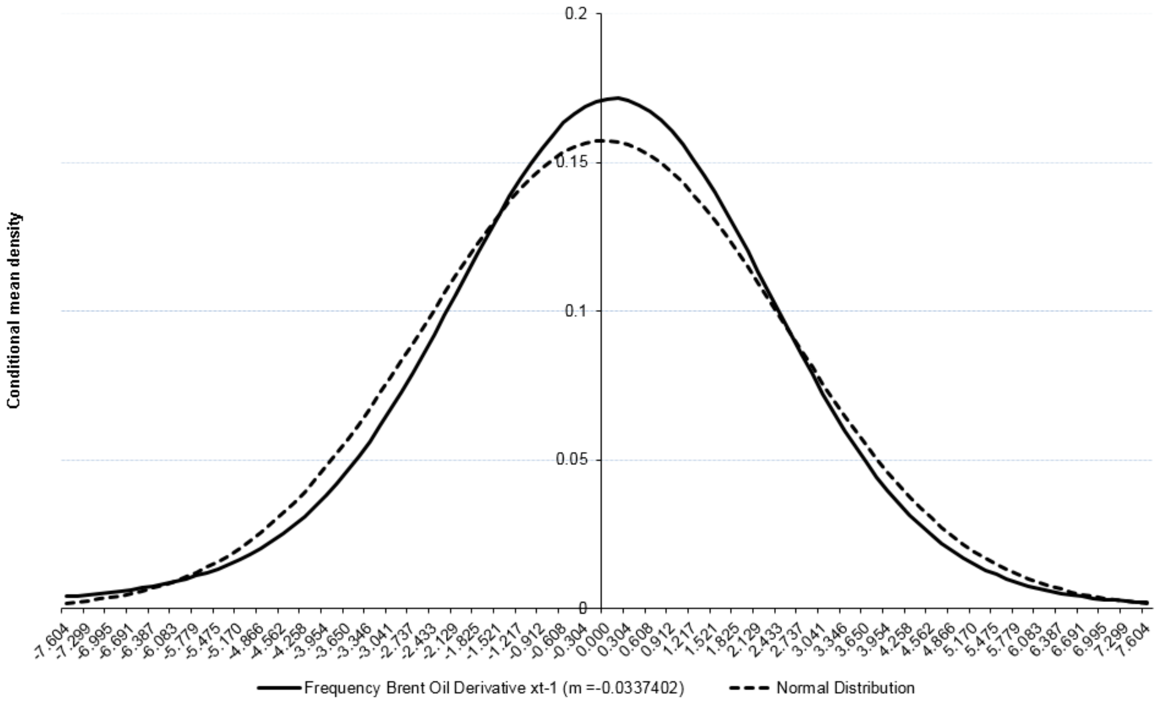

Figure 76 *Brent oil one-step-ahead densities (x_{t-1} = unconditional mean)*

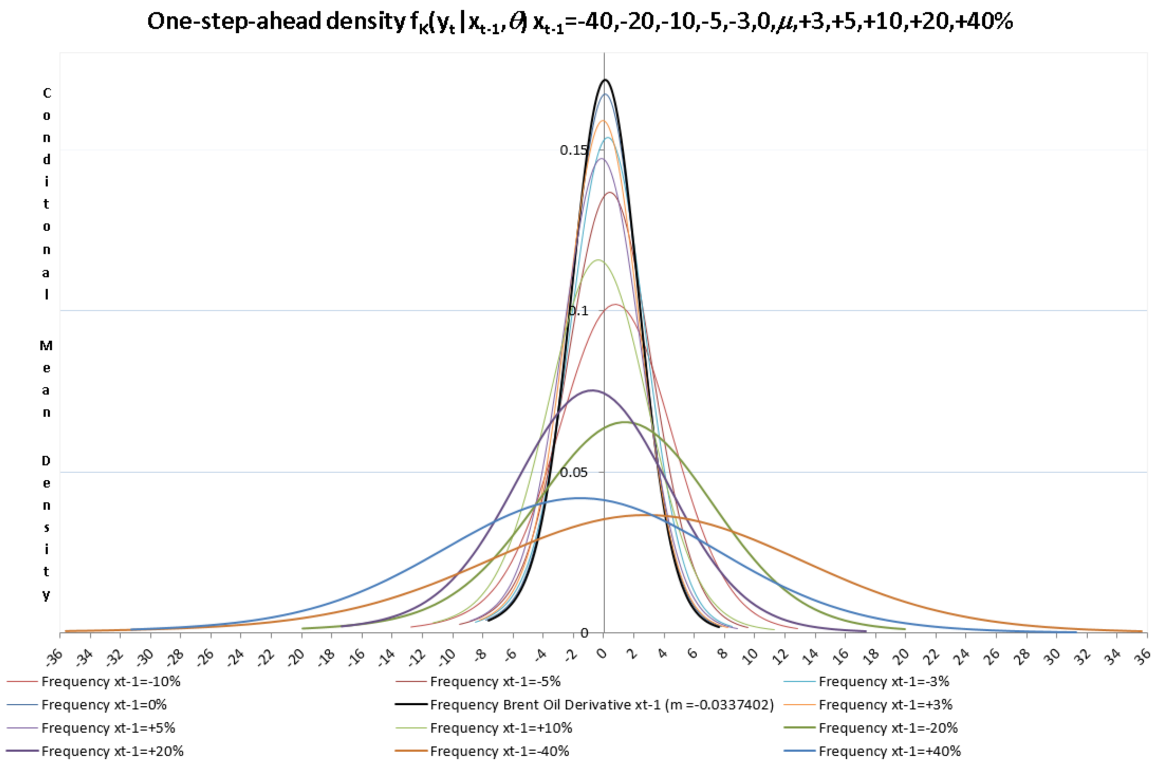

Figure 77 *Brent oil one-step-ahead densities (conditional mean for xt-1 = -40%...40%)*

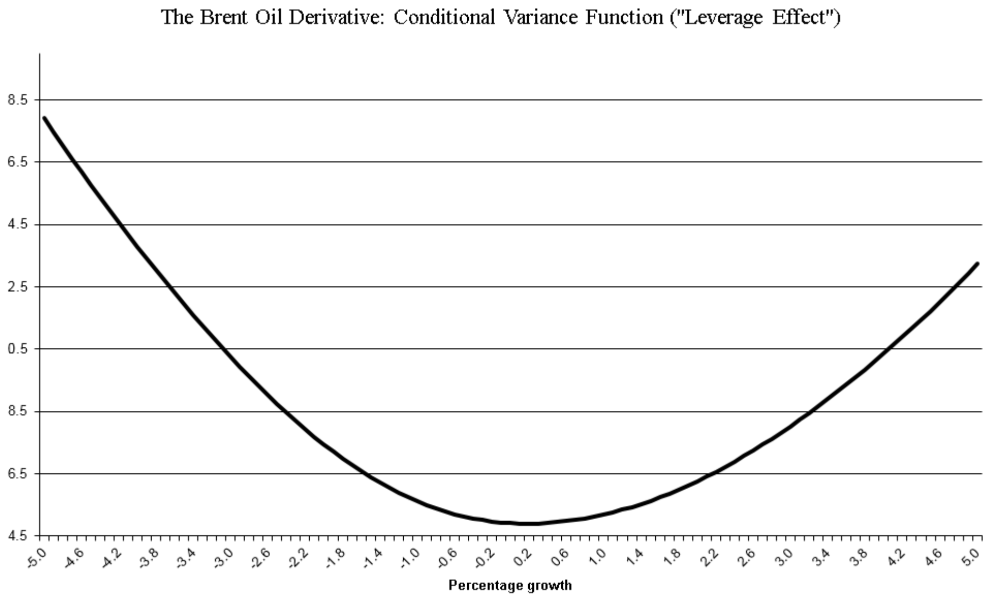

Figure 78 *Brent oil: conditional variance functions*

5.4.2.14 Salmon Forward Contracts

The specification tests for the optimal SNP GARCH model are reported in ***Table 43***. The residual statistics show that the data is closer to the normal distribution, with a kurtosis of 5.8. There is no volatility clustering, having *P*-values of 0.50 and 0.51 for Q^2 (12) and ARCH (12) respectively. The mean is approximately zero, and the standard deviation is one, referring to the normal distribution denoted as N (0, 1). The BDS-test states that the residuals are IID, meaning data dependence is no longer present. By this, the model misspecification seems minimized, and the semi-nonparametric GARCH model is selected for the impulse response analysis

Table 43 *Characteristics of the statistical SNP Model Residuals for Salmon*

Residual Statistics for Salmon one month Future Contract

Mean	Median / Std.dev.	Maximum / Minimum	Moment Kurt/Skew	Quantile Kurt/Skew	Quantile Normal	Cramer-von-Mises	Serial dependence Q(12)	Q^2(12)
0.00641	-0.02809	7.27835	5.81767	0.50109	24.97514	9.63621	27.6580	11.325
	0.99996	-5.51650	0.54979	0.00210	{0.0000}	{0.0000}	{0.0060}	{0.5010}
BDS-statistic (ε=1)				ARCH	VaR	CVaR		
m=2	m=3	m=4	m=5	(12)	2.5%/0.5%	2.5%/0.5%		
0.898695	1.202263	0.891151	0.809836	11.21925	-2.0348	-2.7965		
{0.3688}	{0.2293}	{0.3728}	{0.4180}	{0.5102}	-3.1792	-4.0040		

The figures in braces are P-values for statistical significance

The model selected under the Schwarz Criterion is a semiparametric GARCH with eight Hermite polynomials (K_z) for non-normal features of the series. The model is a GARCH (1,1) (L_g, L_r) model with two lags in VAR (L_u). The asymmetric volatility effect is significant for the time series, which indicates that the volatility of the stock shows greater response to a negative shock than a positive shock. The eigenvalue of variance function is 0.8884, and the eigenvalue of the mean function is 0.2922, as shown in the table below.

***Table 44** Statistical SNP Model Parameters for Salmon*

Salmon one month Forward

Statistical Model SNP-11118000 -fit model
Parameters Semiparametric-GARCH

η		Mode	Standard error
η_1	a0[1]	-0.00270	0.01050
η_2	a0[2]	-0.06211	0.01306
η_3	a0[3]	0.02814	0.01078
η_4	a0[4]	0.18940	0.01033
η_5	a0[5]	-0.01039	0.01111
η_6	a0[6]	-0.05948	0.01214
η_7	a0[7]	0.00953	0.01134
η_8	a0[8]	0.09125	0.01122
η_9	A(1,1)	1.00000	0.00000
η_{10}	B(1,1)	0.09888	0.01760
η_{11}	B(1,2)	0.05648	0.01737
η_{12}	R0[1]	0.26398	0.01995
η_{13}	P(1,1)	0.21582	0.02677
η_{14}	Q(1,1)	0.91750	0.01056
η_{15}	V(1,1)	-0.30768	0.03780

Largest eigen value of mean function companion matrix = 0.29219
Largest eigen value of variance function P & Q companion matrix = 0.888383

Figure 79 displays the characteristics of the projected time series. The plots show the projected conditional volatility, together with a moving average (*m*=number of lags) of the squared residuals of an AR (1) regression model of the returns. It seems like the volatility change randomly, and the projected volatility tends to be relatively compact between *m*=4 and *m*=15. ***Figure 80*** displays the volatility at the mean of the time series, being the one-step-ahead densities $f_k(y_t|x_{t-1}.\theta)$, conditional on the values for x_{t-1} (where x_{t-1} = unconditional mean). The plot shows fatter tails than the normal distribution and advocates only small non-normal elements of the time series. We find that the salmon series has a distribution that is narrower than the normal distribution. These features are commonly seen when analyzing data from a financial market, and confirm the purpose of using Hermite polynomials to describe the density in the best possible way. ***Figure 81*** shows the one-step-ahead densities of shocks ranging from - 40 % to + 40 %, together with the baseline profile (*m*=0.030207). Comparing the different impulse profiles to the baseline profile (the mean), we find that the densities are wider after adding an impulse (shock) to the series. The largest negative shock of - 40 % shows a much wider density compared to the equivalent positive shock. This indicates a higher degree of uncertainty after a negative shock and is a confirmation of the observed asymmetry. The relationship between the one-step-ahead dynamics of the conditional variance and the percentage growth is displayed in ***Figure 82***. The graph represents the reactions to shocks hitting the system (asset price). The difference in responses suggests asymmetry due to the "leverage -" and "risk premium" effects. For the salmon series, we find that the responses from negative shocks are much higher than from positive, showing an apparent asymmetry.

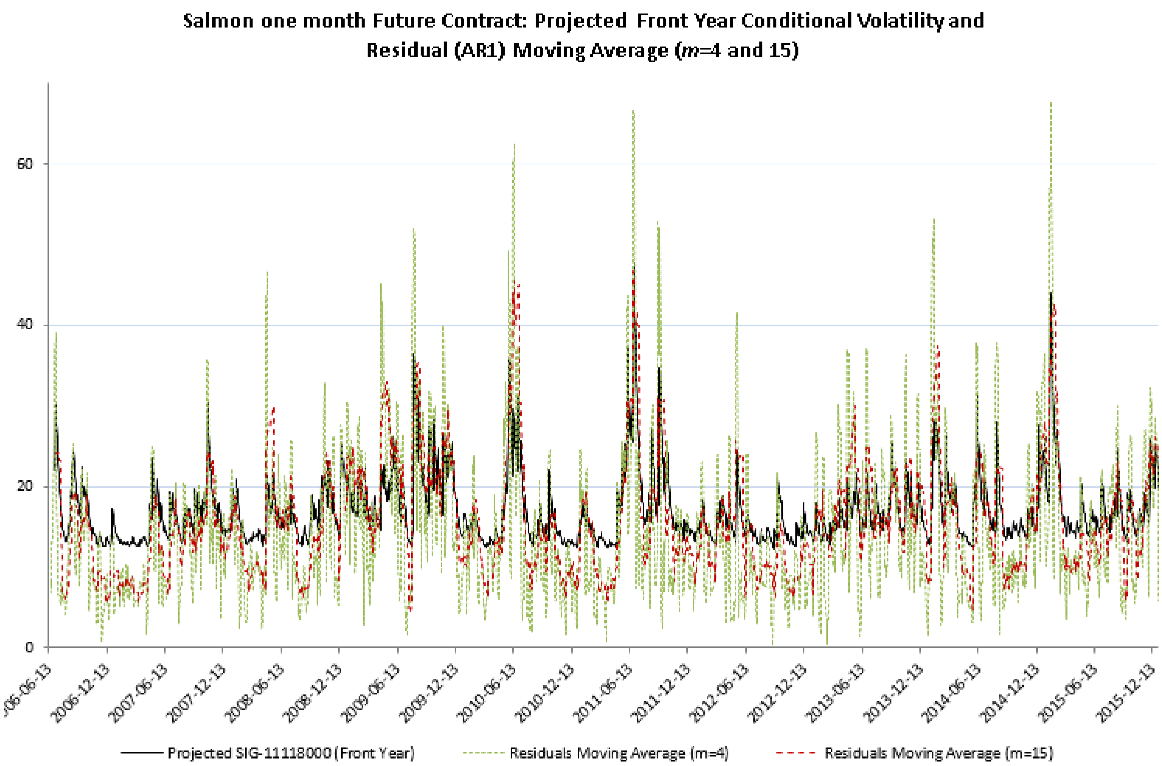

Figure 79 *Projected conditional volatility and residuals AR (1) moving average Salmon*

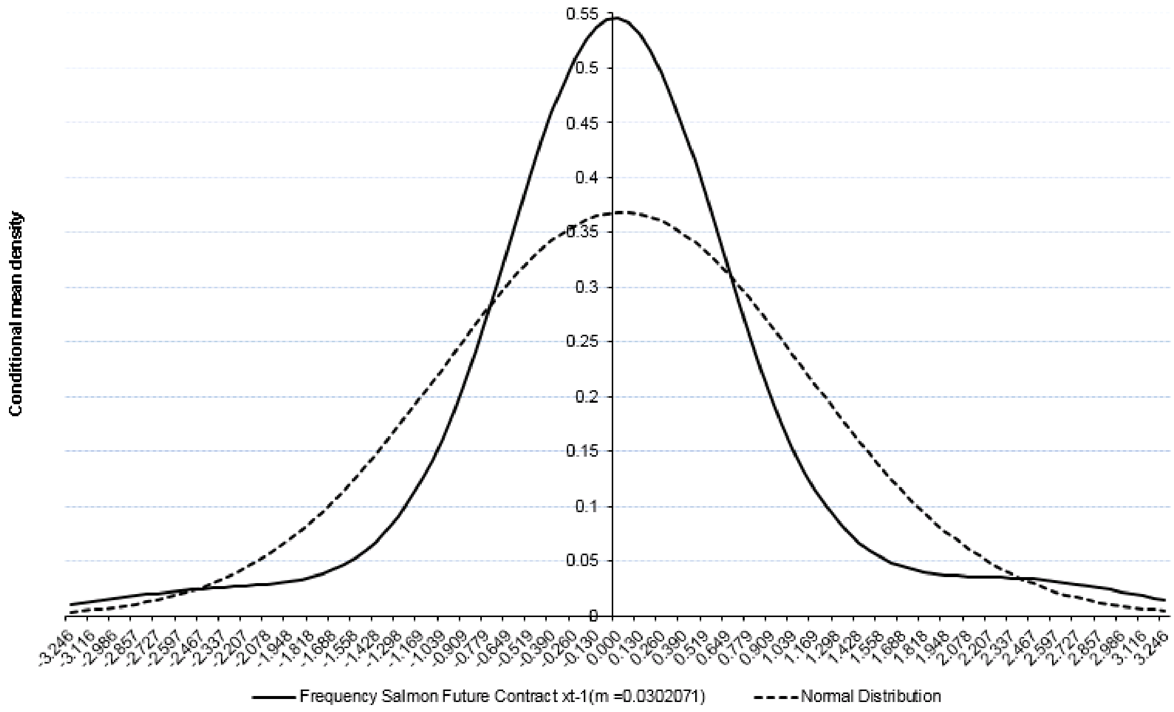

Figure 80 *Salmon one-step-ahead densities (x_{t-1} = unconditional mean)*

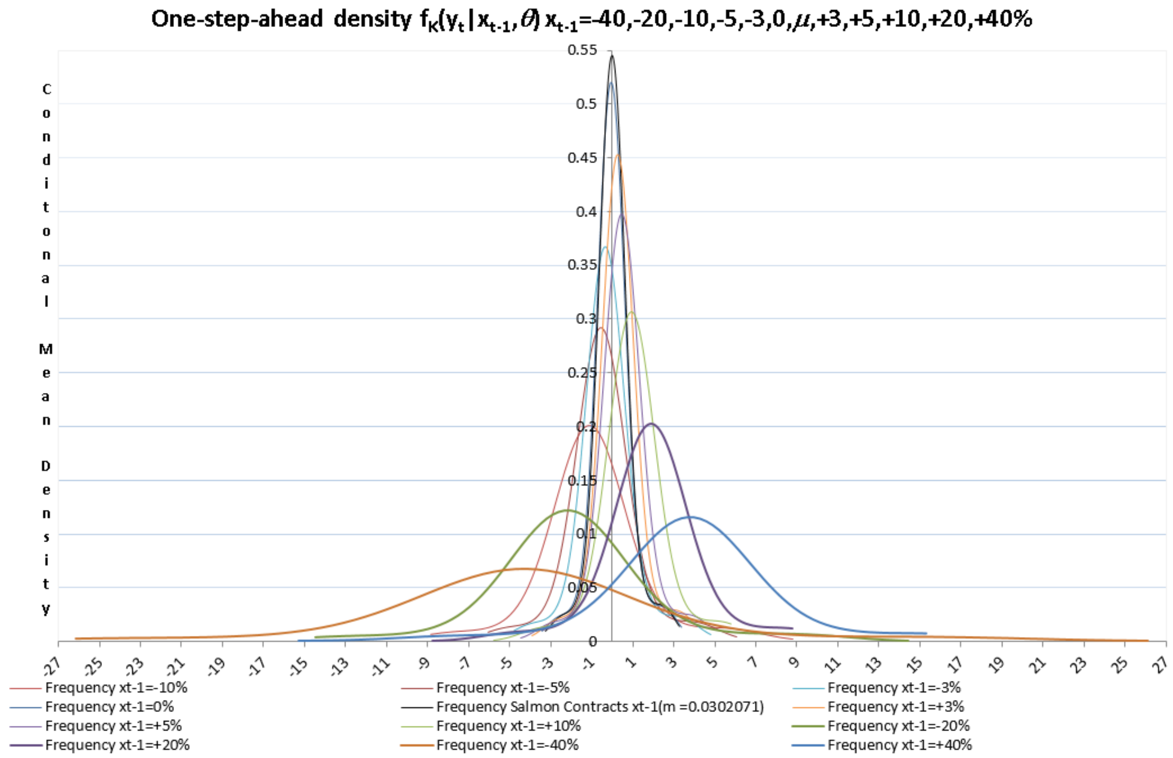

Figure 81 *Salmon one-step-ahead densities (conditional mean for x_{t-1} = -40%...40%)*

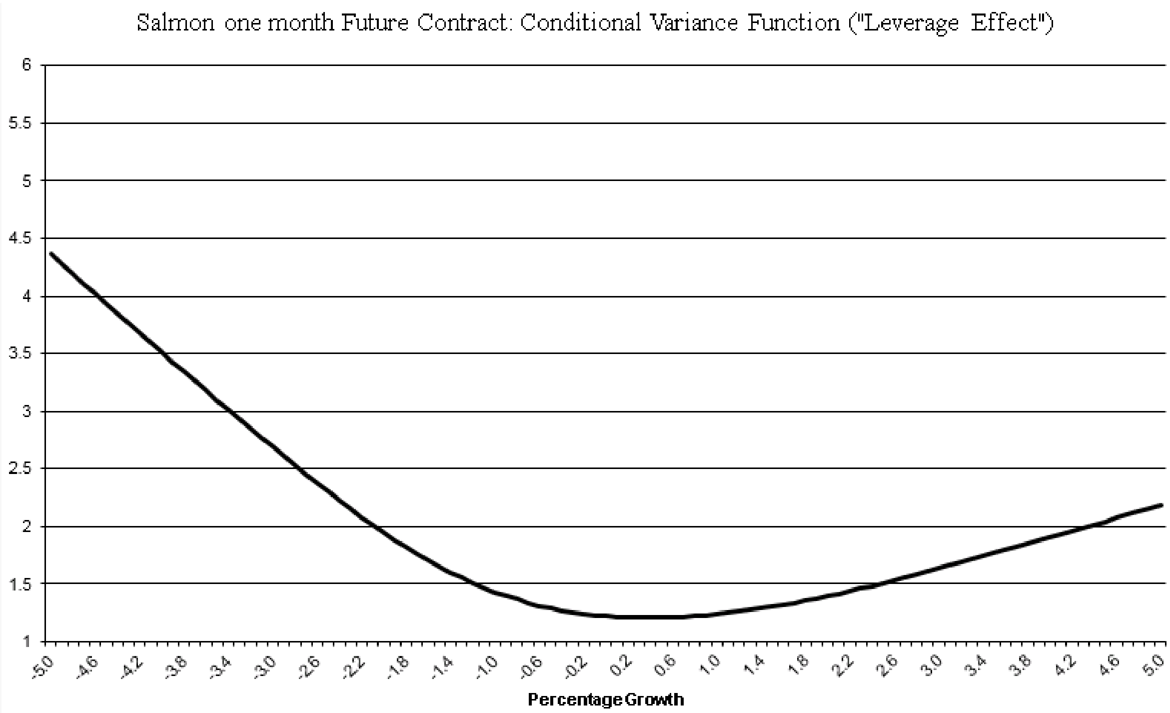

Figure 82 *Salmon: conditional variance functions*

6.0 Empirical Results

Several figures lay out the results of our analysis. We have compiled the impulse-response dynamics for mean return and variance in the first section. Discussion of aspects concerning impulse response characteristics that stand out compared to others follows at the end of the sections.

6.1 Impulse-Response Dynamics for Mean and Variance

This section contains the dynamic impulse responses of future mean return and volatility to price shocks. ***Figure 83*** **(a – n)** shows the *Mean* Impulse Response Dynamics for the time series. One interesting feature is that the impulse responses are symmetric about the baseline, and we observe virtually no serial dependence beyond lag one. The return is clearly mean reverting, returning to its mean within one day, as shown in the figure below. Our results suggest that a positive (negative) price change is met by a slightly negative (positive) expected return in the following days. OSEBX, NHY, and MU stand out in this context in that they show a negative (positive) response to negative (positive) price changes. The results also indicate that both a positive and negative price change for OSEAX is met by a positive subsequent expected return.

a. Dow Jones Industrial Average

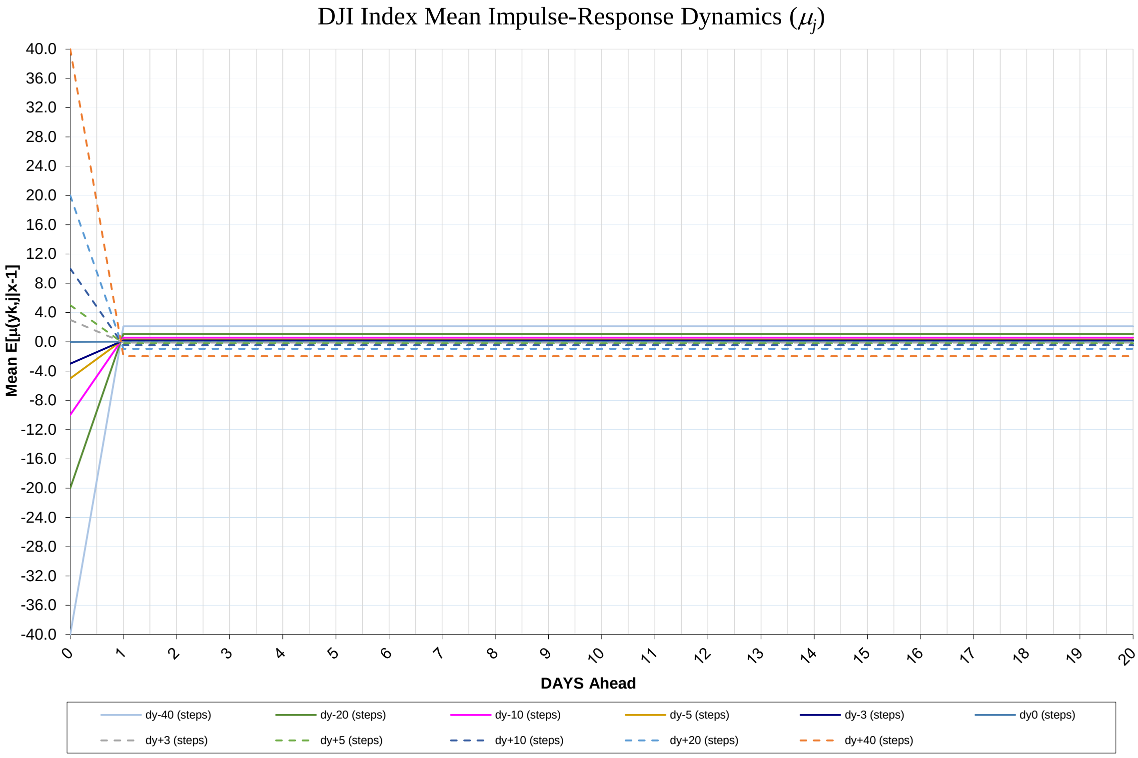

b. FTSE 100 Index

FTSE Index Mean Impulse-Response Dynamics (μ_j)

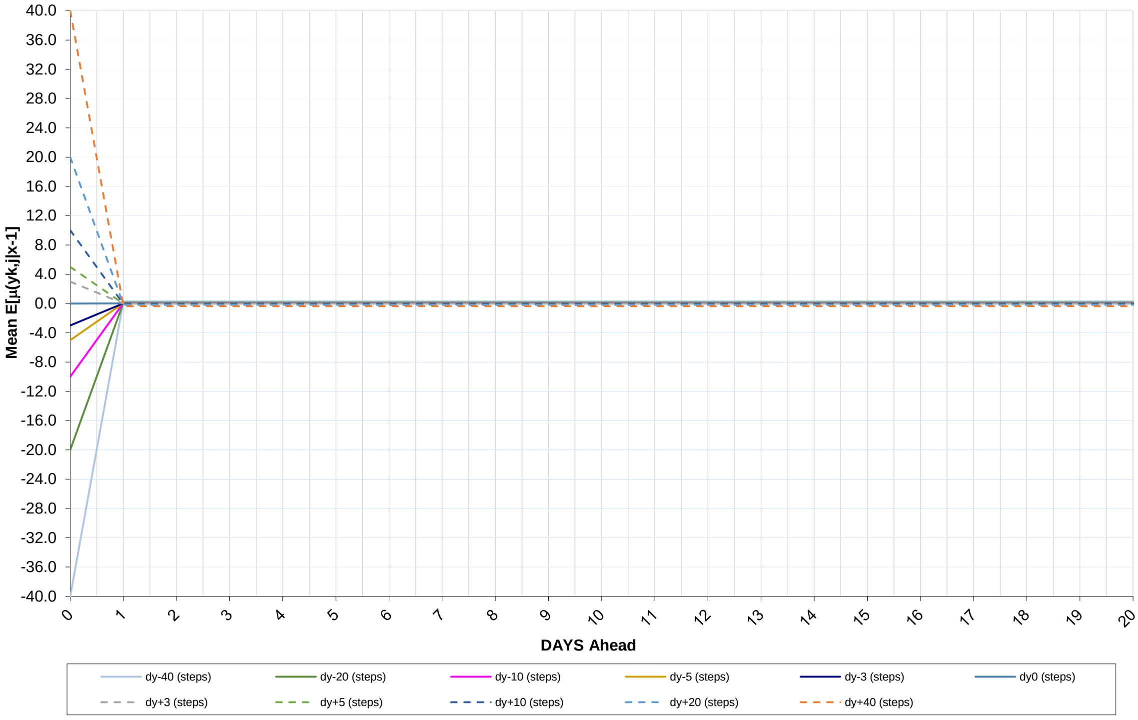

c. S&P 100 Index

S&P 100 Index Mean Impulse-Response Dynamics (μ_j)

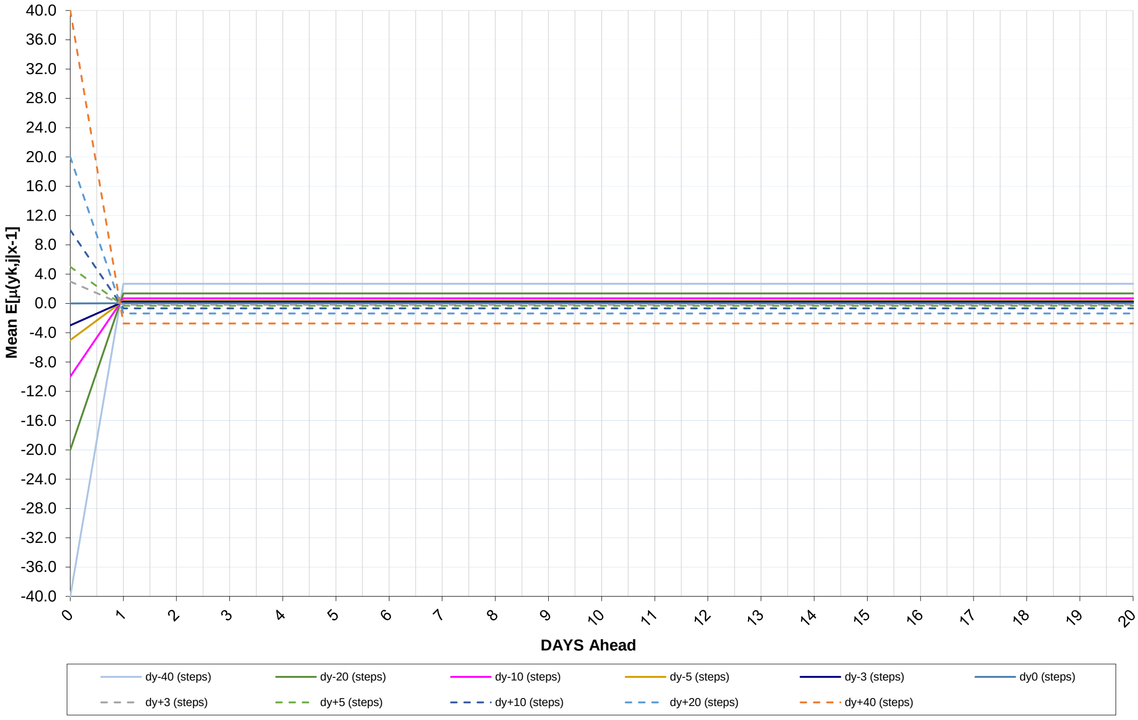

d. S&P 500 Index

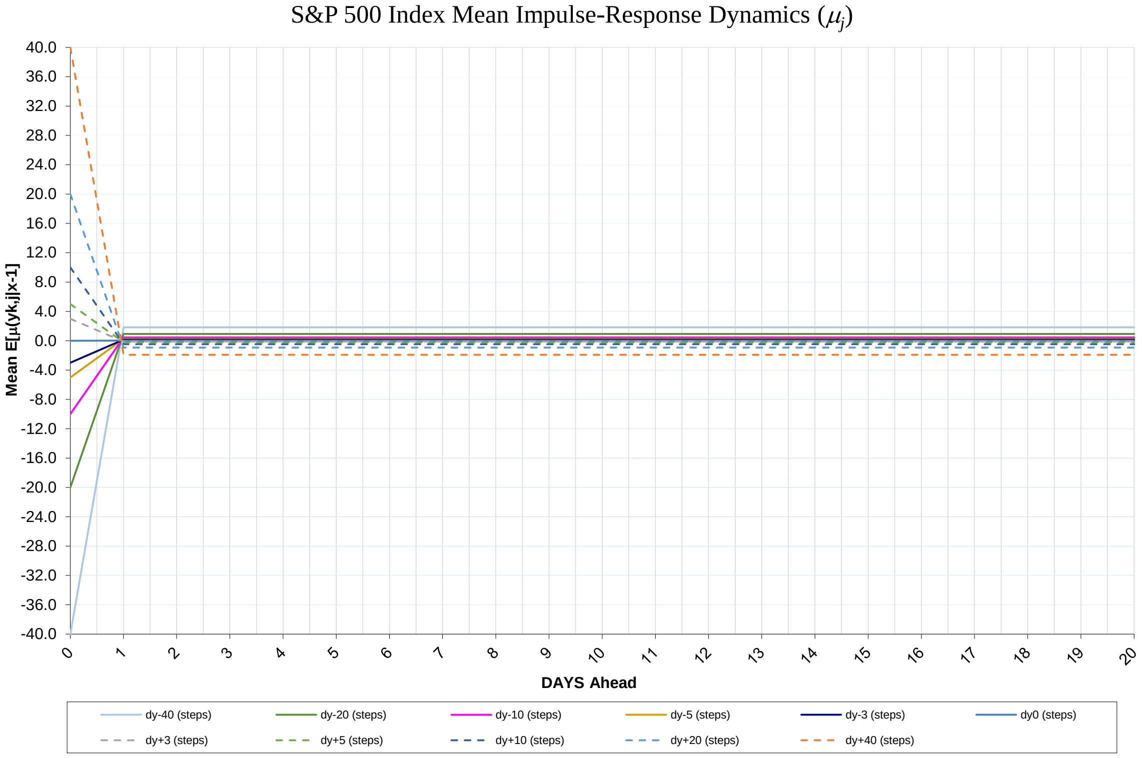

e. Oslo Stock Exchange Benchmark Index

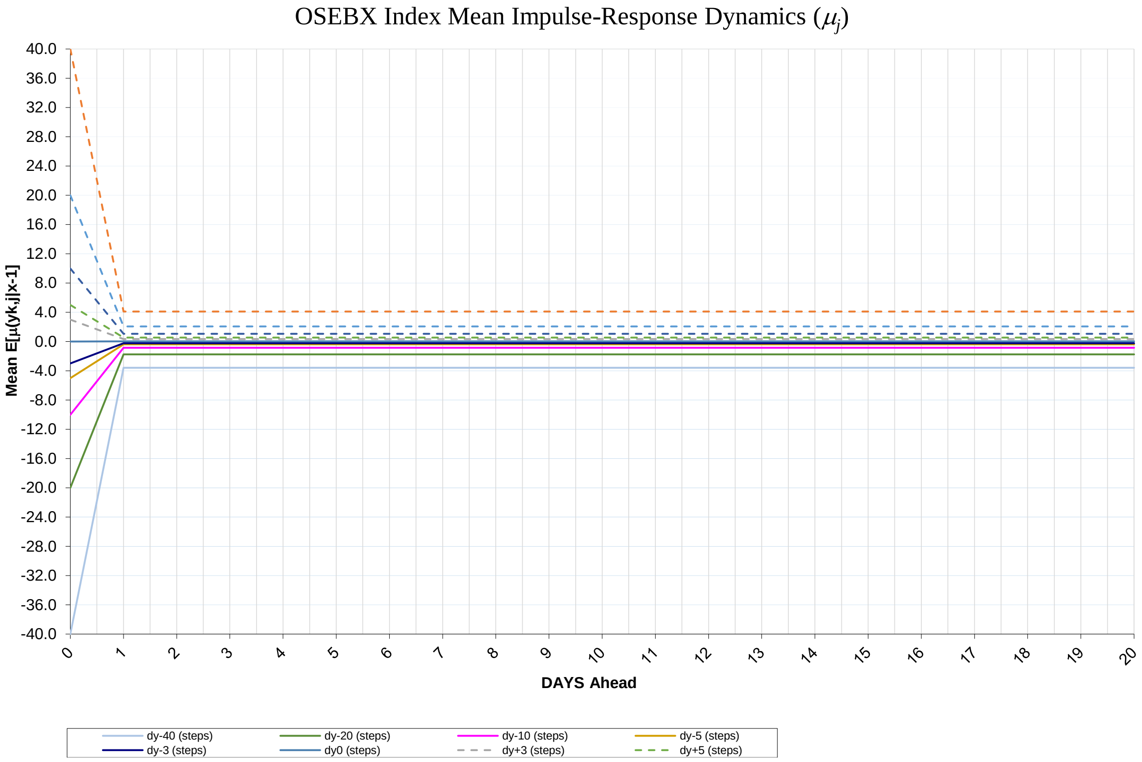

f. Oslo Stock Exchange Index

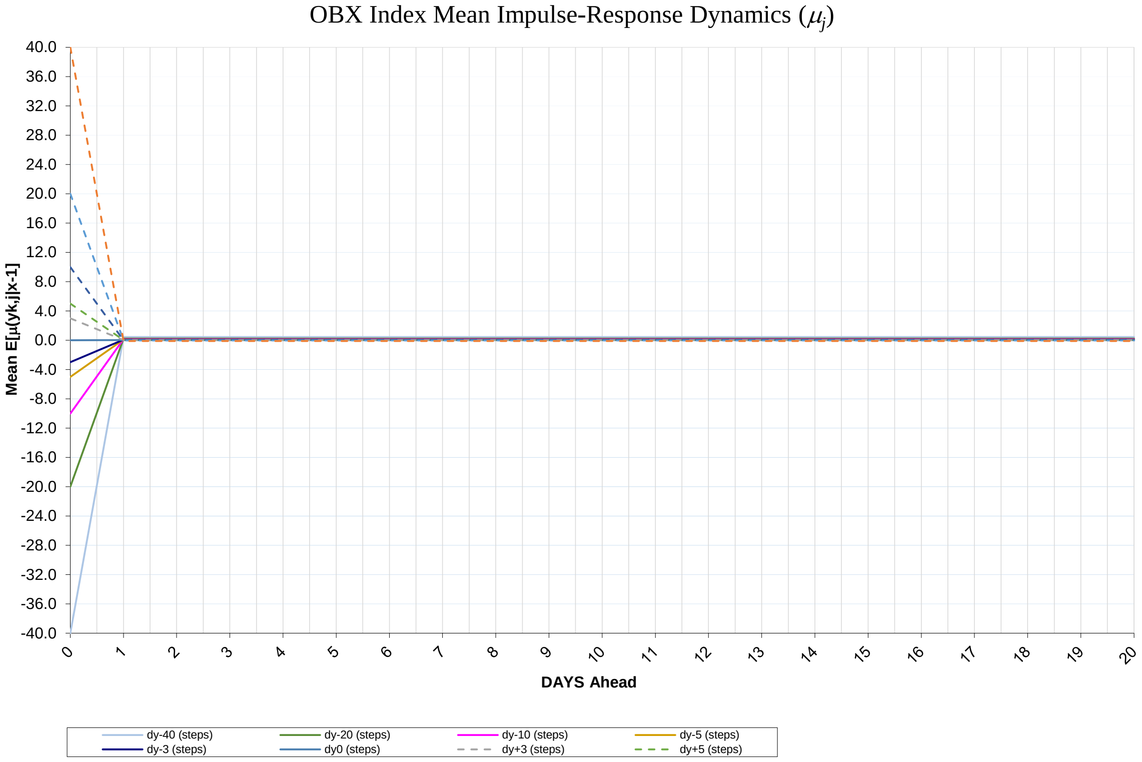

g. Oslo Stock Exchange All Share Index

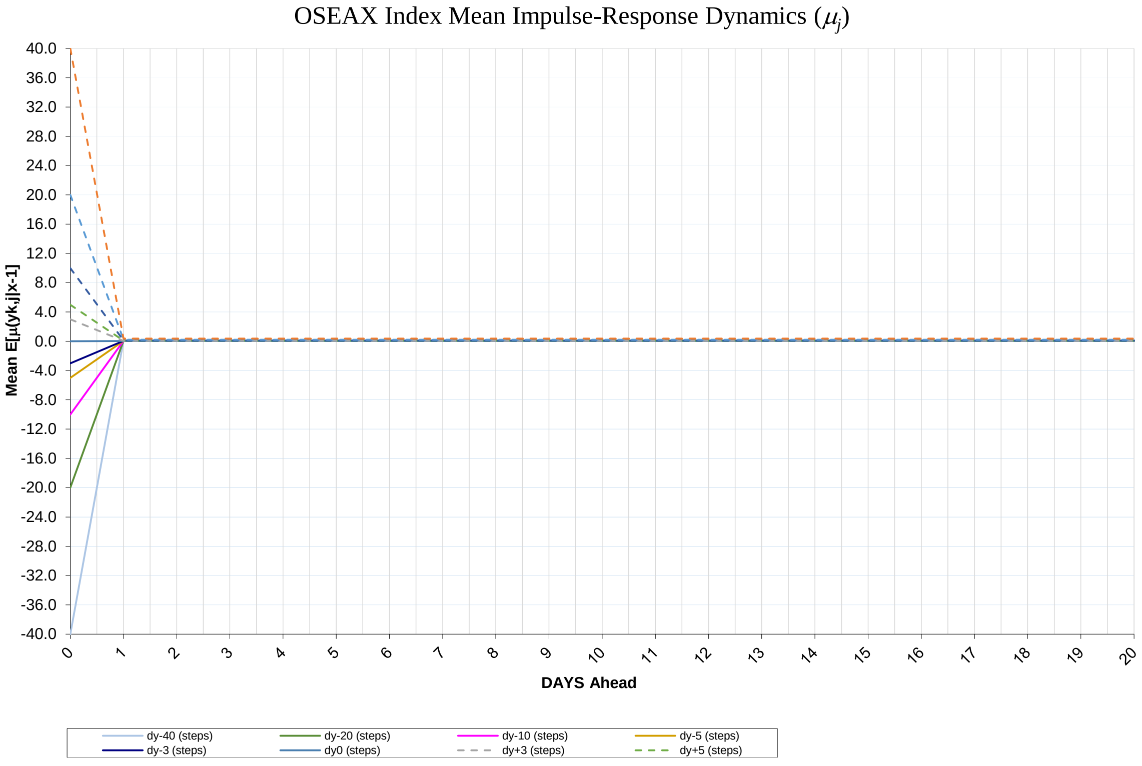

h. Microsoft Corporation

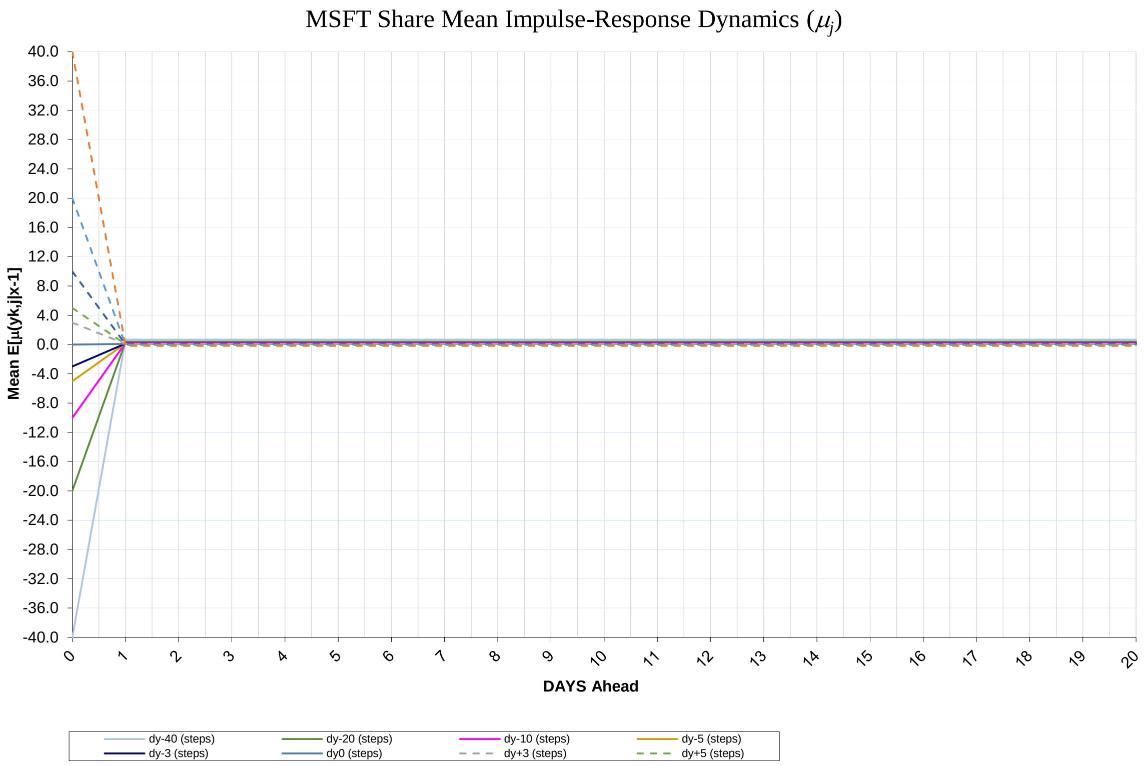

i. Micron Technology Inc.

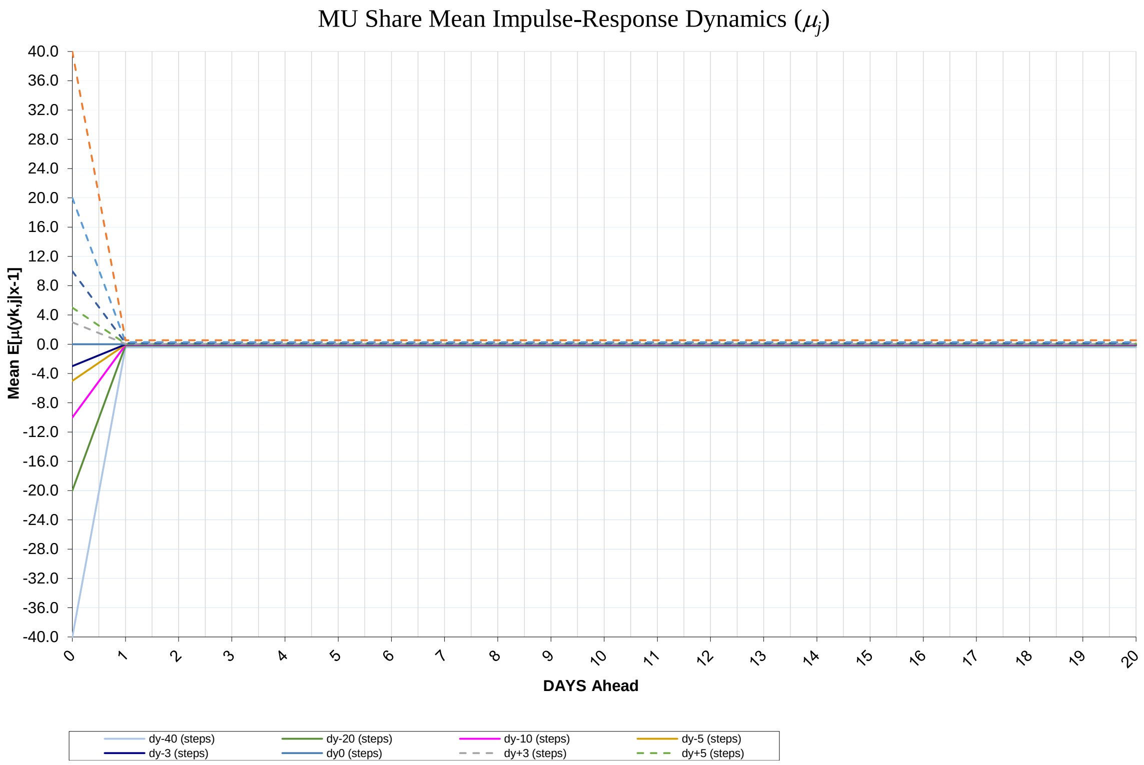

j. Norsk Hydro ASA

NHY Share Mean Impulse-Response Dynamics (μ_j)

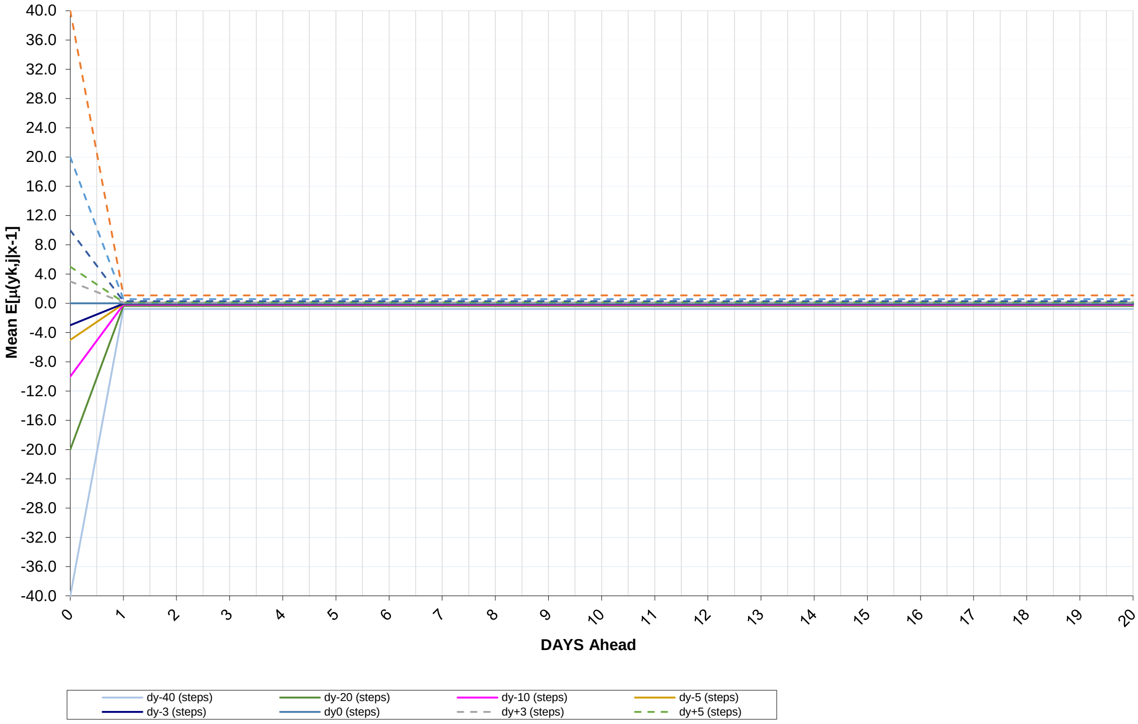

k. Tomra Systems ASA

TOM Share Mean Impulse-Response Dynamics (μ_j)

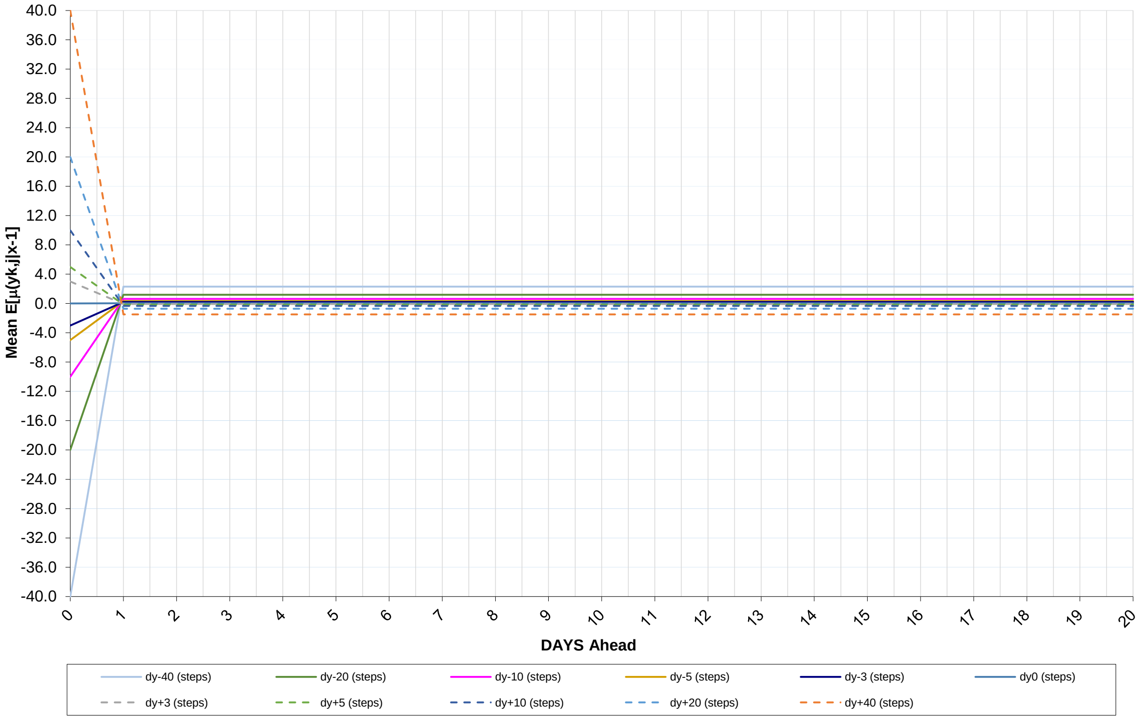

l. The ICE Carbon one month Forward Contracts

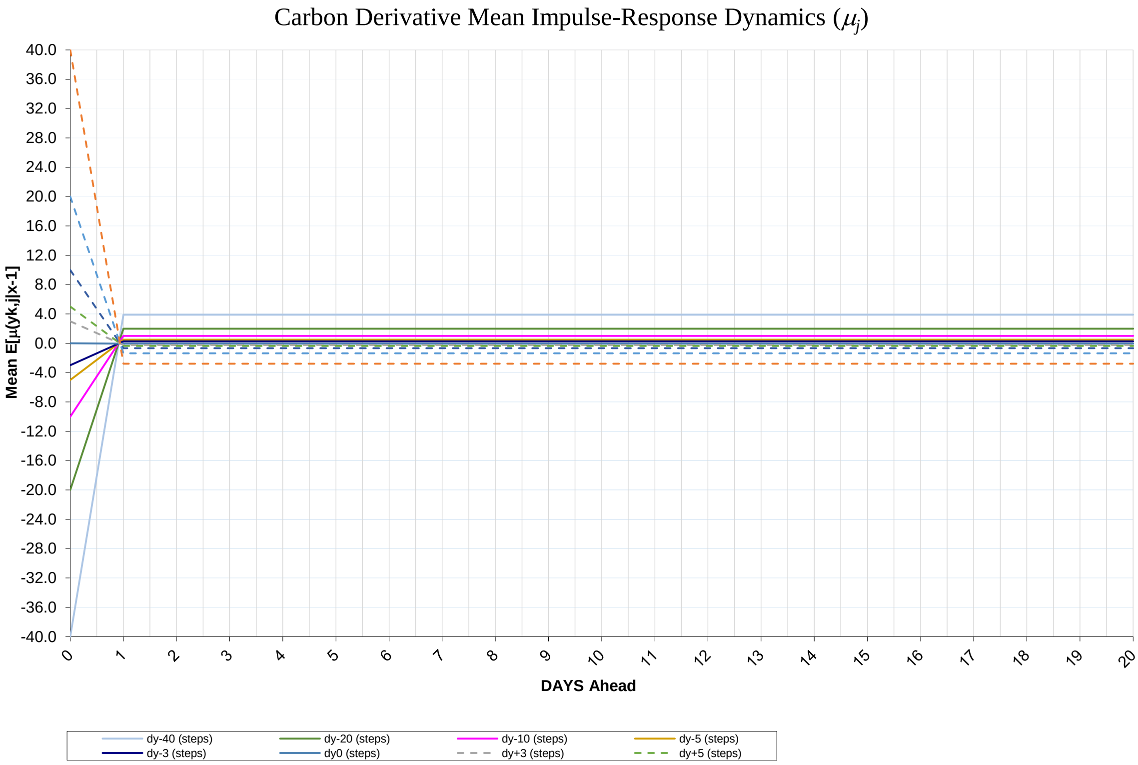

m. Brent oil front month Future Contracts

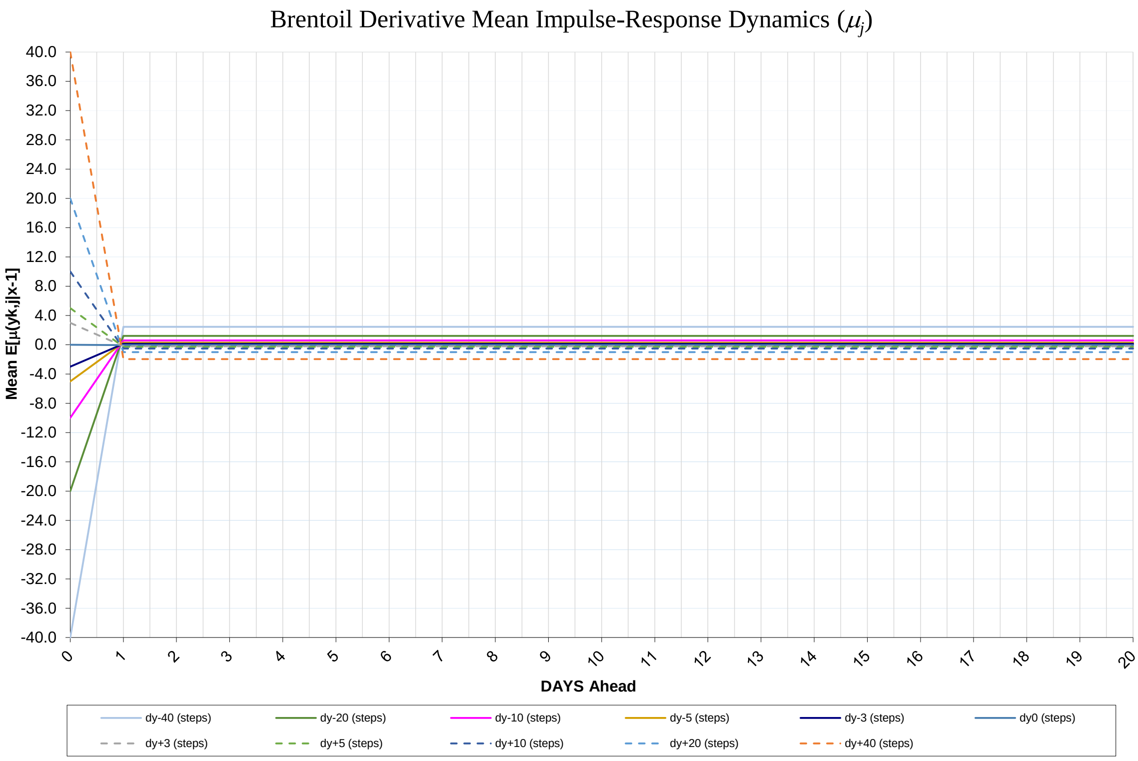

n. Salmon Forward Contracts

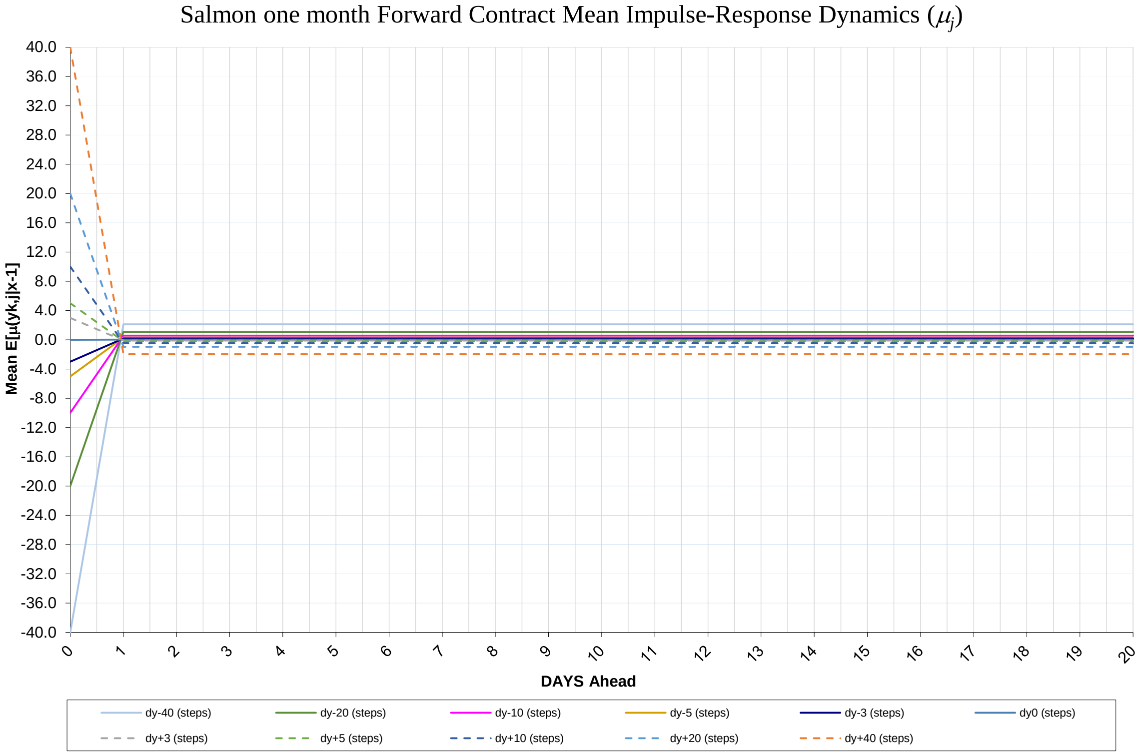

***Figure 83** Mean Impulse-Response Dynamics*

The *Variance* Impulse-Response Dynamics plots ***Figure 84*** **(a – n)** show the change in variance after adding an impulse (a price shock). The expected variance is shown on the second axis. As noted in **5.4.2.1**, the one-step-ahead density plots gave information that the time series had (much) wider densities when hit by negative shocks, compared to positive shocks. It is reasonable to think that the one-step-ahead variance is higher when the density is wider.

The indices show the highest degree of asymmetry among the time series studied. The ratio between the variance impulse-response (at lag one) coming from negative and positive shocks of 5% and 20% are displayed in ***Table 45*****.** The American stock indices stand out, where the variance after a negative shock is about 7 to 26 times higher than for the corresponding positive shock. The impact of a negative shock to the FTSE Index and the Norwegian indices are 3 to 6 times as high, compared to the corresponding positive shocks. The individual shares and commodity indices are showing lower ratios (ranging from 1.5 to 3) for negative and positive impulses, meaning that we observe less asymmetry for these financial assets. The Salmon future contracts are an exception among the commodity indices, showing a variance impulse-response that is about seven times higher for the negative shock, than the corresponding positive shock. Our results suggest that the variance makes a jump the next day and stays almost constant at this level for the coming 50 days that are simulated. The SNP model has detected a high degree of volatility persistence, and it has confirmed the asymmetrical features are present for all the financial time series.

a. Dow Jones Industrial Average

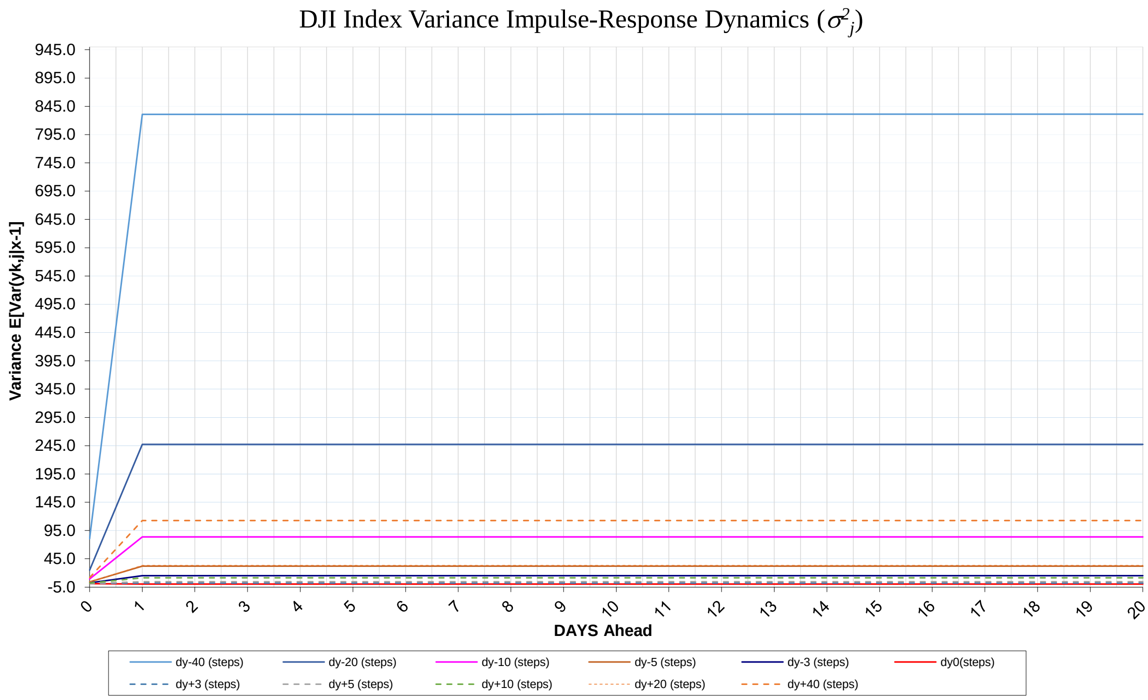

b. FTSE 100 Index

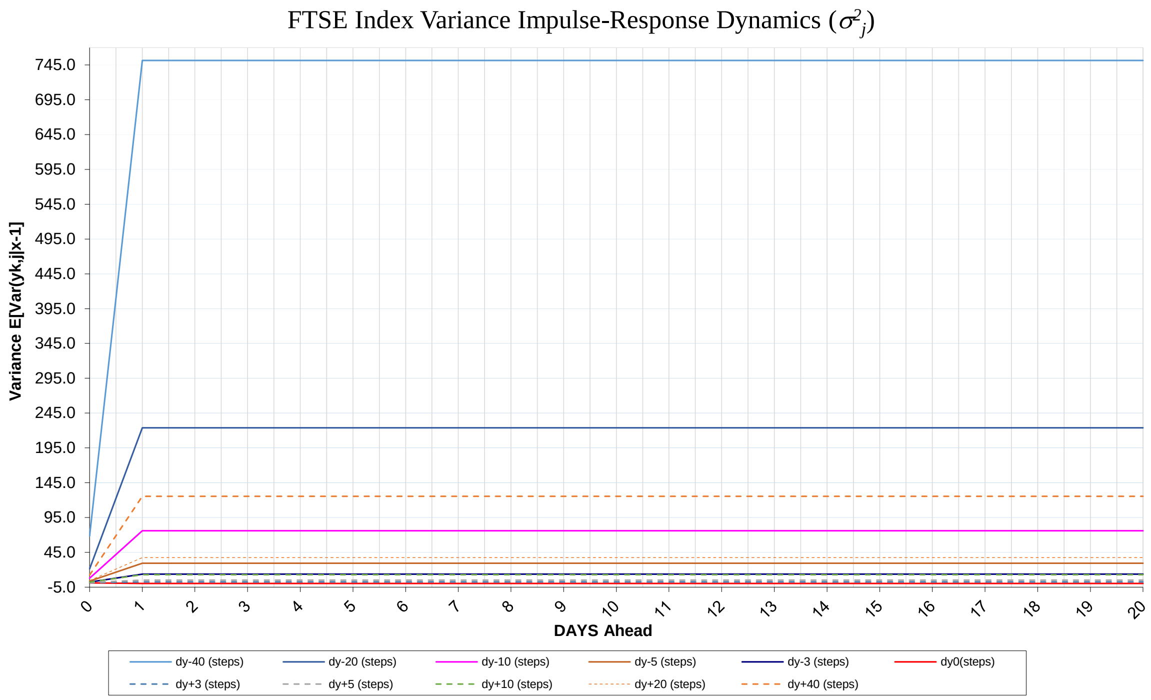

c. S&P 100 Index

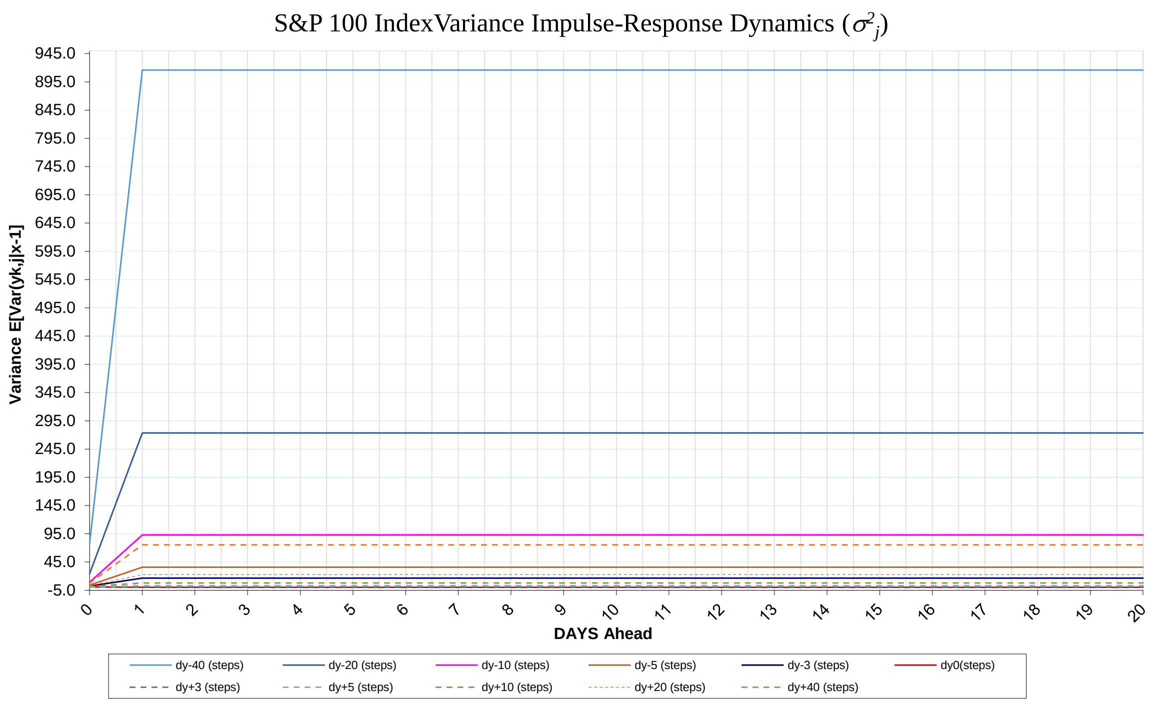

d. S&P 500 Index

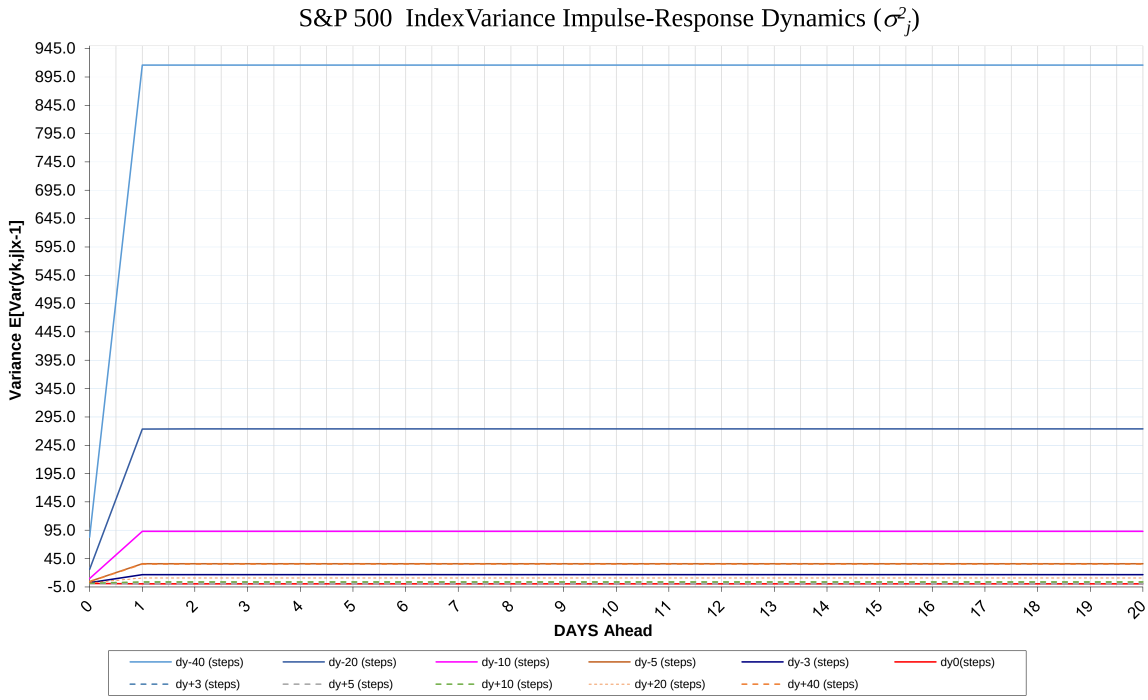

e. Oslo Stock Exchange Benchmark Index

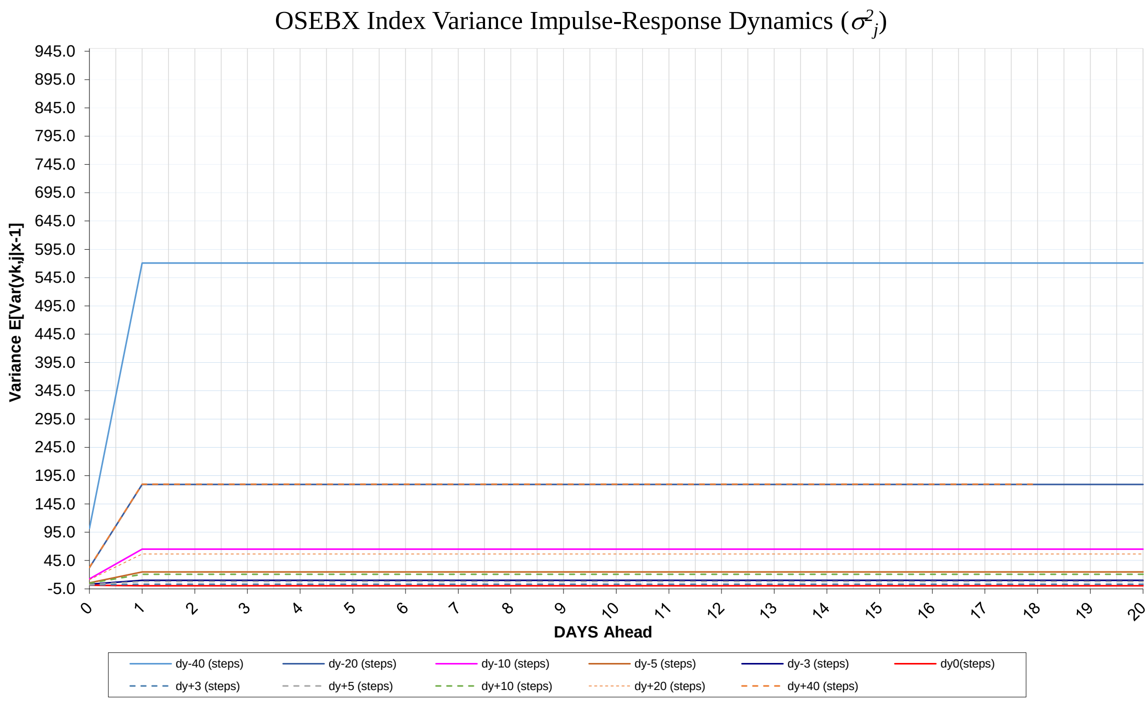

f. Oslo Stock Exchange Index

OBX Index Variance Impulse-Response Dynamics (σ^2_j)

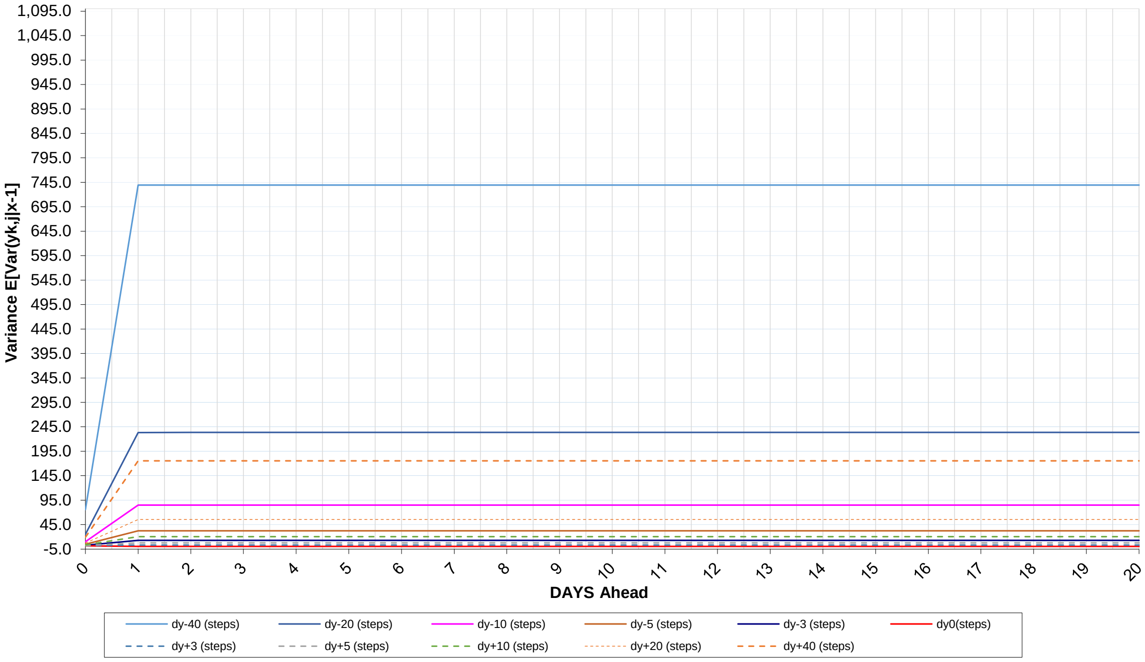

g. Oslo Stock Exchange All Share Index

OSEAX Index Variance Impulse-Response Dynamics (σ^2_j)

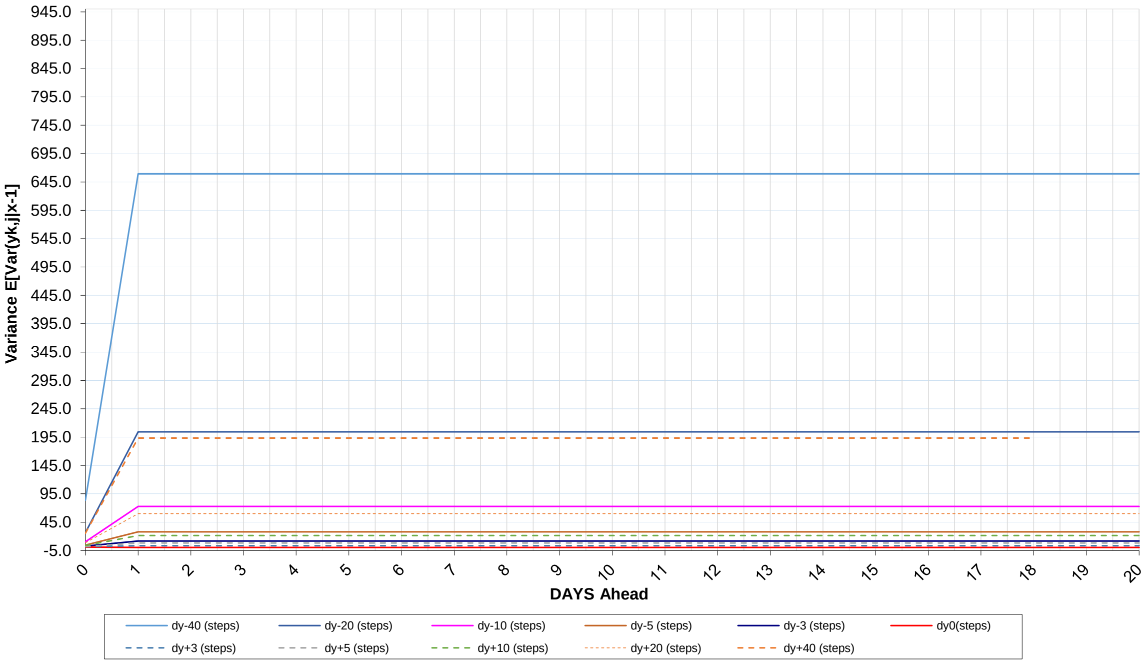

h. Microsoft Corporation

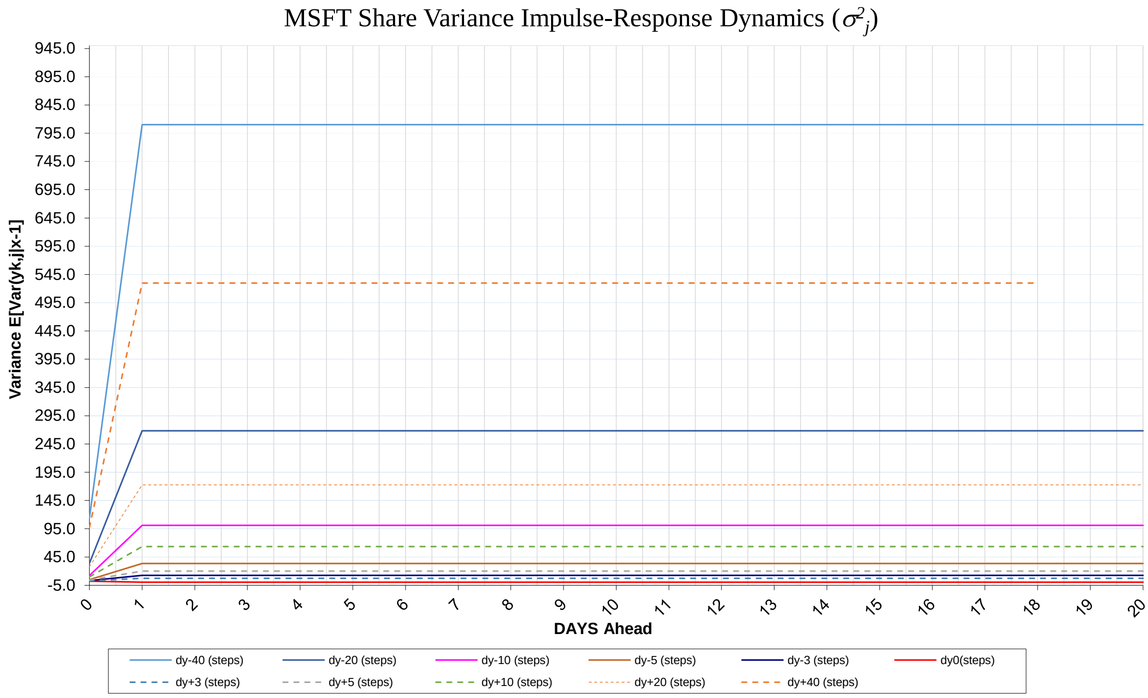

i. Micron Technology Inc.

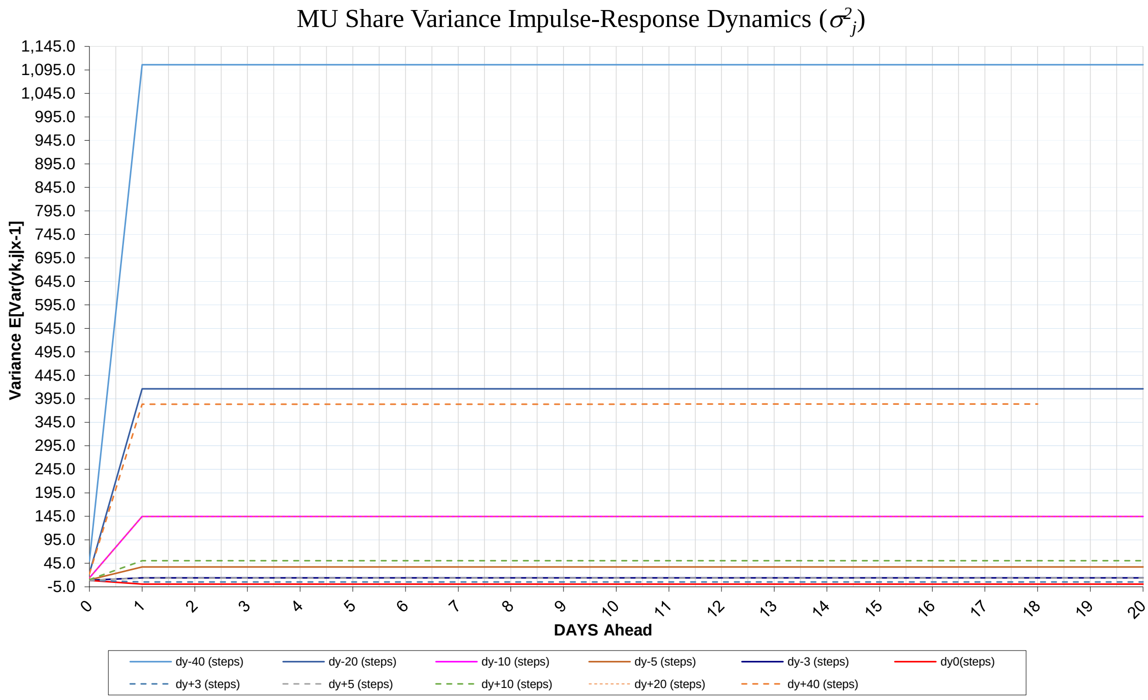

j. Norsk Hydro ASA

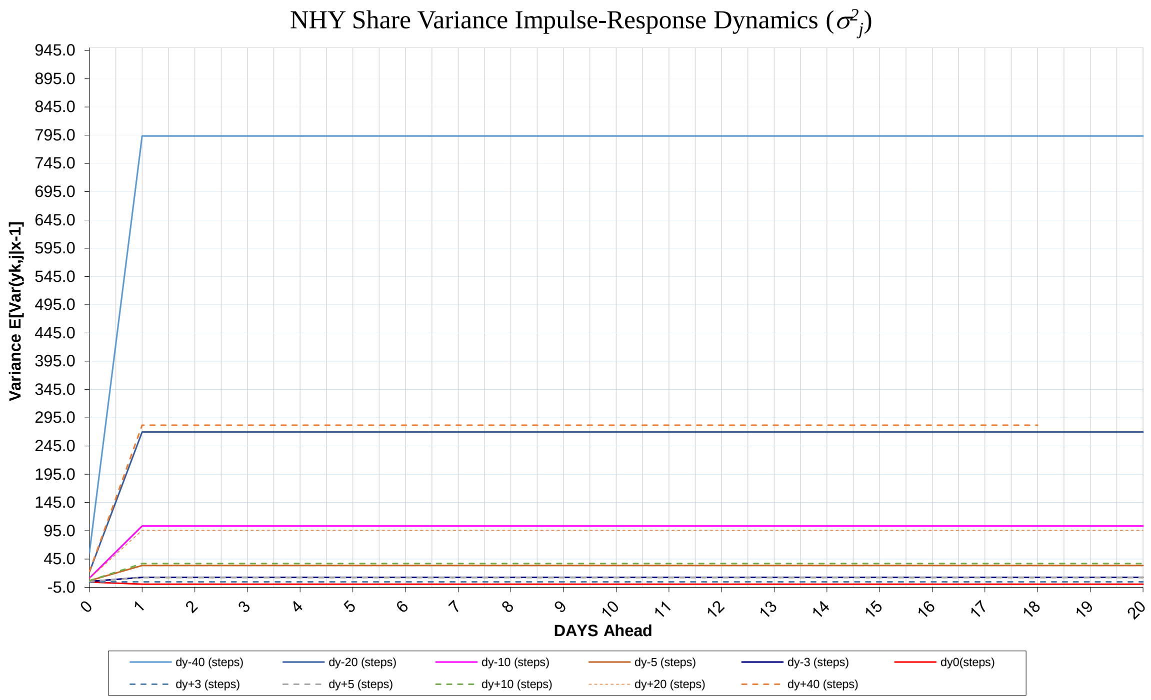

k. Tomra Systems ASA

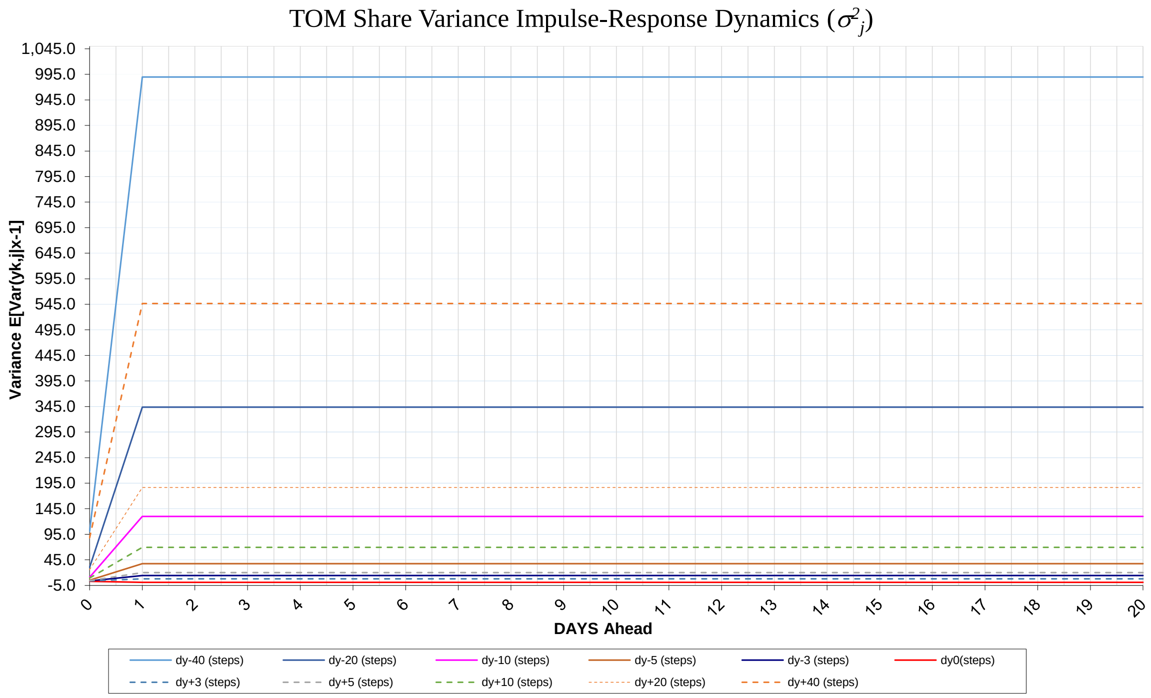

l. The ICE Carbon one month Forward Contracts

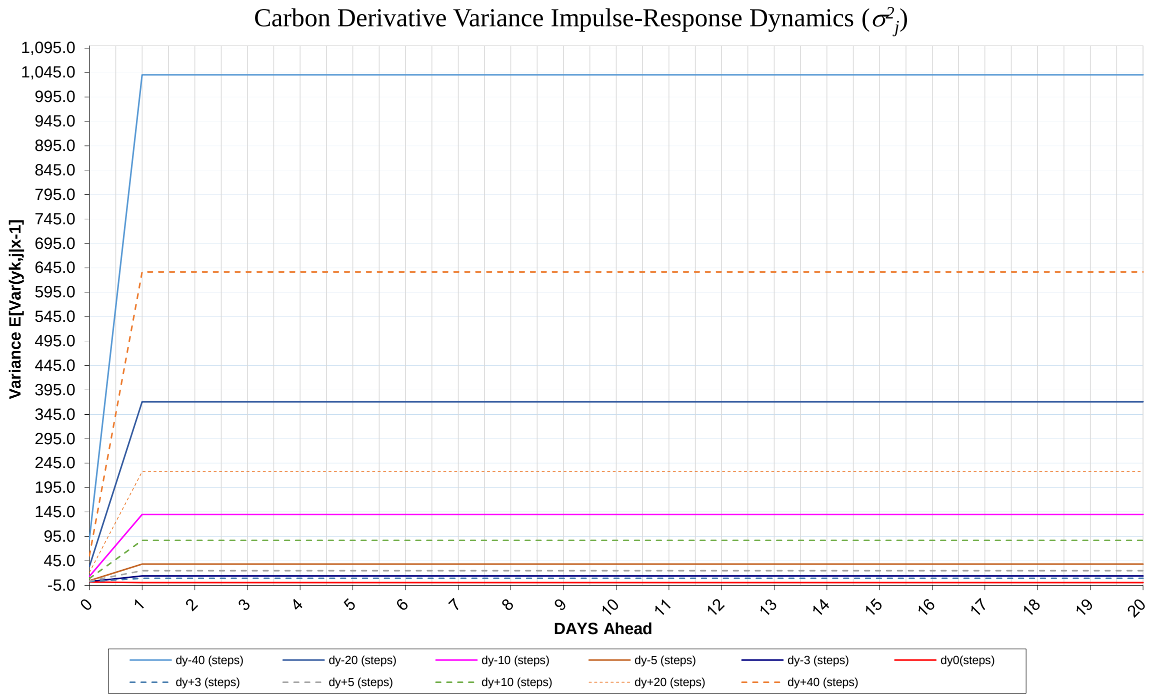

m. Brent oil front month Future Contracts

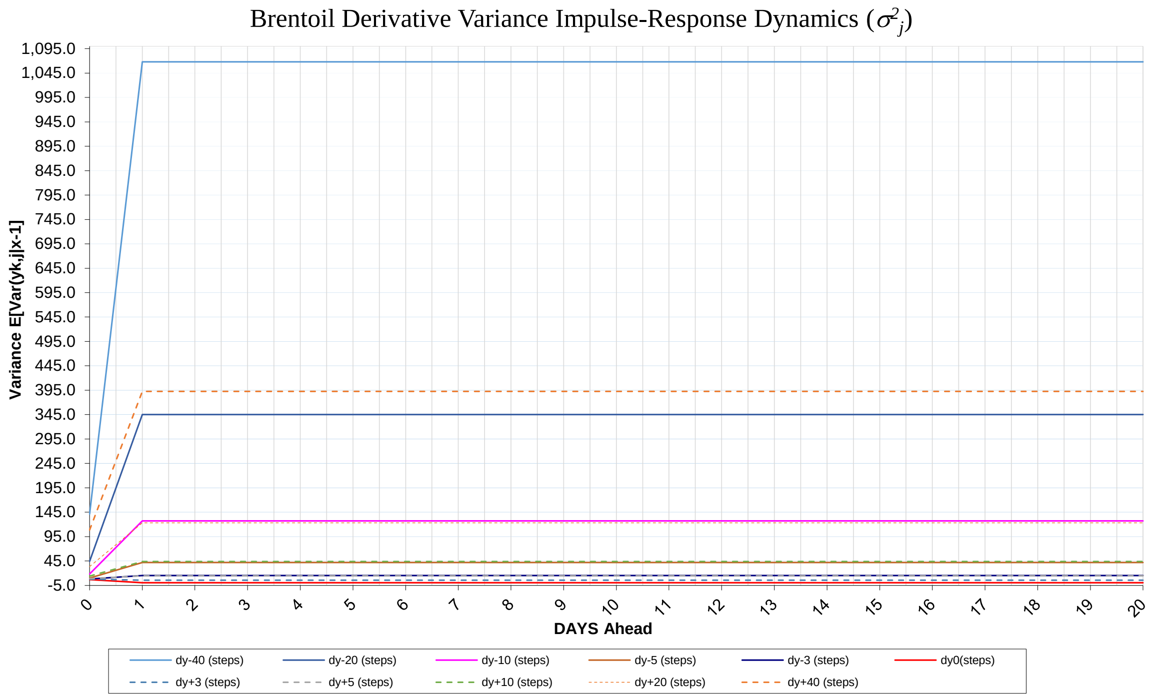

n. Salmon Forward Contracts

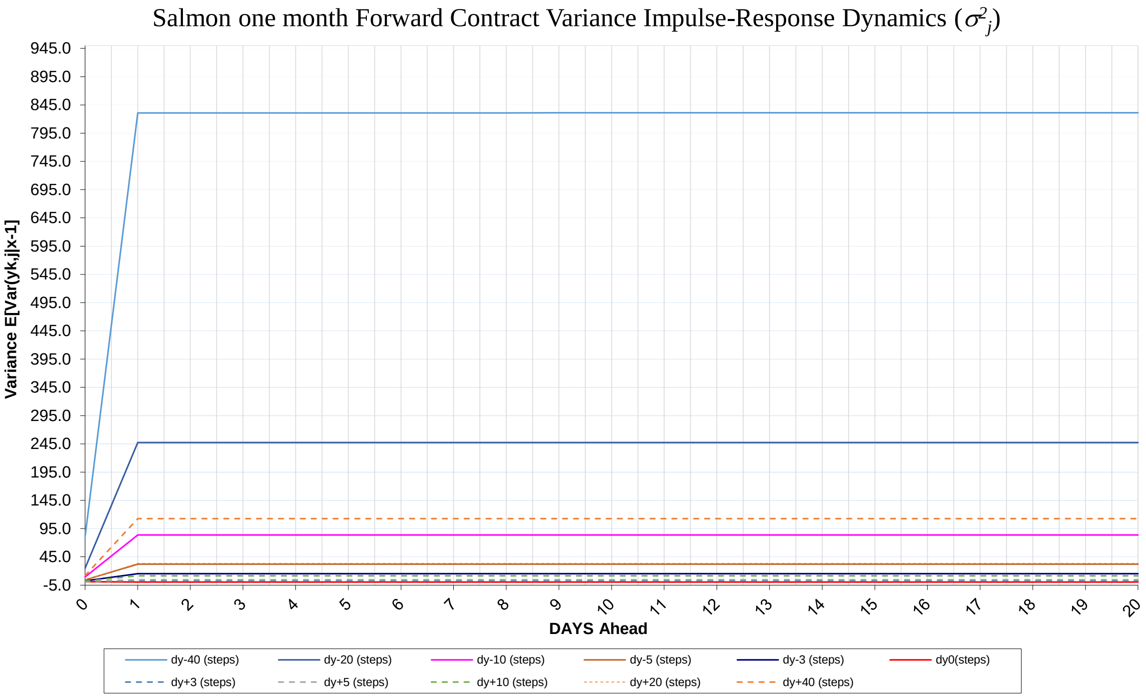

Figure 84 *Variance Impulse-Response Dynamics*

Table 45 *Variance Impulse-Response Dynamics showing the leverage effect*

Series Volatility *x* days ahead												"-/+" 20%	"-/+" 5%
OEX													
Volatility	δy^{-40} (steps)	**δy^{-20} (steps)**	δy^{-10} (steps)	**δy^{-5} (steps)**	δy^{-3} (steps)	δy^{0}(steps)	δy^{+3} (steps)	**δy^{+5} (steps)**	δy^{+10} (steps)	**δy^{+20} (steps)**	δy^{+40} (steps)		
0	77.92775209	**24.34604553**	9.156696362	**4.253056923**	2.559996507	1.14106296	1.245727865	**1.385625504**	1.787279792	**3.033614278**	7.446023599		
1	915.7400656	**273.5888727**	93.05772405	**35.80779361**	16.56939801	0.194586593	1.497940685	**3.081609997**	7.778765016	**22.60404202**	75.40379241	**12.10**	**11.62**
DJI													
Volatility	δy^{-40} (steps)	**δy^{-20} (steps)**	δy^{-10} (steps)	**δy^{-5} (steps)**	δy^{-3} (steps)	δy^{0}(steps)	δy^{+3} (steps)	**δy^{+5} (steps)**	δy^{+10} (steps)	**δy^{+20} (steps)**	δy^{+40} (steps)		
0	80.22631062	**24.83120925**	9.212810744	**4.226628373**	2.535293221	1.086996517	1.267057183	**1.496957978**	2.169266274	**4.279195597**	11.78547607		
1	830.8910826	**247.3139949**	83.74280413	**32.17855722**	15.0457549	0.197269478	2.140390016	**4.463551352**	11.43011556	**33.55225712**	112.5842765	**7.37**	**7.21**
GSPC													
Volatility	δy^{-40} (steps)	**δy^{-20} (steps)**	δy^{-10} (steps)	**δy^{-5} (steps)**	δy^{-3} (steps)	δy^{0}(steps)	δy^{+3} (steps)	**δy^{+5} (steps)**	δy^{+10} (steps)	**δy^{+20} (steps)**	δy^{+40} (steps)		
0	82.77446826	**25.6747752**	9.530489178	**4.344307484**	2.565317289	1.073774016	1.126586583	**1.194934458**	1.3930294	**2.010675179**	4.2007844		
1	915.8185447	**273.6596495**	93.12352803	**35.8407215**	16.56822095	0.19117772	0.793108695	**1.526612534**	3.699643089	**10.55523352**	34.97311587	**25.93**	**23.48**
FTSE													
Volatility	δy^{-40} (steps)	**δy^{-20} (steps)**	δy^{-10} (steps)	**δy^{-5} (steps)**	δy^{-3} (steps)	δy^{0}(steps)	δy^{+3} (steps)	**δy^{+5} (steps)**	δy^{+10} (steps)	**δy^{+20} (steps)**	δy^{+40} (steps)		
0	68.37491645	**21.10288907**	7.831813074	**3.629220456**	2.219004491	1.019810589	1.214949753	**1.450828281**	2.152077319	**4.368270576**	12.27027872		
1	751.5005295	**223.8912889**	75.91137868	**29.14942749**	13.51577325	0.179821709	2.360546695	**4.969948943**	12.75890725	**37.42160362**	125.4222513	**5.98**	**5.87**
OBX													
Volatility	δy^{-40} (steps)	**δy^{-20} (steps)**	δy^{-10} (steps)	**δy^{-5} (steps)**	δy^{-3} (steps)	δy^{0}(steps)	δy^{+3} (steps)	**δy^{+5} (steps)**	δy^{+10} (steps)	**δy^{+20} (steps)**	δy^{+40} (steps)		
0	75.81429764	**25.03525784**	10.11958647	**4.813795909**	2.858371424	1.607516983	1.893568319	**2.355976871**	3.617196444	**7.1601004**	19.23431215		
1	739.2420855	**233.4377523**	84.96790974	**32.26825192**	12.83207716	0.34977755	3.195765303	**7.784452902**	20.2824817	**55.46004501**	175.4280839	**4.21**	**4.15**
OSEAX													
Volatility	δy^{-40} (steps)	**δy^{-20} (steps)**	δy^{-10} (steps)	**δy^{-5} (steps)**	δy^{-3} (steps)	δy^{0}(steps)	δy^{+3} (steps)	**δy^{+5} (steps)**	δy^{+10} (steps)	**δy^{+20} (steps)**	δy^{+40} (steps)		
0	83.67454999	**26.73584488**	10.31650106	**4.735237587**	2.690674781	1.272910377	1.677877054	**2.27742726**	3.915425043	**8.734157272**	25.45934135		
1	659.2996172	**204.1893865**	72.83906368	**28.11240991**	11.71088553	0.322983605	3.535794427	**8.335501686**	21.43393123	**59.88828435**	193.2765544	**3.41**	**3.37**
OSEBX													
Volatility	δy^{-40} (steps)	**δy^{-20} (steps)**	δy^{-10} (steps)	**δy^{-5} (steps)**	δy^{-3} (steps)	δy^{0}(steps)	δy^{+3} (steps)	**δy^{+5} (steps)**	δy^{+10} (steps)	**δy^{+20} (steps)**	δy^{+40} (steps)		
0	101.5553598	**32.25393967**	12.24921424	**5.505505128**	3.05	1.259918221	1.782781421	**2.554780862**	4.672896974	**10.95482821**	32.76578808		
1	570.752086	**179.4935772**	65.00949425	**24.91828321**	10.1	0.302740771	3.245147752	**7.892385301**	20.51142215	**56.51345281**	179.7107407	**3.18**	**3.16**
NHY													
Volatility	δy^{-40} (steps)	**δy^{-20} (steps)**	δy^{-10} (steps)	**δy^{-5} (steps)**	δy^{-3} (steps)	δy^{0}(steps)	δy^{+3} (steps)	**δy^{+5} (steps)**	δy^{+10} (steps)	**δy^{+20} (steps)**	δy^{+40} (steps)		
0	56.11203378	**21.85974357**	11.06040833	**6.560143209**	5.179223346	4.395789446	4.668888518	**5.156171587**	6.755648661	**10.59414302**	22.77431921		
1	793.5654953	**269.629925**	103.4052148	**33.4278012**	12.42567636	0.554146051	4.717948938	**12.14089328**	36.9747012	**95.95183596**	281.8724433	**2.81**	**2.75**
TOM													
Volatility	δy^{-40} (steps)	**δy^{-20} (steps)**	δy^{-10} (steps)	**δy^{-5} (steps)**	δy^{-3} (steps)	δy^{0}(steps)	δy^{+3} (steps)	**δy^{+5} (steps)**	δy^{+10} (steps)	**δy^{+20} (steps)**	δy^{+40} (steps)		
0	100.70	**30.09**	10.85	**4.93**	3.58	2.83	3.41	**4.45**	9.13	**25.56**	88.05		
1	989.77	**343.81**	129.71	**37.45**	14.10	0.87	7.74	**20.05**	69.32	**186.51**	546.49	**1.84**	**1.87**
MU													
Volatility	δy^{-40} (steps)	**δy^{-20} (steps)**	δy^{-10} (steps)	**δy^{-5} (steps)**	δy^{-3} (steps)	δy^{0}(steps)	δy^{+3} (steps)	**δy^{+5} (steps)**	δy^{+10} (steps)	**δy^{+20} (steps)**	δy^{+40} (steps)		
0	50.01722882	**24.0485057**	13.88868783	**9.82378401**	8.938553435	8.437593601	8.609032117	**8.914443389**	10.32137119	**13.85151621**	22.86970197		
1	1106.008433	**416.3414932**	144.7883423	**37.24109842**	13.92211949	0.794590048	5.331882103	**13.40470906**	50.65644883	**144.7558043**	383.7320786	**2.88**	**2.78**
MSFT													
Volatility	δy^{-40} (steps)	**δy^{-20} (steps)**	δy^{-10} (steps)	**δy^{-5} (steps)**	δy^{-3} (steps)	δy^{0}(steps)	δy^{+3} (steps)	**δy^{+5} (steps)**	δy^{+10} (steps)	**δy^{+20} (steps)**	δy^{+40} (steps)		
0	113.8164589	**33.95782187**	12.06352897	**5.069948**	3.191571657	2.091470649	2.834622704	**4.208940073**	9.720816428	**28.0621902**	96.87831769		
1	810.06264	**268.4015365**	100.8766483	**33.54883516**	12.60853065	0.36769961	7.360045537	**20.22851397**	63.4857099	**172.6381422**	529.8083426	**1.55**	**1.66**
Brentoil													
Volatility	δy^{-40} (steps)	δy^{-20} (steps)	δy^{-10} (steps)	δy^{-5} (steps)	δy^{-3} (steps)	δy^{0}(steps)	δy^{+3} (steps)	δy^{+5} (steps)	δy^{+10} (steps)	δy^{+20} (steps)	δy^{+40} (steps)		
0	140.9343222	44.27518162	18.21467239	10.14013983	7.999295795	6.768637502	7.48265628	8.743812118	14.10368813	33.4941446	108.5255969		
1	1067.97825	345.2519489	127.1102415	41.78847462	14.98590428	0.203646823	5.529049284	14.66837653	43.97261517	123.1123425	392.6385257	**2.80**	**2.85**
Salmon													
Volatility	δy^{-40} (steps)	δy^{-20} (steps)	δy^{-10} (steps)	δy^{-5} (steps)	δy^{-3} (steps)	δy^{0}(steps)	δy^{+3} (steps)	δy^{+5} (steps)	δy^{+10} (steps)	δy^{+20} (steps)	δy^{+40} (steps)		
0	80.22631062	24.83120925	9.212810744	4.226628373	2.535293221	1.086996517	1.267057183	1.496957978	2.169266274	4.279195597	11.78547607		
1	830.8910826	247.3139949	83.74280413	32.17855722	15.0457549	0.197269478	2.140390016	4.463551352	11.43011556	33.55225712	112.5842765	**7.37**	**7.21**
Carbon													
Volatility	δy^{-40} (steps)	δy^{-20} (steps)	δy^{-10} (steps)	δy^{-5} (steps)	δy^{-3} (steps)	δy^{0}(steps)	δy^{+3} (steps)	δy^{+5} (steps)	δy^{+10} (steps)	δy^{+20} (steps)	δy^{+40} (steps)		
0	89.84731996	33.4239169	13.34462744	4.652963749	2.658446656	1.570165318	2.299000474	3.557877737	8.90987397	21.16559743	55.65008797		
1	1040.270214	370.7774325	140.0005193	38.46610124	14.02339461	0.579176587	9.36265941	24.64592325	86.87769006	227.6858061	636.4070393	**1.63**	**1.56**

6.2 Persistence

As described in section **3.1**, we use the half-life measure to describe the persistence of volatility. A program in EViews is used to feed coefficients from a GARCH model into a loop, going from 0-992, 1-993, and 2-994 to the end of the time series. ***Figure 85*** **(a – n)** display the output, being the persistence of volatility for each time series. The half-life of the studied time series varies between 17 and 113 days, as summarized in ***Table 46*.**

The stock market indices show relatively low persistence after a shock, with a half-life of 17-23 days. The three Norwegian indices OSEAX, OBX and OSEBX show the lowest degree of persistence while the British FTSE Index shows the highest degree of persistence.

Among the individual shares, we observe different results for the half-life measure. The volatility of the two Norwegian shares TOM and NHY uses less than half as many days to return halfway back to its unconditional mean, compared to the American company shares (MSFT and MU). The standard deviation of TOM is very high, suggesting that the stated value of persistence comes with a great amount of uncertainty. MSFT has the highest degree of persistence with a half-life of 113 days. This suggests that the volatility of MSFT has a long memory. The sum of the alpha and beta is lower than one, indicating that it is mean reverting (Engle and Patton 2001). The average half-life time is higher for all the individual shares, compared to the stock indices.

The three commodity derivatives also show different outputs regarding the half-life measure for volatility persistence.

***Table 46** Measures of Persistence*

	Average half-life	Standard Deviation
DJI	21.72	1.99
FTSE	22.86	2.8
OEX	21.81	2.63
GSPC	20.73	2.08
OSEBX	20.42	0.94
OBX	18.19	1.44
OSEAX	16.97	1.58
MSFT	113.19	15.06
MU	75.4	15.22
NHY	34.97	4.29
TOM	35.87	35.54
CARBON	46.02	15.14
BRENTOIL	33.86	23.31
SALMON	17.81	4.3

a. Dow Jones Industrial Average

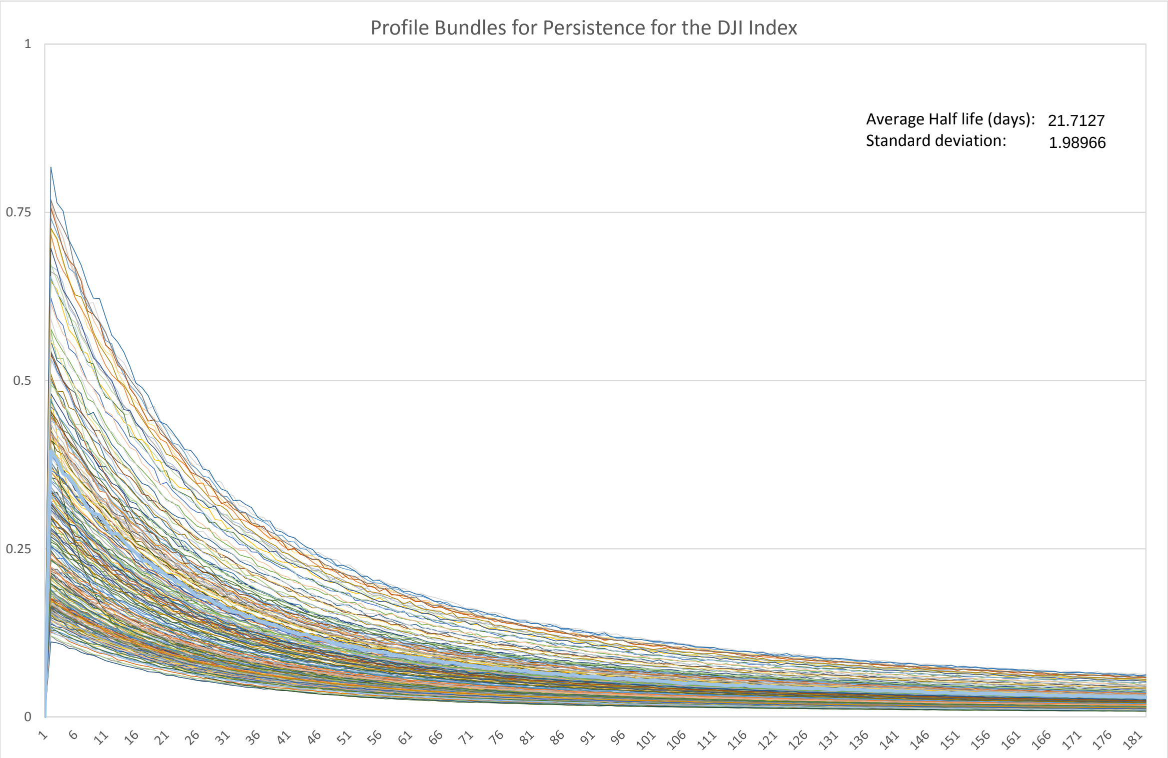

b. FTSE 100 Index

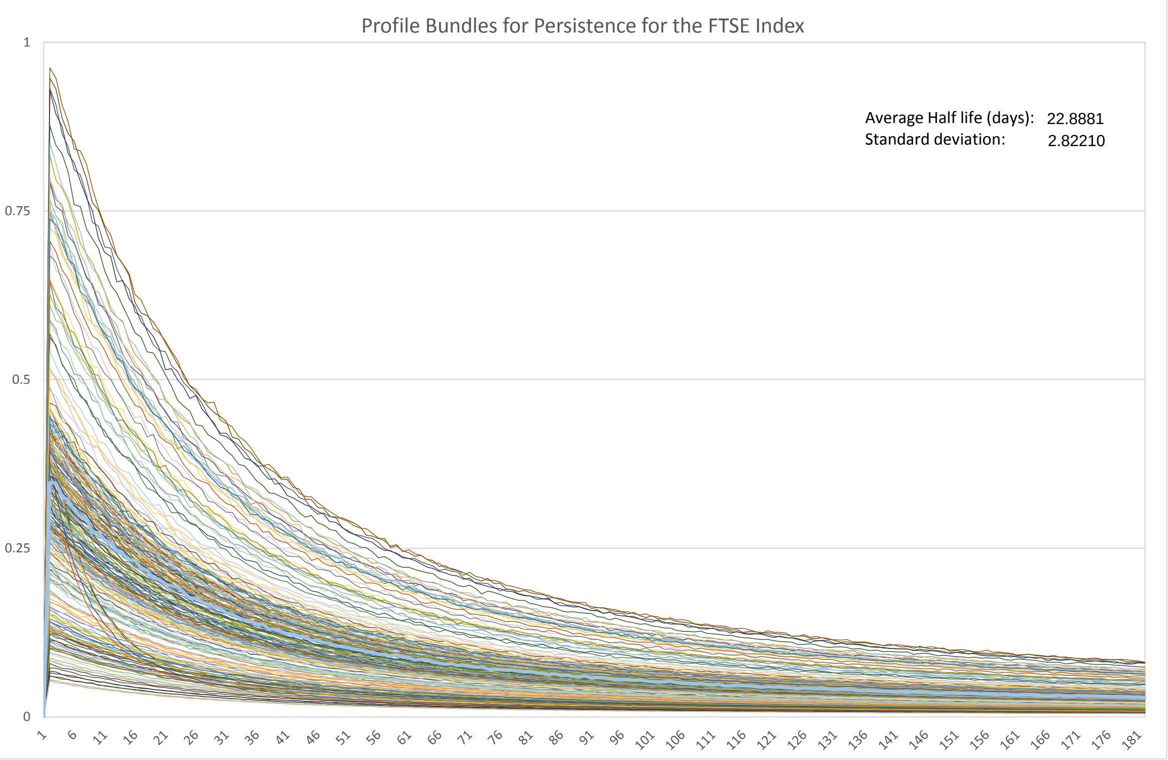

c. S&P 100 Index

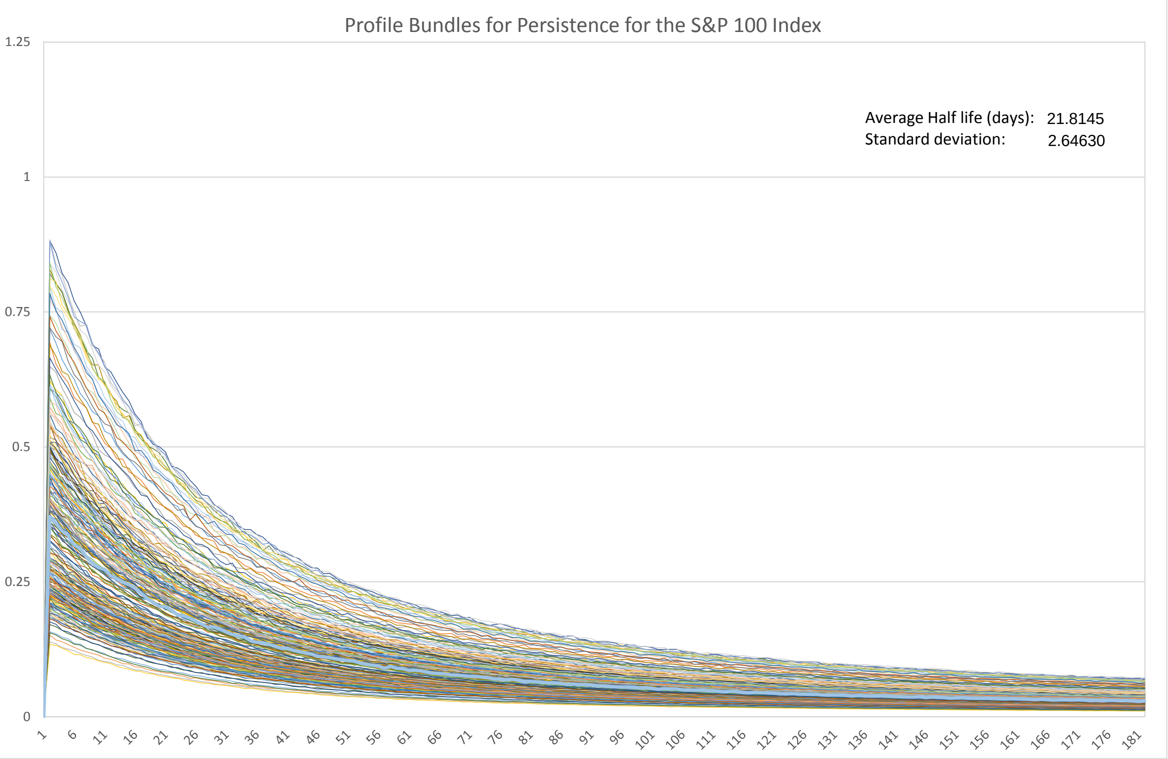

d. S&P 500 Index

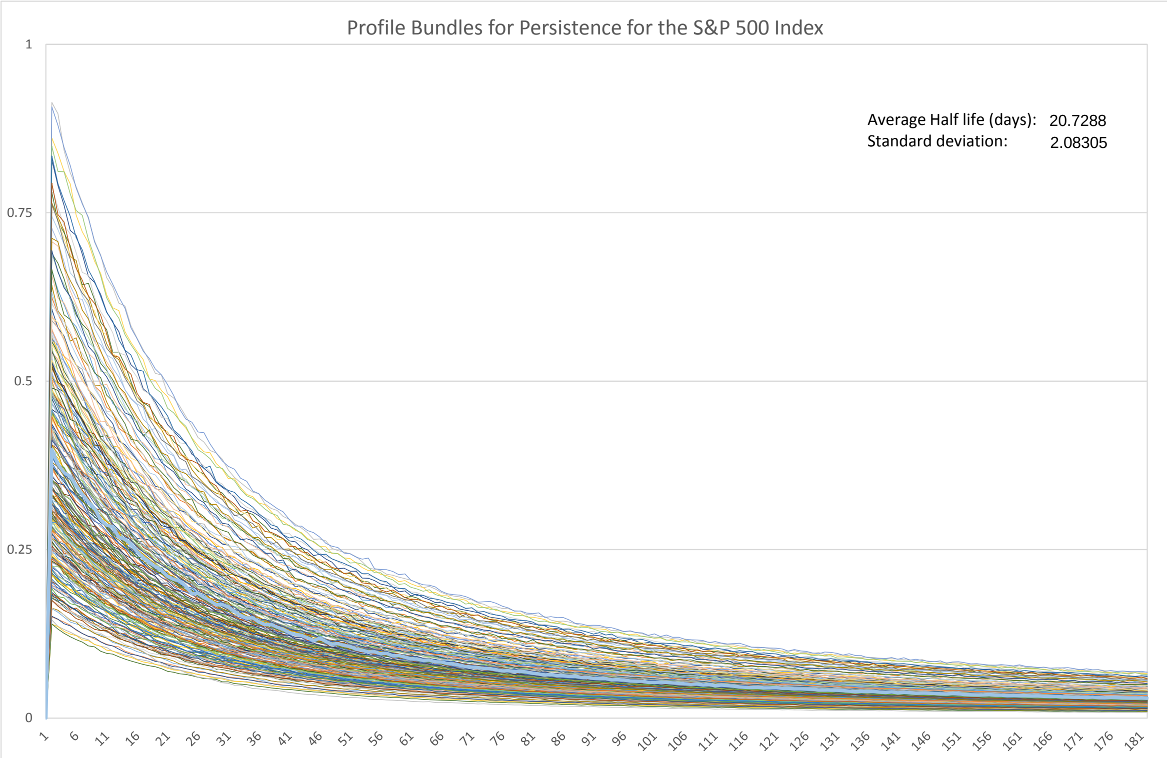

e. Oslo Stock Exchange Benchmark Index

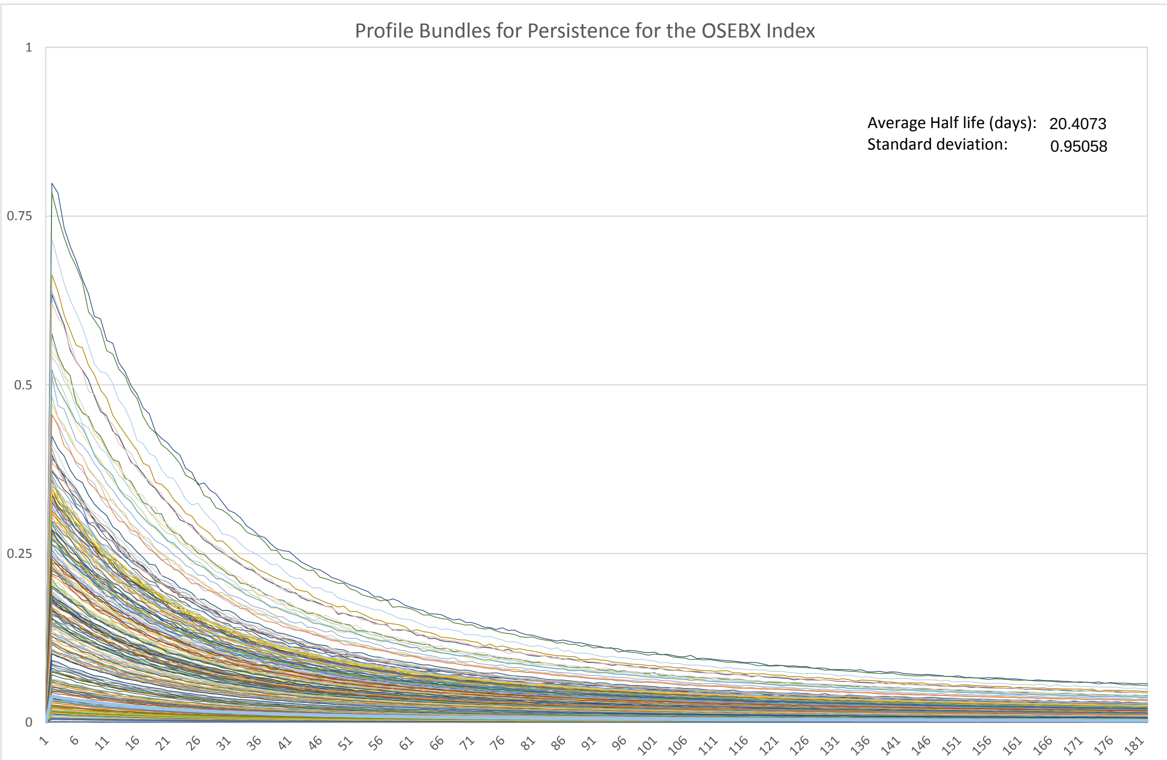

f. Oslo Stock Exchange Index

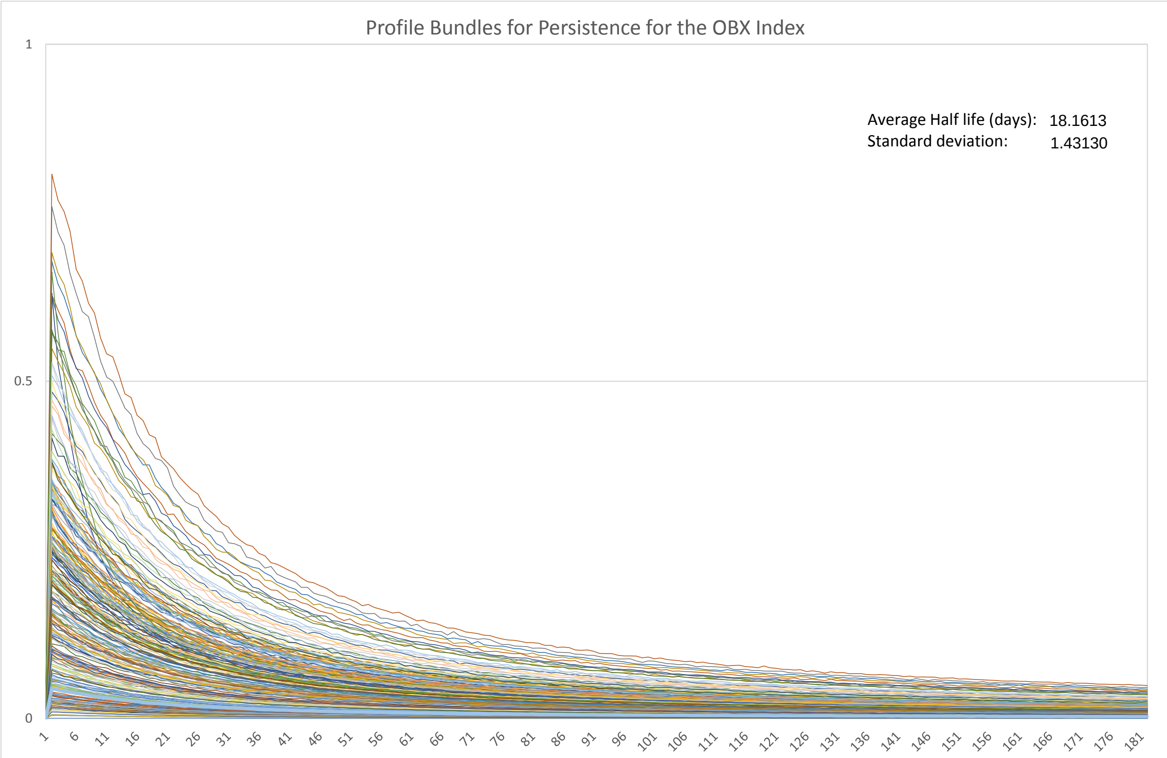

g. Oslo Stock Exchange All Share Index

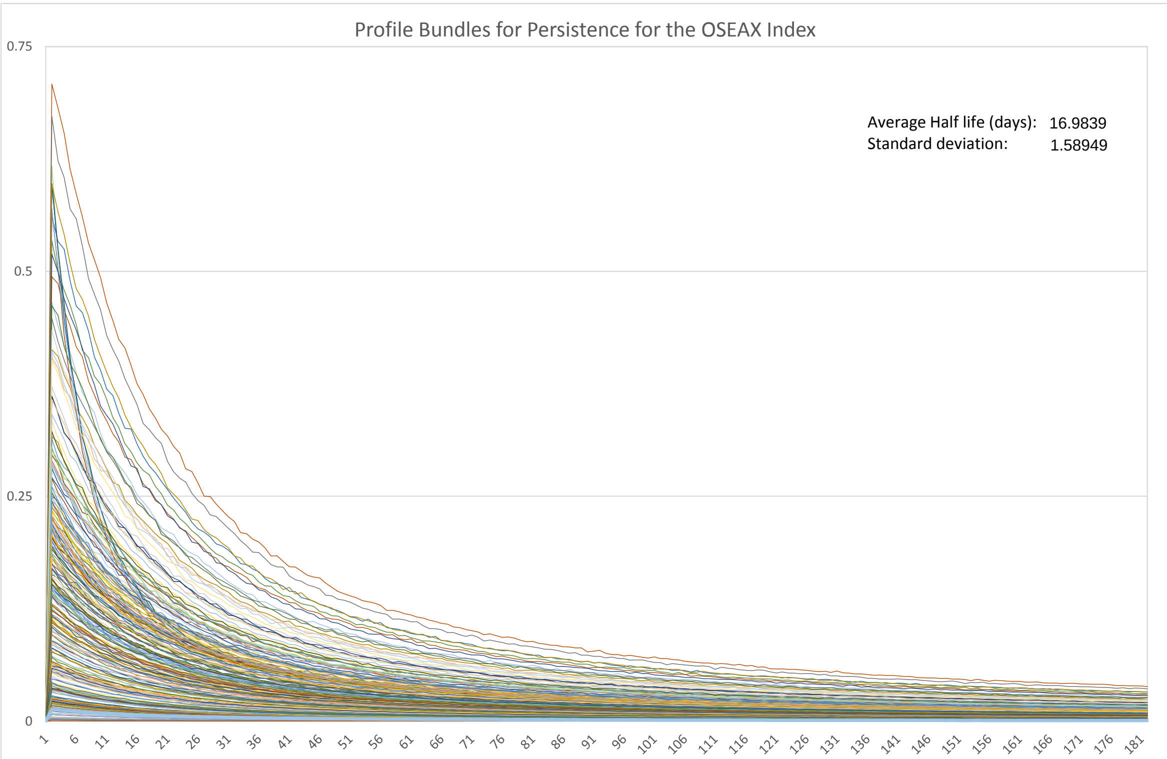

h. Microsoft Corporation

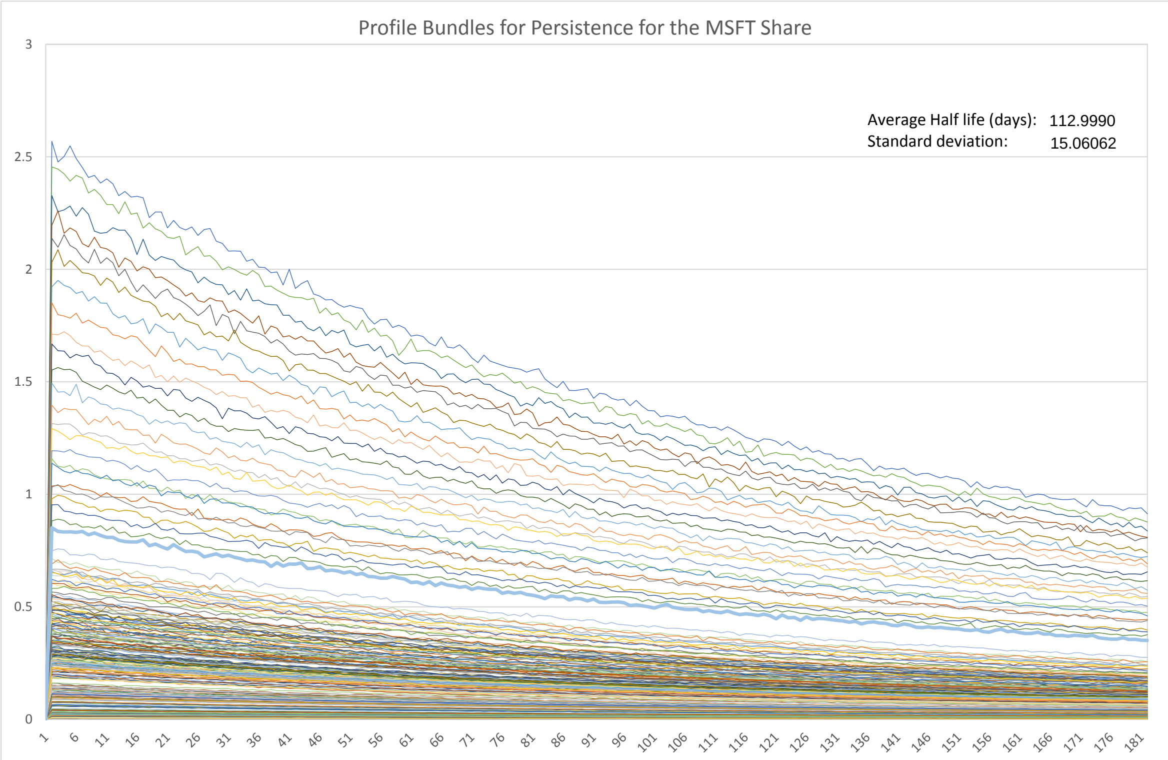

i. Micron Technology Inc.

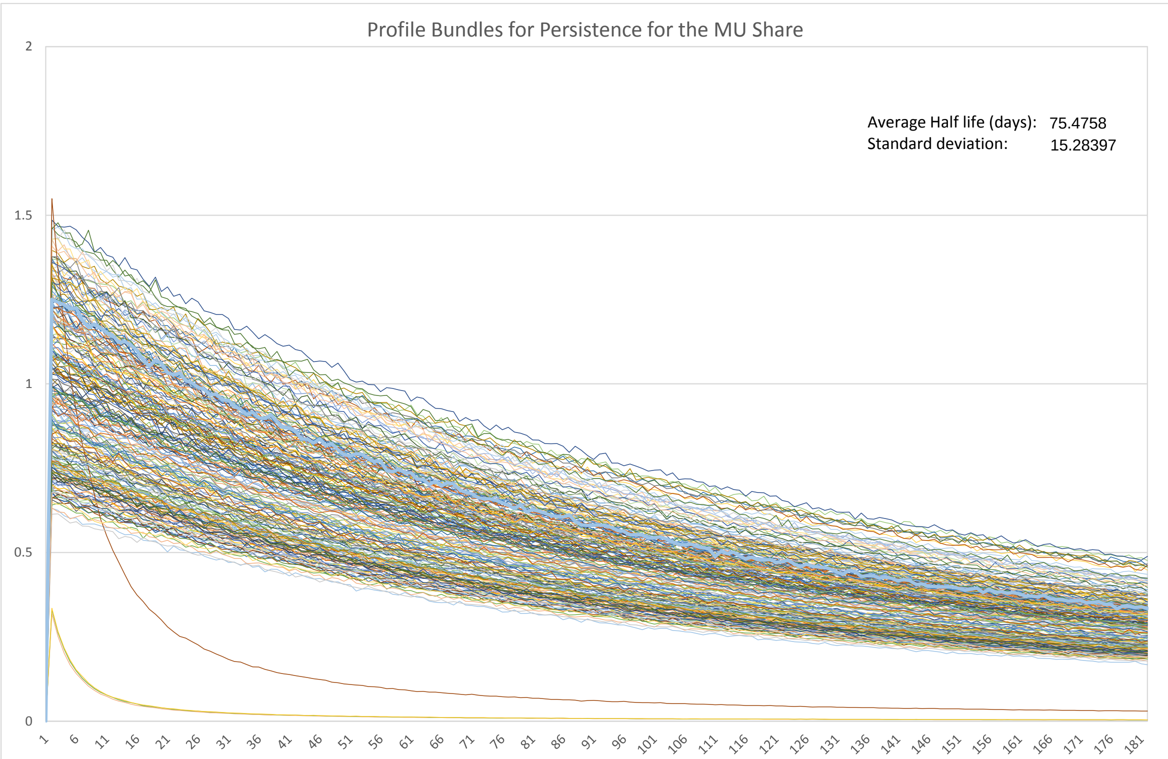

j. Norsk Hydro ASA

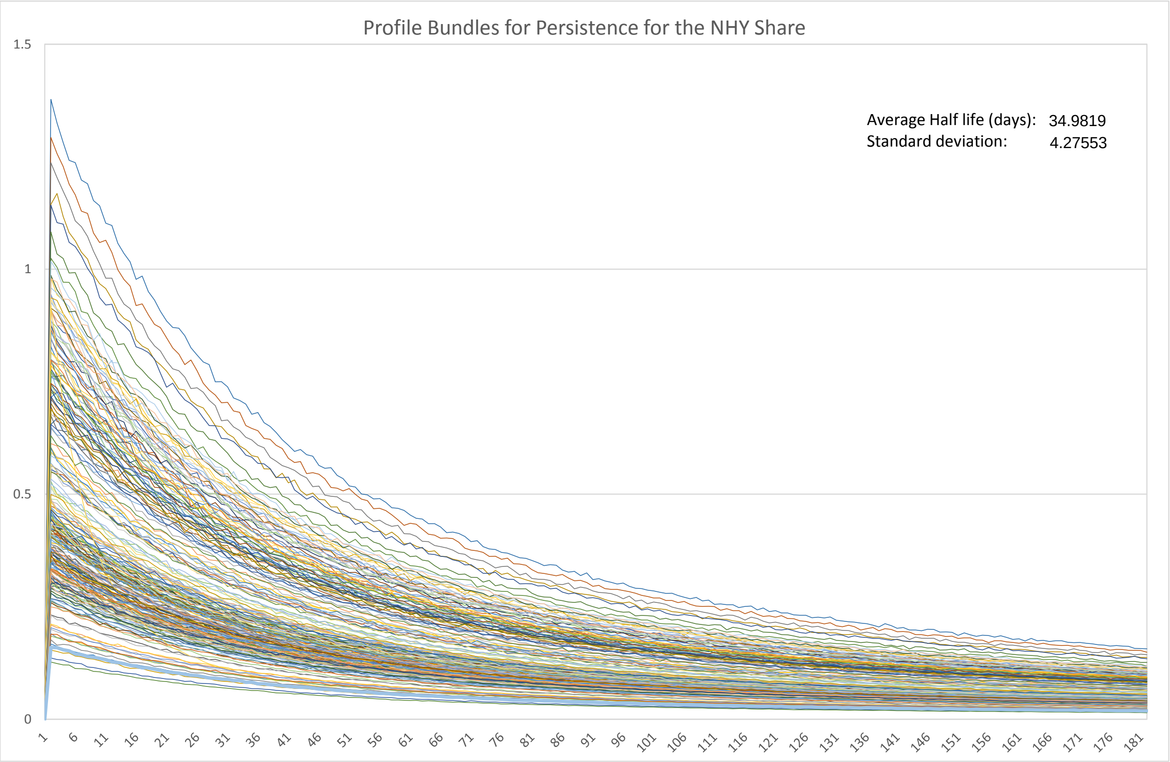

k. Tomra Systems ASA

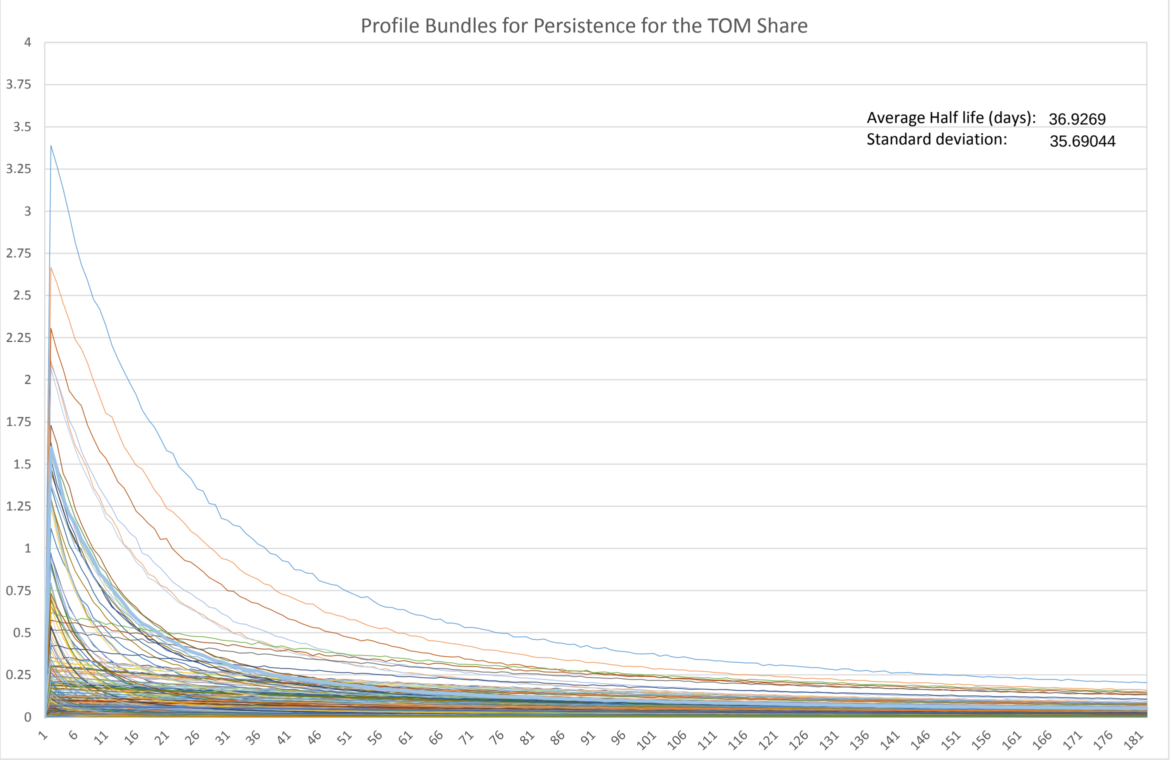

l. The ICE Carbon one month Forward Contracts

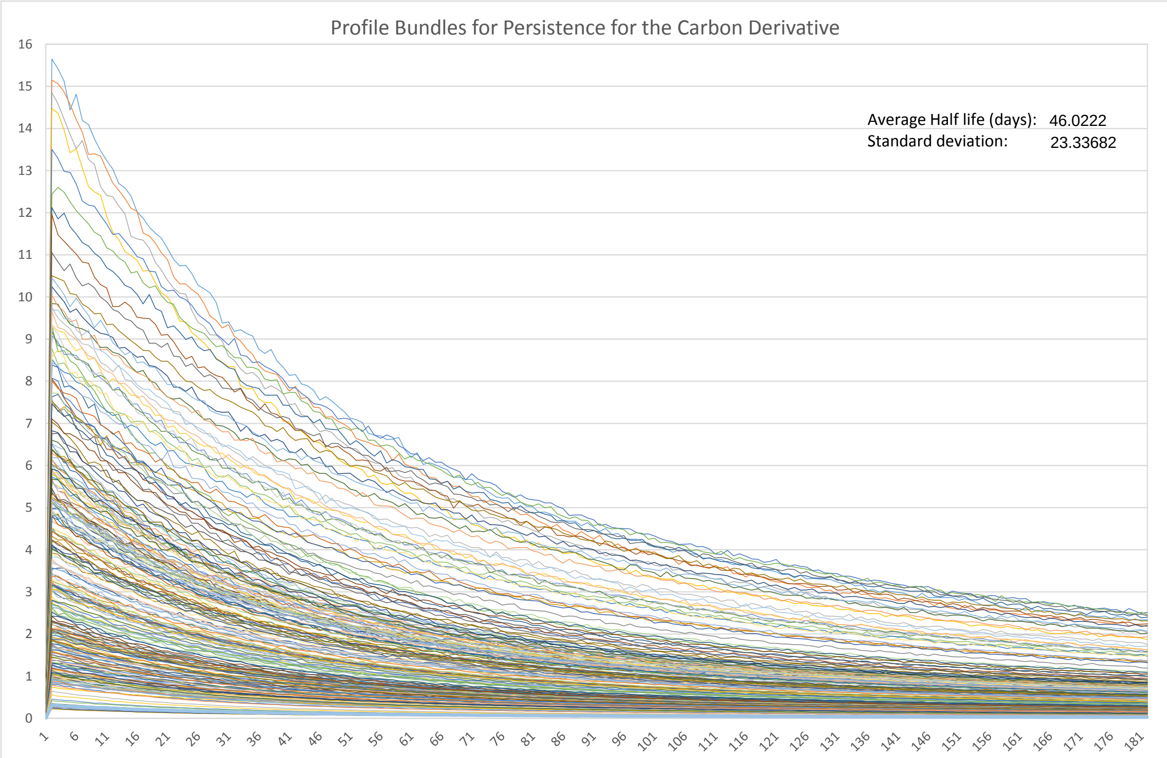

m. Brent oil front month Future Contracts

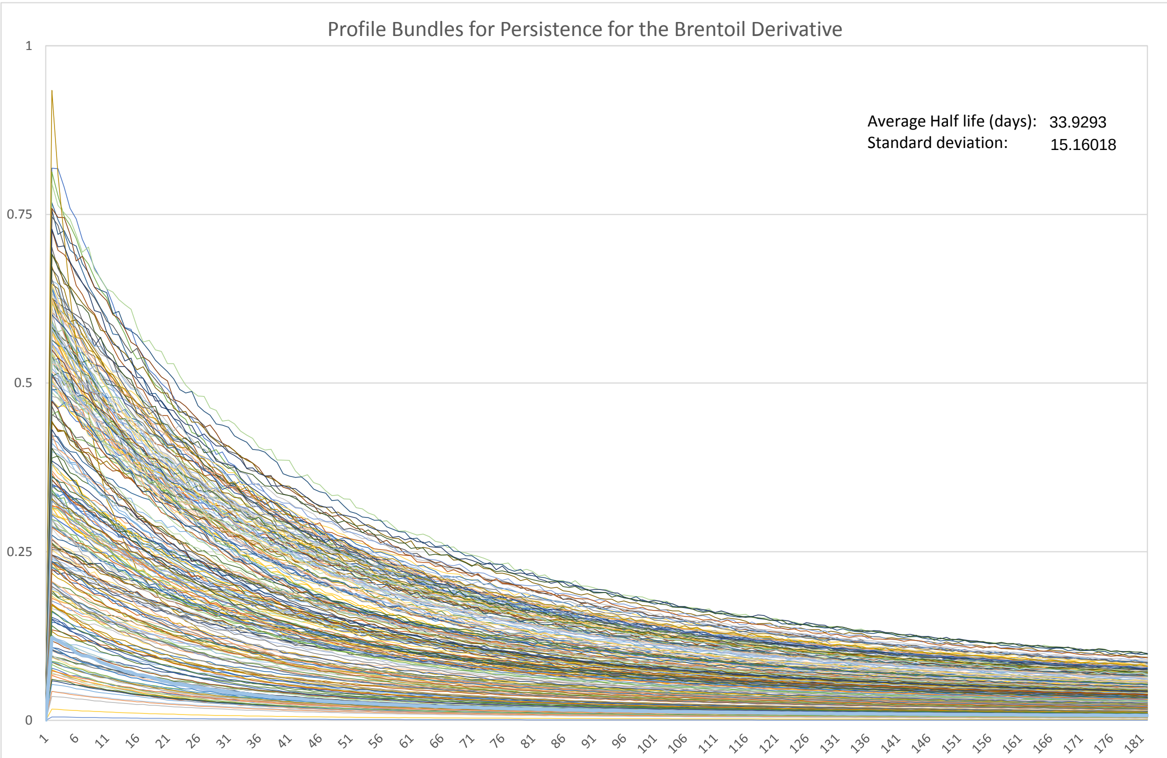

n. Salmon Forward Contracts

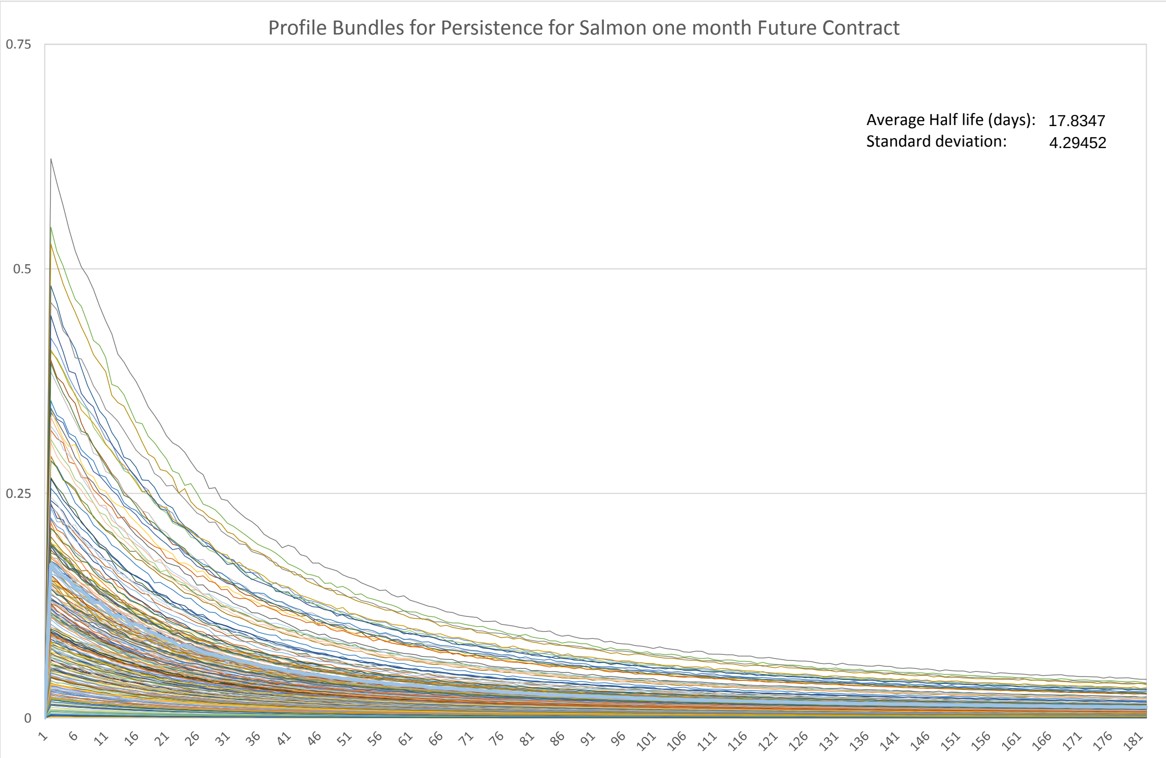

Figure 85 *Profile Bundles for Persistence*

7.0 Conclusion

7.1 Summary of main results

This thesis features a study of the dynamics of return and volatility, in response to a shock hitting the financial assets. Using a semi-nonparametric GARCH model, we have been able to examine profile bundles for evidence of damping or persistence, generating empirical evidence on the multi-step-ahead price dynamics. We have studied the extent to which the impulse responses indicate a leverage effect, where price decrease has a greater effect on subsequent volatility than the price increase. The thesis is relevant for the understanding of risk aspects that apply to the pricing of hedging instruments and fund management. The approach is similar to the univariate part of a study done by Gallant, Rossi et al. (1993), though this thesis conducts several different financial assets.

Our results reveal that the mean impulse responses are symmetric about the baseline, and we observe almost no serial dependence beyond lag one. Our results suggest that a positive (negative) price change is met by a slightly negative (positive) expected return in the following days. OSEBX, NHY, and MU stand out in this context in that they show a negative (positive) response to negative (positive) price changes. The results also indicate that both a positive and negative price change for OSEAX is met by a positive subsequent expected return.

The results reveal that an increase in volatility after a shock does not lead to a permanent change in the volatility. This is consistent with the results of Engle and Patton (2001). However, the results suggest that the “leverage effect” is quite persistent and not only a heavily damped transient phenomenon as claimed by Gallant, Rossi et al. (1993). The high persistence of the leverage effect is different from the results of Gallant, Rossi et al. (1993) and Tauchen, Zhang et al. (1996). Both papers suggest that the leverage effect is heavily damped after about 15 (S&P composite price index) and 4 days (IBM) accordingly. Our results deviate from earlier studies, suggesting that it remains constant for many days. Although we cannot argue that the results are significant, it can be a feature of interest for further studies.

Our results show that the degree of asymmetry in variance differs between the financial assets. We find the highest degree of asymmetry for stock indices and the asymmetry seems to be quite persistent. This is consistent with (Figlewski and Wang (2000)), who studied the individual stocks in the S&P 100 Index and the index itself. They found larger effects for negative returns compared to positive and a higher degree of asymmetry for the index itself.

The persistence of volatility, measured by its half-life, explains how many days the volatility uses to return halfway back to its unconditional mean after a shock. The half-life of the volatility of the 14 financial assets ranges from 17 to 113 days. Using a data set consisting of daily returns from 1988-2000, Engle and Patton (2001) found the volatility half-life for the DJIA to be around 73 days. Our results give a half-life of 22 days for this asset, which is substantially lower. An important difference between the two studies is the selection of data. Engle and Patton (2001) did not include the great crash of 1987 and the financial crisis of 2007/2008. The average half-life of volatility is higher for all the individual shares, compared to the stock indices.

The plots displaying the variance impulse-response dynamics (***Figure 84*** **a - n**) and the persistence of volatility (***Figure 85*** **a - n**) reveal a pattern between different types of assets. The results suggest that the stock indices have the highest degree of asymmetry in variance and at the same time, the lowest degree of persistence. The stock indices are portfolios consisting of several shares; hence, they offer a value of diversification. They are characterized by having lower standard deviations, CVaR and a low degree of persistence compared to the individual shares. When a shock occurs, the correlation between the assets in a portfolio approaches one, which indicates diminishing portfolio effects. This may be explained by the nature of such assets.
The individual stocks and commodity indices have the lowest degree of asymmetry in variance and the highest persistence (except the salmon derivative, which is more similar to the stock indices).

We have found that the financial assets with the highest degree of asymmetry in variance also have the lowest degree of persistence. Furthermore, the volatility dynamics of commodity indices seem to be quite similar to individual stocks. We believe that our thesis reveals some interesting features that motivate for further studies.

7.2 Further studies

For further studies, sup-norm bands can be constructed by bootstrapping as described in Gallant, Rossi et al. (1993). This method uses simulation to make confidence bands at a 95% level. It is done by comparing the sup-norm confidence bands of the profile with a null profile. Here, the null profile shows the profile of a null response, usually a horizontal line. If the null profile is inside the bands, the effect of the impulse profile is insignificant. By using this method, we can state the statistical significance of our findings.

References

Akaike, H. (1969). "Fitting Autoregressive Models for Prediction." Annals of the Institute of Statistical Mathematics **21**: 243-247.

Black, F. (1976). Studies of stock market volatility changes. Meetings of the American Statistical Association, Business and Economic Statistics Section 177-181.

Bollerslev, T. (1986). "Generalized Autoregressive Conditional Heteroscedasticity " Journal of Econometrics **31**: 307-327.

Brock, W. A., et al. (1996). "A test for Independence based on the Correlation Dimension." Econometric Reviews **15**: 197-235.

Chatfield, C. (2000). Time-series forecasting. Boca Raton, Fla, Chapman & Hall/CRC.

Christie, A. A. (1982). "The stochastic behavior of common stock variance: value, leverage and interest rate effects." Financial Economics **10**: 407-432.

Clark, P. K. (1973). "A subordinated stochastic process model with finite variance for speculative prices " Econometrica **41**: 135-156.

Dickey, D. A. and W. A. Fuller (1979). "Distribution of the Estimators for Autoregressive Time Series with a Unit Root." Journal of the American Statistical Assosiation **74**(366): 427-431.

Engle, R. F. (1982). "Autoregressive Conditional Heretoscedasticity with Estimates of the Variance of United Kingdom Inflation " Econometrica **50**(4): 987-1007.

Engle, R. F. and K. F. Kroner (1995). "Multivariate Simultaneous Generalized ARCH " Econometric Theory **11**: 122-150.

Engle, R. F. and A. J. Patton (2001). "What good is a volatility model?" Quantitative Finance **1**: 237-245.

Figlewski, S. and X. Wang (2000). Is the "leverage effect" a Leverage Effect? New York, NYU Stern School of Business
City University of Hong Kong.

Fish Pool ASA (2016). "About Fish Pool ASA." Retrieved 01. April, 2016, from http://fishpool.eu/about/.

Gallant, A. R., et al. (1993). "Nonlinear Dynamic Structures." Econometrica **61**(4): 871-907.

Gallant, A. R. and G. Tauchen (1990, April 2014). "SNP: A Program for Nonparametric Time Series Analysis ". from http://www.aronaldg.org.

Hull, J. (2015). Risk Management & Financial Institutions Wiley Finance Series.

Intercontinental Exchange, I. (2016). "The Intercontinental Exchange (ICE): About ". Retrieved 01. April 2016, from https://www.intercontinentalexchange.com https://www.theice.com/index.

Koop, G. (1996). "Parameter uncertainty and impulse response analysis." Journal of Econometrics **72**: 135-149.

Koop, G., et al. (1996). "Impulse response analysis in nonlinear multivariate models." Journal of Econometrics **74**: 119-147.

Kwiatowski, D., et al. (1992). "Testing the null hypothesis of stationary against the alternative of aa unit root: How sure are we that economic series have a unit root." Journal of Econometrics **54**: 159-178.

Ljung, G. M. and G. E. P. Box (1978). "On a Measure of Lack of Fit in Time Series Models " Biometrika **65**: 297-303.

Markowitz, H. (1952). "Portfolio Selection." Journal of Finance **7**(1): 77-91.

Nelson, D. B. (1991). "Conditional Heteroskedasticity in Asset Returns: A New Approach." Econometrica **59**(2): 347-370.

Netfonds Bank (2016). "Netfonds Bank: Market Quotes." Retrieved 10. January 2016, from http://www.netfonds.no/quotes/kurs.php.

Poterba, J. M. and L. H. Summers (1986). "The Persistence of Volatility and Stock Market Fluctuations." The American Economic Review **76**(5): 1142-1151.

Schwarz, G. (1978). "Estimating the Dimension of a Model." Annals of Statistics **6**(2): 461-464.

Tauchen, G., et al. (1996). "Volume, Volatility, and leverage: A dynamic analysis." Journal of Econometrics **74**: 177-208.

Verbeek, M. (2012). A Guide to Modern Econometrics. Rotterdam School of Management, Erasmus University, Rotterdam Wiley.

Walter, G. G. (1977). "Properties of Hermite Series Estimation of Probability Density " The Annals of Statistics **5**(6): 1258-1264.

Yahoo! Finance (2016). "Yahoo! Finance: Market Data ". Retrieved 10. January, 2016, from https://finance.yahoo.com/market-overview/.